Electronic Supplementary Material (ESI) for Green Chemistry.

Supporting Information

Halometallate Ionic Liquids: Thermal Properties, Decomposition Pathways, and Life Cycle Considerations

Coby J. Clarke,*[ab] Husain Baaquel,[a] Richard P. Matthews,[a] Yiyan Chen,[a] Kevin R. J. Lovelock,[c] Jason P. Hallett[a] and Peter Licence[b]

(a) Department of Chemical Engineering, Imperial College London, London UK
(b) Department of Chemistry, The University of Nottingham, Nottingham, UK
(c) Department of Chemistry, University of Reading, Reading, UK

*Correspondence: coby.clarke@nottingham.ac.uk

Synthesis

Anhydrous metal halides with ≥ 99.99 % purity were purchased from either Tokyo Chemical Industry, Sigma Aldrich, or Solvionic. 1-Butyl-3-methylimidazolium chloride ($[C_4C_1Im]Cl$) was prepared by a previously published procedure.[1] 1-Octyl-3-methylimidazolium chloride ($[C_8C_1Im]Cl$) and 1-octyl-3-methylimidazolium bromide ($[C_8C_1Im]Br$) were purchased from IOLITEC and trihexyl(tetradecyl)phosphonium chloride ($[P_{66614}]Cl$) was purchased from Sigma Aldrich. All ionic liquids were analysed by ^1H, ^{13}C, and ^{31}P NMR to check purity before being dried on a Schlenk line at $<2 \times 10^{-2}$ mbar at 70 °C and loaded into a LABstar MBraun glovebox with < 0.5 ppm O_2 and < 0.5 ppm H_2O. Halometallate ionic liquids were prepared by mixing the desired ratios in screw top glass vials and heating at 70 °C for 48-72 hr until clear solutions were obtained. Details of the procedures have previously been published elsewhere.[2] All ionic liquids have previously been analysed by a range of lab based and synchrotron based X-ray spectroscopies to confirm speciation of the metal components.[2–4] Purity of the organic components was confirmed by NMR which was recorded on a Bruker AV(III)400HD in deuterated solvents and spectra were referenced to the residual solvent signals. High resolution mass spectrometry (HRMS) was measured using a Bruker micrOTOF II and solutions were prepared in analytical grade acetonitrile.

NMR Data

$[C_8C_1Im]Cl$: ^1H NMR (400 MHz, DMSO) δ = 9.33 (s, 1H), 7.82 (s, 1H), 7.75 (s, 1H), 4.17 (t, *J* = 7.2 Hz, 2H), 3.86 (s, 3H), 1.85 – 1.68 (m, 2H), 1.35 – 1.14 (m, 10H), 0.84 (t, 3H). ^{13}C NMR (101 MHz, DMSO) δ = 136.61, 123.57, 48.70, 35.71, 31.14, 29.39, 28.46, 28.32, 25.48, 22.04, 13.92.

$[C_8C_1Im]Cl_{0.1}ZnCl_2$: ^1H NMR (400 MHz, DMSO) δ = 9.31 (s, 1H), 7.81 (s, 1H), 7.74 (s, 1H), 4.17 (t, *J* = 7.2 Hz, 2H), 3.86 (s, 3H), 1.91 – 1.65 (m, 2H), 1.36 – 1.14 (m, 10H), 0.84 (t, 3H). ^{13}C NMR (101 MHz, DMSO) δ = 135.99, 123.57, 122.24, 48.72, 39.52, 35.73, 31.15, 29.40, 28.47, 28.33, 24.86, 22.04, 13.93.

$[C_8C_1Im]Cl_{0.33}ZnCl_2$: ^1H NMR (400 MHz, DMSO) δ = 9.20 (s, 1H), 7.78 (s, 1H), 7.71 (s, 1H), 4.16 (t, *J* = 7.3 Hz, 2H), 3.86 (s, 3H), 1.90 – 1.66 (m, 2H), 1.47 – 1.06 (m, 10H), 0.84 (t, 3H). ^{13}C NMR (101 MHz, DMSO) δ = 136.51, 123.58, 122.24, 48.14, 39.52, 35.77, 31.15, 29.39, 28.46, 27.93, 25.49, 21.47, 13.21.

$[C_8C_1Im]Cl_{0.4}ZnCl_2$: ^1H NMR (400 MHz, DMSO) δ = 9.14 (s, 1H), 7.77 (s, 1H), 7.70 (s, 1H), 4.15 (t, *J* = 7.3 Hz, 3H), 3.85 (s, 3H), 1.93 – 1.65 (m, 2H), 1.37 – 1.16 (m, 10H), 0.85 (t, 3H). ^{13}C NMR (101 MHz, DMSO) δ = 136.02, 123.60, 122.25, 48.76, 39.52, 35.77, 30.54, 29.38, 28.46, 28.32, 25.48, 22.71, 13.94.

$[C_8C_1Im]Cl_{0.43}ZnCl_2$: ^1H NMR (400 MHz, DMSO) δ = 9.16 (s, 1H), 7.77 (s, 1H), 7.70 (s, 1H), 4.16 (t, *J* = 7.2 Hz, 3H), 3.86 (s, 3H), 1.87 – 1.69 (m, 2H), 1.38 – 1.12 (m, 10H), 0.85 (t, *J* = 6.9 Hz, 3H). ^{13}C NMR (101 MHz, DMSO) δ = 136.45, 123.57, 122.23, 48.78, 35.82, 31.14, 29.41, 28.46, 28.33, 25.48, 22.04, 13.92.

$[C_8C_1Im]Cl_{0.5}ZnCl_2$: ^1H NMR (400 MHz, DMSO) δ = 9.10 (s, 1H), 7.76 (s, 1H), 7.69 (s, 1H), 4.15 (t, *J* = 7.2 Hz, 2H), 3.85 (s, 3H), 1.86 – 1.70 (m, 2H), 1.32 – 1.16 (m, 10H), 0.84 (t, 3H). ^{13}C NMR (101 MHz, DMSO) δ = 136.42, 123.60, 122.25, 48.80, 39.52, 35.82, 31.15, 29.39, 28.46, 28.32, 25.48, 22.04, 13.94.

$[C_8C_1Im]Cl_{0.6}ZnCl_2$: ^1H NMR (400 MHz, DMSO) δ = 9.07 (s, 1H), 7.74 (s, 1H), 7.68 (s, 1H), 4.14 (t, *J* = 7.3 Hz, 2H), 3.85 (s, 3H), 1.82 – 1.71 (m, 2H), 1.29 – 1.14 (m, 10H), 0.83 (t, 3H). ^{13}C NMR (101 MHz, DMSO) δ = 136.41, 123.62, 122.29, 48.86, 39.52, 35.90, 31.18, 29.43, 28.50, 28.36, 25.52, 22.08, 13.98.

$[C_8C_1Im]Cl_{0.67}ZnCl_2$: ^1H NMR (400 MHz, DMSO) δ 9.08 (s, 1H), 7.75 (s, 1H), 7.69 (s, 1H), 4.14 (t, *J* = 7.2 Hz, 2H), 3.84 (s, 3H), 1.85 – 1.70 (m, 2H), 1.35 – 1.11 (m, 10H), 0.84 (t, 3H). ^{13}C NMR (101 MHz, DMSO) δ = 136.45, 123.62, 122.28, 48.81, 39.52, 35.82, 31.17, 29.39, 28.48, 28.34, 25.50, 22.06, 13.96.

[C_8C_1Im]$Br_{0.1}ZnBr_2$: ^{1}H NMR (400 MHz, DMSO) δ = 9.17 (s, 1H), 7.79 (s, 1H), 7.72 (s, 1H), 4.16 (t, *J* = 7.2 Hz, 2H), 3.85 (s, 3H), 1.83 – 1.70 (m, 2H), 1.34 – 1.18 (m, 10H), 0.84 (t, 3H). ^{13}C NMR (101 MHz, DMSO) δ = 136.48, 123.58, 122.25, 48.74, 39.52, 35.75, 31.14, 29.37, 28.45, 28.31, 25.47, 22.03, 13.93.

[C_8C_1Im]$Br_{0.33}ZnBr_2$: ^{1}H NMR (400 MHz, DMSO) δ = 9.14 (s, 1H), 7.78 (s, 1H), 7.71 (s, 1H), 4.15 (t, *J* = 7.2 Hz, 3H), 3.85 (s, 3H), 1.92 – 1.65 (m, 2H), 1.36 – 1.16 (m, 10H), 0.84 (t, 3H). ^{13}C NMR (101 MHz, DMSO) δ = 136.46, 123.59, 122.25, 48.76, 39.52, 35.77, 31.14, 29.37, 28.46, 28.31, 25.47, 22.04, 13.93.

[C_8C_1Im]$Br_{0.5}ZnBr_2$: ^{1}H NMR (400 MHz, DMSO) δ = 9.12 (s, 1H), 7.77 (s, 1H), 7.70 (s, 1H), 4.16 (t, *J* = 7.3 Hz, 2H), 3.85 (s, 3H), 1.92 – 1.66 (m, 2H), 1.38 – 1.10 (m, 10H), 0.86 (t, *J* = 6.8 Hz, 3H). ^{13}C NMR (101 MHz, DMSO) δ = 136.43, 123.59, 122.25, 48.78, 39.52, 35.81, 31.14, 29.37, 28.45, 28.31, 25.48, 22.04, 13.94.

[C_8C_1Im]$Br_{0.6}ZnBr_2$: ^{1}H NMR (400 MHz, DMSO) δ 9.08 (s, 1H), 7.74 (s, 1H), 7.67 (s, 1H), 4.14 (t, *J* = 7.3 Hz, 3H), 3.84 (s, 3H), 1.86 – 1.68 (m, 2H), 1.40 – 1.09 (m, 10H), 0.83 (t, 3H). ^{13}C NMR (101 MHz, DMSO) δ = 136.44, 123.64, 122.31, 48.89, 35.92, 31.20, 29.43, 28.51, 28.37, 25.54, 22.10, 14.01.

[C_8C_1Im]$Br_{0.67}ZnBr_2$: ^{1}H NMR (400 MHz, DMSO) δ = 9.08 (s, 1H), 7.75 (s, 1H), 7.68 (s, 1H), 4.14 (t, *J* = 7.2 Hz, 2H), 3.84 (s, 3H), 1.85 – 1.68 (m, 2H), 1.32 – 1.15 (m, 10H), 0.84 (d, *J* = 6.9 Hz, 3H). ^{13}C NMR (101 MHz, DMSO) δ 136.43, 123.62, 122.28, 48.84, 35.88, 31.16, 29.40, 28.48, 28.34, 25.50, 22.07, 13.98.

[C_8C_1Im]$Br_{0.33}ZnCl_2$: ^{1}H NMR (400 MHz, DMSO) δ = 9.18 (s, 1H), 7.79 (s, 1H), 7.72 (s, 1H), 4.16 (t, *J* = 7.2 Hz, 2H), 3.86 (s, 3H), 1.86 – 1.68 (m, 2H), 1.34 – 1.12 (m, 10H), 0.84 (d, *J* = 7.0 Hz, 3H). ^{13}C NMR (101 MHz, DMSO) δ = 136.44, 123.56, 122.23, 48.75, 35.79, 31.13, 29.37, 28.45, 28.31, 25.46, 22.02, 13.91.

[C_8C_1Im]$Br_{0.5}ZnCl_2$: ^{1}H NMR (400 MHz, DMSO) δ = 9.12 (s, 1H), 7.77 (s, 1H), 7.70 (s, 1H), 4.15 (t, *J* = 7.2 Hz, 2H), 3.85 (s, 3H), 1.83 – 1.68 (m, 2H), 1.35 – 1.12 (m, 10H), 0.94 – 0.76 (m, 3H). ^{13}C NMR (101 MHz, DMSO) δ = 135.59, 123.60, 122.26, 48.78, 39.52, 35.80, 31.15, 29.37, 28.46, 28.32, 25.48, 22.04, 13.94.

[C_4C_1Im]$Cl_{0.33}ZnCl_2$: ^{1}H NMR (400 MHz, DMSO) δ = 9.48 (s, 1H), 7.86 (s, 1H), 7.78 (s, 1H), 4.19 (t, *J* = 7.2 Hz, 2H), 3.87 (s, 3H), 1.89 – 1.64 (m, 2H), 1.33 – 1.17 (m, 2H), 0.88 (t, *J* = 7.4 Hz, 3H). ^{13}C NMR (101 MHz, DMSO) δ = 136.70, 123.58, 122.28, 48.41, 35.72, 31.40, 18.77, 13.29.

[C_4C_1Im]$Cl_{0.5}ZnCl_2$: ^{1}H NMR (400 MHz, DMSO) δ = 9.02 (s, 1H), 7.70 (s, 1H), 7.63 (s, 1H), 4.13 (t, *J* = 7.2 Hz, 3H), 3.82 (s, 3H), 1.88 – 1.60 (m, 2H), 1.41 – 1.09 (m, 2H), 0.85 (t, *J* = 7.4 Hz, 3H). ^{13}C NMR (101 MHz, DMSO) δ 136.51, 123.77, 122.44, 48.82, 36.12, 31.55, 18.98, 13.52.

[C_8C_1Im]$Cl_{0.33}NiCl_2$: ^{1}H NMR (400 MHz, DMSO) δ = 9.17 (s, 1H), 7.62 (s, 1H), 7.55 (s, 1H), 4.03 – 3.87 (m, 2H), 3.65 (s, 3H), 1.64 – 1.47 (m, 2H), 1.18 – 0.91 (m, 10H), 0.74 – 0.55 (m, 3H). ^{13}C NMR (101 MHz, DMSO) δ = 131.90, 119.28, 117.93, 44.52, 31.75, 26.63, 25.07, 23.97, 23.88, 21.08, 17.53, 9.47.

[C_8C_1Im]$Cl_{0.5}InCl_3$: ^{1}H NMR (400 MHz, DMSO) δ = 9.33 (s, 1H), 7.81 (s, 1H), 7.74 (s, 1H), 4.18 (t, *J* = 7.2 Hz, 2H), 3.87 (s, 3H), 1.90 – 1.65 (m, 2H), 1.30 – 1.12 (m, 10H), 0.83 (t, *J* = 6.9 Hz, 2H). ^{13}C NMR (101 MHz, DMSO) δ = 136.66, 123.65, 122.31, 48.80, 39.52, 35.92, 31.22, 29.55, 28.55, 28.42, 25.57, 22.11, 14.01.

[P_{66614}]Cl: ^{1}H NMR (400 MHz, DMSO) δ = 2.28 – 2.08 (m, 8H), 1.53 – 1.41 (m, 8H), 1.43 – 1.33 (m, 8H), 1.34 – 1.19 (m, 32H), 0.95 – 0.78 (m, 12H). ^{13}C NMR (101 MHz, DMSO) δ 31.27, 30.80, 30.39, 30.02, 29.87, 29.81, 29.66, 29.05, 29.03, 29.01, 28.99, 28.94, 28.69, 28.62, 28.07, 22.07, 21.80, 20.55, 20.51, 20.44, 17.73, 17.63, 17.26, 17.16, 13.92, 13.84.

[P_{66614}]$Cl_{0.1}ZnCl_2$: ^{1}H NMR (400 MHz, DMSO) δ = 2.26 – 2.12 (m, 8H), 1.55 – 1.42 (m, 8H), 1.41 – 1.34 (m, 8H), 1.33 – 1.20 (m, 32H), 0.97 – 0.78 (m, 12H). ^{13}C NMR (101 MHz, DMSO) δ = 31.28, 30.39, 30.02, 29.87, 29.81, 29.66, 29.05, 29.03, 29.01, 28.99, 28.94, 28.69, 28.63, 28.07, 22.07, 21.80, 20.55, 20.51, 17.73, 17.26, 13.92, 13.84.

[P_{66614}]$Cl_{0.33}ZnCl_2$: ^{1}H NMR (400 MHz, DMSO) δ = 2.27 – 2.10 (m, 8H), 1.52 – 1.42 (m, 8H), 1.42 – 1.34 (m, 8H), 1.34 – 1.19 (m, 32H), 0.99 – 0.81 (m, 12H). ^{13}C NMR (101 MHz, DMSO) δ = 31.28, 30.38, 29.80, 29.65, 29.05, 29.02, 29.00, 28.99, 28.94, 28.69, 28.62, 28.07, 22.08, 21.79, 20.54, 20.49, 17.72, 17.25, 13.93, 13.85.

[C_4C_1Im]Cl: ^{1}H NMR (400 MHz, DMSO) δ = 9.55 (s, 1H), 7.88 (s, 1H), 7.81 (s, 1H), 4.20 (t, *J* = 7.2 Hz, 3H), 3.88 (s, 3H), 1.89 – 1.66 (m, 2H), 1.35 – 1.14 (m, 2H), 0.88 (t, *J* = 7.4 Hz, 3H). ^{13}C NMR (101 MHz, DMSO) δ = 136.73, 123.54, 122.25, 48.35, 35.67, 31.37, 18.73, 13.26.

[C_8C_1Im]Br: ^{1}H NMR (400 MHz, DMSO) δ = 9.27 (s, 1H), 7.83 (s, 1H), 7.75 (s, 1H), 4.17 (t, *J* = 7.2 Hz, 3H), 3.86 (s, 3H), 1.86 – 1.70 (m, 2H), 1.32 – 1.15 (m, 10H), 0.84 (d, *J* = 6.9 Hz, 3H). ^{13}C NMR (101 MHz, DMSO) δ = 136.49, 123.54, 122.23, 48.70, 35.74, 31.13, 29.38, 28.45, 28.31, 25.46, 22.02, 13.90.

[C_8C_1Im]$Cl_{0.33}$AgCl: ^{1}H NMR (400 MHz, DMSO) δ = 9.28 (s, 1H), 7.80 (s, 1H), 7.73 (s, 1H), 4.17 (t, *J* = 7.2 Hz, 2H), 3.86 (s, 3H), 1.77 (s, 2H), 1.24 (s, 10H), 0.84 (d, *J* = 7.0 Hz, 3H). ^{13}C NMR (101 MHz, DMSO) δ = 136.56, 123.57, 122.24, 48.74, 35.76, 31.15, 29.40, 28.47, 28.34, 25.50, 22.04, 13.93.

[C_8C_1Im]$Cl_{0.33}PtCl_2$: ^{1}H NMR (400 MHz, DMSO) δ = 9.31 (s, 1H), 7.82 (s, 1H), 7.74 (s, 1H), 4.17 (t, *J* = 7.3 Hz, 2H), 3.87 (s, 3H), 1.84 – 1.66 (m, 2H), 1.34 – 1.18 (m, 10H), 0.84 (d, *J* = 7.0 Hz, 3H). ^{13}C NMR (101 MHz, DMSO) δ = 136.53, 123.54, 122.22, 48.71, 39.52, 35.73, 31.12, 29.38, 28.44, 28.31, 25.47, 22.01, 13.90.

[P_{66614}]$Cl_{0.33}$AgCl: ^{1}H NMR (400 MHz, DMSO) δ =2.28 – 2.10 (m, 8H), 1.54 – 1.42 (m, 8H), 1.42 – 1.33 (m, 8H), 1.35 – 1.18 (m, 32H), 0.95 – 0.77 (m, 12H). ^{13}C NMR (101 MHz, DMSO) δ = 31.28, 30.39, 30.02, 29.87, 29.81, 29.66, 29.05, 29.03, 29.01, 28.99, 28.94, 28.69, 28.62, 28.07, 22.08, 21.80, 20.55, 20.51, 17.74, 17.64, 17.27, 17.17, 13.92, 13.84.

[C_8C_1Im]$Cl_{0.33}ZnBr_2$: ^{1}H NMR (400 MHz, DMSO) δ = 9.22 (s, 1H), 7.80 (s, 1H), 7.73 (s, 1H), 4.17 (t, *J* = 7.2 Hz, 2H), 3.87 (s, 3H), 1.84 – 1.71 (m, 2H), 1.40 – 1.15 (m, 10H), 0.86 (d, *J* = 7.0 Hz, 3H). ^{13}C NMR (101 MHz, DMSO) δ = 136.51, 123.58, 122.24, 48.74, 39.52, 35.76, 31.14, 29.39, 28.46, 28.32, 25.48, 22.04, 13.93.

[C_8C_1Im]$Cl_{0.5}ZnBr_2$: ^{1}H NMR (400 MHz, DMSO) δ = 9.11 (s, 1H), 7.77 (s, 1H), 7.70 (s, 1H), 4.15 (t, *J* = 7.2 Hz, 2H), 3.85 (s, 3H), 1.85 – 1.67 (m, 1H), 1.34 – 1.16 (m, 10H), 0.85 (d, *J* = 6.9 Hz, 3H). ^{13}C NMR (101 MHz, DMSO) δ = 136.93, 124.08, 122.74, 49.26, 36.27, 31.63, 29.85, 28.94, 28.80, 25.96, 22.52, 14.42.

[C_8C_1Im]$Cl_{0.33}CoCl_2$: ^{1}H NMR (400 MHz, DMSO) δ = 9.31 (s, 1H), 7.71 (s, 1H), 7.63 (s, 1H), 4.05 (s, 2H), 3.76 (s, 3H), 1.32 (s, 10H), 0.88 (s, 3H). ^{13}C NMR (101 MHz, DMSO) δ = 133.61, 123.14, 121.60, 49.27, 37.08, 29.94, 29.04, 27.41, 27.33, 24.91, 20.80, 12.85.

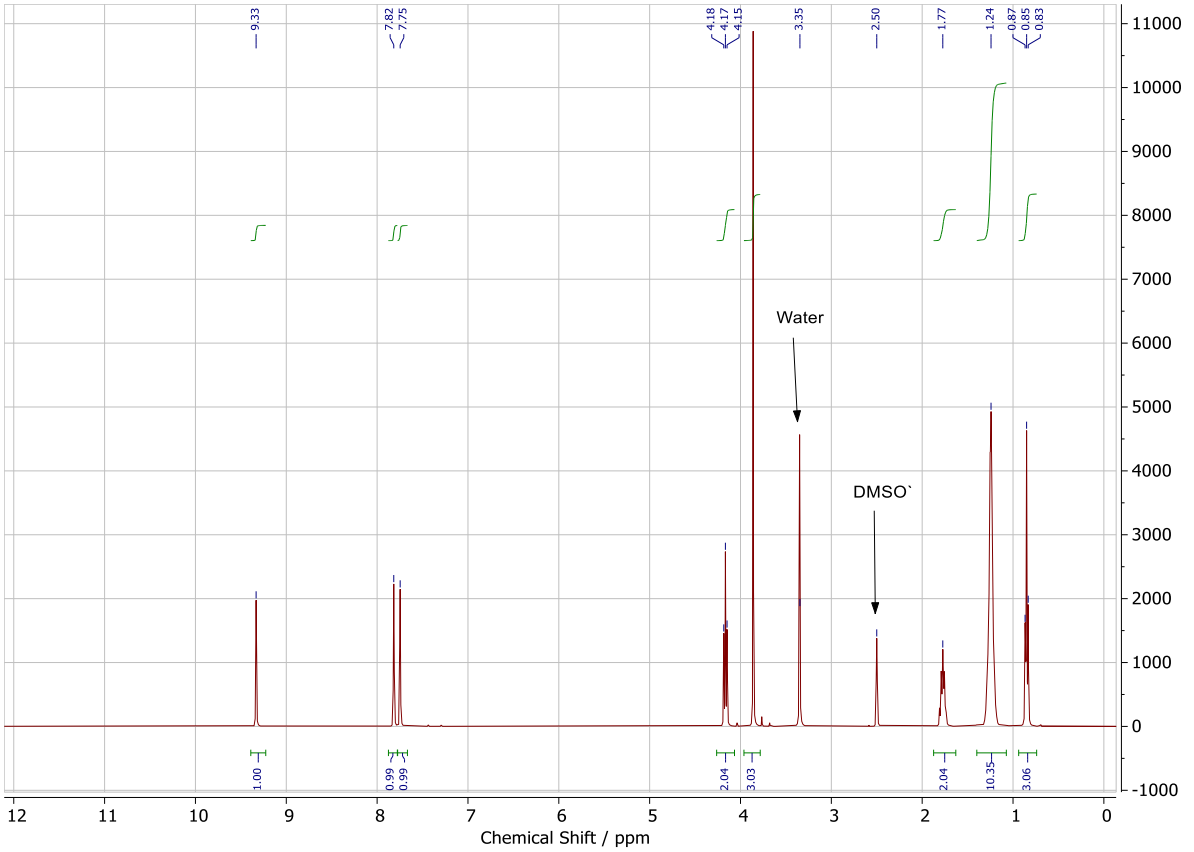

Figure S1 ^{1}H NMR of $[C_8C_1Im]Cl$ in DMSO-d_6.

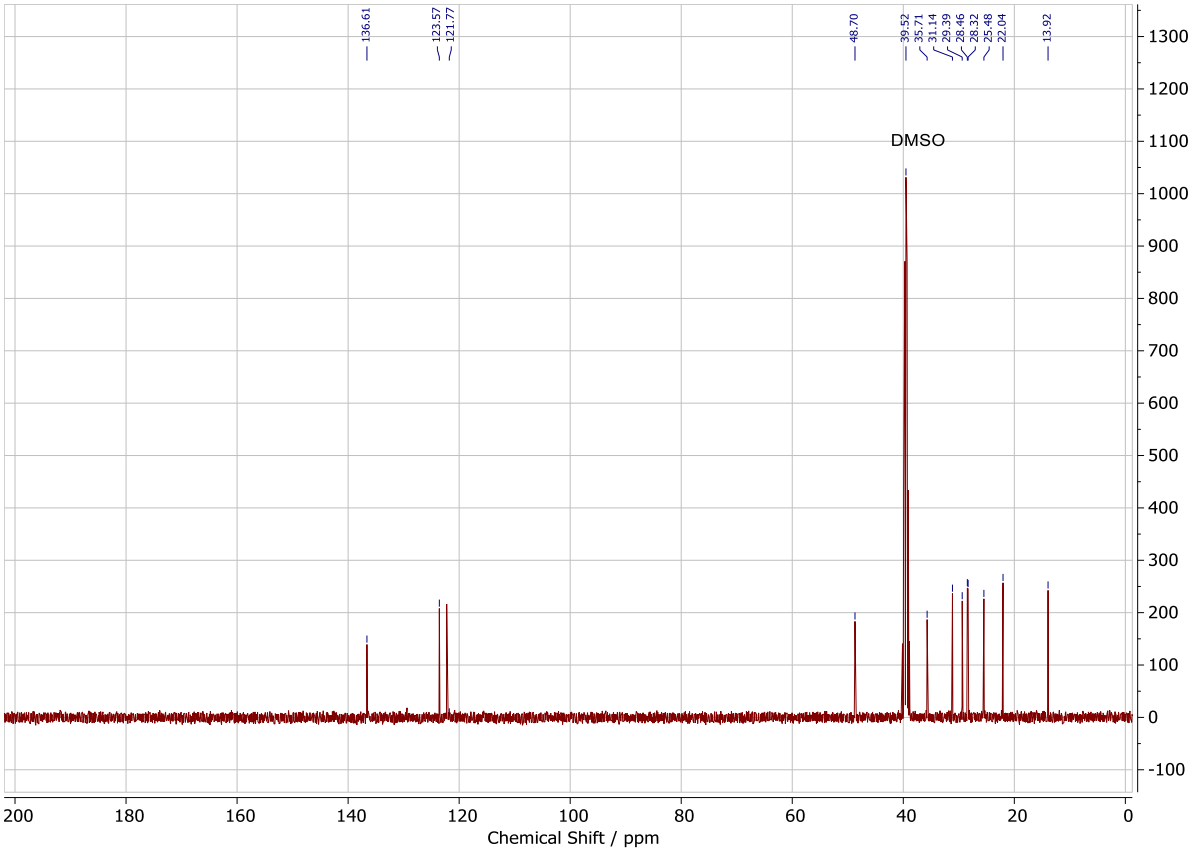

Figure S2 ^{13}C NMR of $[C_8C_1Im]Cl$ in DMSO-d_6.

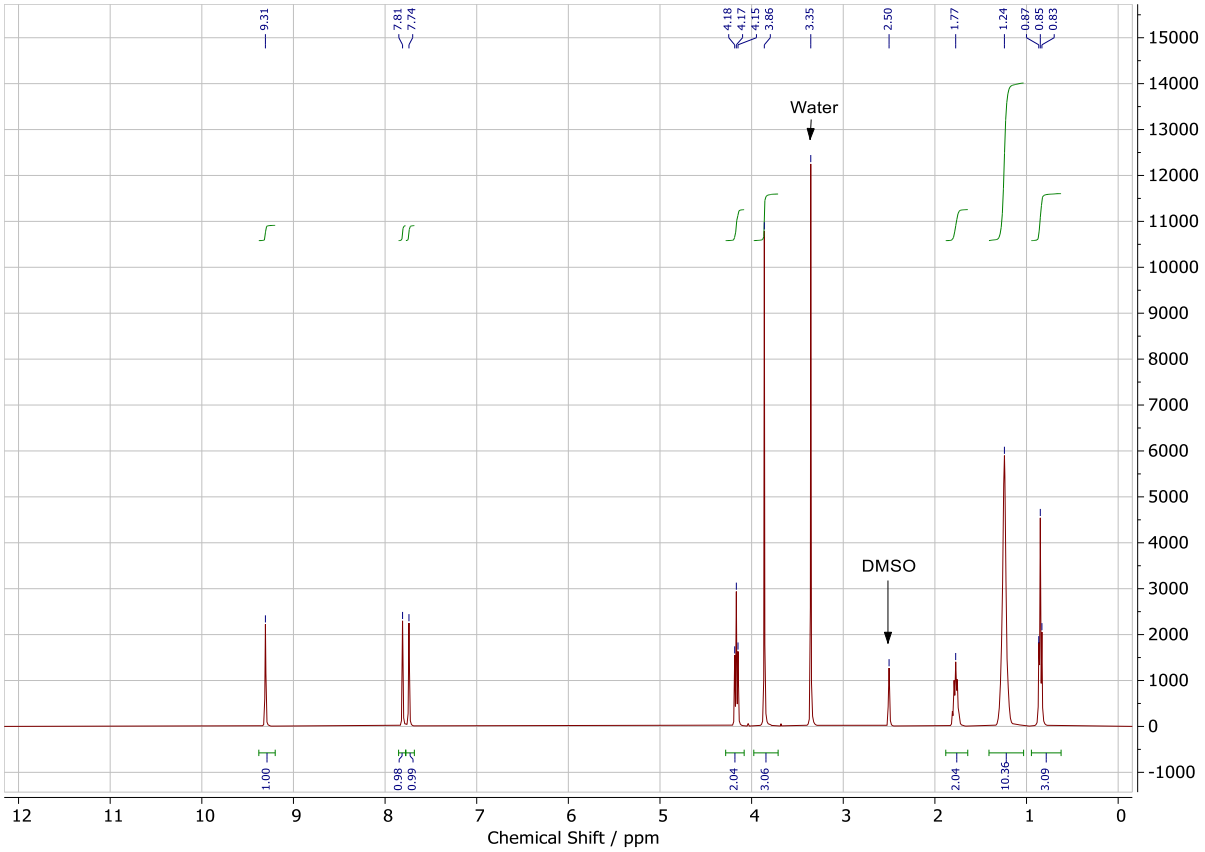

Figure S3 ^{1}H NMR of $[C_8C_1Im]Cl_{0.1}ZnCl_2$ in DMSO-d_6.

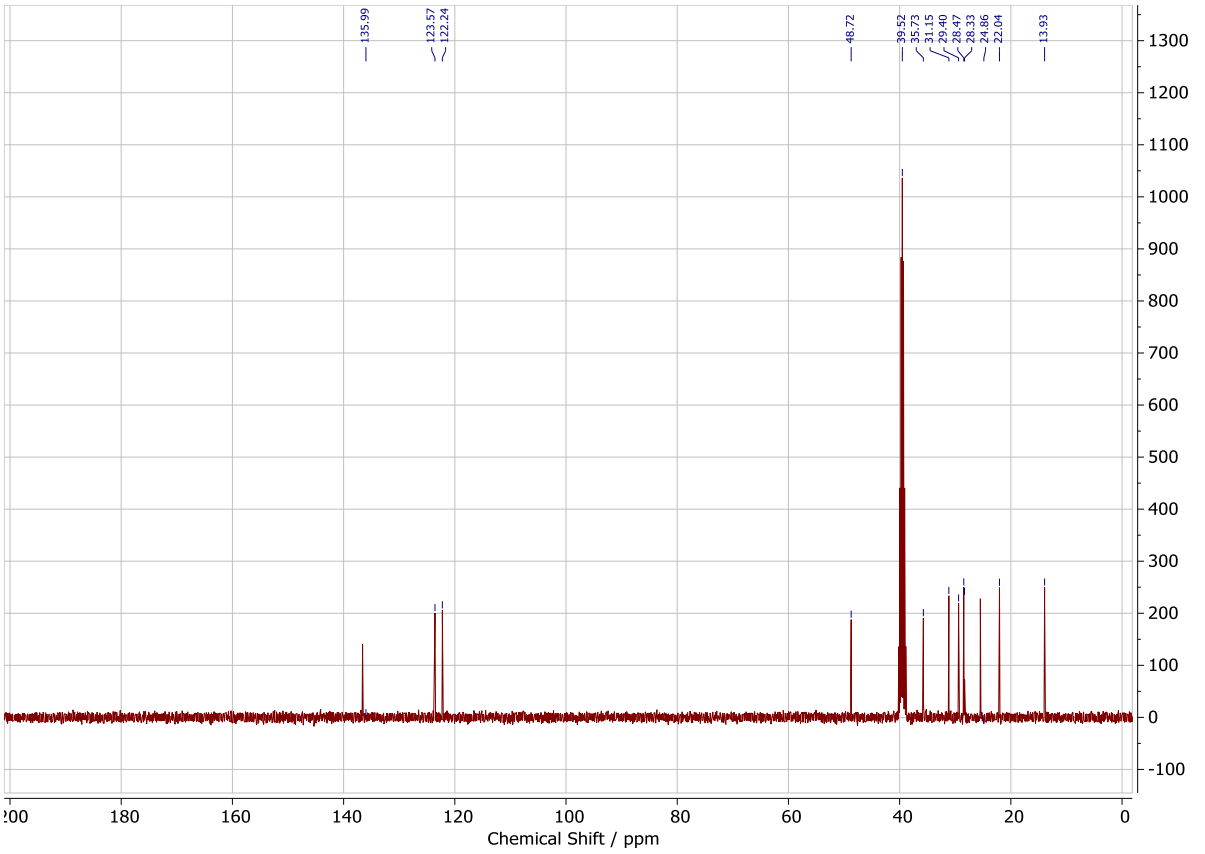

Figure S4 ^{13}C NMR of $[C_8C_1Im]Cl_{0.1}ZnCl_2$ in DMSO-d_6.

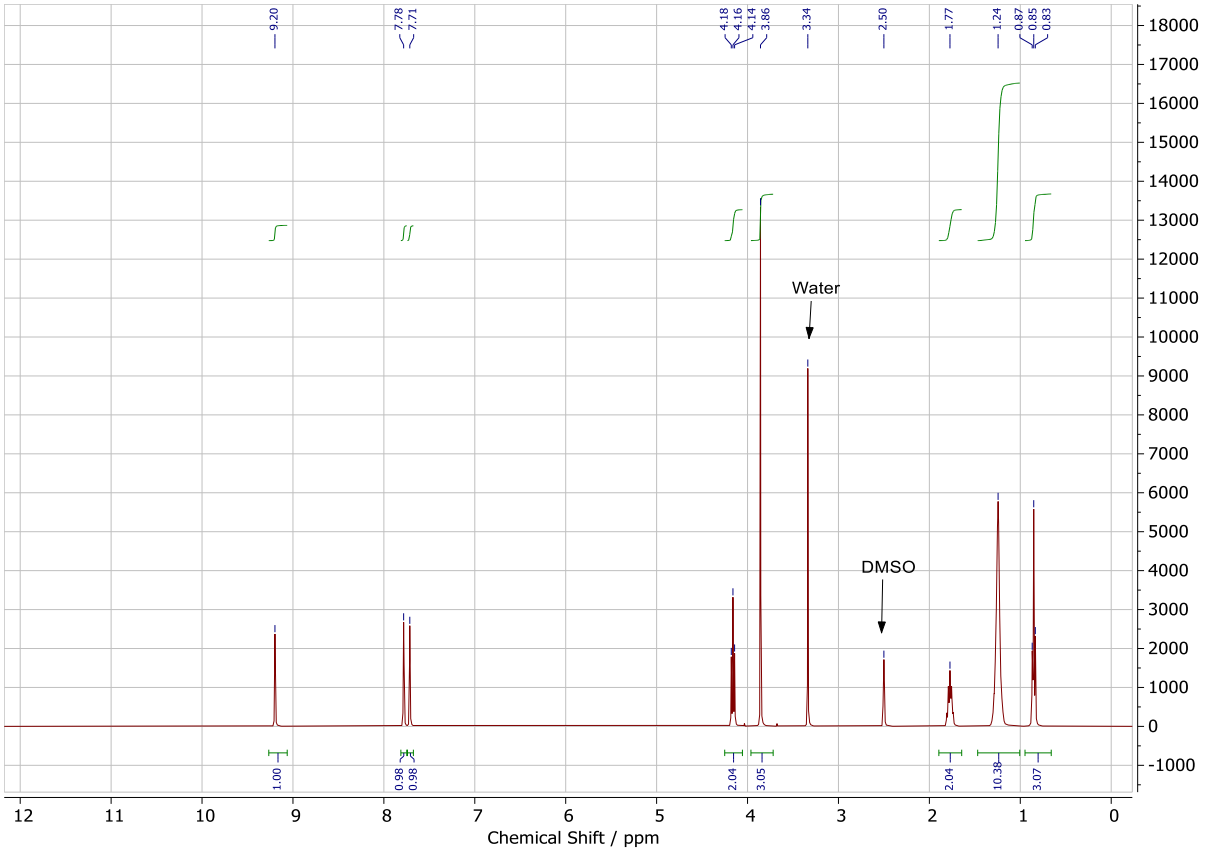

Figure S5 ^{1}H NMR of $[C_8C_1Im]Cl_{0.33}ZnCl_2$ in DMSO-d_6.

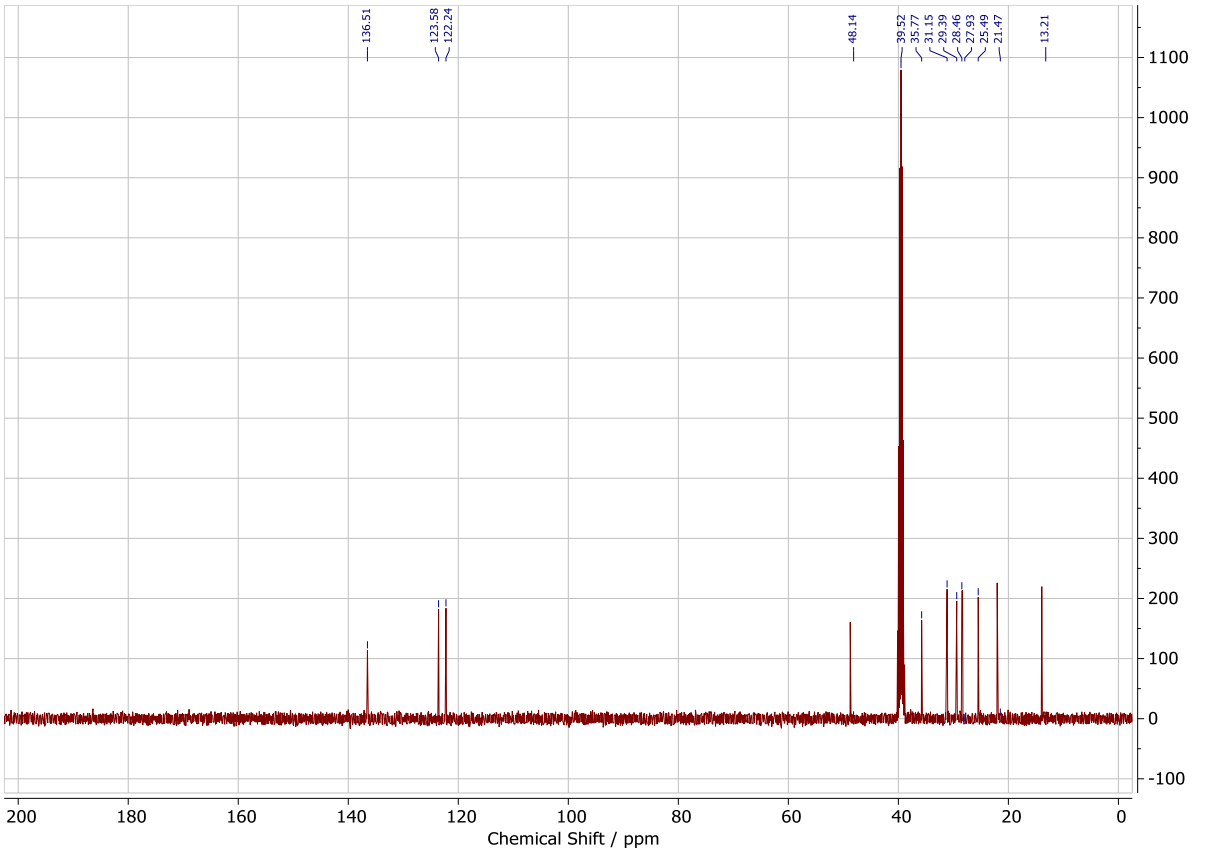

Figure S6 ^{13}C NMR of $[C_8C_1Im]Cl_{0.33}ZnCl_2$ in DMSO-d_6.

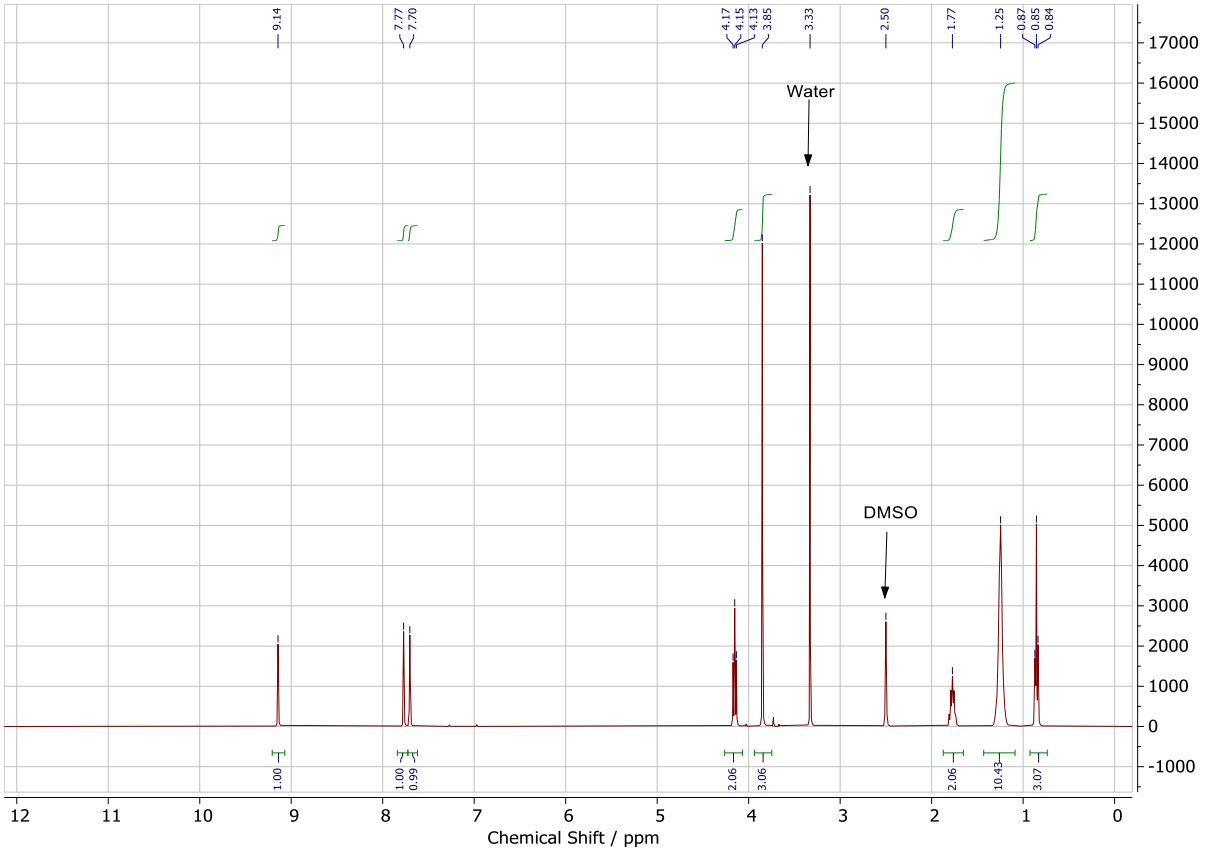

Figure S7 ^{1}H NMR of $[C_8C_1Im]Cl_{0.4}ZnCl_2$ in DMSO-d_6.

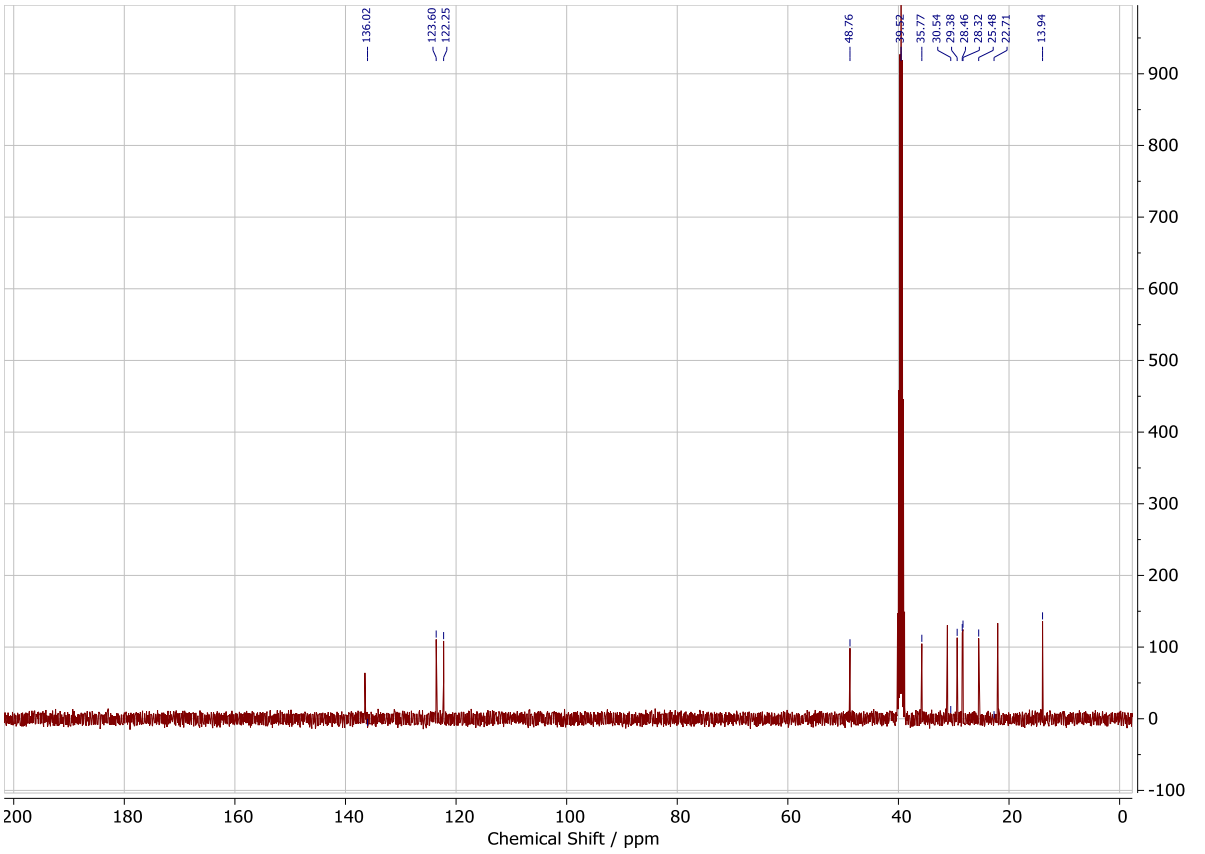

Figure S8 ^{13}C NMR of $[C_8C_1Im]Cl_{0.4}ZnCl_2$ in DMSO-d_6.

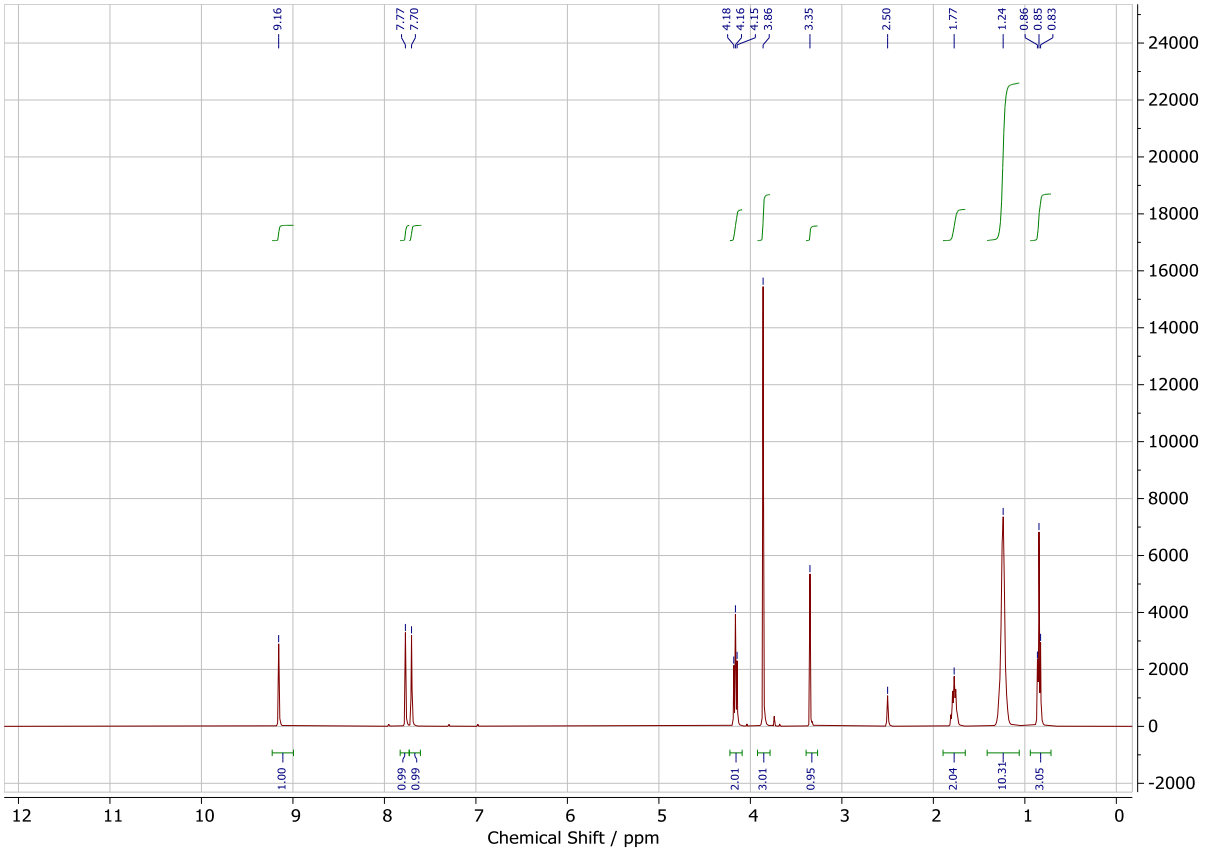

Figure S9 ^{1}H NMR of $[C_8C_1Im]Cl_{0.43}ZnCl_2$ in DMSO-*d*$_6$.

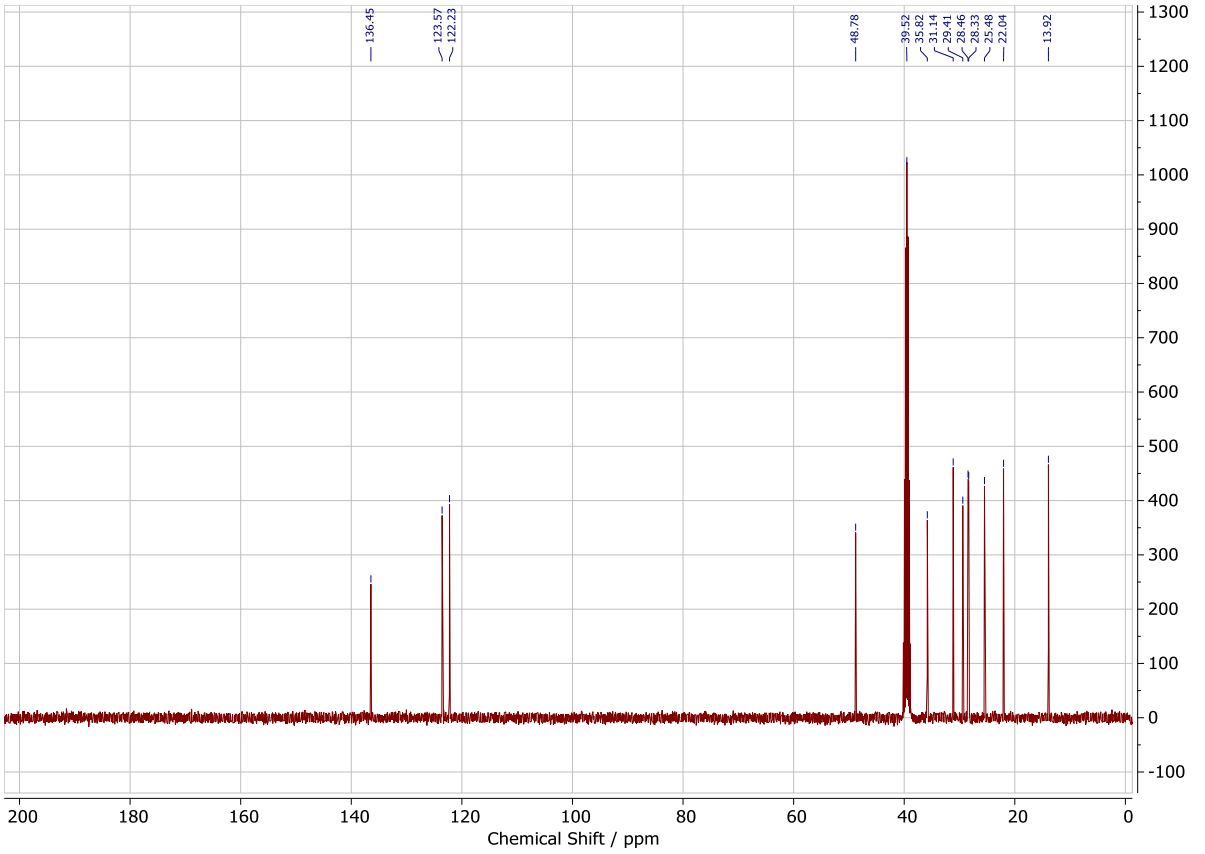

Figure S10 ^{13}C NMR of $[C_8C_1Im]Cl_{0.43}ZnCl_2$ in DMSO-*d*$_6$.

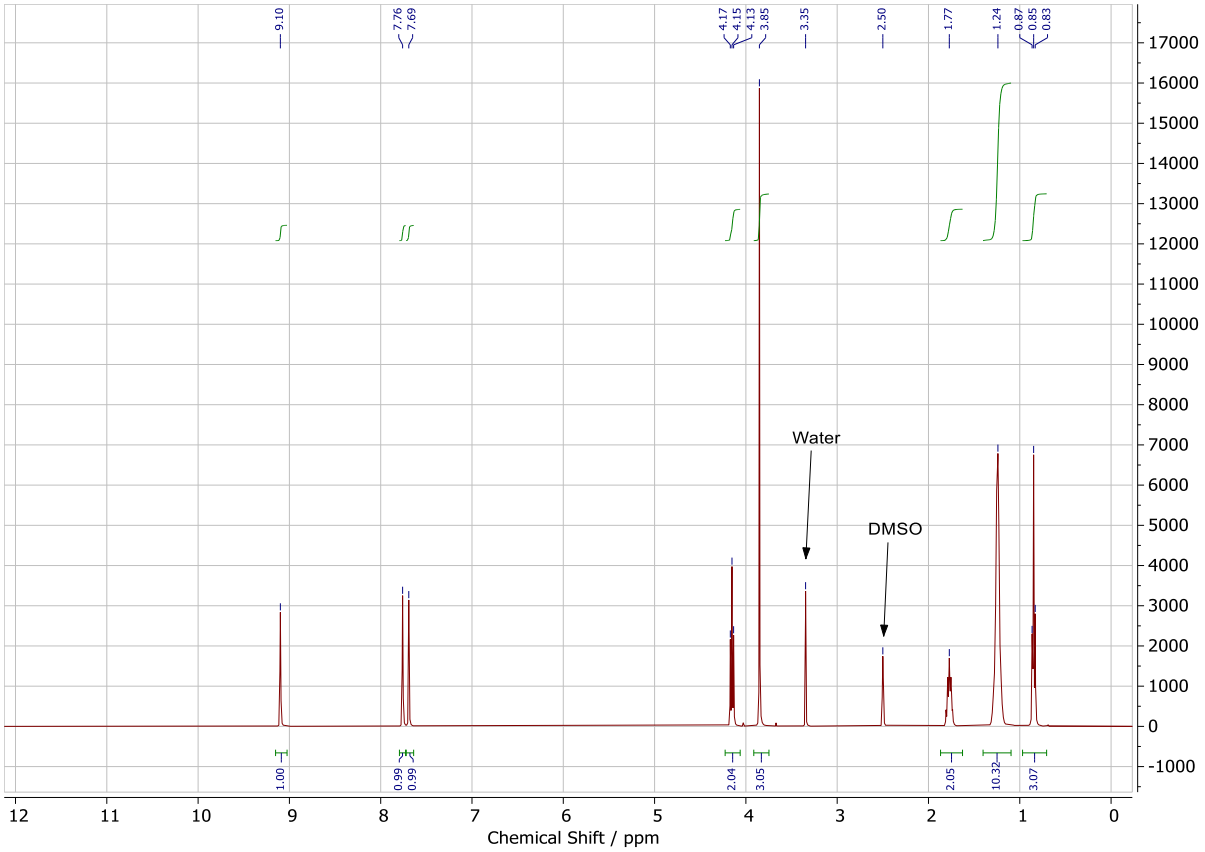

Figure S11 ^{1}H NMR of $[C_8C_1Im]Cl_{0.5}ZnCl_2$ in DMSO-d_6.

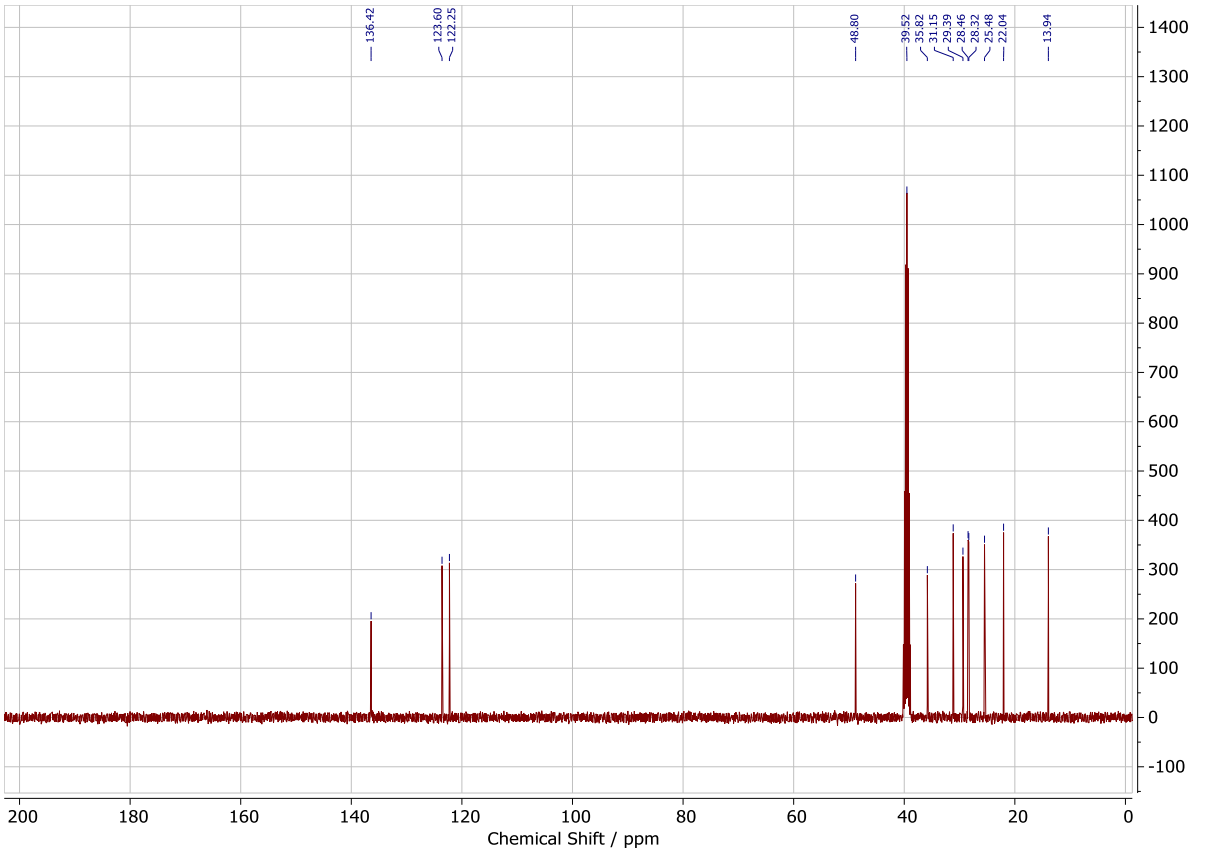

Figure S12 ^{13}C NMR of $[C_8C_1Im]Cl_{0.5}ZnCl_2$ in DMSO-d_6.

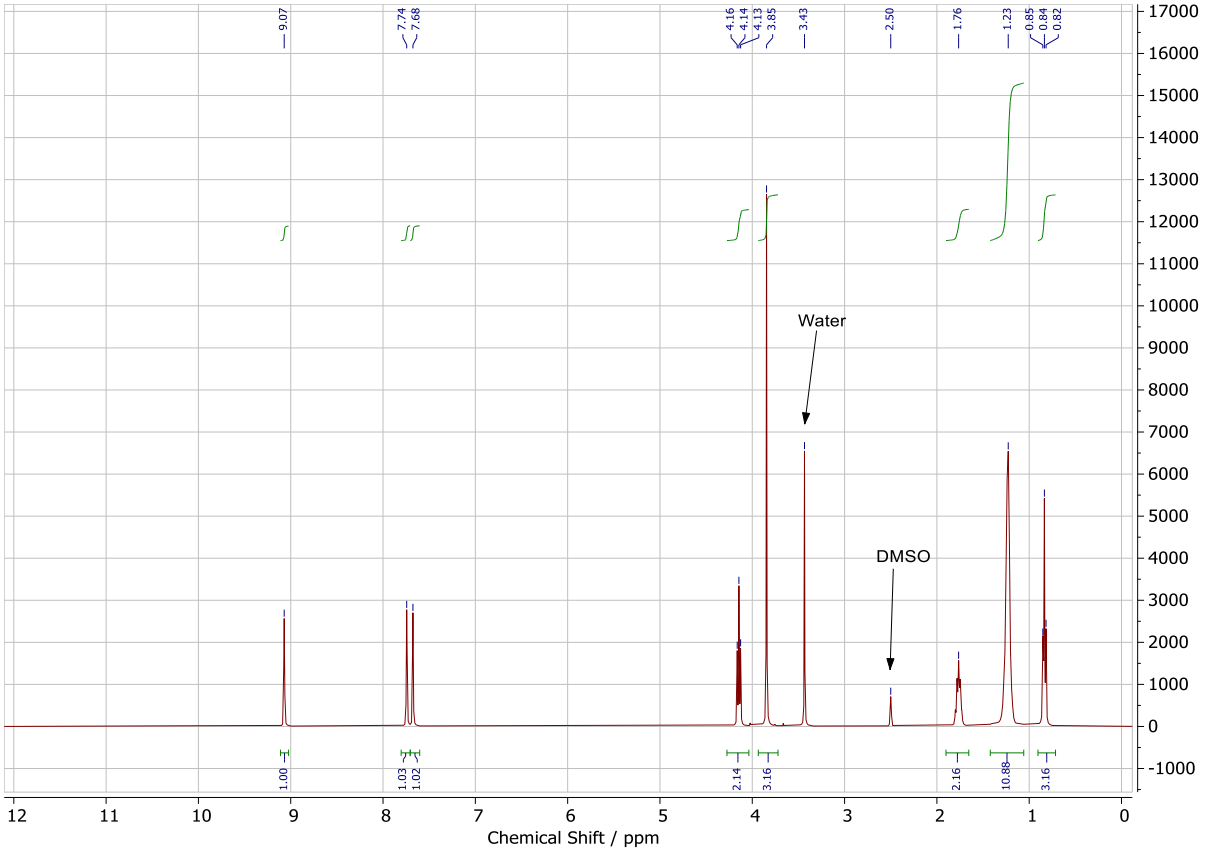

Figure S13 ^{1}H NMR of $[C_8C_1Im]Cl_{0.6}ZnCl_2$ in DMSO-d_6.

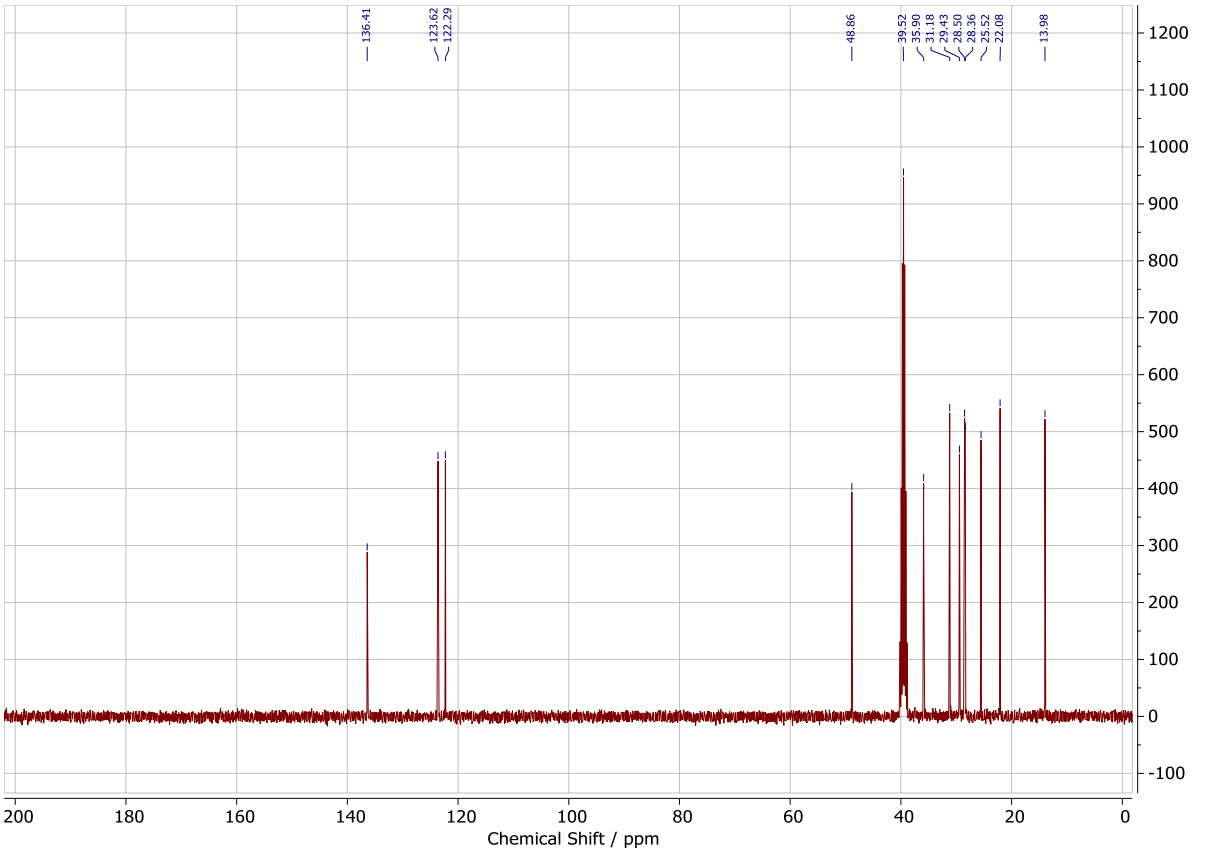

Figure S14 ^{13}C NMR of $[C_8C_1Im]Cl_{0.6}ZnCl_2$ in DMSO-d_6.

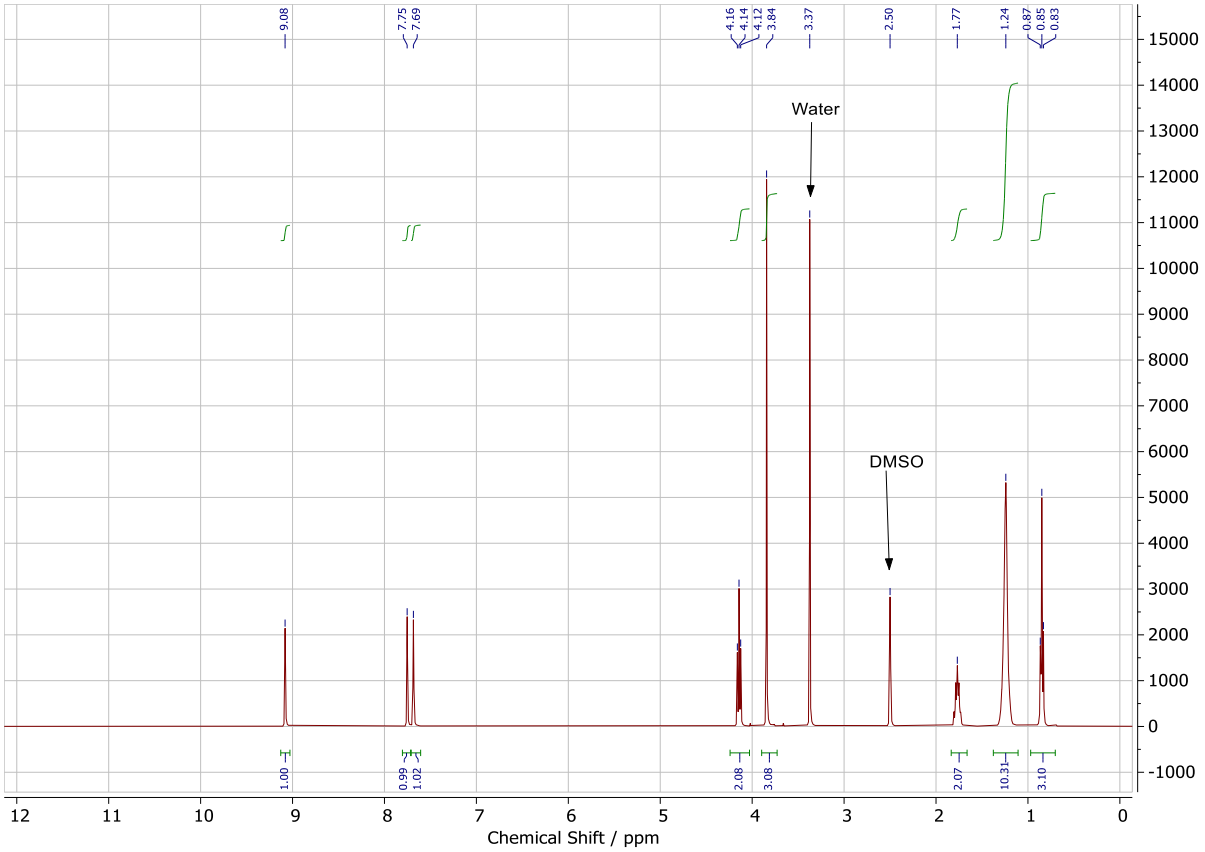

Figure S15 ^{1}H NMR of $[C_8C_1Im]Cl_{0.67}ZnCl_2$ in DMSO-d_6.

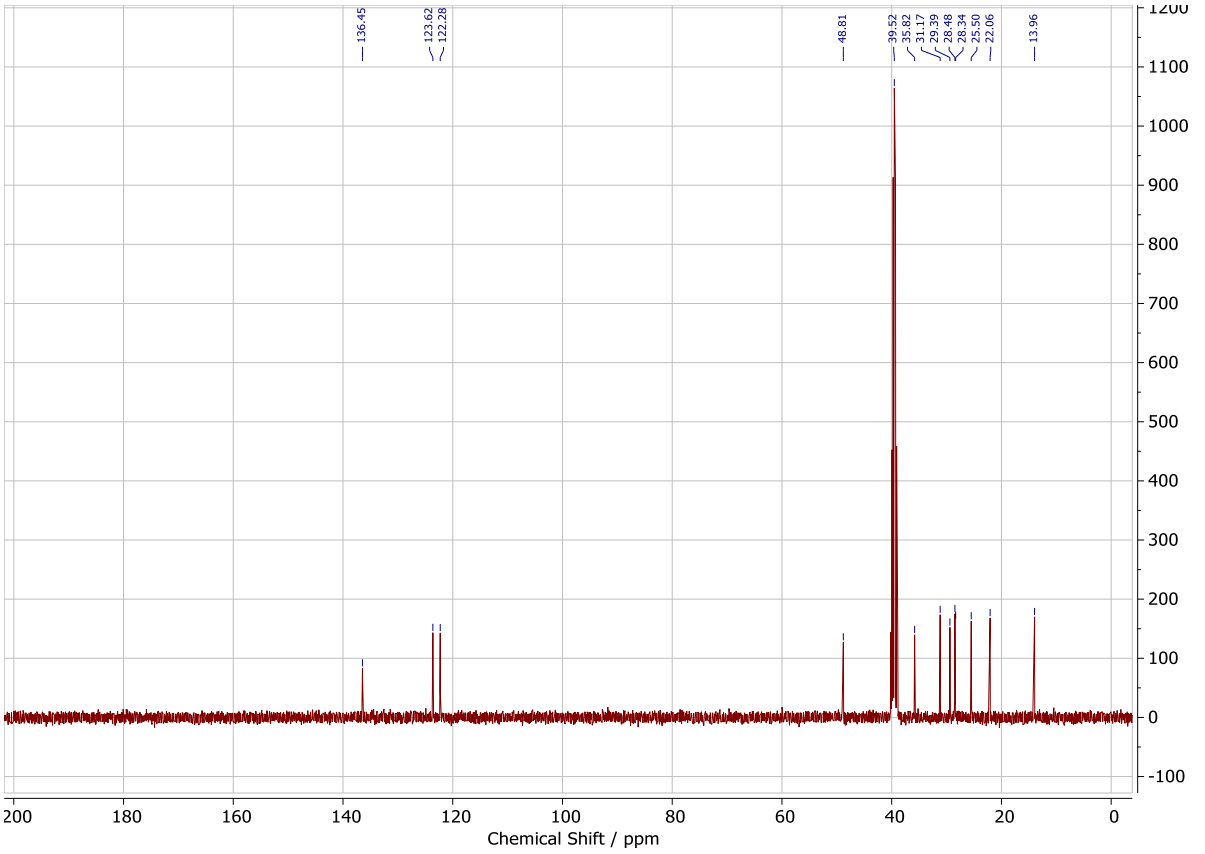

Figure S16 ^{13}C NMR of $[C_8C_1Im]Cl_{0.67}ZnCl_2$ in DMSO-d_6.

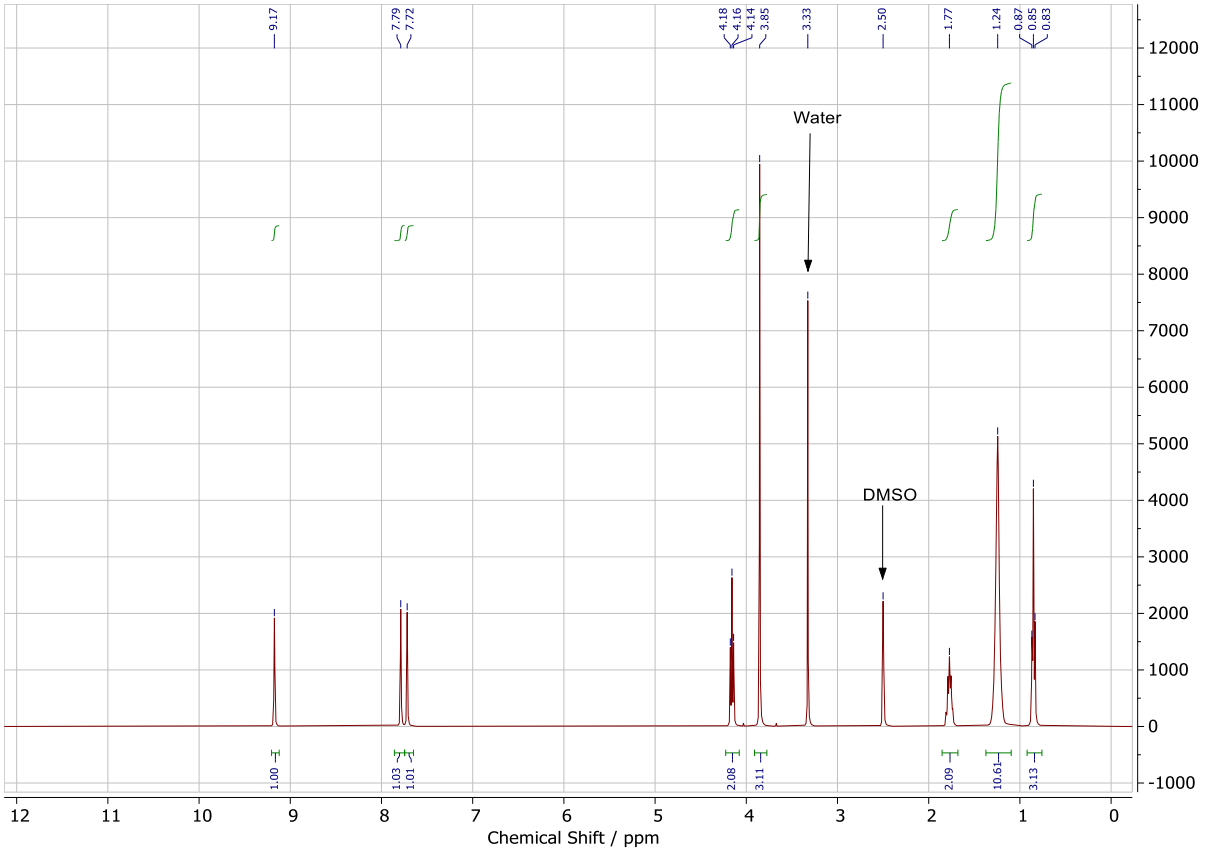

Figure S17 ^{1}H NMR of $[C_8C_1Im]Br_{0.1}ZnBr_2$ in DMSO-d_6.

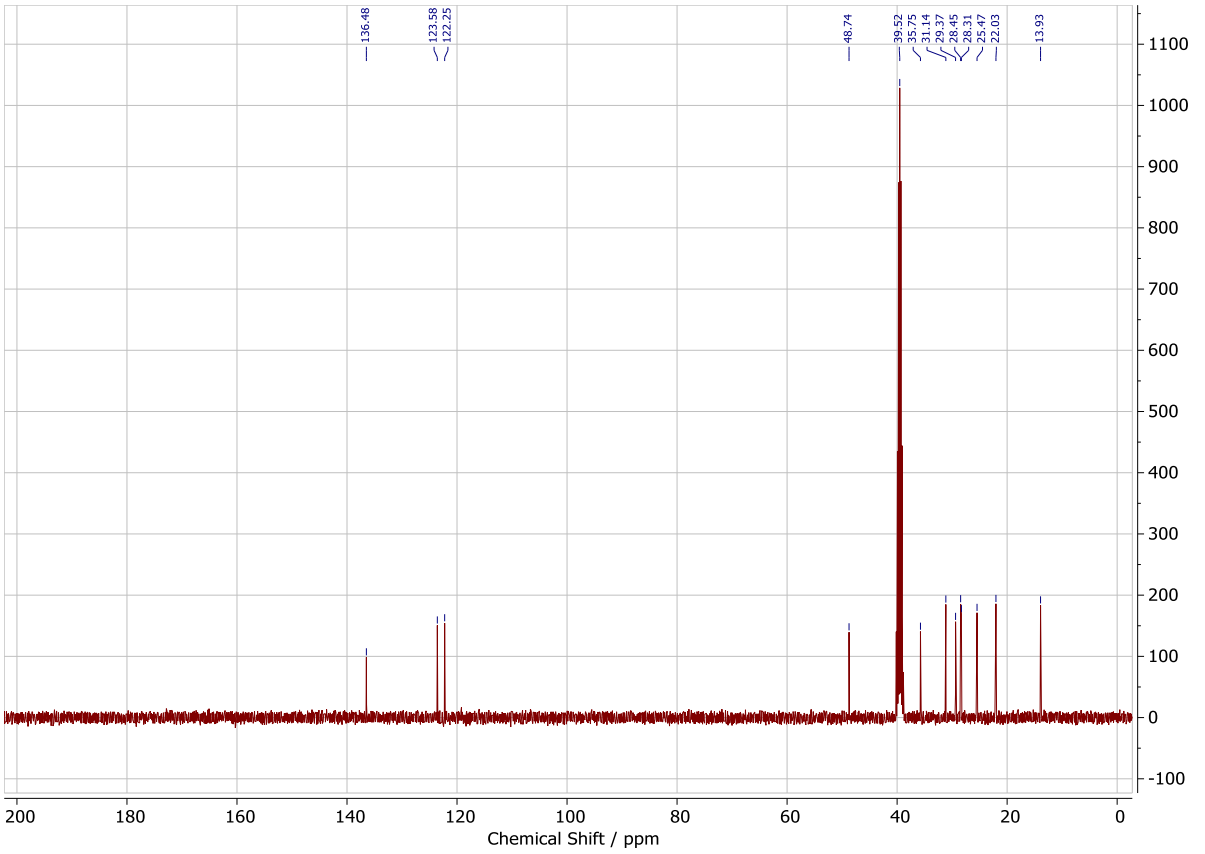

Figure S18 ^{13}C NMR of $[C_8C_1Im]Br_{0.1}ZnBr_2$ in DMSO-d_6.

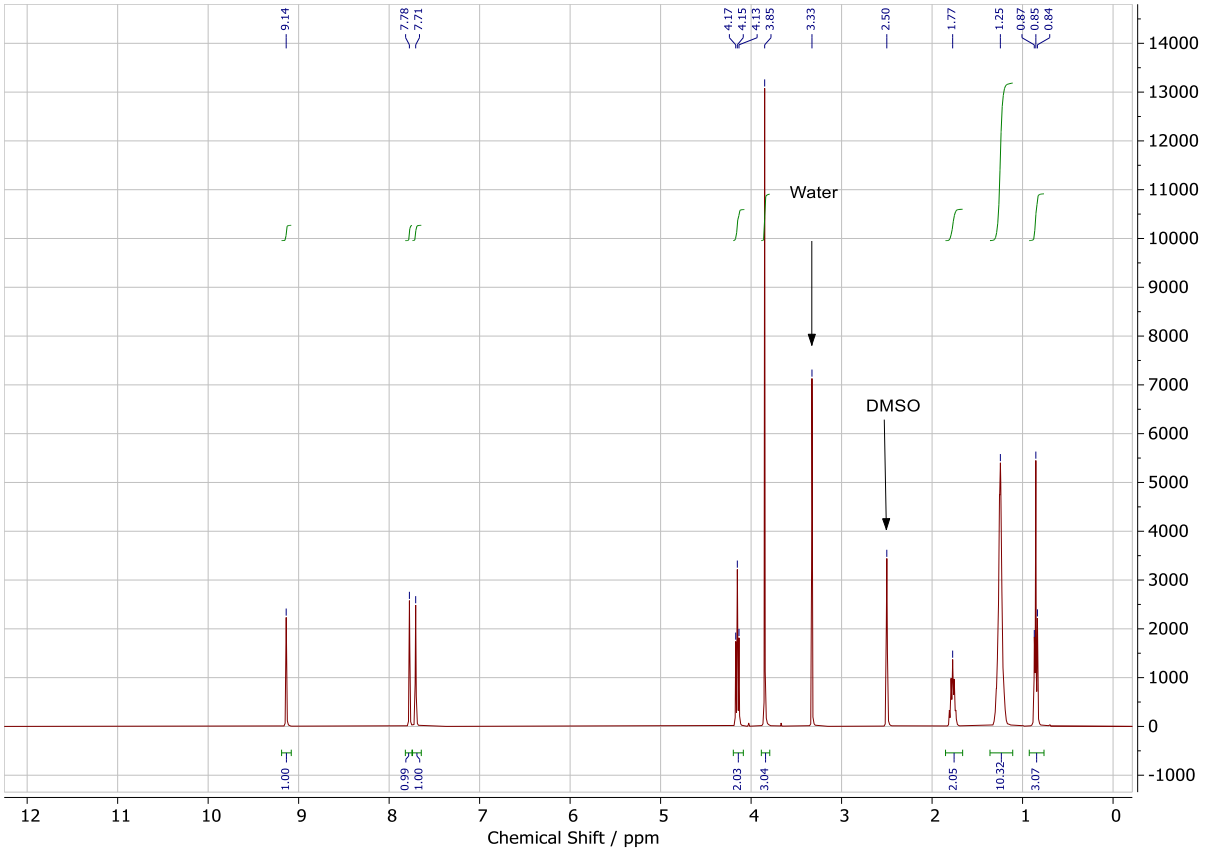

Figure S19 ^{1}H NMR of $[C_8C_1Im]Br_{0.33}ZnBr_2$ in DMSO-d_6.

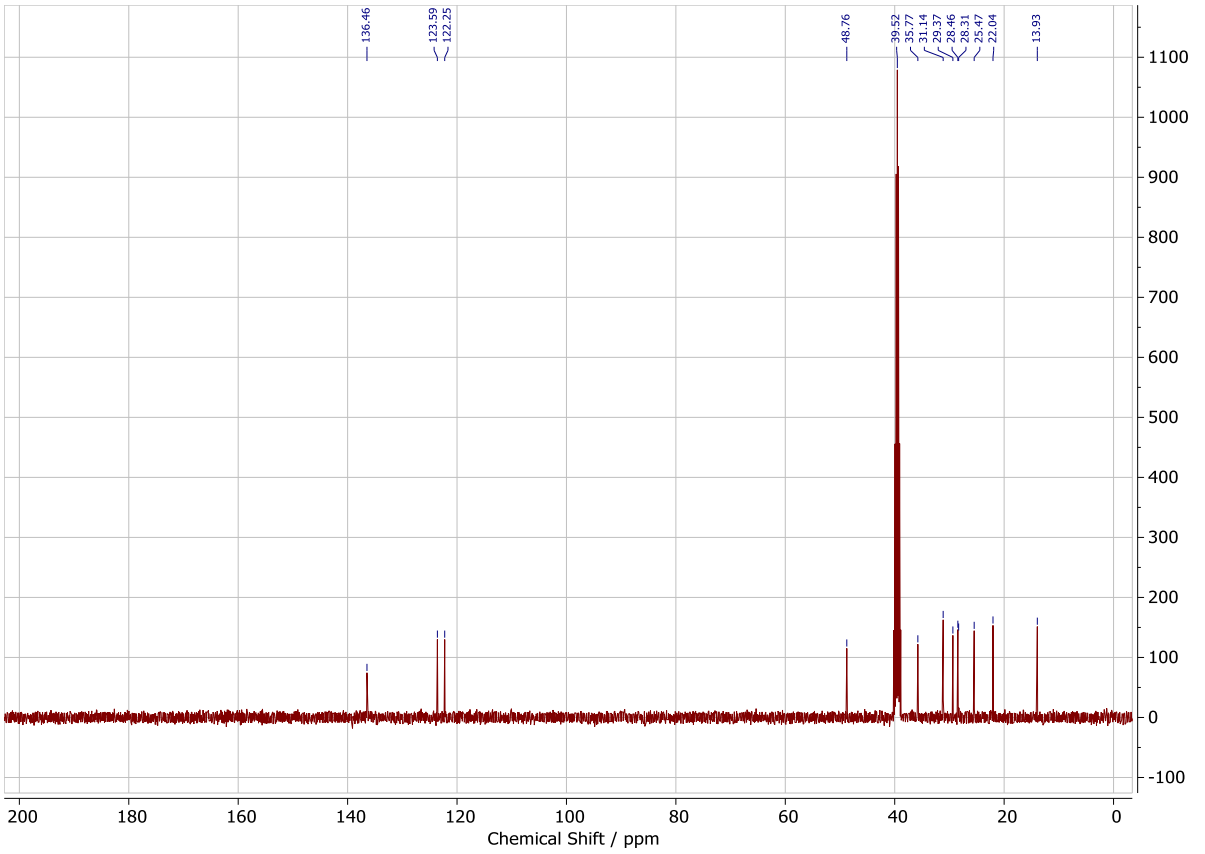

Figure S20 ^{13}C NMR of $[C_8C_1Im]Br_{0.33}ZnBr_2$ in DMSO-d_6.

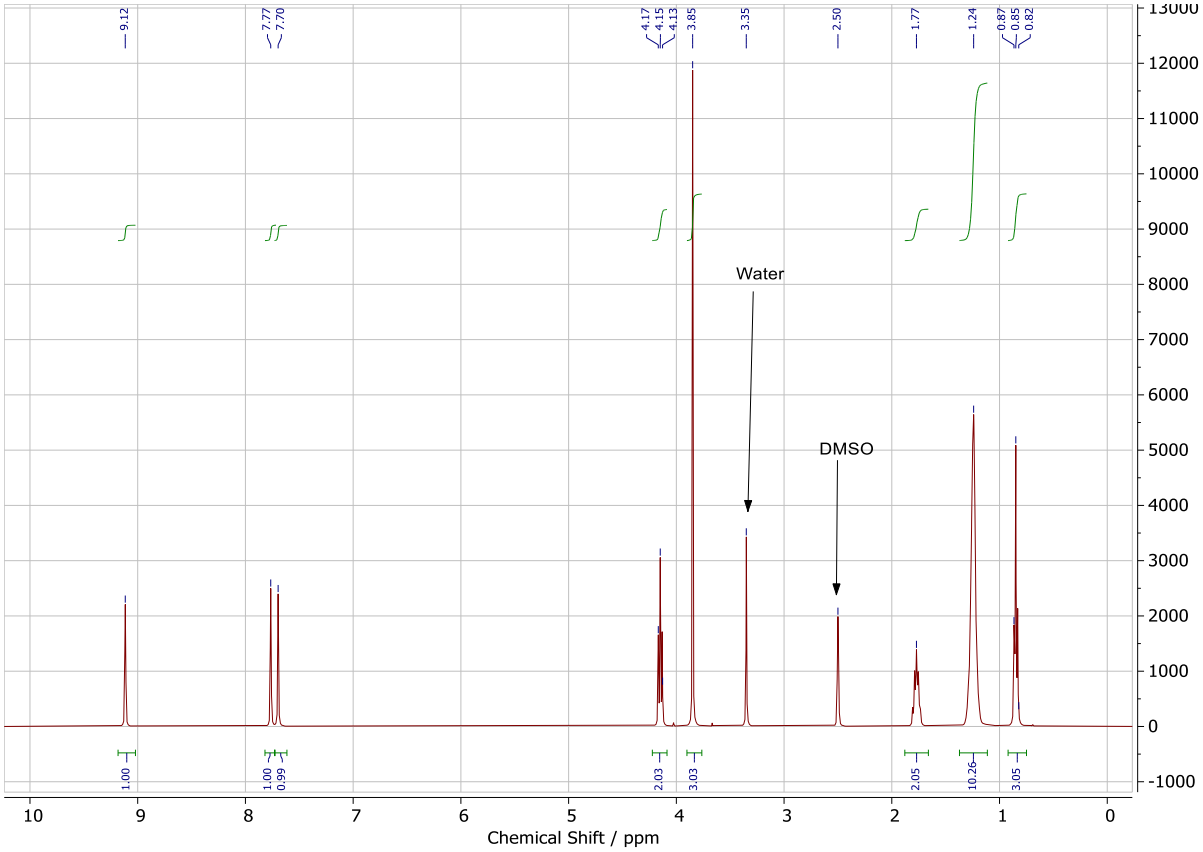

Figure S21 ^{1}H NMR of $[C_8C_1Im]Br_{0.5}ZnBr_2$ in DMSO-d_6.

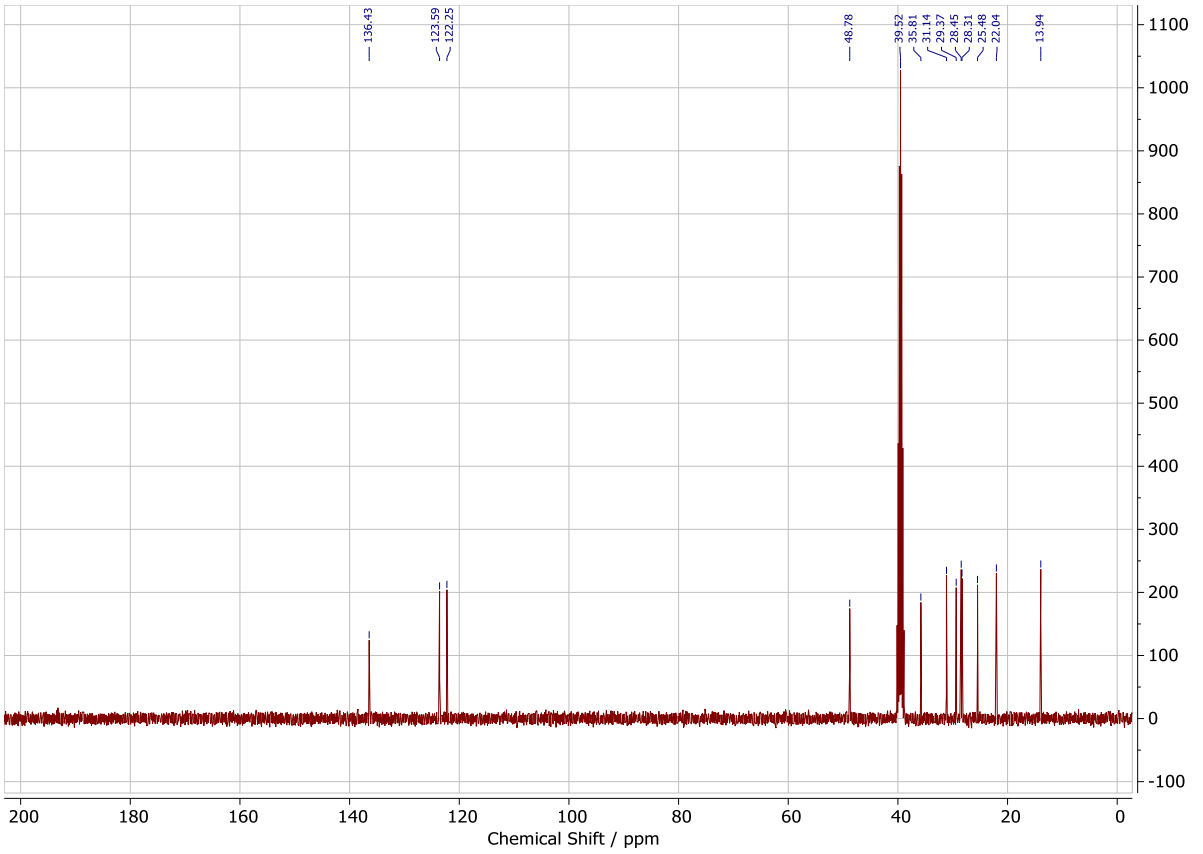

Figure S22 ^{13}C NMR of $[C_8C_1Im]Br_{0.5}ZnBr_2$ in DMSO-d_6.

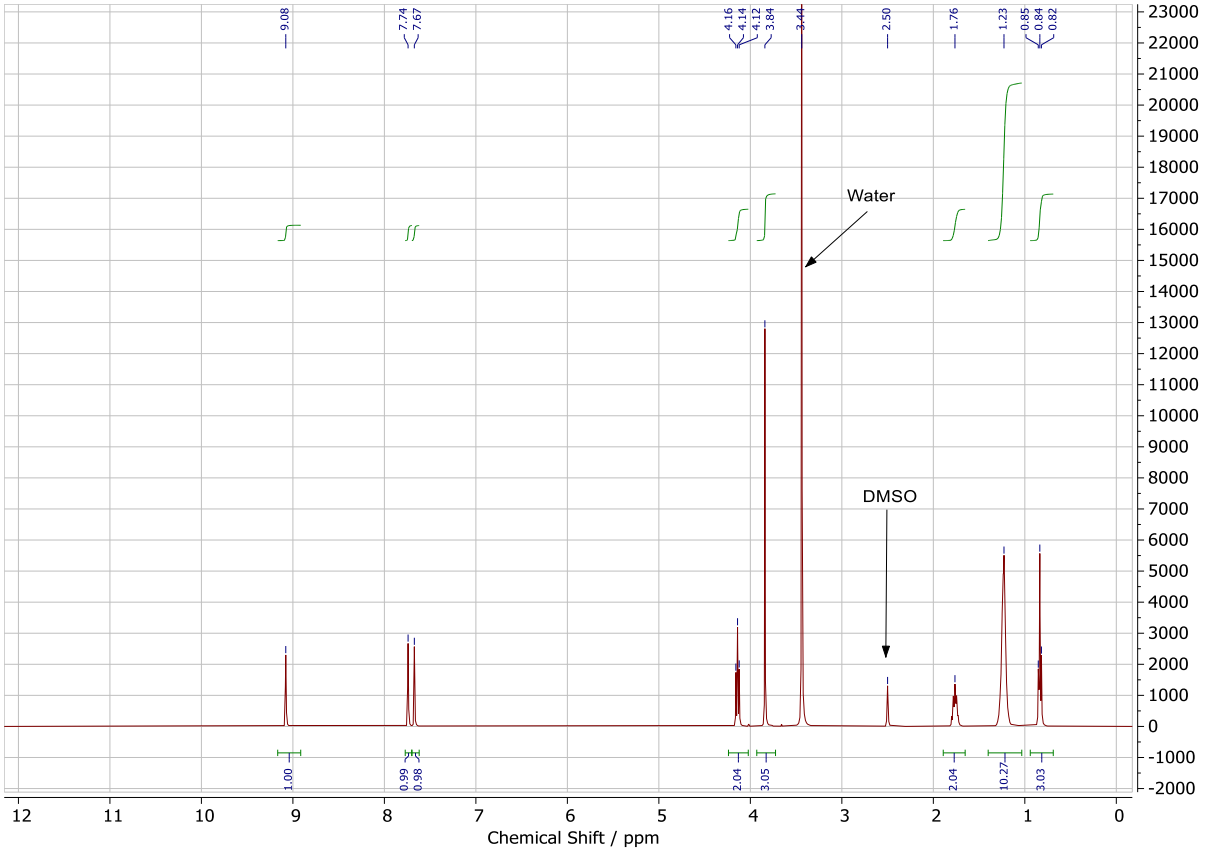

Figure S23 ^{1}H NMR of $[C_8C_1Im]Br_{0.6}ZnBr_2$ in DMSO-d_6.

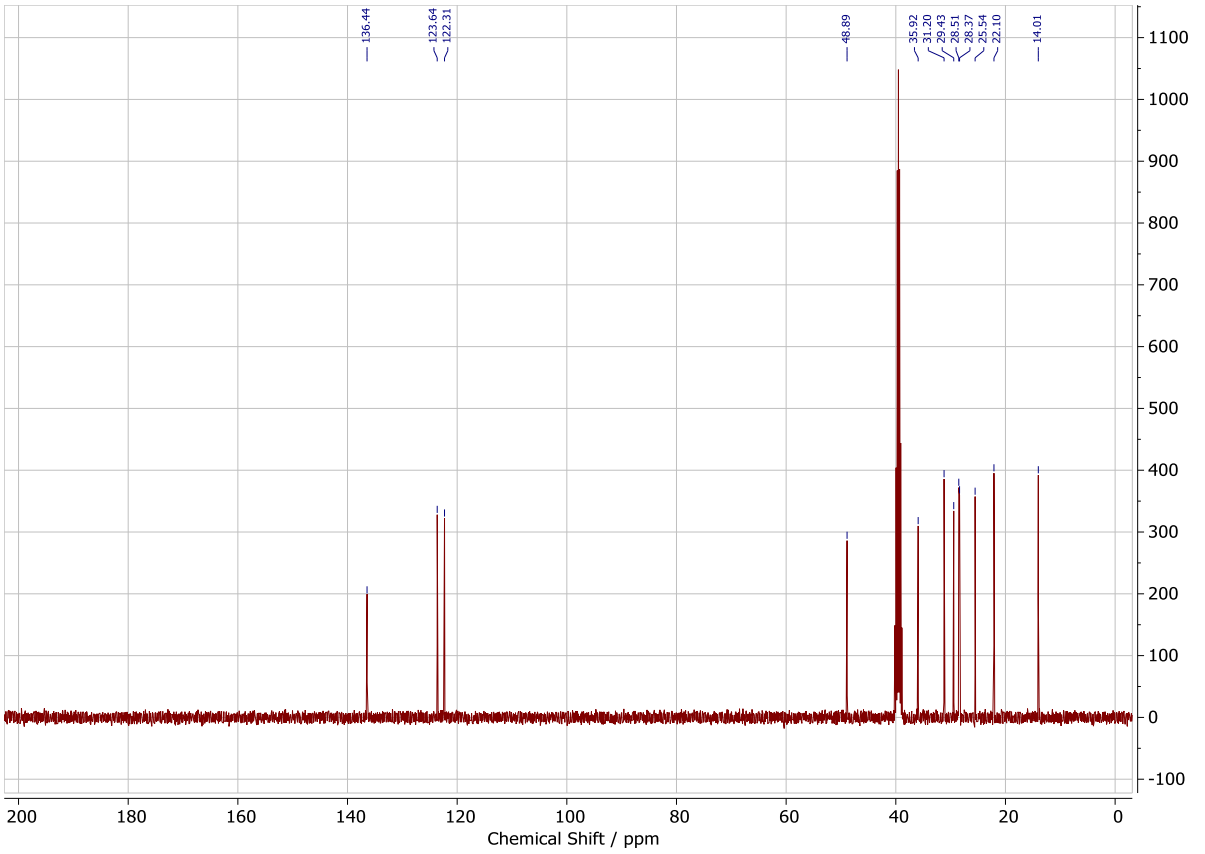

Figure S24 ^{13}C NMR of $[C_8C_1Im]Br_{0.6}ZnBr_2$ in DMSO-d_6.

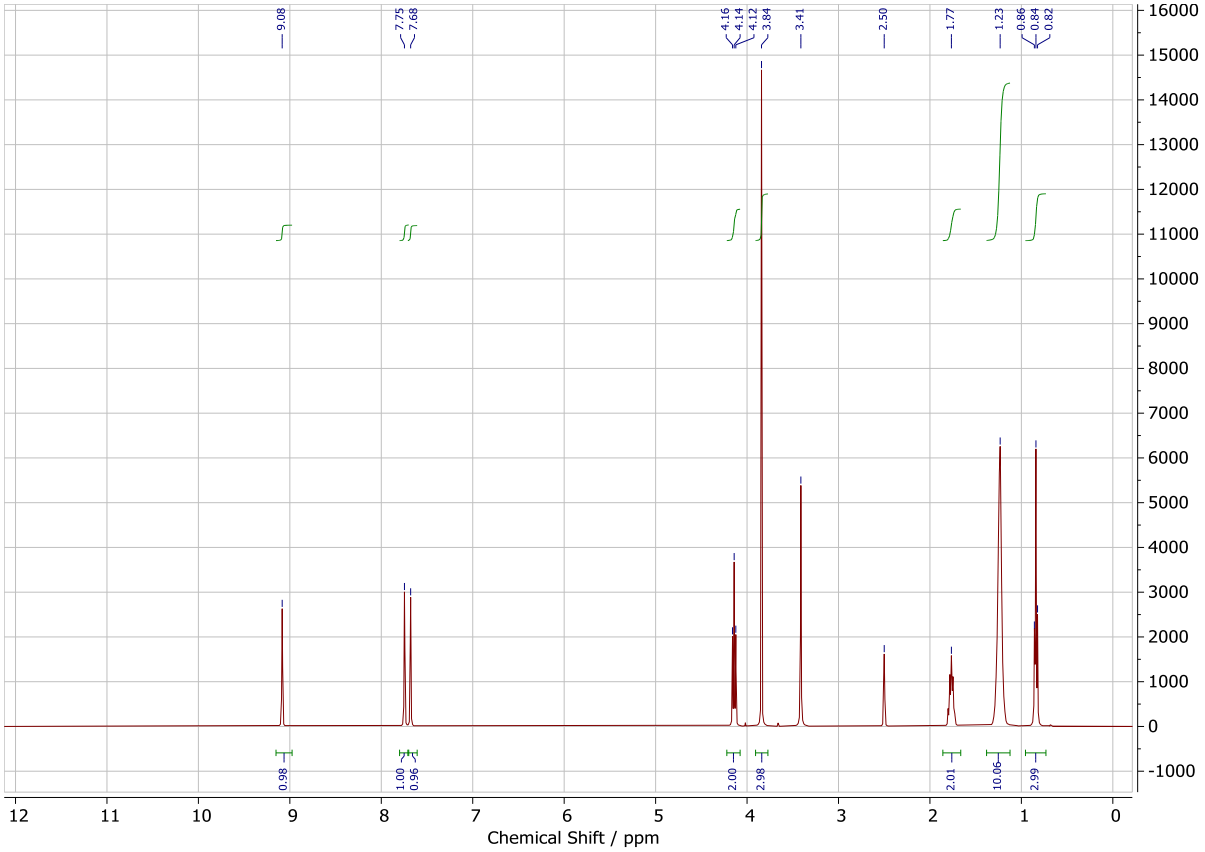

Figure S25 ^{1}H NMR of $[C_8C_1Im]Br_{0.67}ZnBr_2$ in DMSO-d_6.

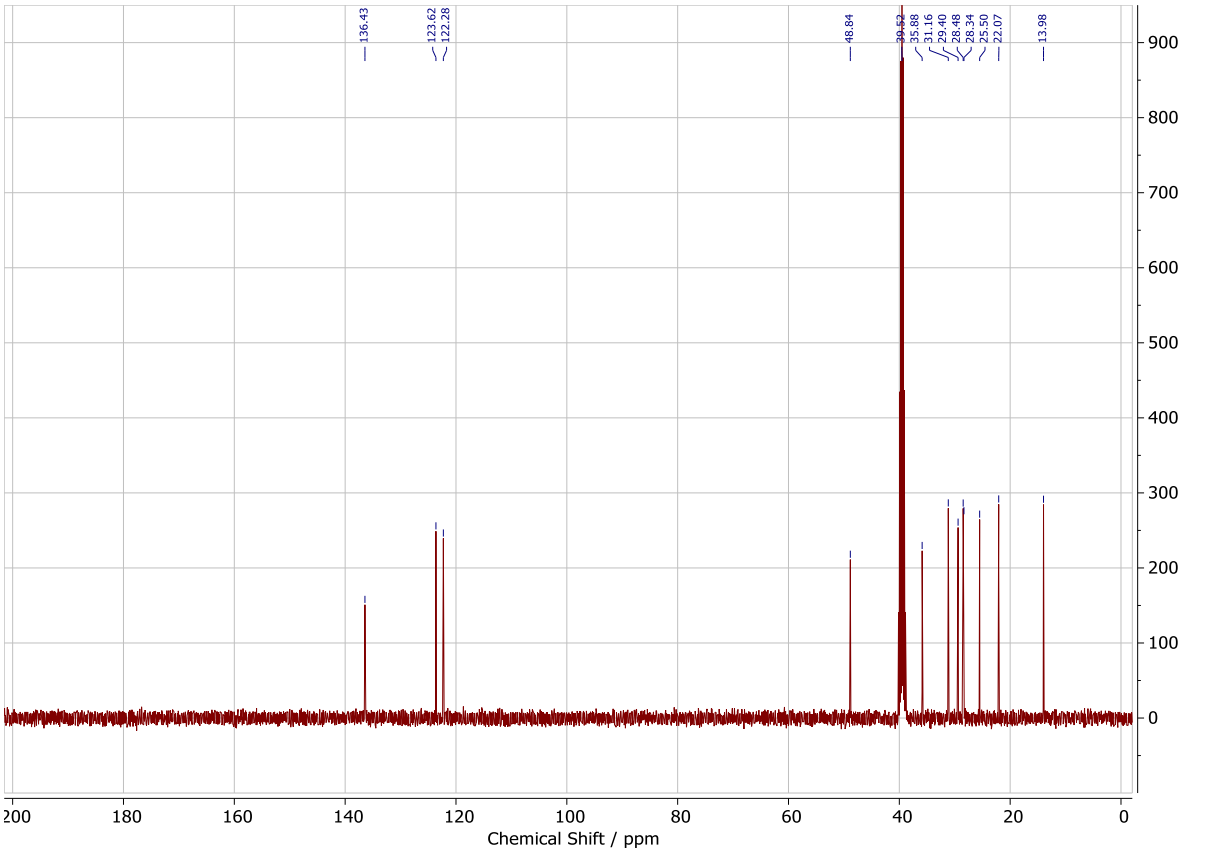

Figure S26 ^{13}C NMR of $[C_8C_1Im]Br_{0.67}ZnBr_2$ in DMSO-d_6.

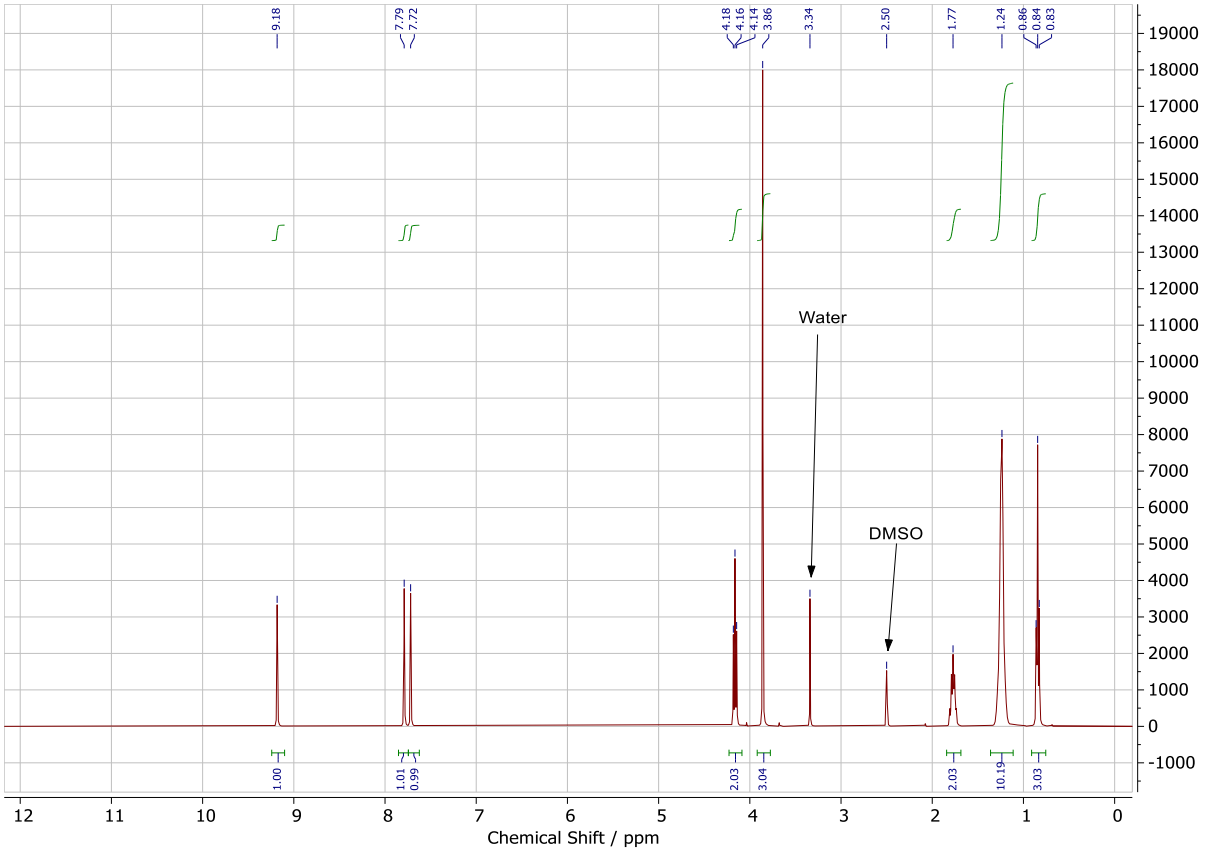

Figure S27 ^{1}H NMR of $[C_8C_1Im]Br_{0.33}ZnCl_2$ in DMSO-d_6.

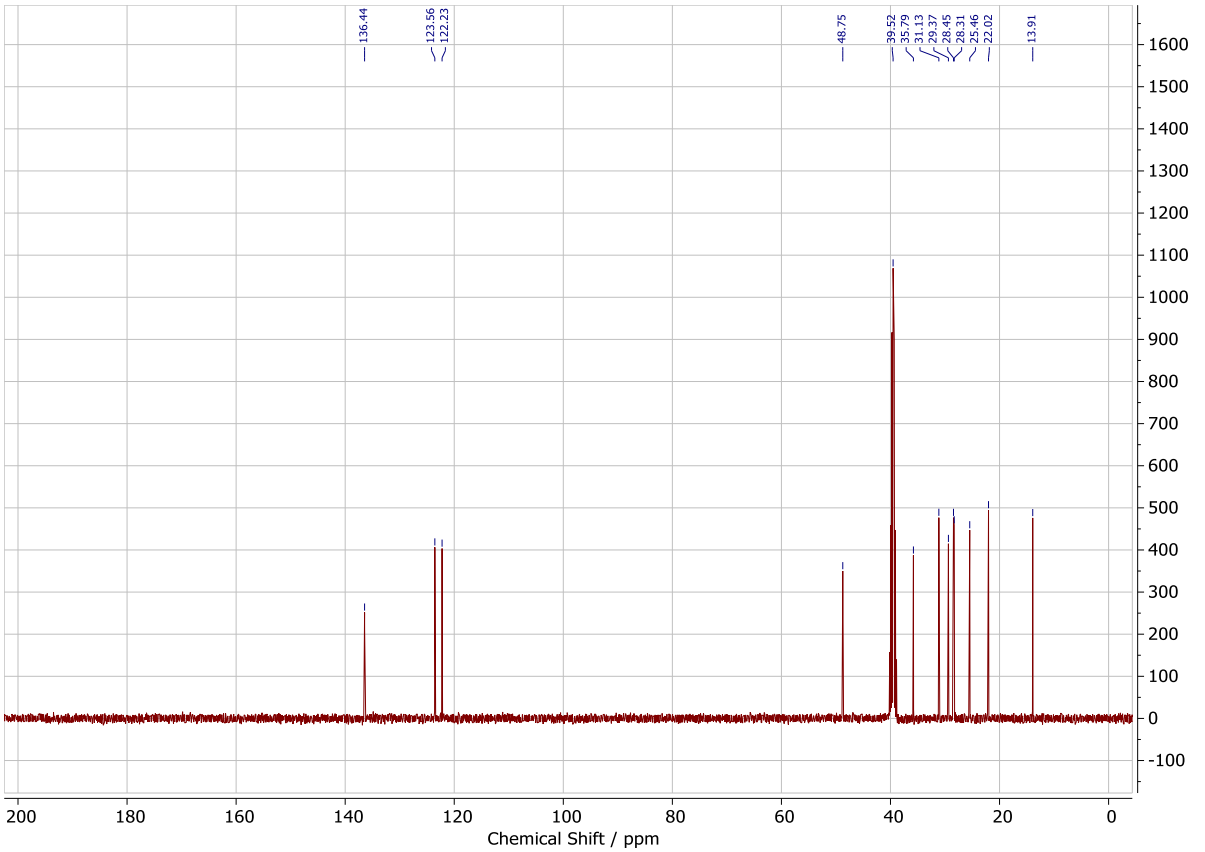

Figure S28 ^{13}C NMR of $[C_8C_1Im]Br_{0.33}ZnCl_2$ in DMSO-d_6.

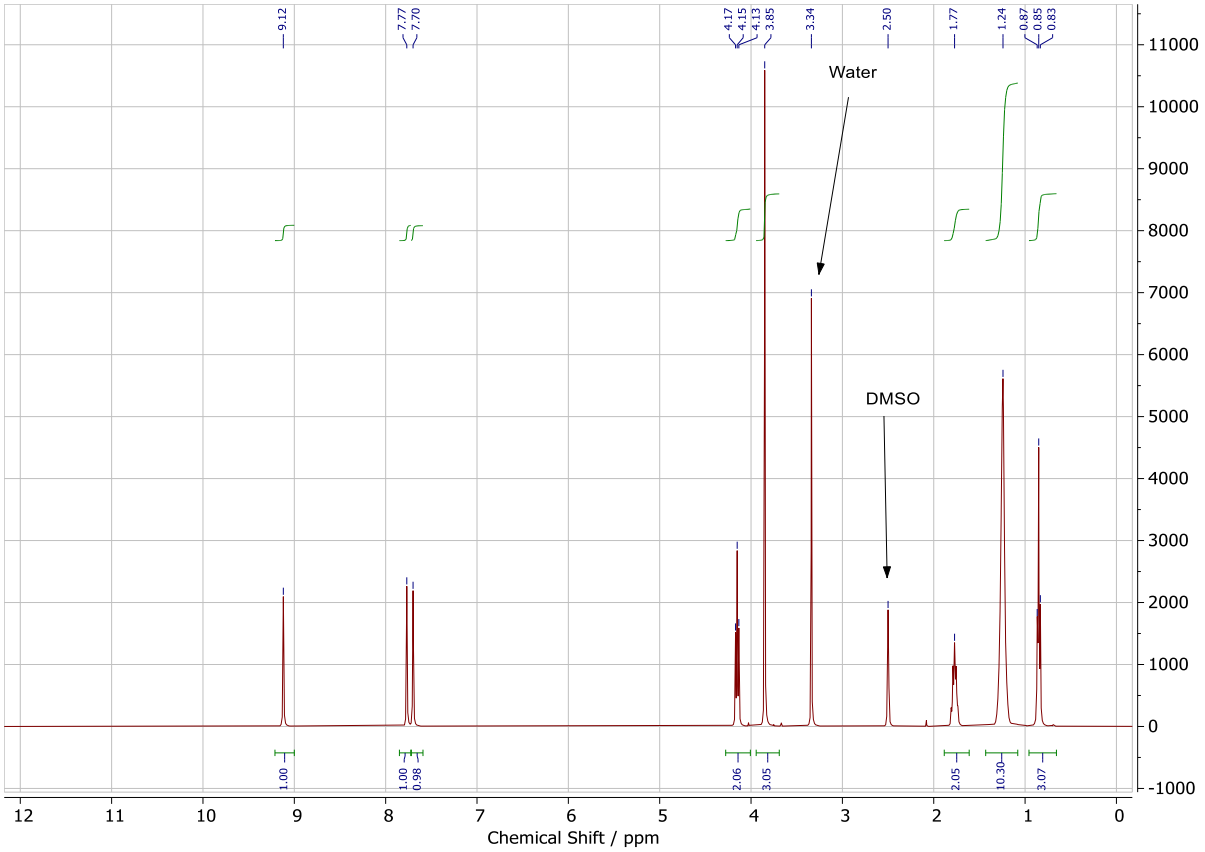

Figure S29 ^{1}H NMR of $[C_8C_1Im]Br_{0.5}ZnCl_2$ in DMSO-d_6.

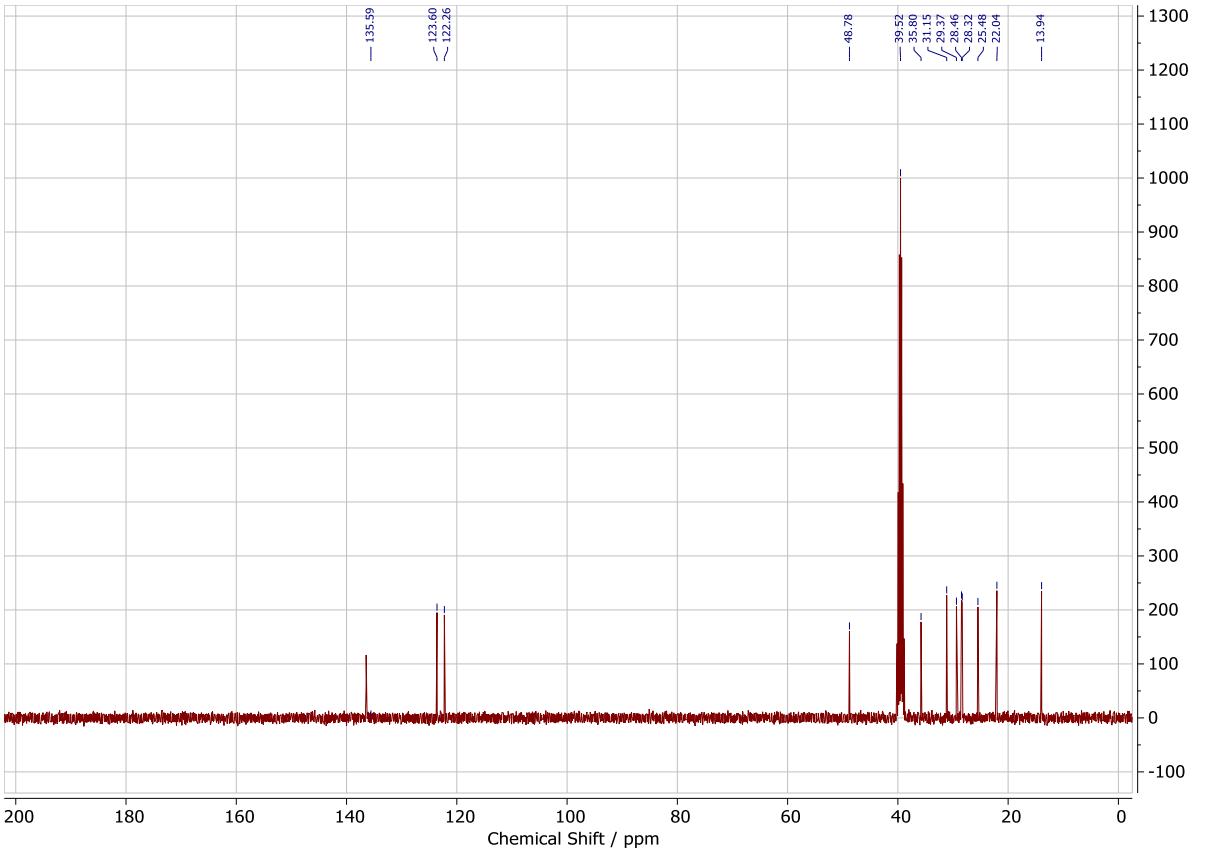

Figure S30 ^{13}C NMR of $[C_8C_1Im]Br_{0.5}ZnCl_2$ in DMSO-d_6.

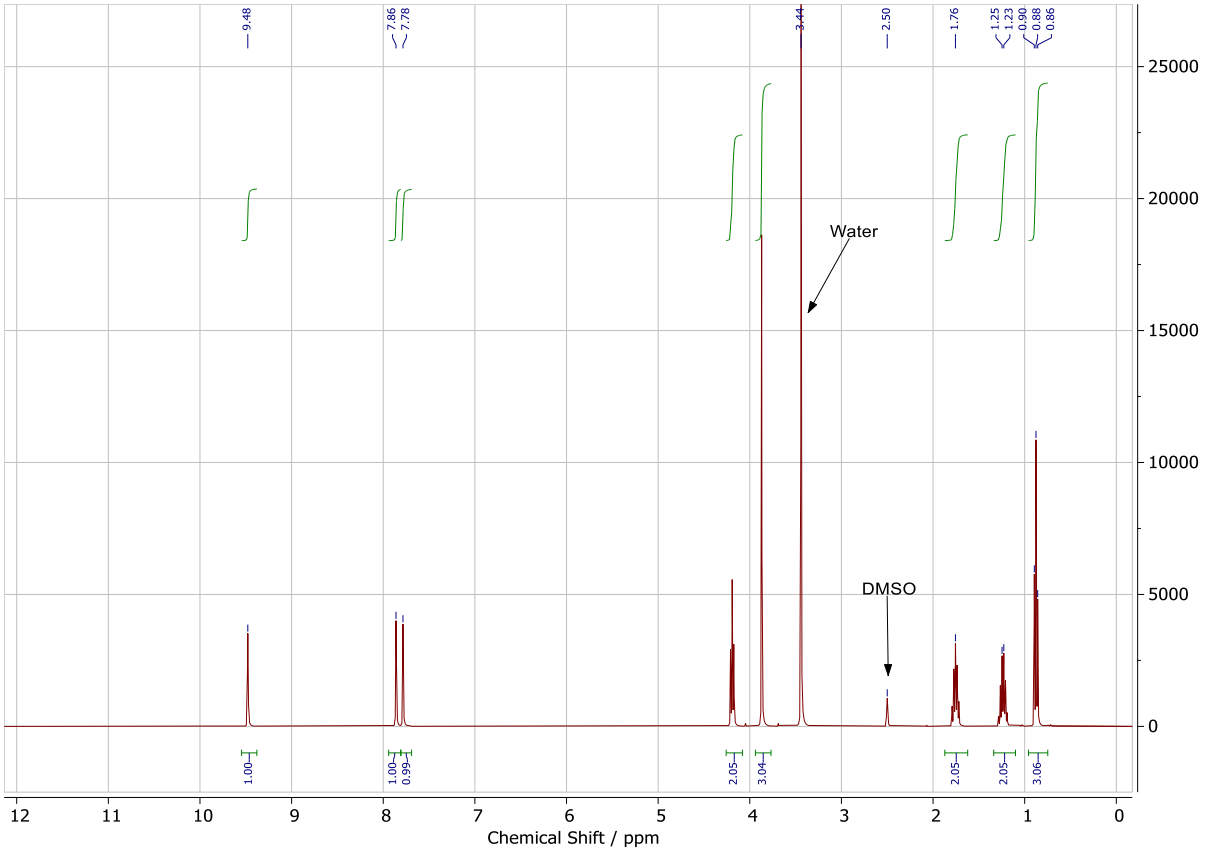

Figure S31 ^{1}H NMR of $[C_4C_1Im]Cl_{0.33}ZnCl_2$ in DMSO-d_6.

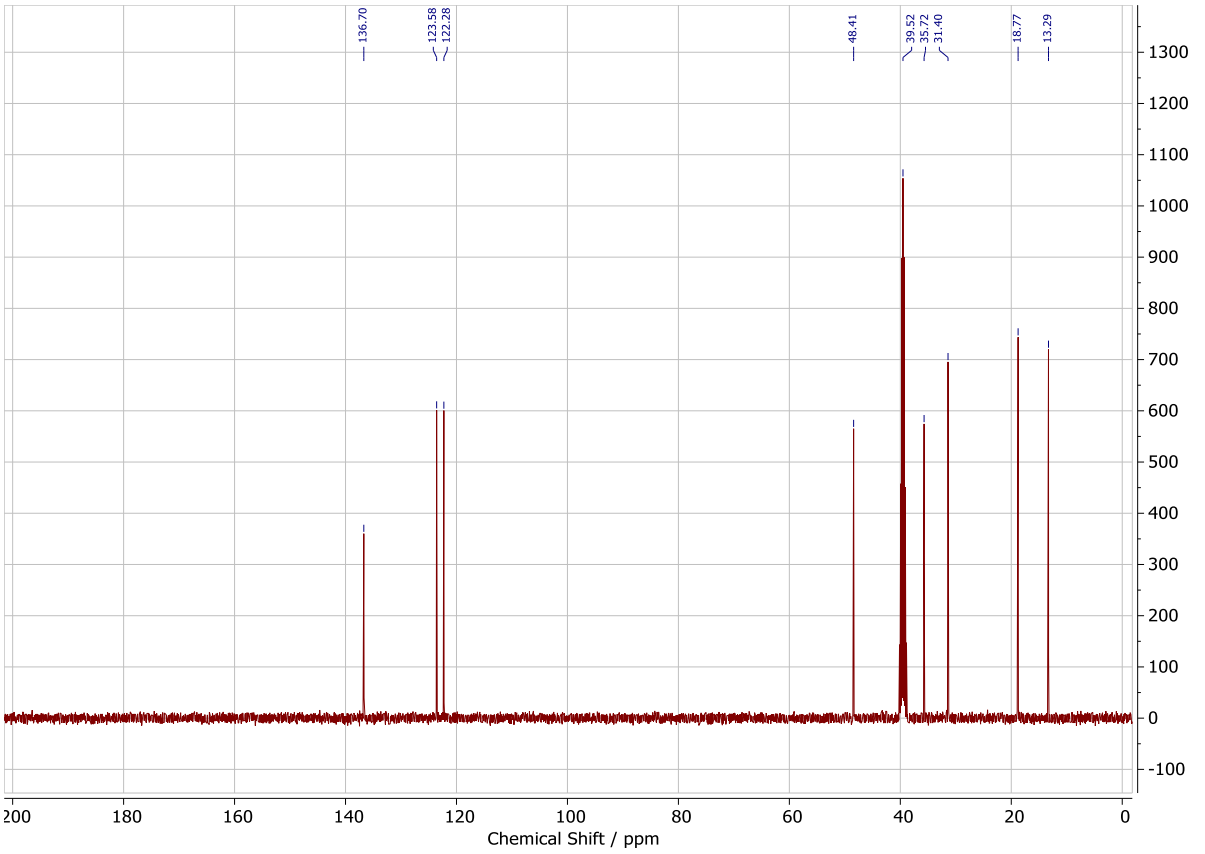

Figure S32 ^{13}C NMR of $[C_4C_1Im]Cl_{0.33}ZnCl_2$ in DMSO-d_6.

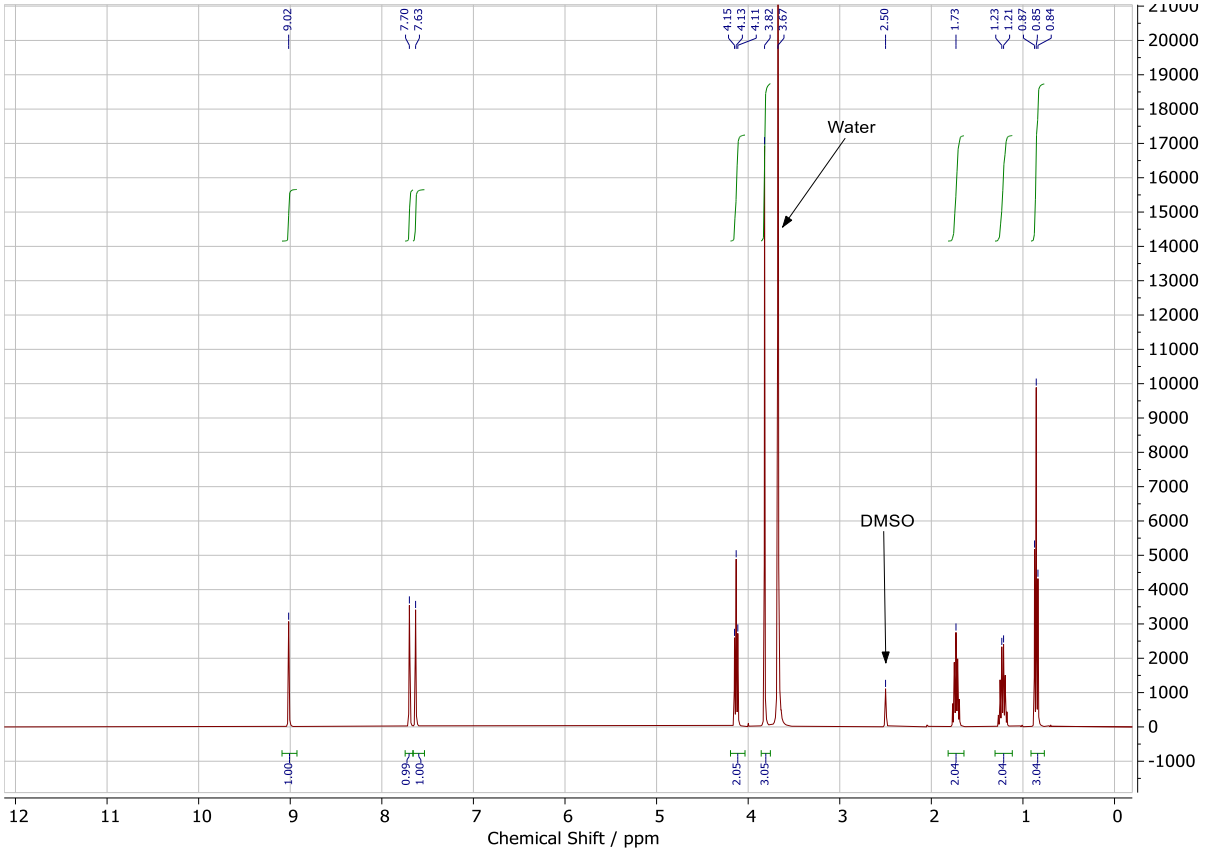

Figure S33 ^{1}H NMR of $[C_4C_1Im]Cl_{0.5}ZnCl_2$ in DMSO-d_6.

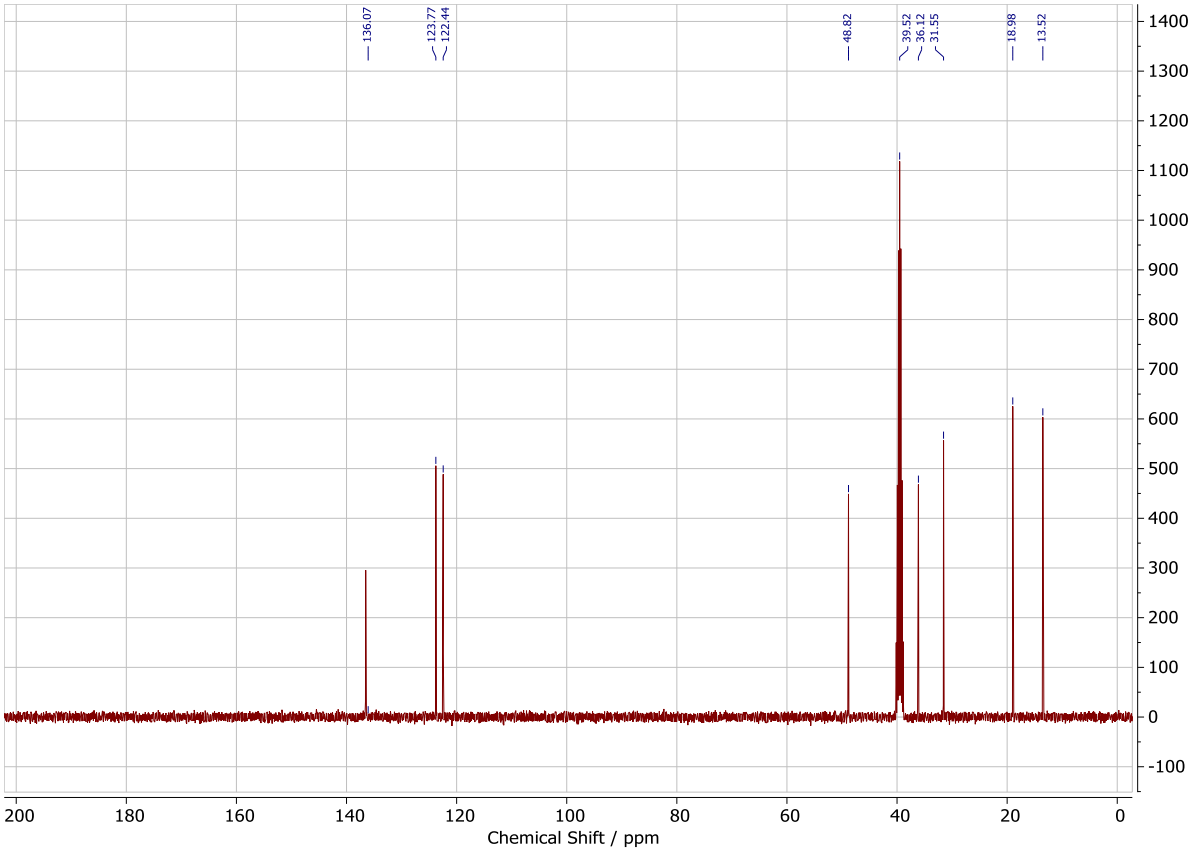

Figure S34 ^{13}C NMR of $[C_4C_1Im]Cl_{0.5}ZnCl_2$ in DMSO-d_6.

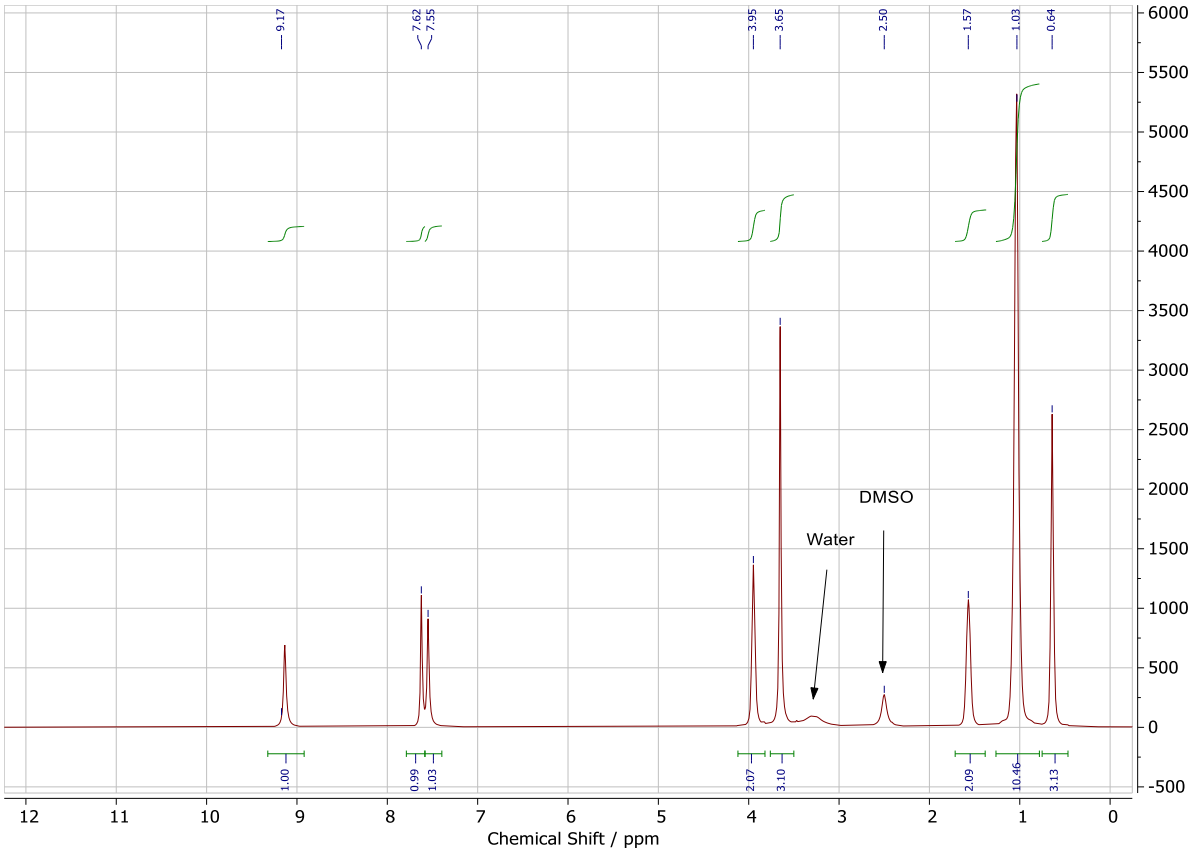

Figure S35 ^{1}H NMR of $[C_8C_1Im]Cl_{0.33}NiCl_2$ in DMSO-d_6.

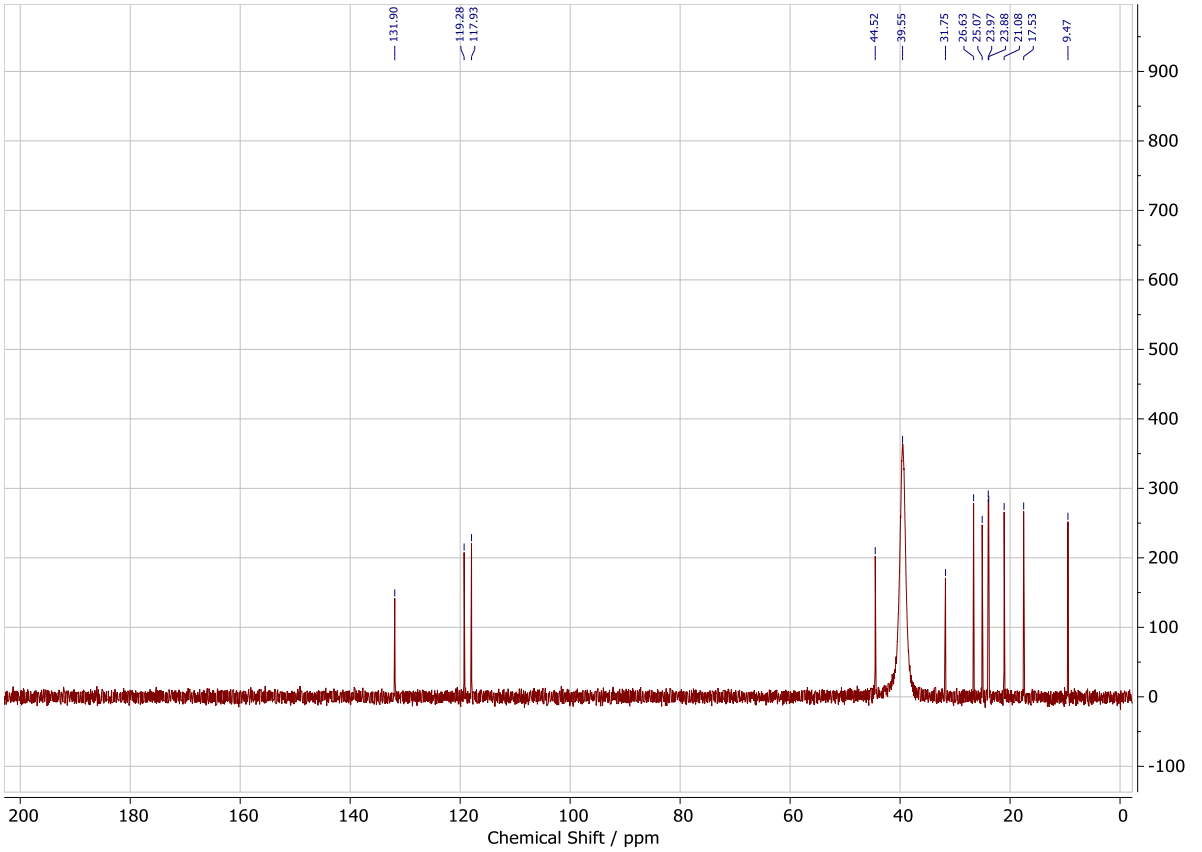

Figure S36 ^{13}C NMR of $[C_8C_1Im]Cl_{0.33}NiCl_2$ in DMSO-d_6.

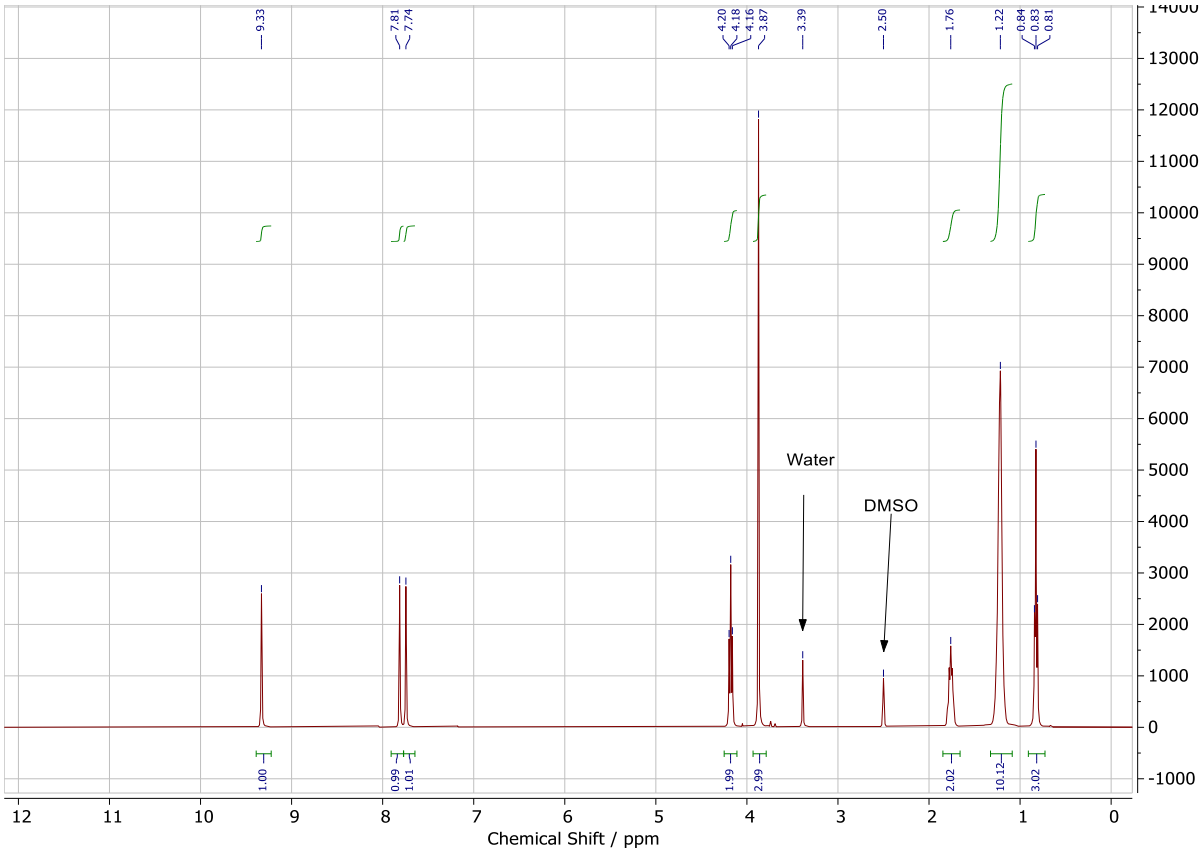

Figure S37 ^{1}H NMR of $[C_8C_1Im]Cl_{0.5}InCl_3$ in DMSO-d_6.

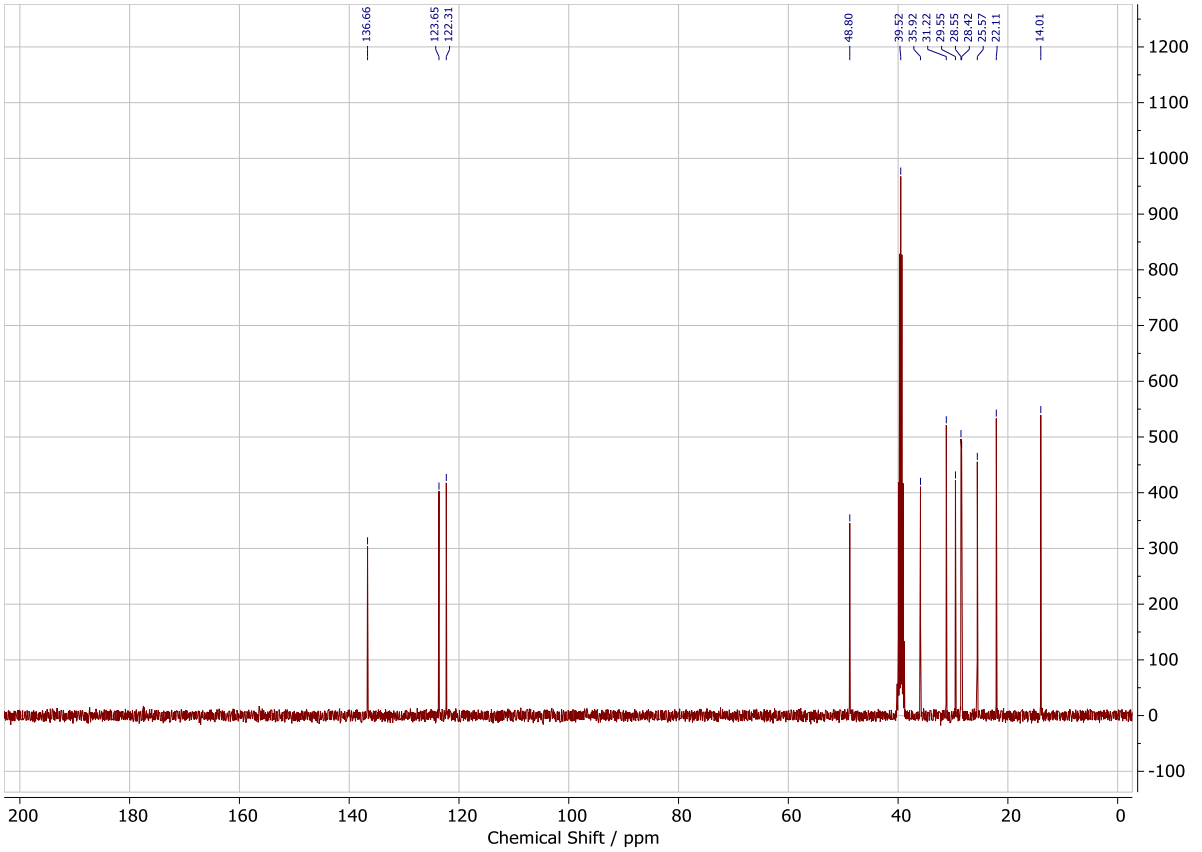

Figure S38 ^{13}C NMR of $[C_8C_1Im]Cl_{0.5}InCl_3$ in DMSO-d_6.

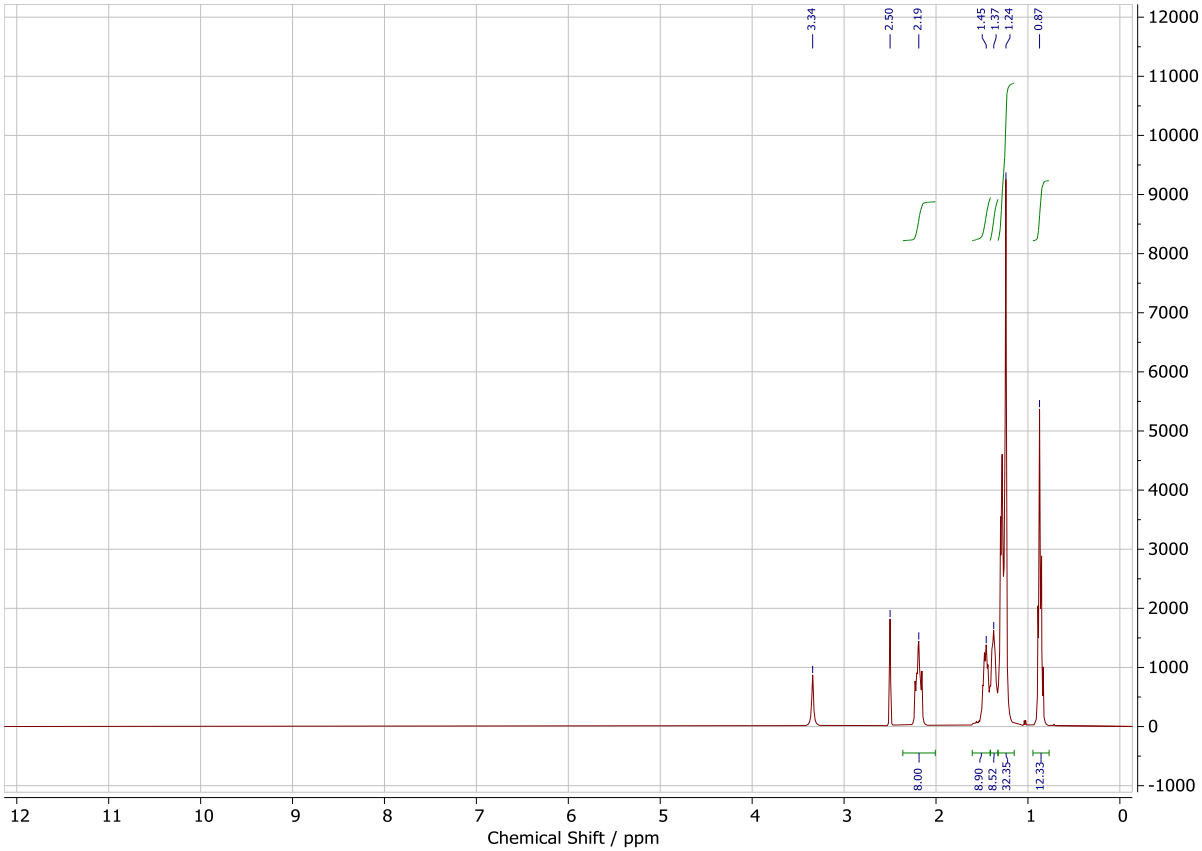

Figure S39 ^{1}H NMR of $[P_{66614}]Cl$ in DMSO-d_6.

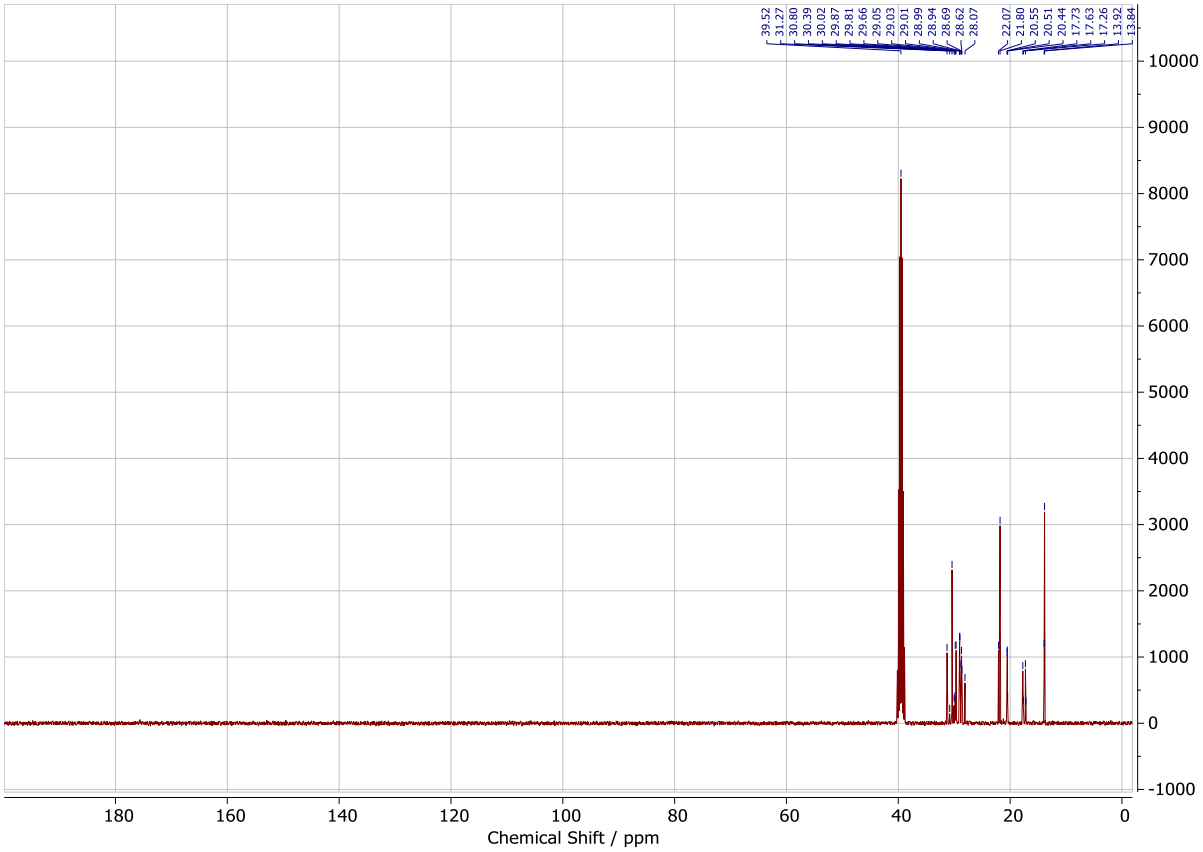

Figure S40 ^{13}C NMR of $[P_{66614}]Cl$ in DMSO-d_6.

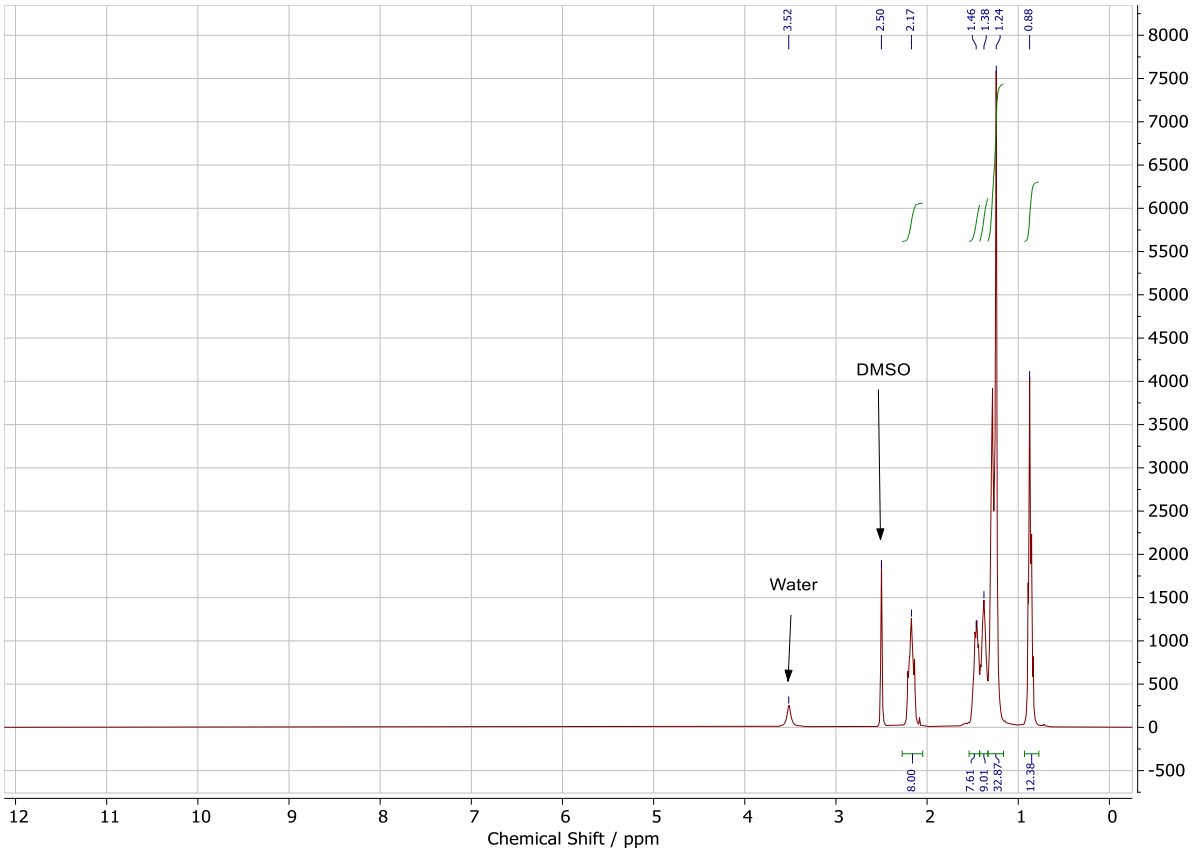

Figure S41 ^{1}H NMR of $[P_{66614}]Cl_{0.33}ZnCl_2$ in DMSO-d_6.

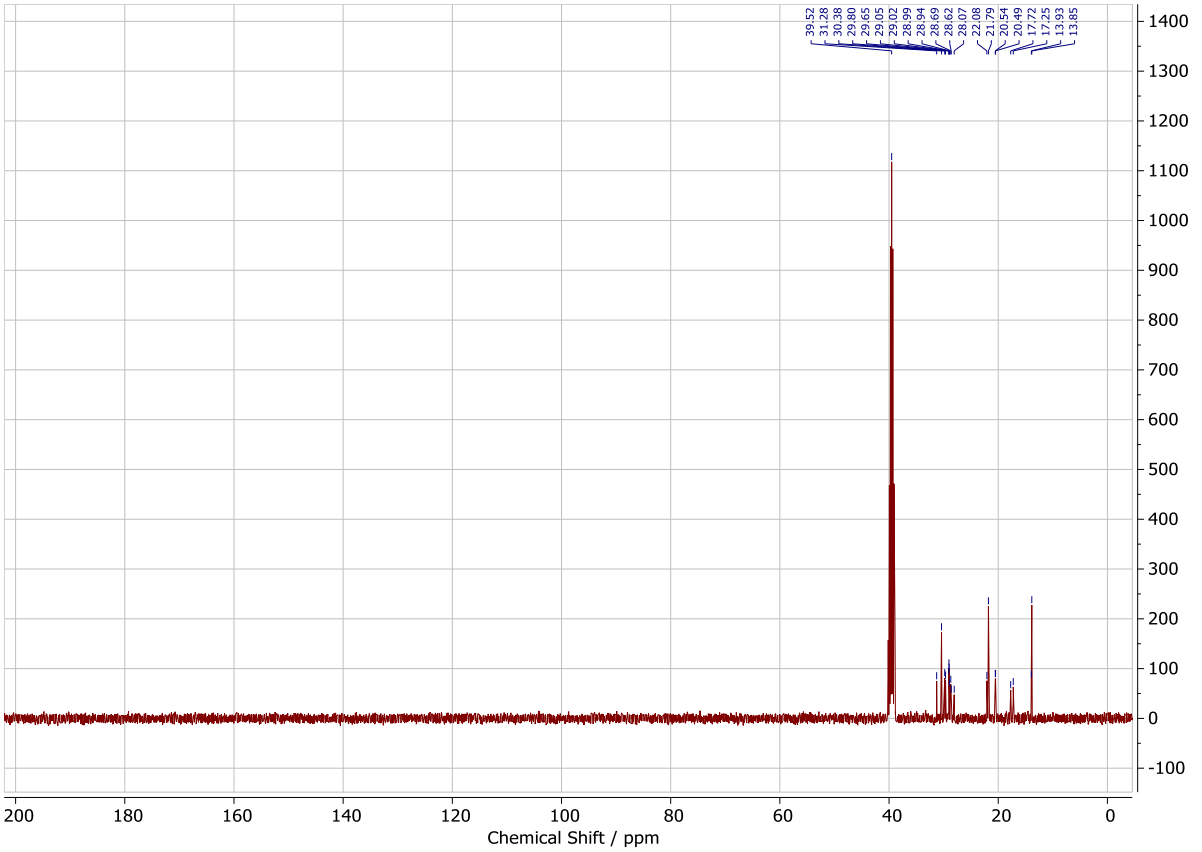

Figure S42 ^{13}C NMR of $[P_{66614}]Cl_{0.33}ZnCl_2$ in DMSO-d_6.

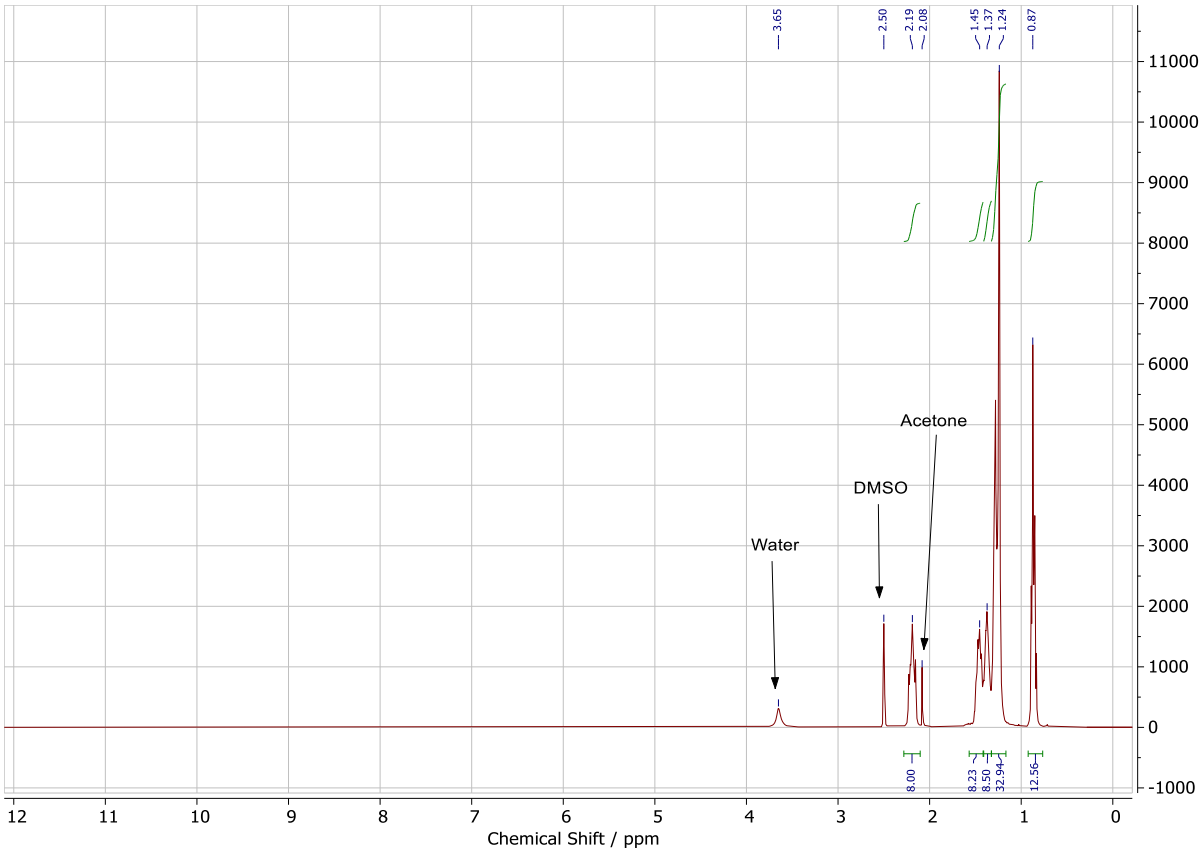

Figure S43 ^{1}H NMR of $[P_{66614}]Cl_{0.1}ZnCl_2$ in DMSO-d_6.

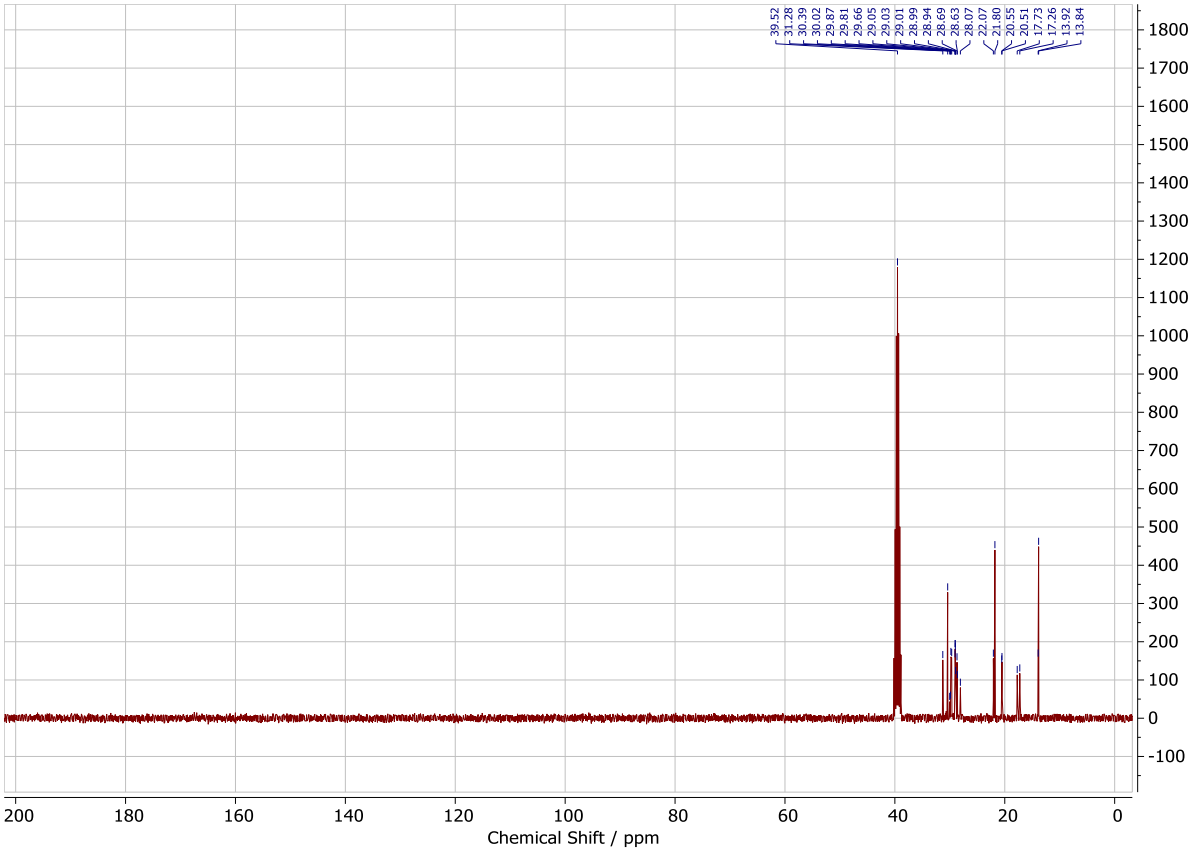

Figure S44 ^{13}C NMR of $[P_{66614}]Cl_{0.1}ZnCl_2$ in DMSO-d_6.

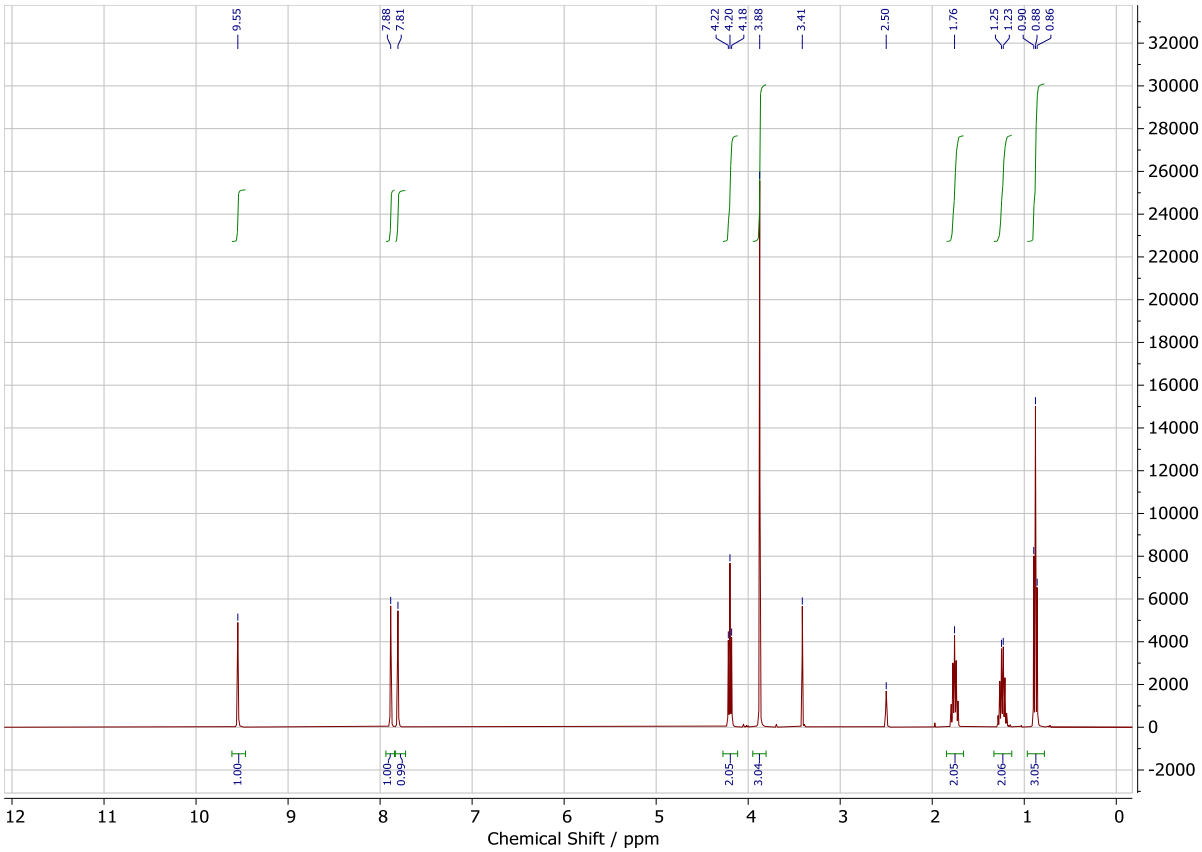

Figure S45 ^{1}H NMR of $[C_4C_1Im]Cl$ in DMSO-d_6.

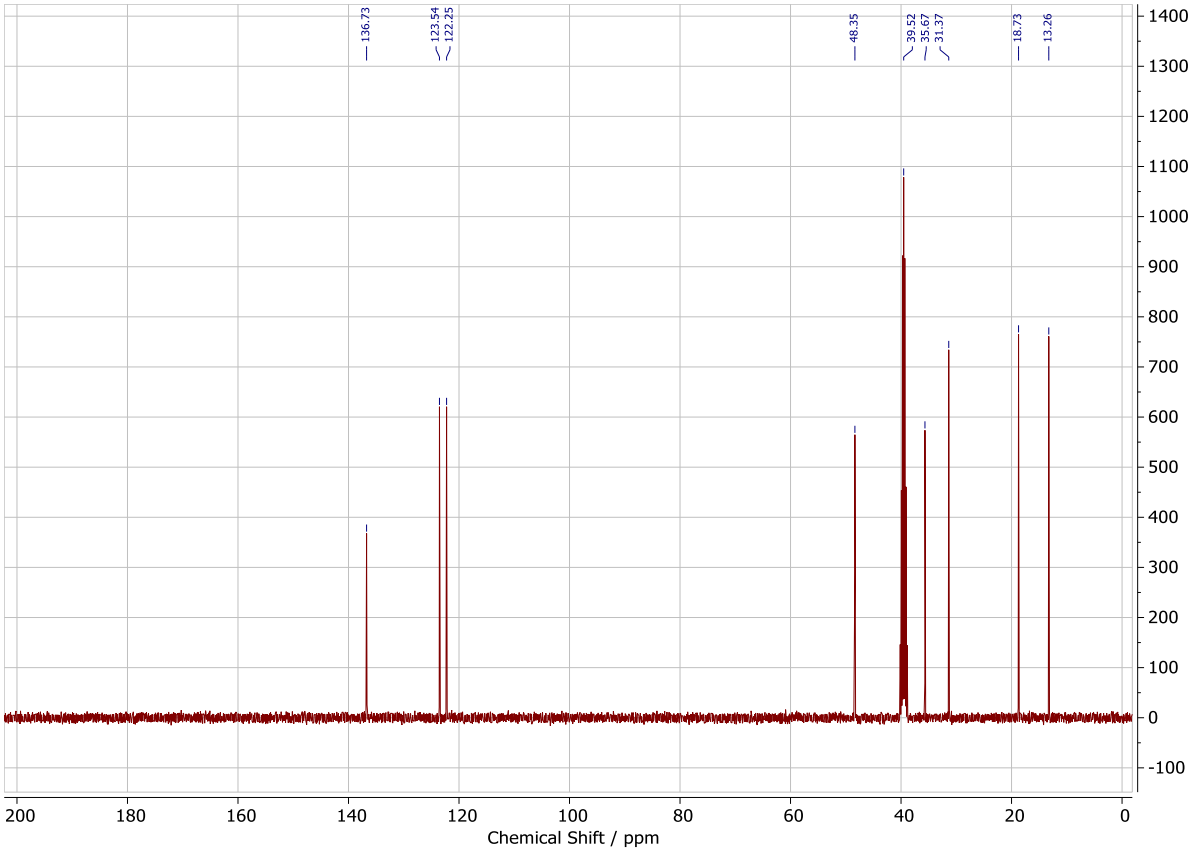

Figure S46 ^{13}C NMR of [C_4C_1Im]Cl in DMSO-d_6.

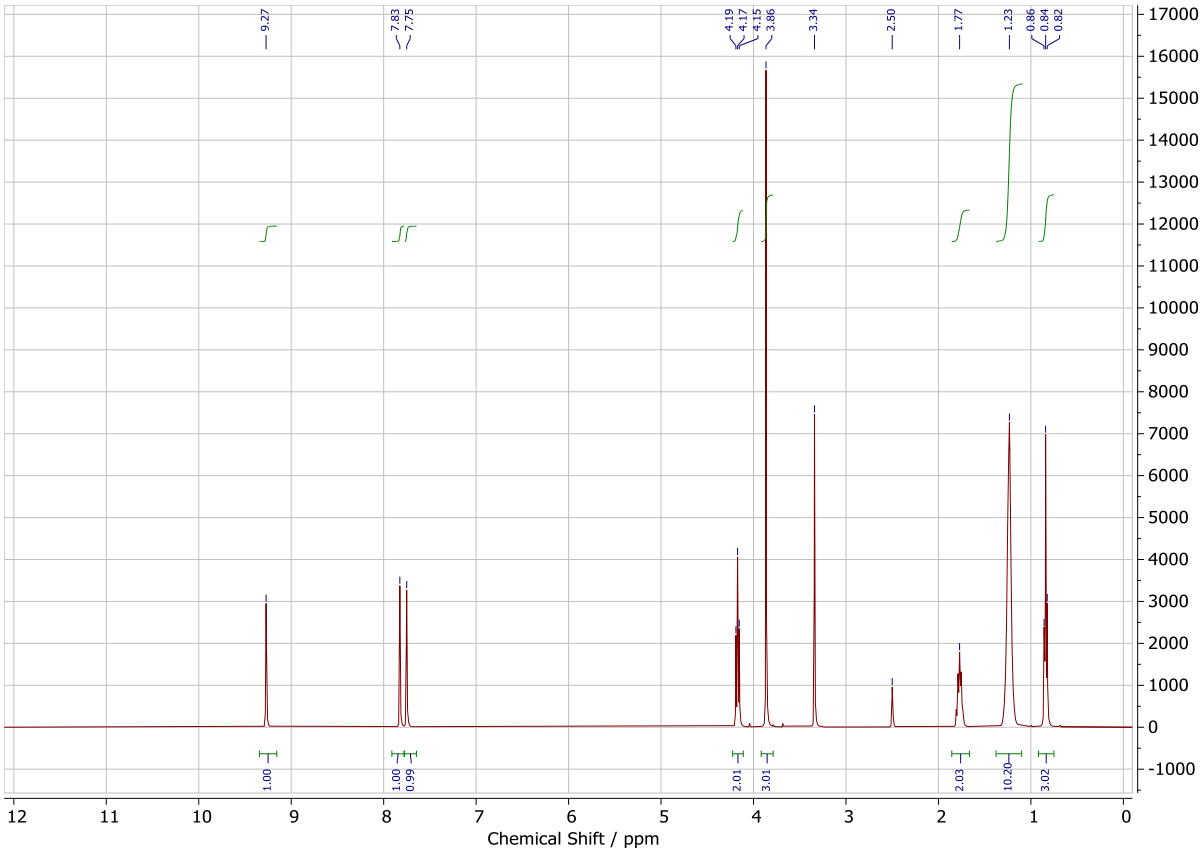

Figure S47 ^{1}H NMR of [C_8C_1Im]Br in DMSO-d_6.

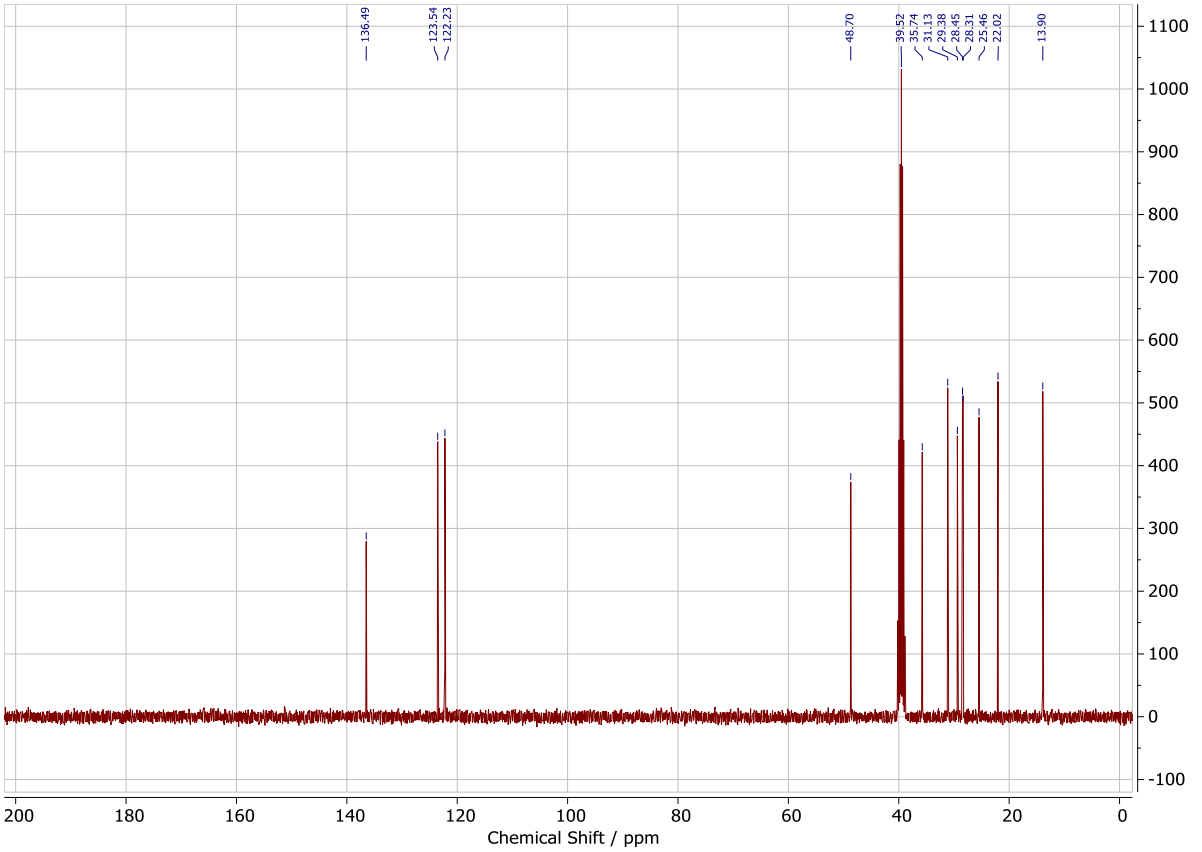

Figure S48 ^{13}C NMR of $[C_8C_1Im]Br$ in DMSO-d_6.

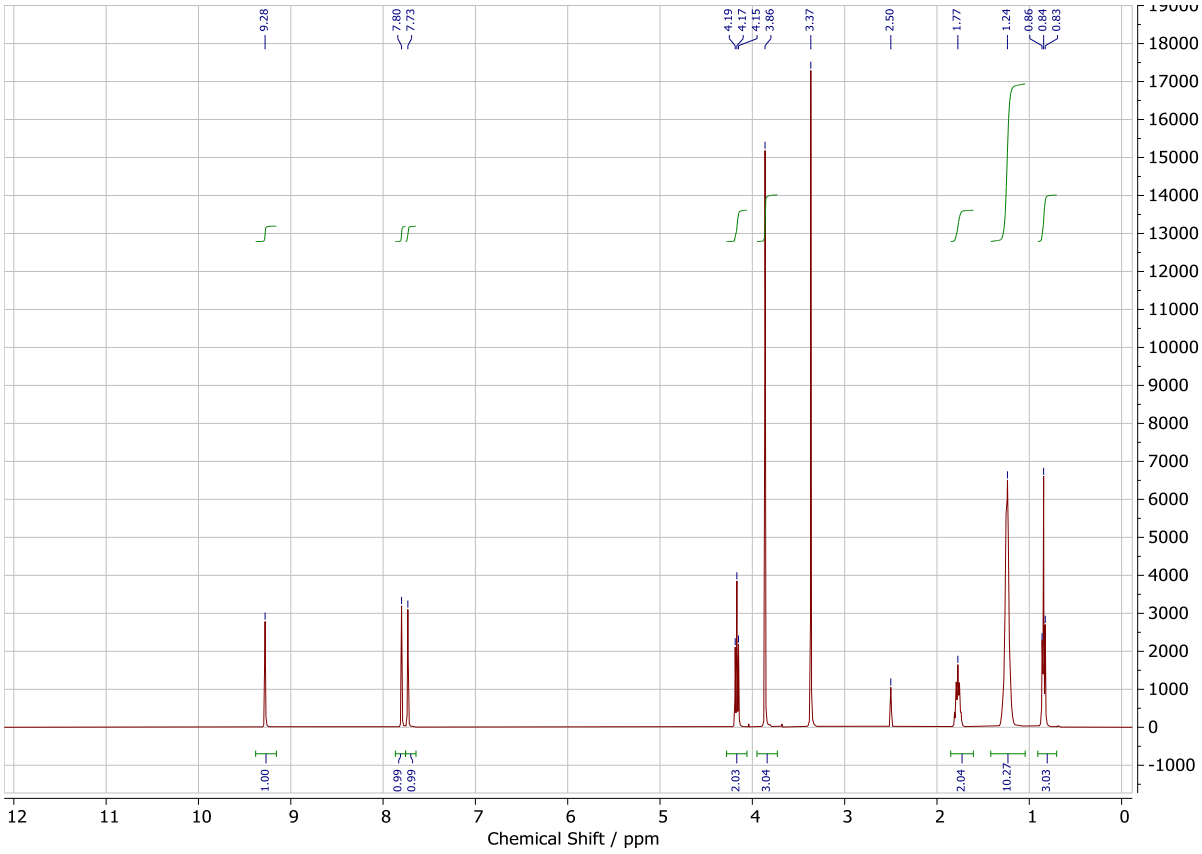

Figure S49 ^{1}H NMR of $[C_8C_1Im]Cl_{0.33}AgCl$ in DMSO-d_6.

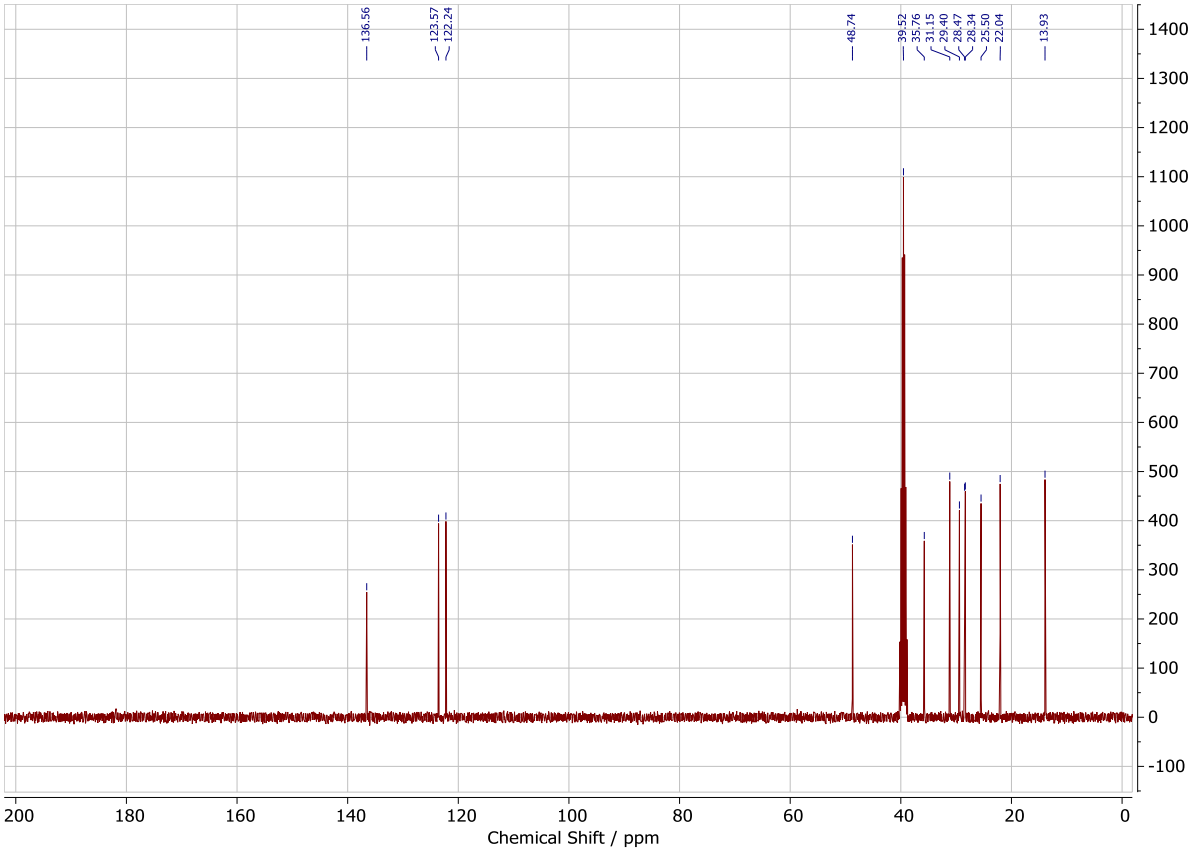

Figure S50 ^{13}C NMR of $[C_8C_1Im]Cl_{0.33}AgCl$ in DMSO-d_6.

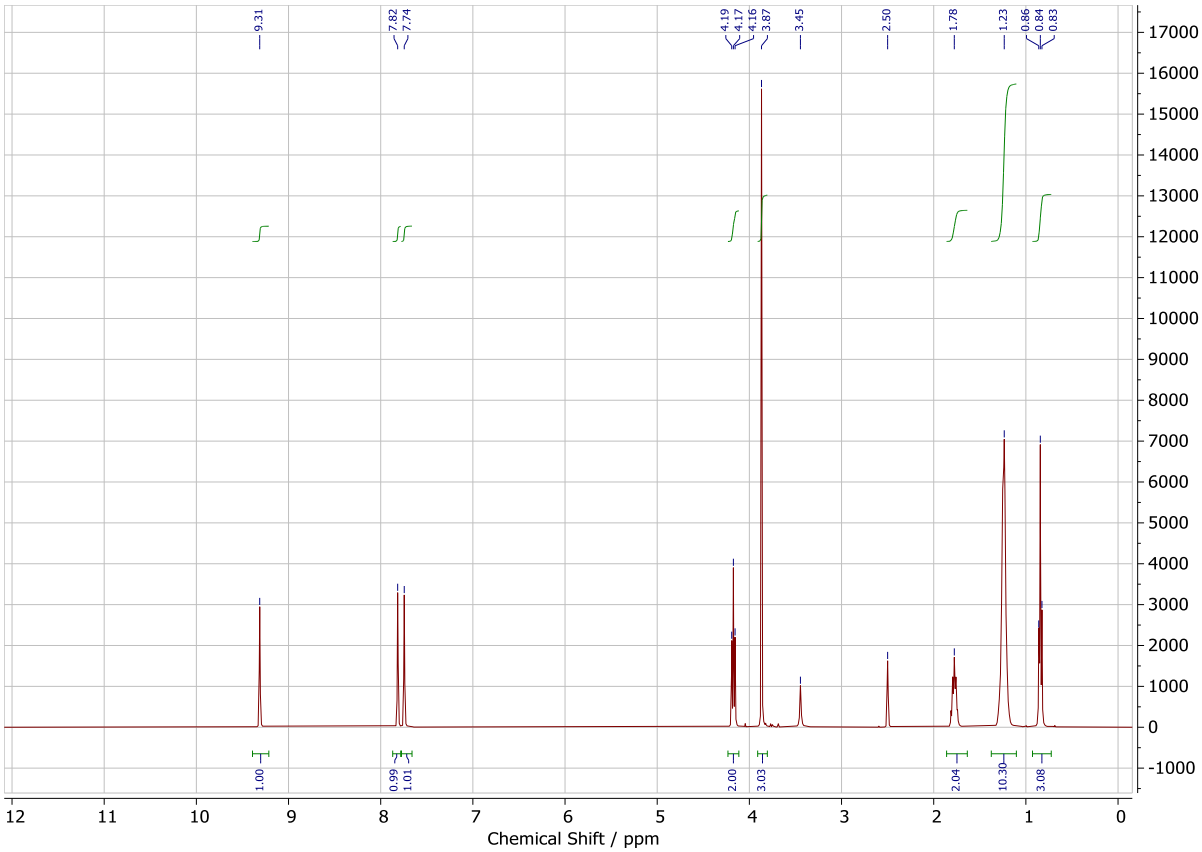

Figure S51 ^{1}H NMR of $[C_8C_1Im]Cl_{0.33}PtCl_2$ in DMSO-d_6.

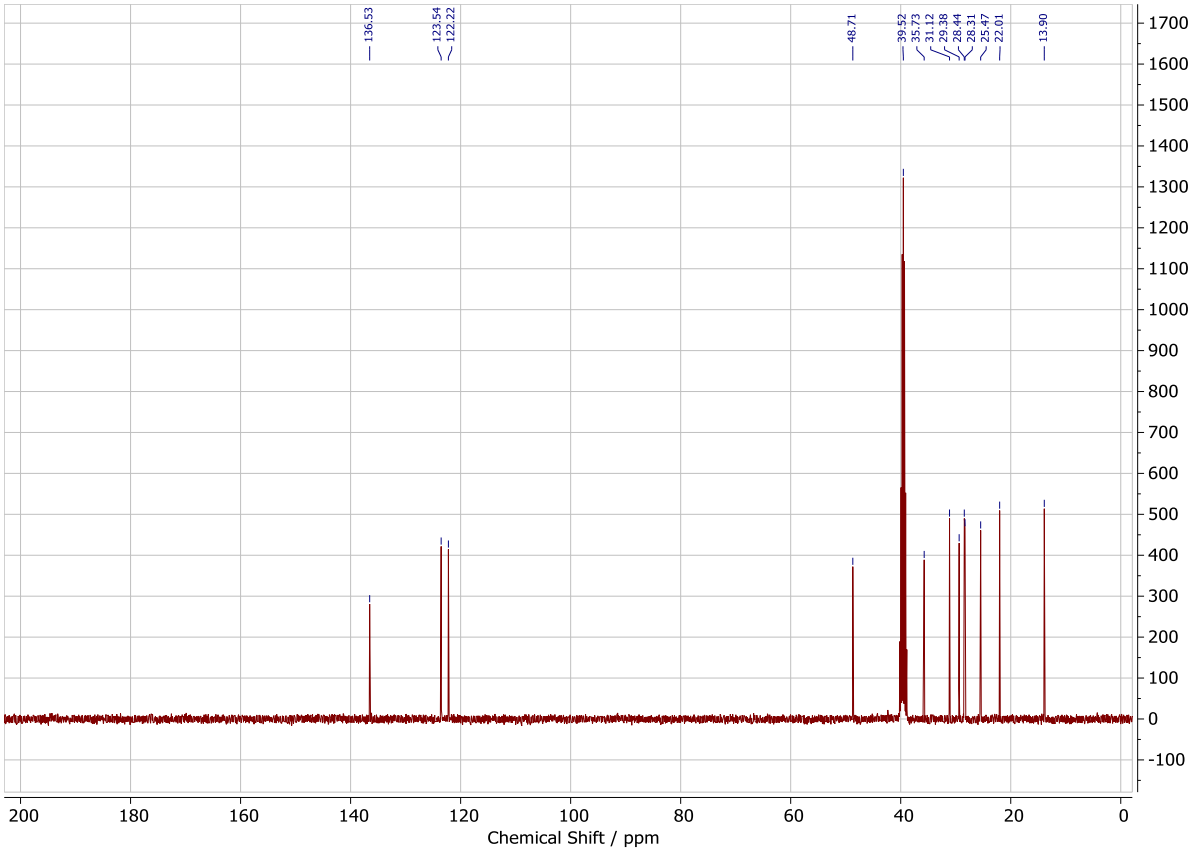

Figure S52 ^{13}C NMR of $[C_8C_1Im]Cl_{0.33}PtCl_2$ in DMSO-d_6.

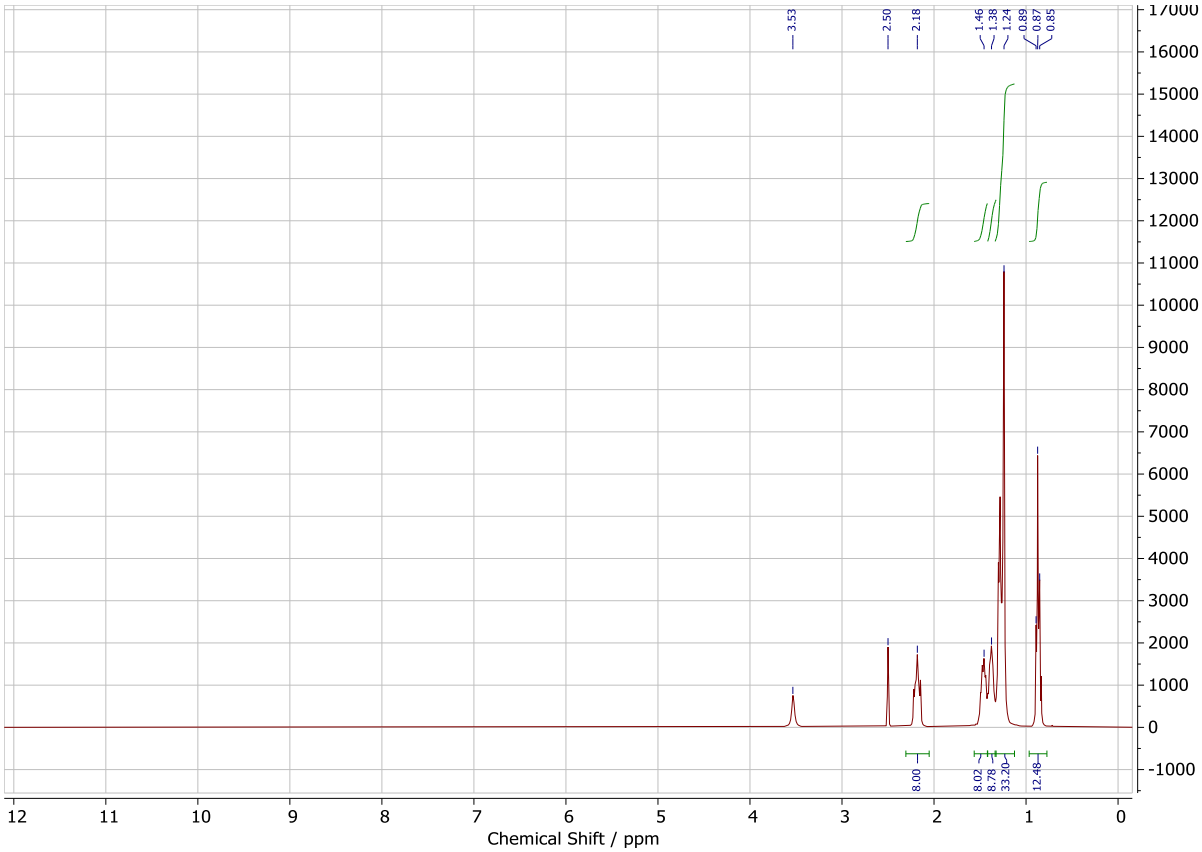

Figure S53 ^{1}H NMR of $[P_{66614}]Cl_{0.33}AgCl$ in DMSO-d_6.

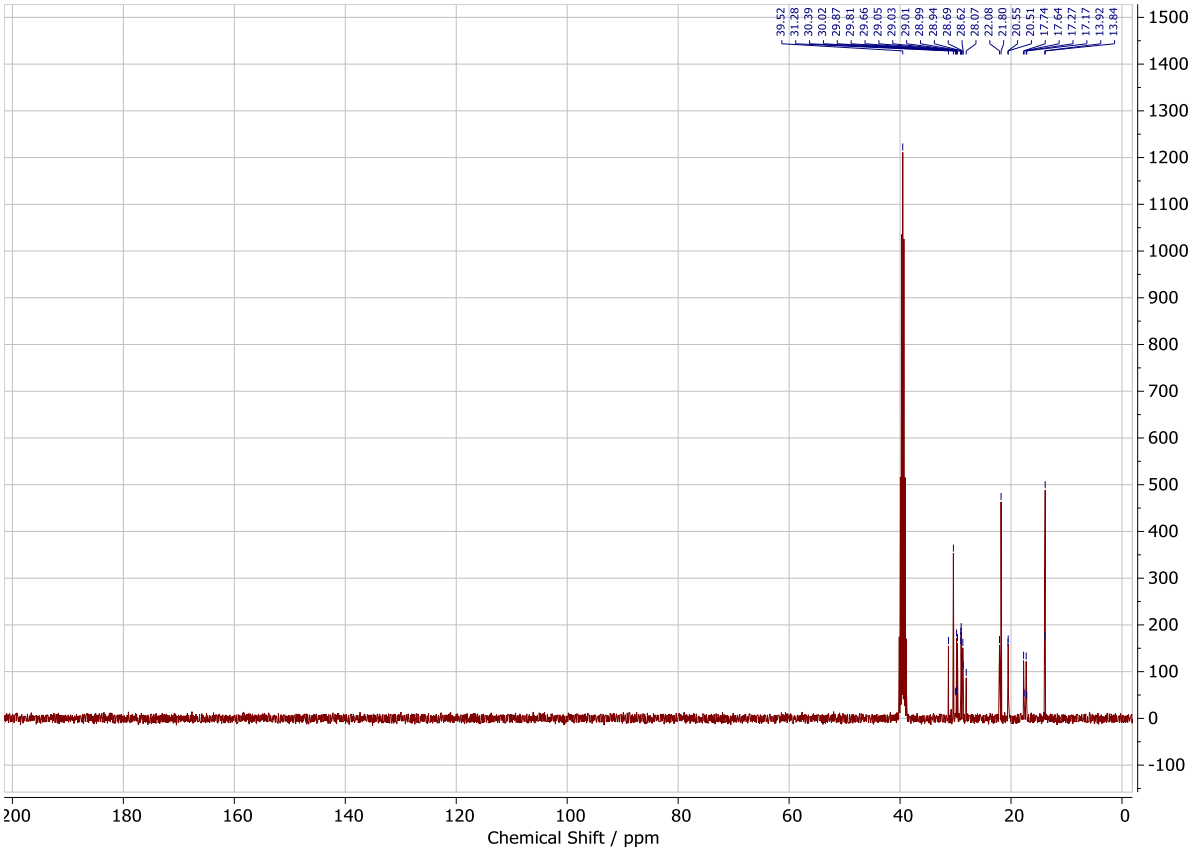

Figure S54 ^{13}C NMR of $[P_{66614}]Cl_{0.33}AgCl$ in DMSO-d_6.

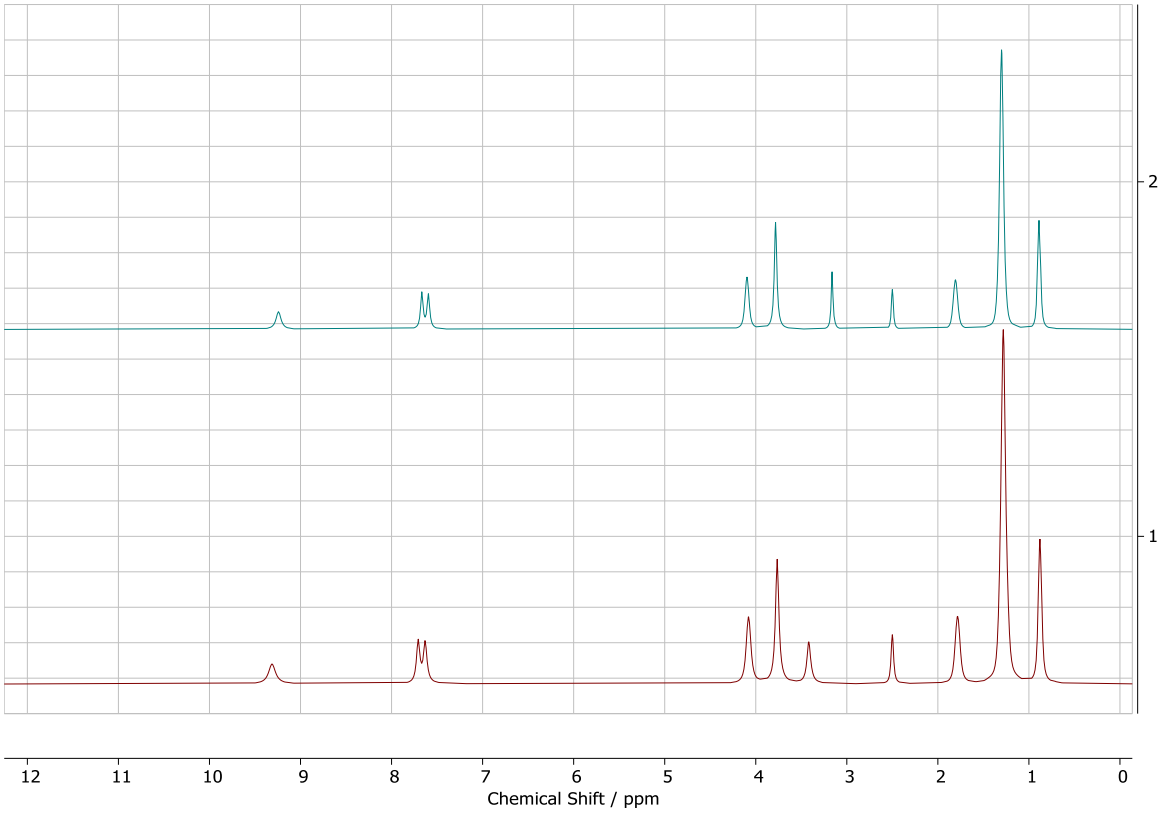

Figure S55 ^{1}H NMR of $[C_8C_1Im]Cl_{0.33}CoCl_2$ in DMSO-d_6 at 25 °C (top) and 70 °C (bottom).

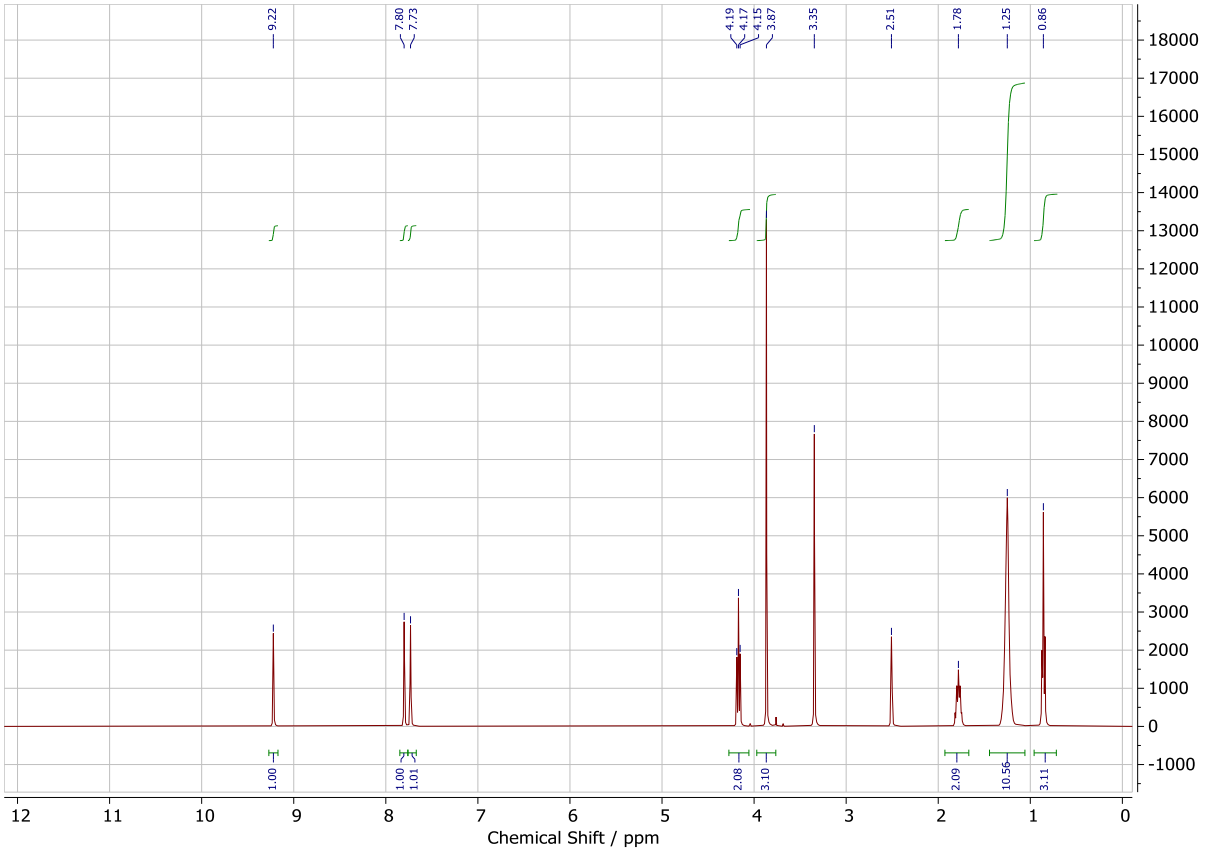

Figure S56 ^{1}H NMR of $[C_8C_1Im]Cl_{0.33}ZnBr_2$ in DMSO-d_6.

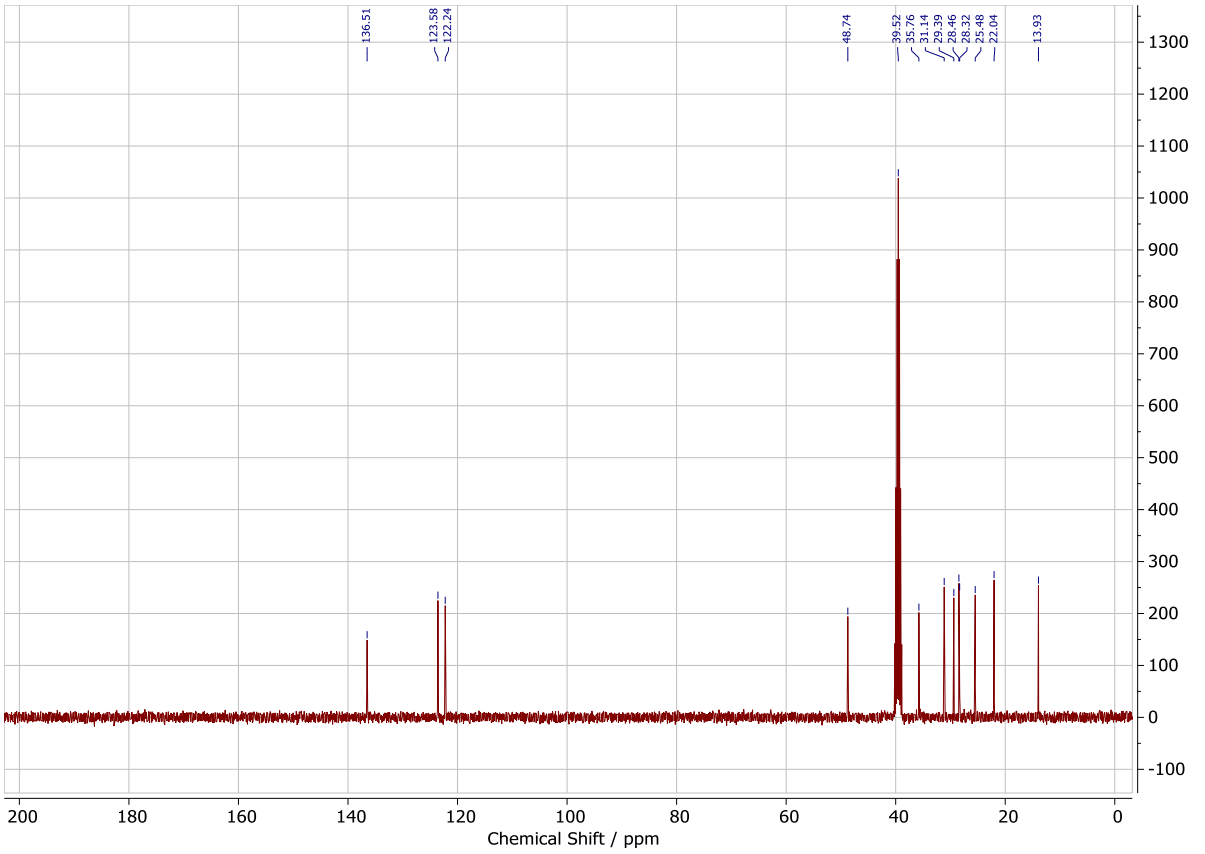

Figure S57 ^{13}C NMR of $[C_8C_1Im]Cl_{0.33}ZnBr_2$ in DMSO-d_6.

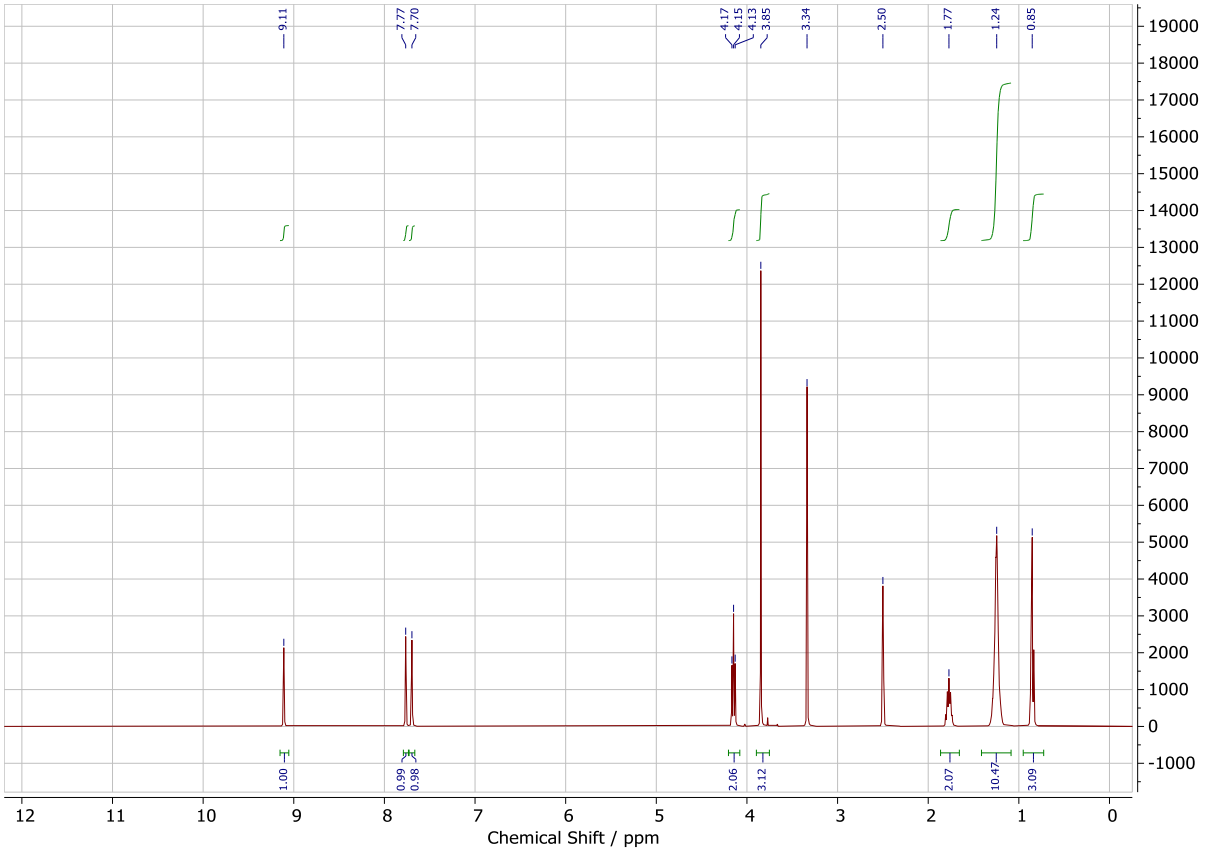

Figure S58 ^{1}H NMR of $[C_8C_1Im]Cl_{0.5}ZnBr_2$ in DMSO-d_6.

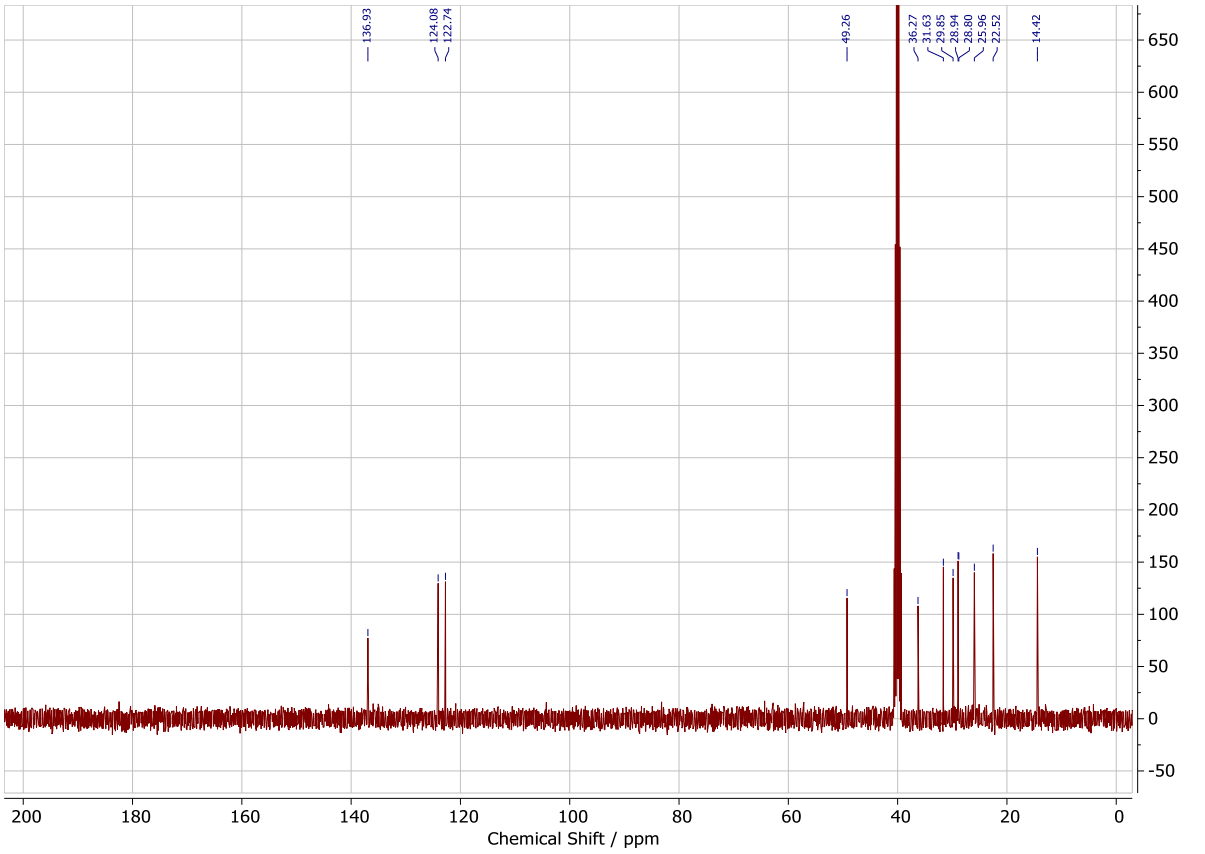

Figure S59 ^{13}C NMR of $[C_8C_1Im]Cl_{0.5}ZnBr_2$ in DMSO-d_6.

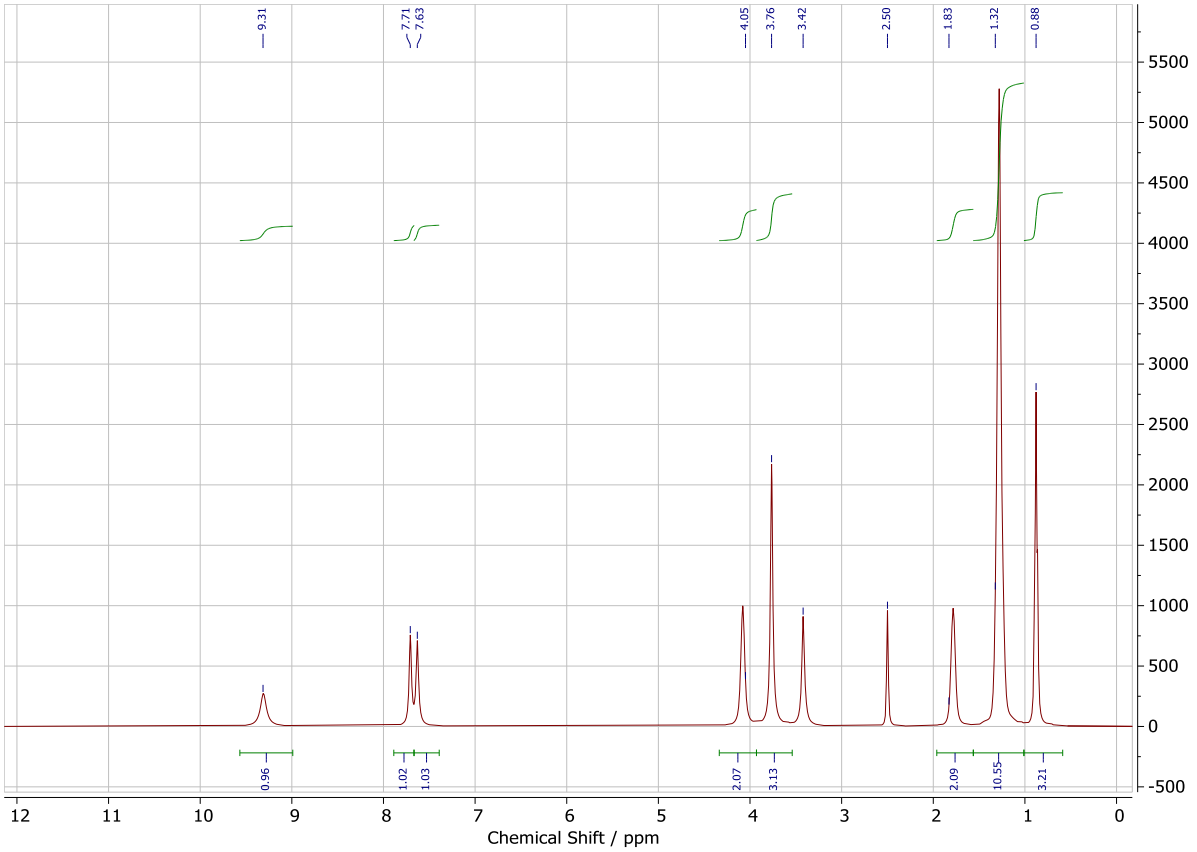

Figure S60 ^{1}H NMR of $[C_8C_1Im]Cl_{0.33}CoCl_2$ in DMSO-d_6.

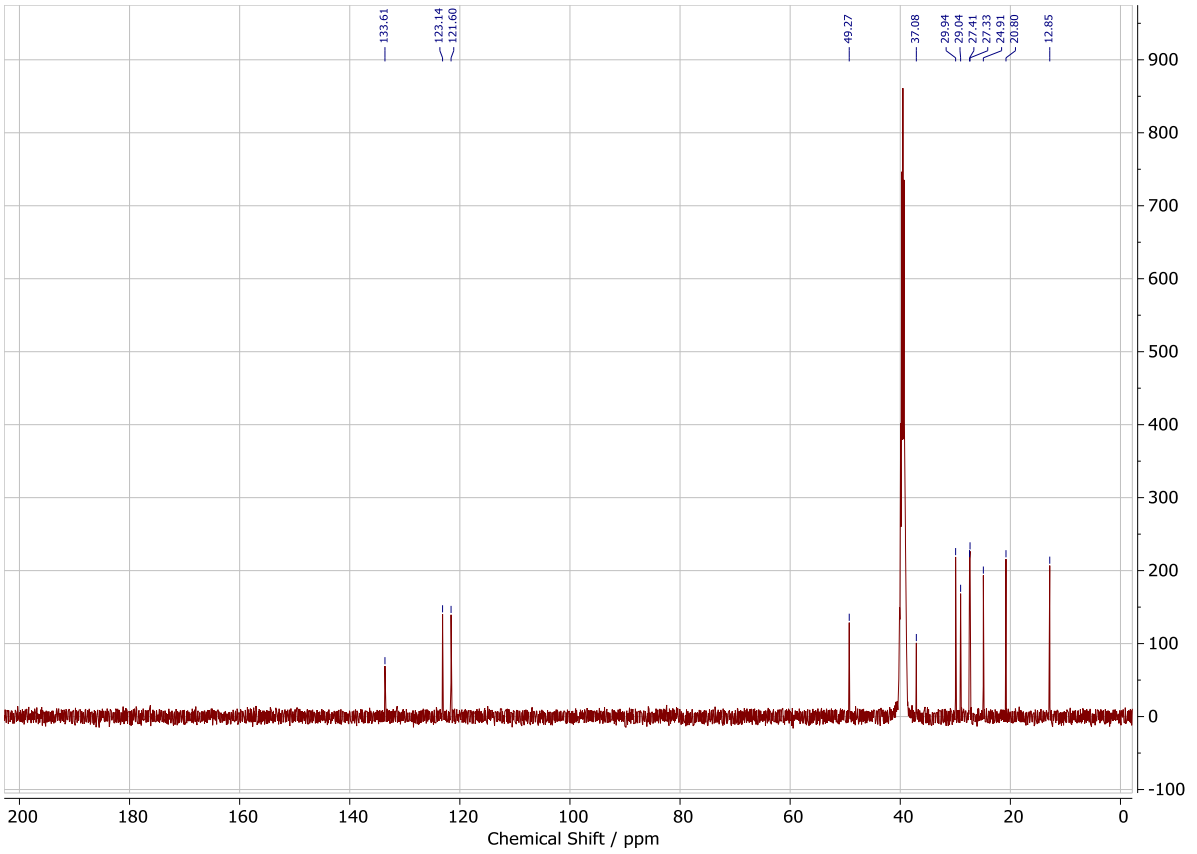

Figure S61 ^{13}C NMR of $[C_8C_1Im]Cl_{0.33}CoCl_2$ in DMSO-d_6.

Residue NMR and MS Data

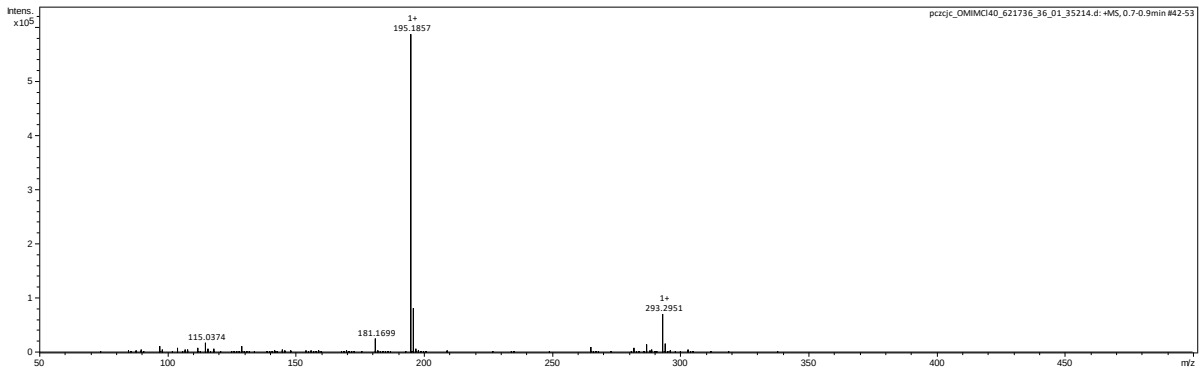

Figure S62 High resolution ESI-MS of $[C_8C_1Im]Cl$ after 60% thermal decomposition under a nitrogen atmosphere in a TGA instrument.

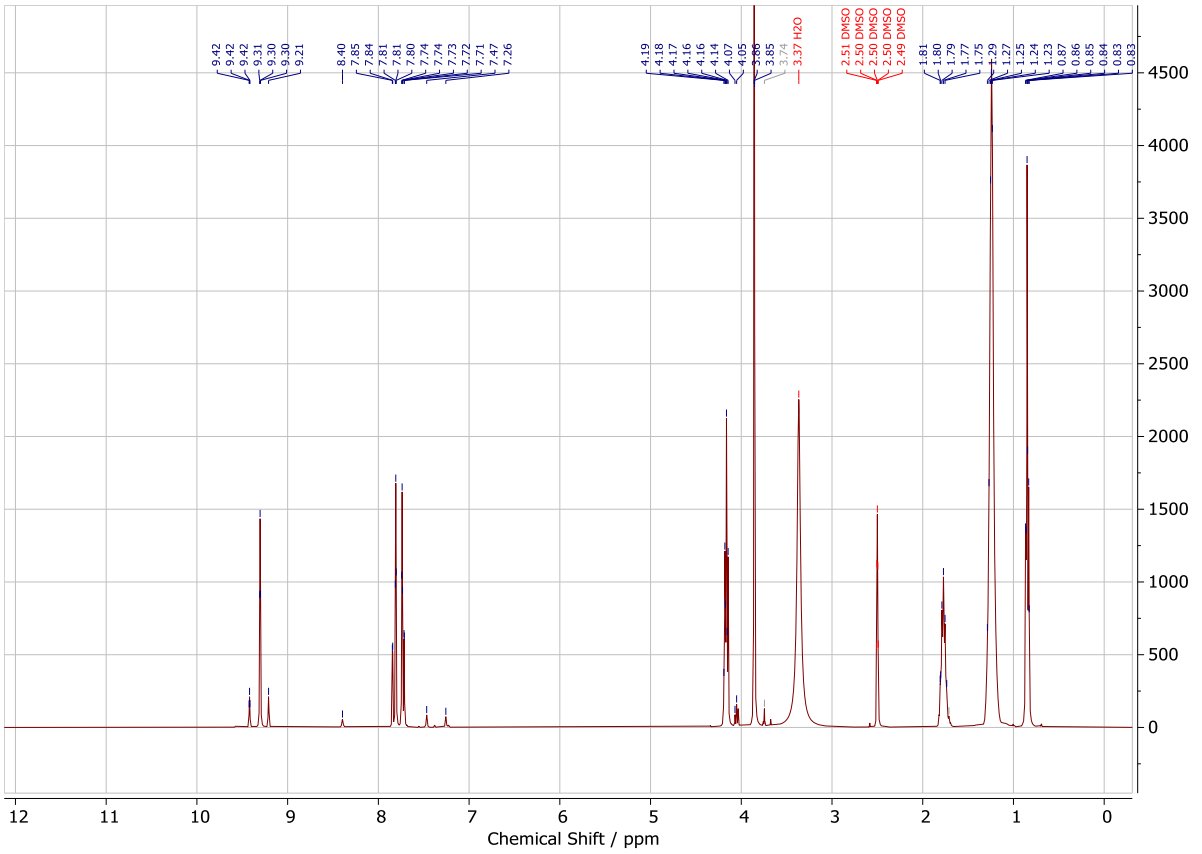

Figure S63 ^1H NMR of $[C_8C_1Im]Cl$ after 60% thermal decomposition under a nitrogen atmosphere in a TGA instrument.

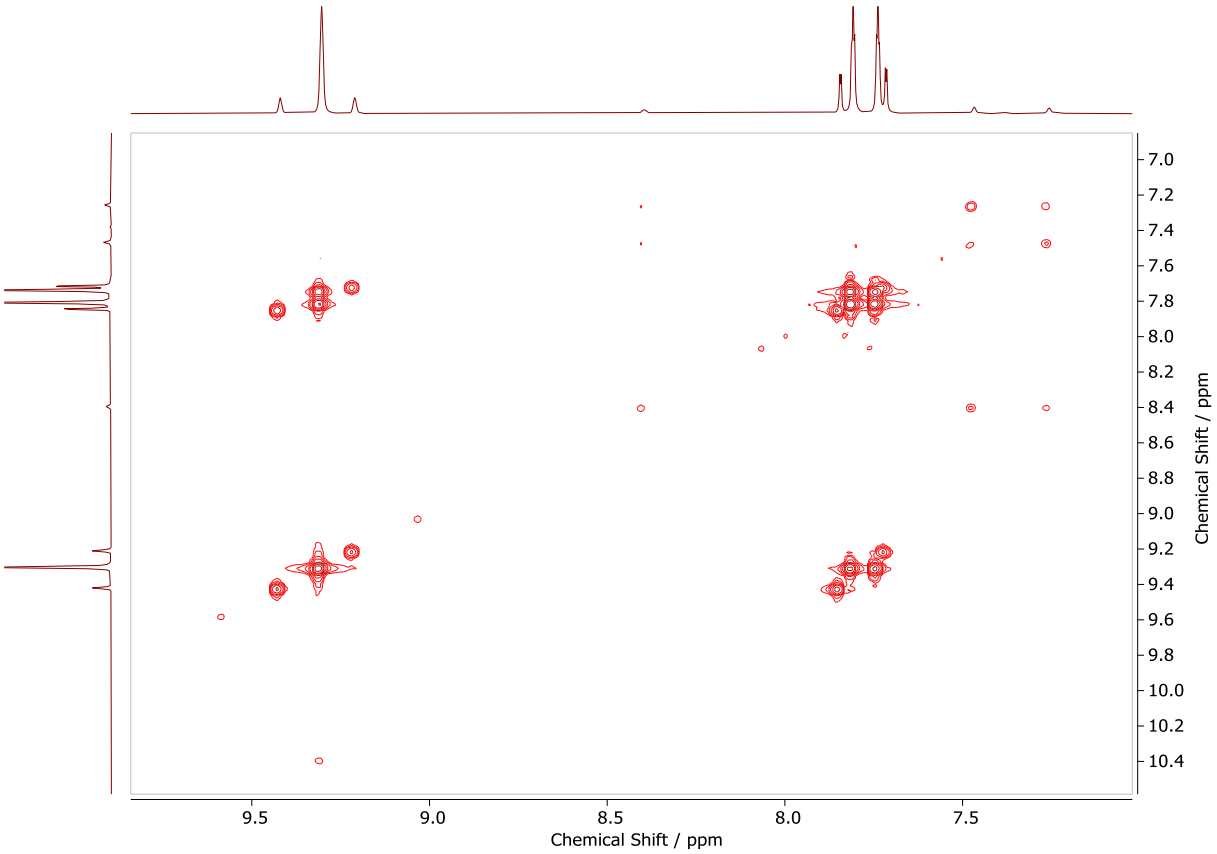

Figure S64 ^{1}H-^{1}H COSY spectrum (aromatic region) of $[C_8C_1Im]Cl$ after 60% thermal decomposition under a nitrogen atmosphere in a TGA instrument.

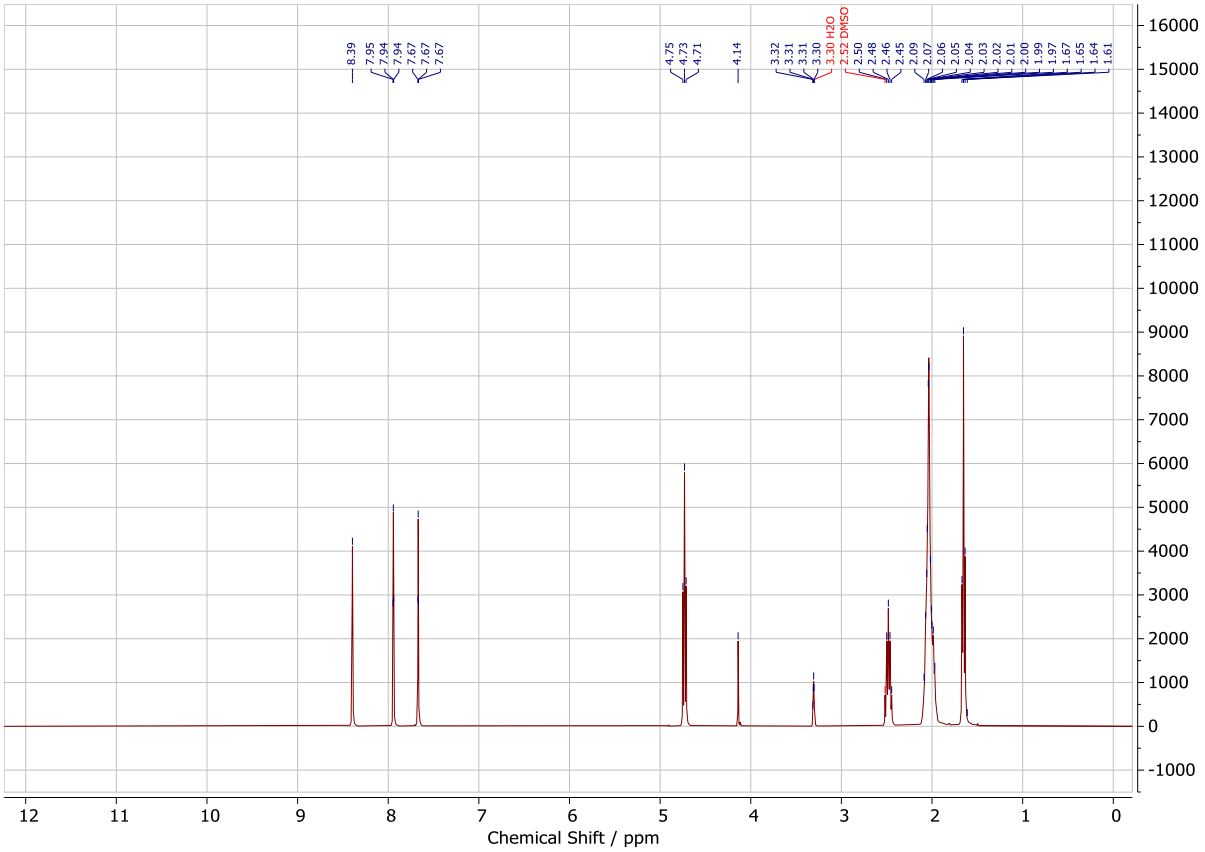

Figure S65 ^{1}H NMR of N-octylimidazole (C_8Im) in d_6-DMSO.

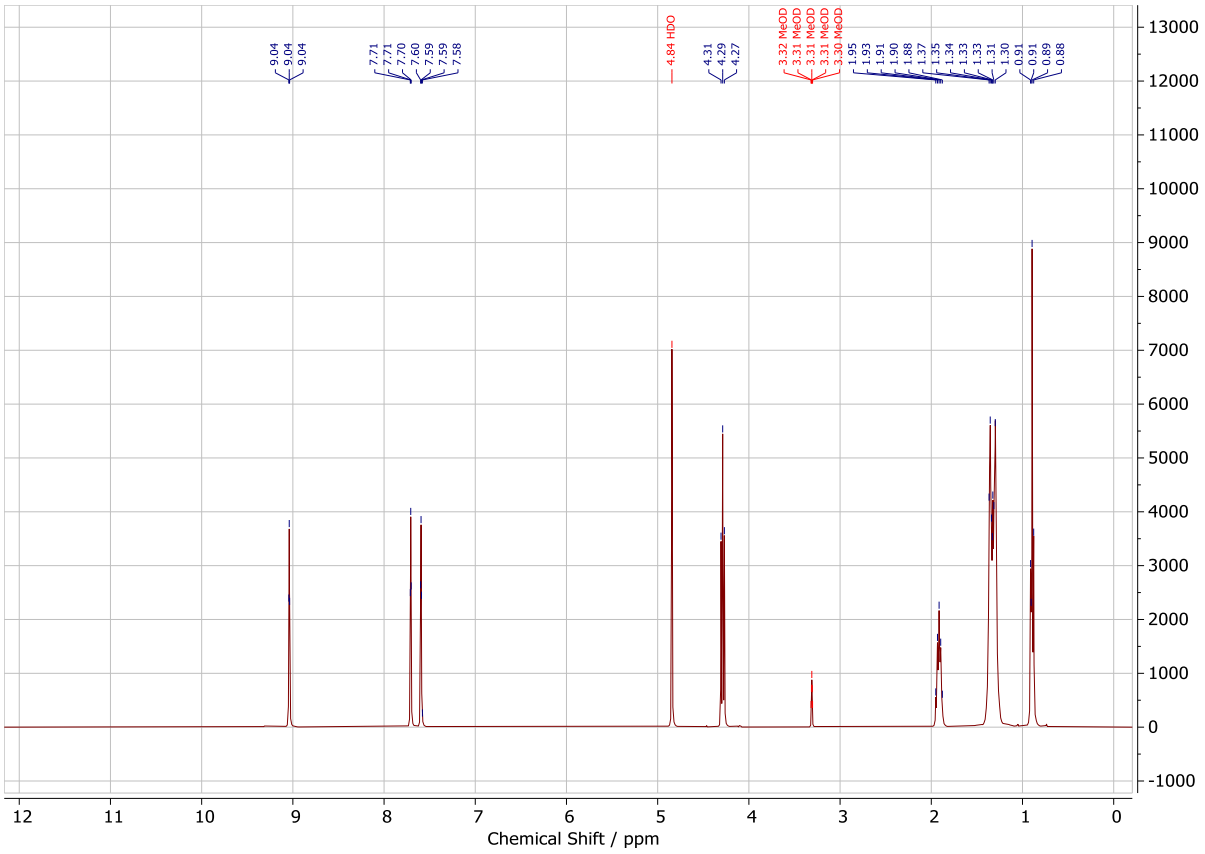

Figure S66 ^{1}H NMR spectrum of protonated [HC_8Im]Cl in d_4-MeOD.

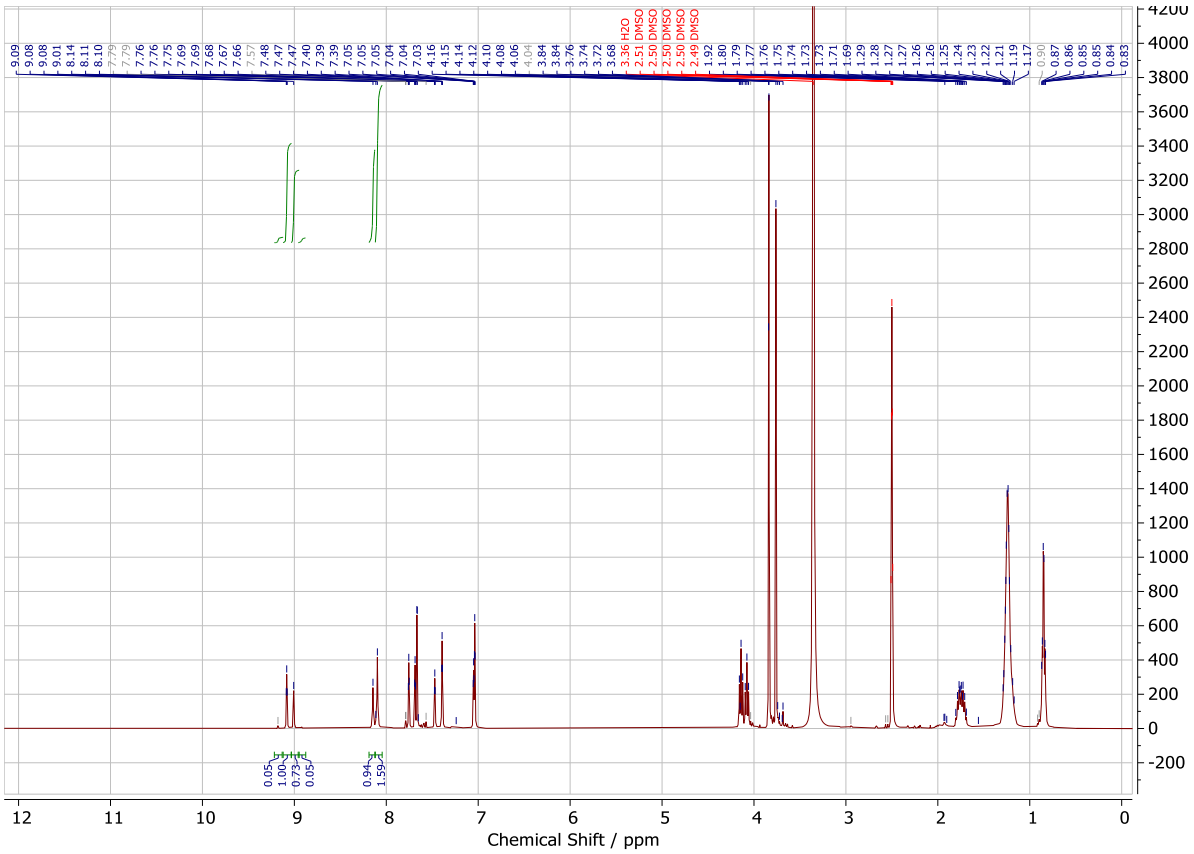

Figure S67 ^{1}H NMR of $[C_8C_1Im]Cl_{0.33}ZnCl_2$ after 60% thermal decomposition under a nitrogen atmosphere in a TGA instrument.

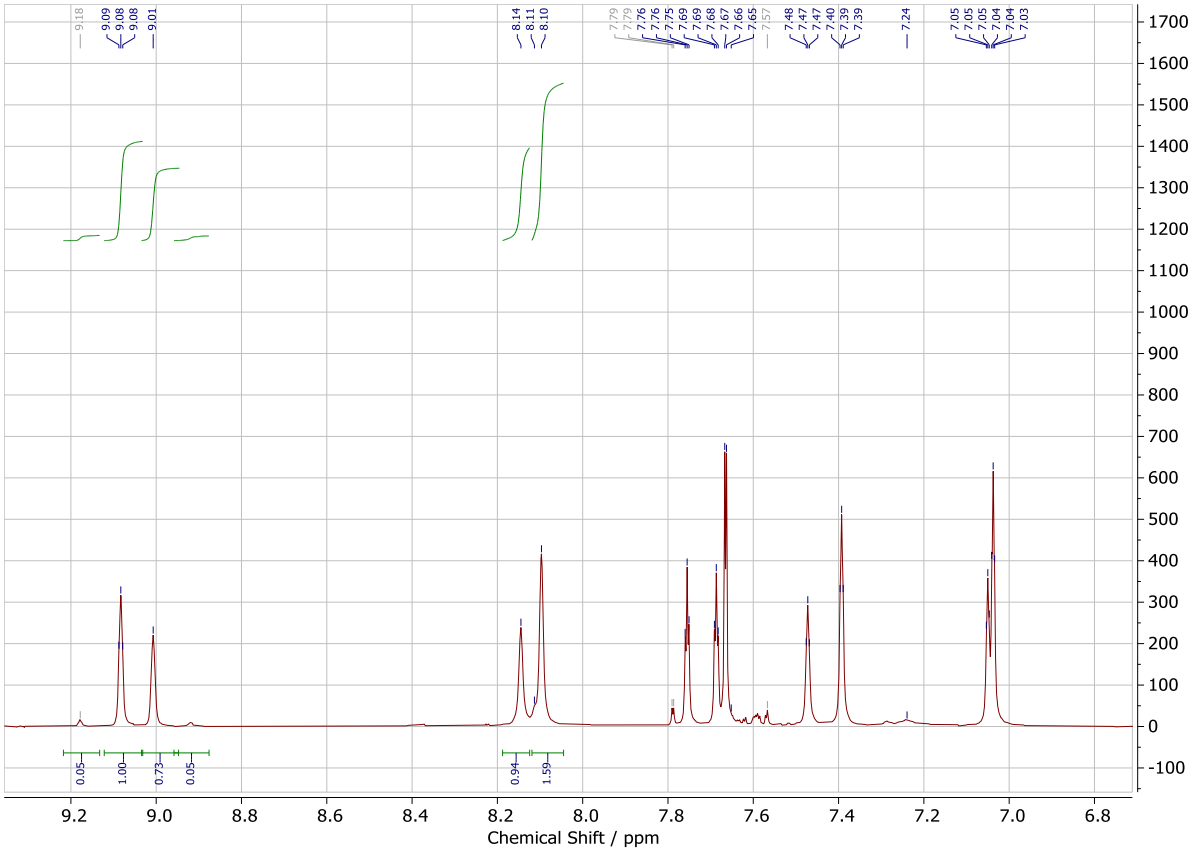

Figure S68 Aromatic region expansion of ^{1}H NMR of $[C_8C_1Im]Cl_{0.33}ZnCl_2$ after 60% thermal decomposition under a nitrogen atmosphere in a TGA instrument.

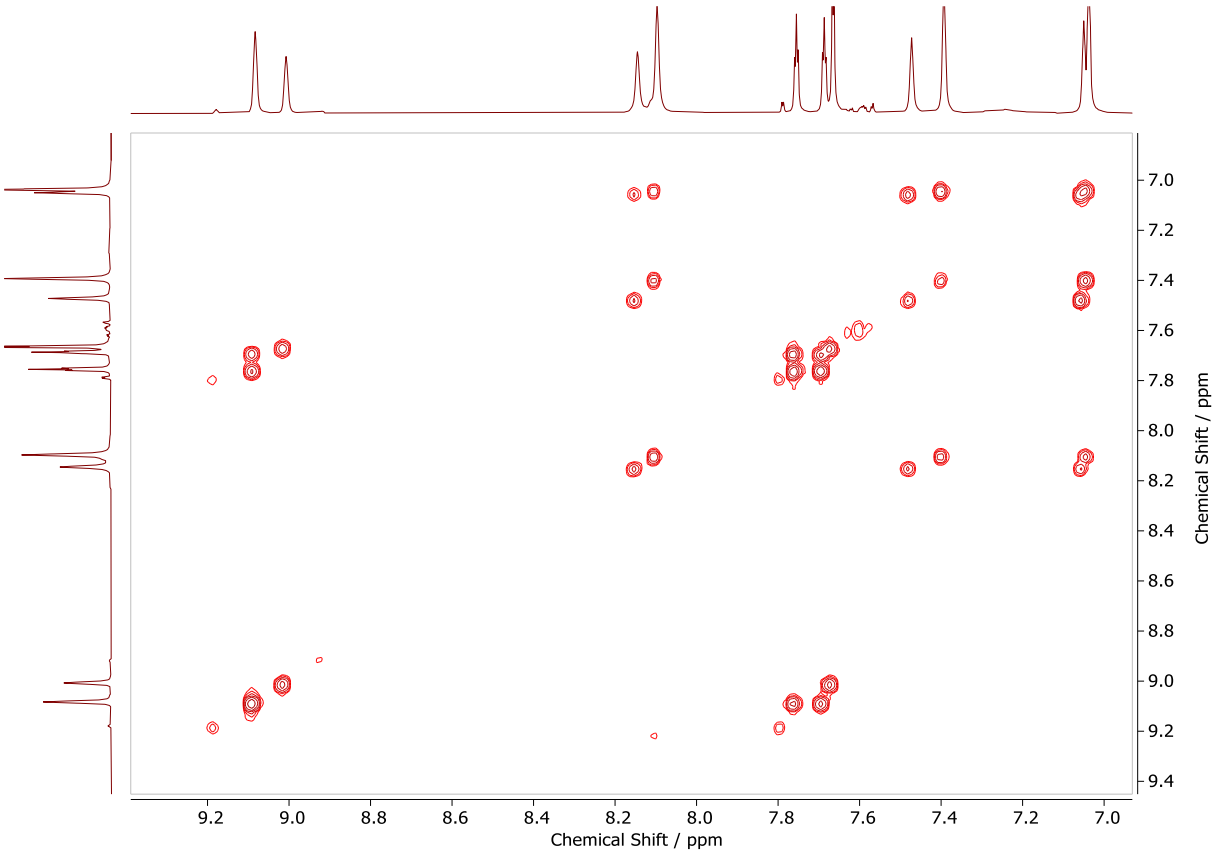

Figure S69 ^{1}H-^{1}H COSY spectrum (aromatic region) of $[C_8C_1Im]Cl_{0.33}ZnCl_2$ after 60% thermal decomposition under a nitrogen atmosphere in a TGA instrument.

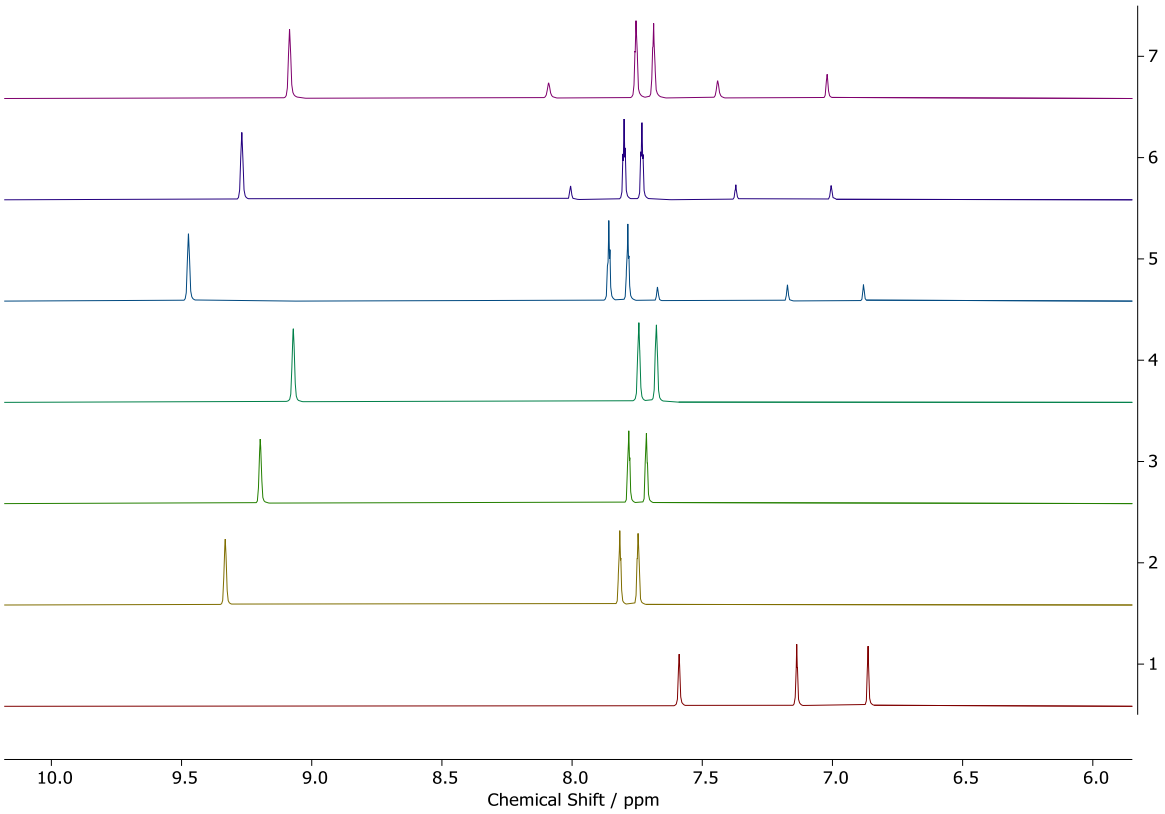

Figure S70 ^{1}H NMR (aromatic region) of ionic liquids with and without N-octylimidazole. Bottom to top: C_8Im (red), $[C_8C_1Im]Cl$ (yellow), $[C_8C_1Im]Cl_{0.33}ZnCl_2$ (pale green), $[C_8C_1Im]Cl_{0.6}ZnCl_2$ (dark green), $[C_8C_1Im]Cl$ + 15.4 % C_8Im (blue), $[C_8C_1Im]Cl_{0.33}ZnCl_2$ + 14.1 % C_8Im (dark purple), $[C_8C_1Im]Cl_{0.6}ZnCl_2$ + 13.9 % C_8Im (light purple).

Table S1 ^{1}H NMR chemical shifts (ppm) in DMSO-d_6 at room temperature for pure $[C_8C_1Im]Cl_\chi ZnCl_2$ (χ = 0, 0.33, 0.6) ionic liquids and mixtures of the same ionic liquids spiked with ≈15 % C_8Im.

					δ / ppm					
					IL			C_8Im		
Cation	Anion	Metal	χ	C8Im / wt%	C^2	C^4	C^5	C^2	C^4	C^5
$[C_8C_1Im]^+$	Cl^-	$ZnCl_2$	0	0	9.33	7.82	7.75			
			0.33	0	9.2	7.78	7.71			
			0.6	0	9.07	7.74	7.68			
$[C_8C_1Im]^+$	Cl^-	$ZnCl_2$	0	15.4	9.47	7.86	7.79	7.67	7.17	6.88
			0.33	14.1	9.27	7.80	7.73	8.01	7.37	7.01
			0.6	13.9	9.09	7.75	7.69	8.09	7.44	7.02
C_8Im								7.59	7.14	6.86
$[HC_8Im]^+$	Cl^-				9.04	7.71	7.59			

Table S2 Variable temperature chemical shifts (ppm) for the C_8Im mixtures in from Figure S70 and Table S1.

						δ/ ppm					
						IL			C_8Im		
Cation	Anion	Metal	χ	C_8Im	Temperature / °C	C^2	C^4	C^5	C^2	C^4	C^5
$[C_8C_1Im]^+$	Cl^-	$ZnCl_2$	0	15.4	25	9.47	7.86	7.78	7.67	7.17	6.88
					80	9.51	7.81	7.75	7.63	7.12	6.88
Δδ						0.04	-0.05	-0.03	-0.04	-0.05	0.00
$[C_8C_1Im]^+$	Cl^-	$ZnCl_2$	0.33	14.1	25	9.27	7.80	7.73	8.01	7.37	7.01
					80	9.28	7.76	7.70	7.87	7.26	7.00
Δδ						0.01	-0.04	-0.03	-0.14	-0.11	-0.01
$[C_8C_1Im]^+$	Cl^-	$ZnCl_2$	0.6	13.9	25	9.08	7.75	7.69	8.09	7.45	7.02
					80	9.06	7.71	7.65	7.99	7.35	7.03
Δδ						-0.02	-0.04	-0.04	-0.10	-0.10	0.01

TGA Data

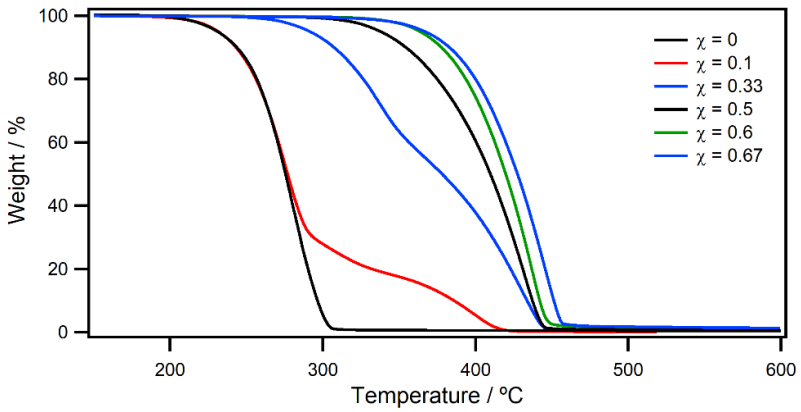

Figure S71 Temperature ramping TGA data for $[C_8C_1Im]Br_\chi ZnBr_2$ under nitrogen at 10 °C min^{-1}.

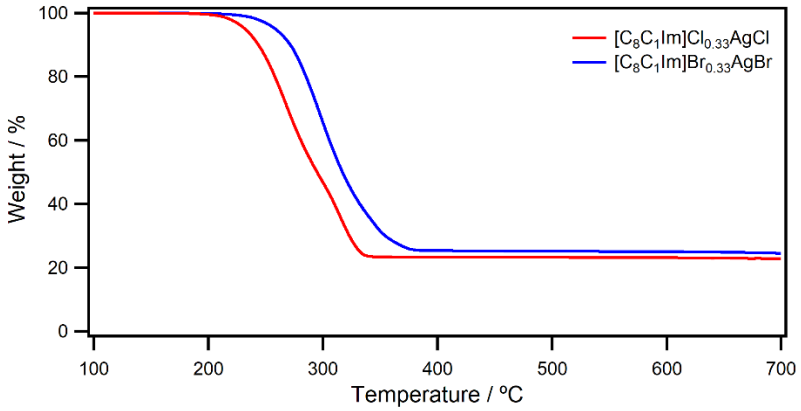

Figure S72 Temperature ramping TGA data for $[C_8C_1Im]X_{0.33}AgX$ under nitrogen at 10 °C min^{-1}.

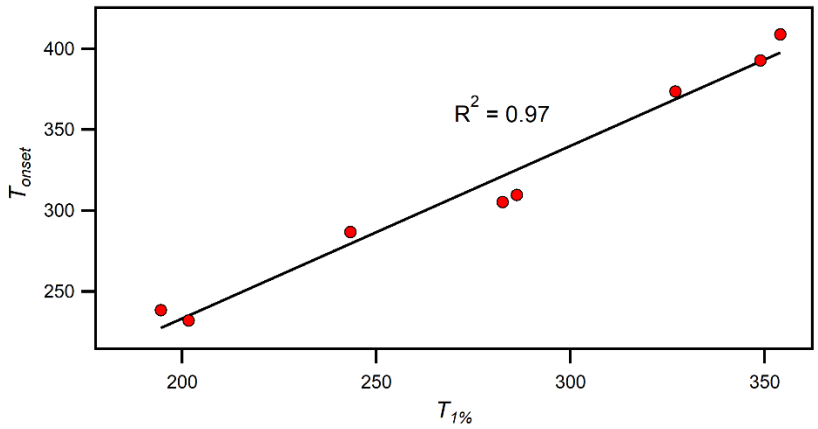

Figure S73 Correlation between T_{onset} and $T_{1\%}$ for $[C_8C_1Im]_\chi ZnCl_2$.

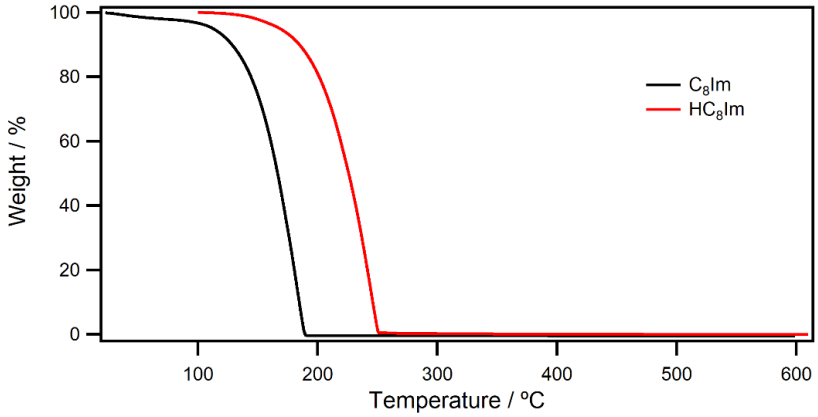

Figure S74 TGA ramping data at 10 °C min^{-1} in an N_2 atmosphere for neutral C_8Im and ionic HC_8Im.

TGA Kinetics

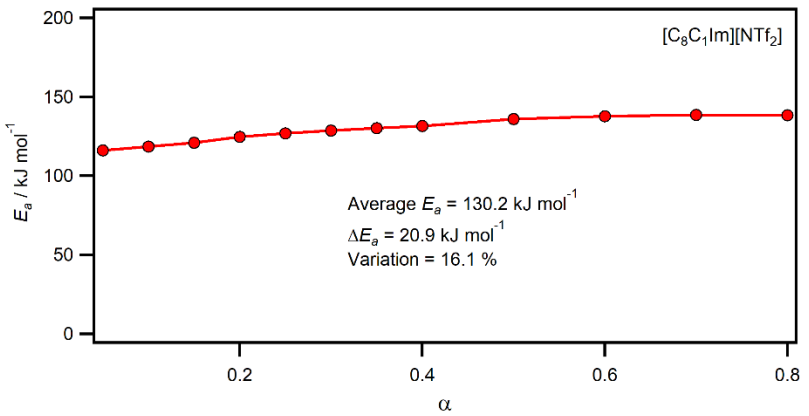

Figure S75 Activation energy with degree of conversion for $[C_8C_1Im][NTf_2]$ under nitrogen from Flynn-Wall isoconversion.

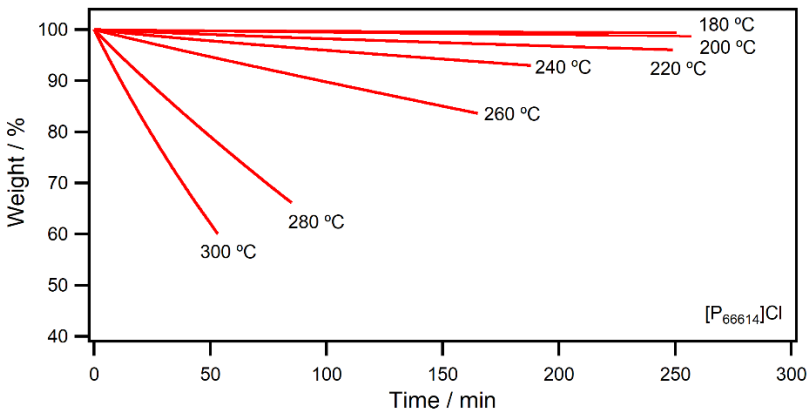

Figure S76 Isothermal decompositions of $[P_{66614}]Cl$ at several temperatures.

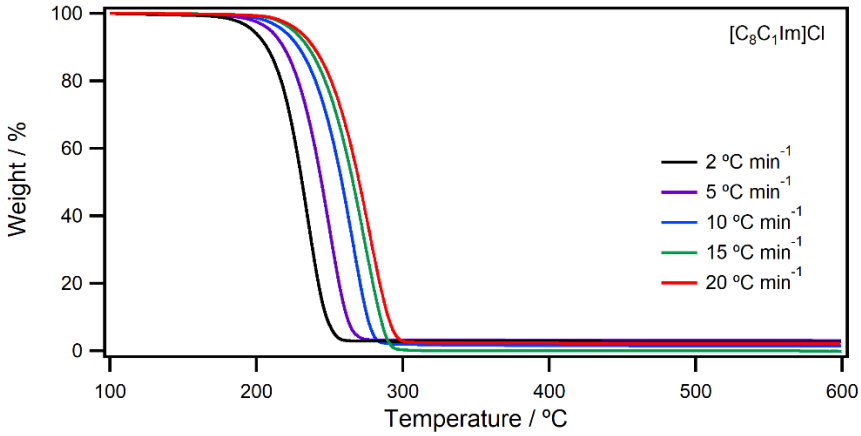

Figure S77 Variable heating rate TGA data for $[C_8C_1Im]Cl$ under nitrogen for Flynn-Wall isoconversion analysis.

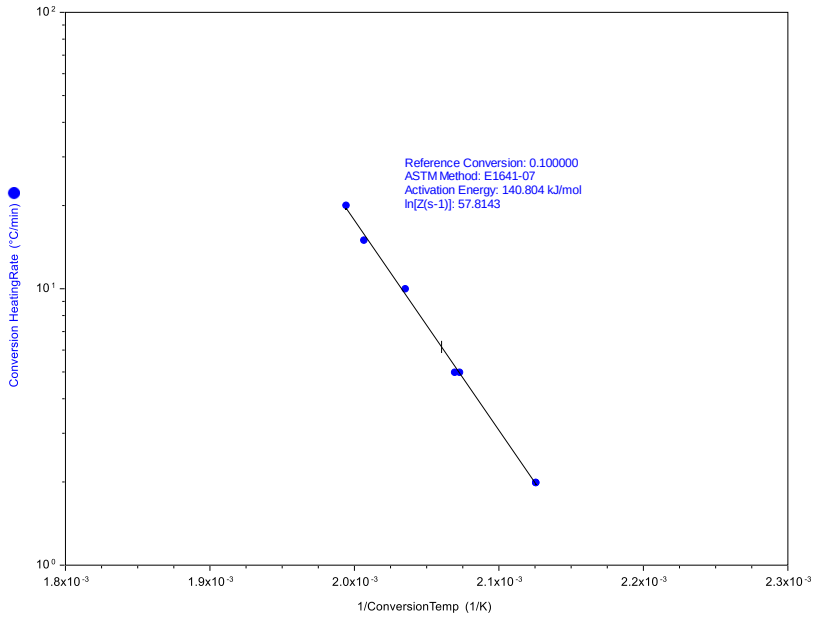

Figure S78 Flynn-Wall isoconversion (ASTM E1641) for $[C_8C_1Im]Cl$ at 0.05 conversion (5 %) under a nitrogen atmosphere using heating rates of 2 °C min^{-1}, 5 °C min^{-1}, 10 °C min^{-1}, 15 °C min^{-1}, and 20 °C min^{-1}.

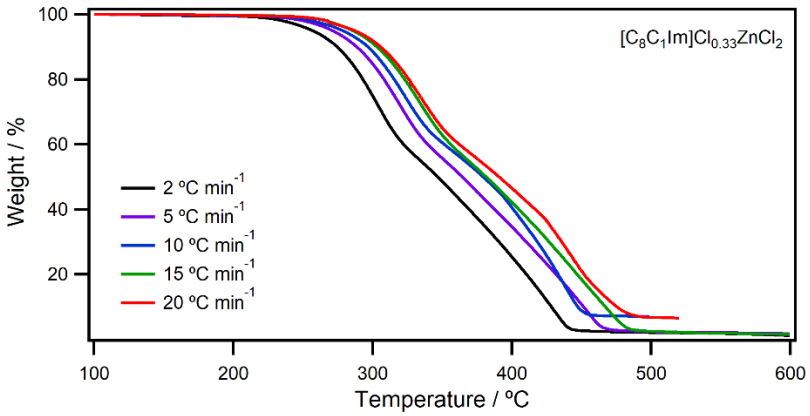

Figure S79 Variable heating rate TGA data for $[C_8C_1Im]Cl_{0.33}ZnCl_2$ under nitrogen for Flynn-Wall isoconversion analysis.

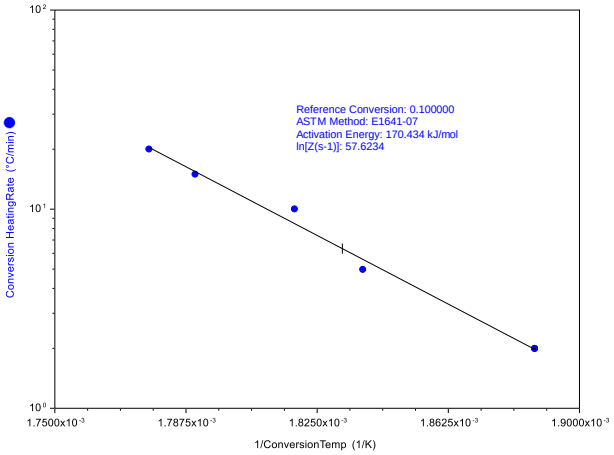

Figure S80 Flynn-Wall isoconversion (ASTM E1641) for $[C_8C_1Im]Cl_{0.33}ZnCl_2$ at 0.05 conversion (5 %) under a nitrogen atmosphere using heating rates of 2 °C min^{-1}, 5 °C min^{-1}, 10 °C min^{-1}, 15 °C min^{-1}, and 20 °C min^{-1}.

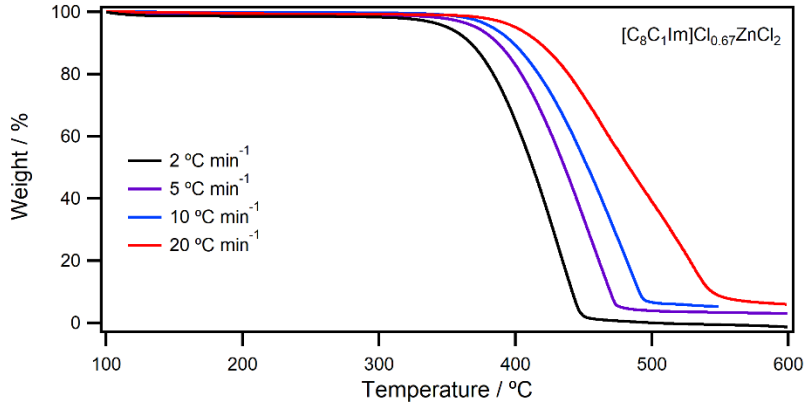

Figure S81 Variable heating rate TGA data for $[C_8C_1Im]Cl_{0.67}ZnCl_2$ under nitrogen for Flynn-Wall isoconversion analysis.

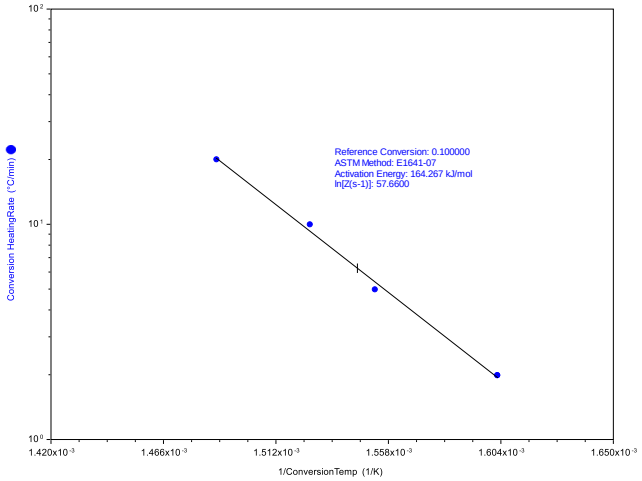

Figure S82 Flynn-Wall isoconversion (ASTM E1641) for $[C_8C_1Im]Cl_{0.67}ZnCl_2$ at 0.05 conversion (5 %) under a nitrogen atmosphere using heating rates of 2 °C min^{-1}, 5 °C min^{-1}, 10 °C min^{-1}, 15 °C min^{-1}, and 20 °C min^{-1}.

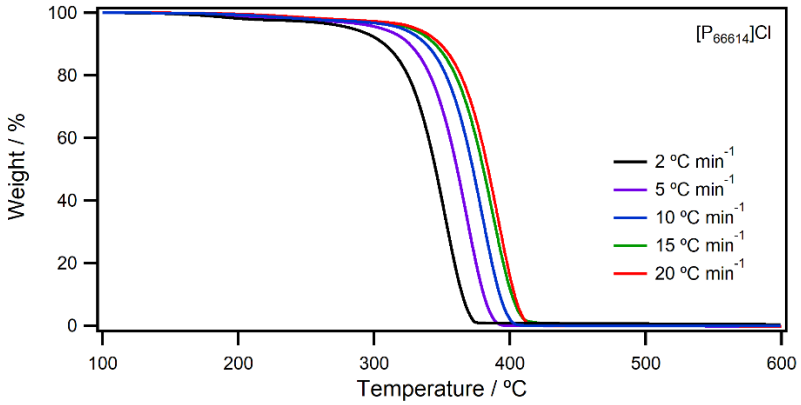

Figure S83 Variable heating rate TGA data for $[P_{66614}]Cl$ under nitrogen for Flynn-Wall isoconversion analysis.

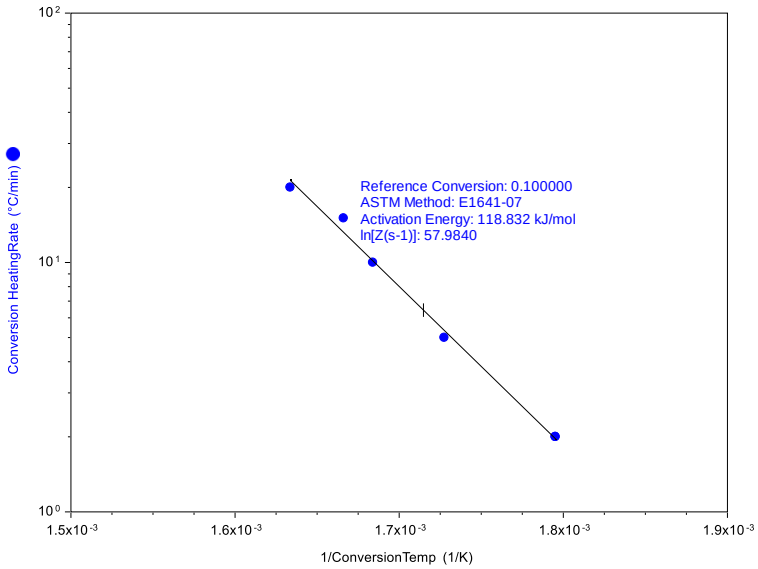

Figure S84 Flynn-Wall isoconversion (ASTM E1641) for $[P_{66614}]Cl$ at 0.05 conversion (5 %) under a nitrogen atmosphere using heating rates of 2 °C min^{-1}, 5 °C min^{-1}, 10 °C min^{-1}, 15 °C min^{-1}, and 20 °C min^{-1}.

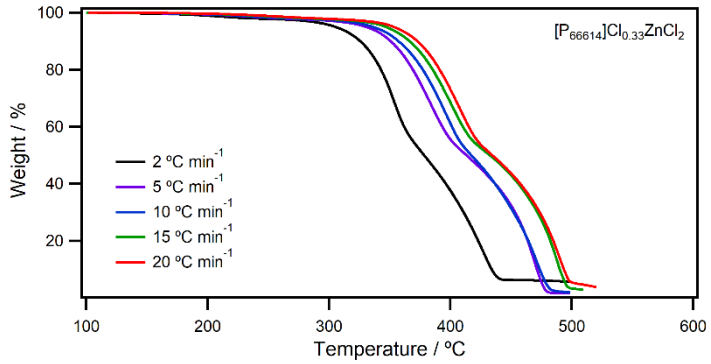

Figure S85 Variable heating rate TGA data for $[P_{66614}]Cl_{0.33}ZnCl_2$ under nitrogen for Flynn-Wall isoconversion analysis.

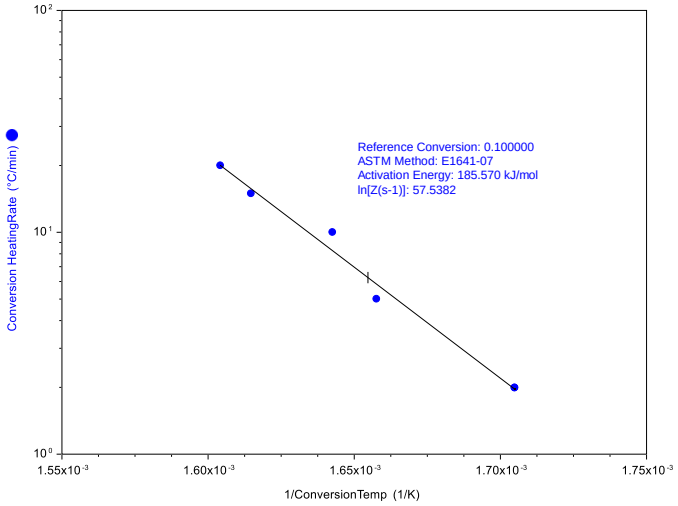

Figure S86 Flynn-Wall isoconversion (ASTM E1641) for $[P_{66614}]Cl_{0.33}ZnCl_2$ at 0.05 conversion (5 %) under a nitrogen atmosphere using heating rates of 2 °C min^{-1}, 5 °C min^{-1}, 10 °C min^{-1}, 15 °C min^{-1}, and 20 °C min^{-1}.

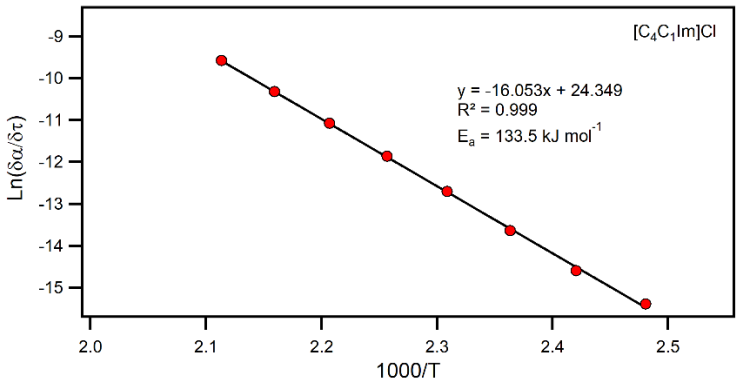

Figure S87 Stepwise isothermal kinetics for $[C_4C_1Im]Cl$ under a nitrogen atmosphere using a heating rate of 10 °C min^{-1}.

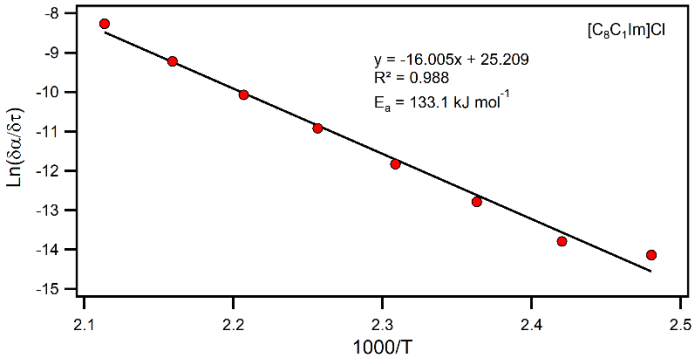

Figure S88 Stepwise isothermal kinetics for $[C_8C_1Im]Cl$ under a nitrogen atmosphere using a heating rate of 10 °C min^{-1}.

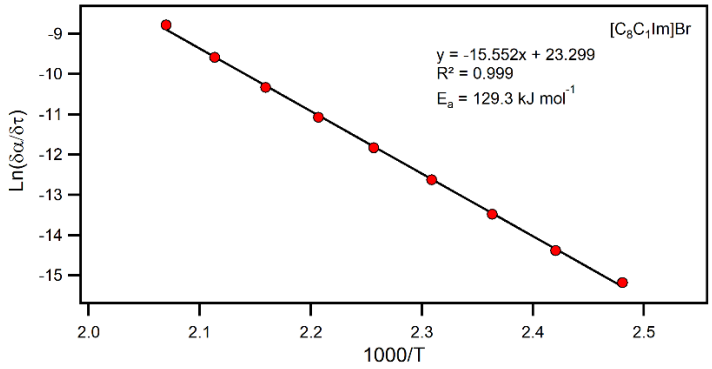

Figure S89 Stepwise isothermal kinetics for $[C_8C_1Im]Br$ under a nitrogen atmosphere using a heating rate of 10 °C min^{-1}.

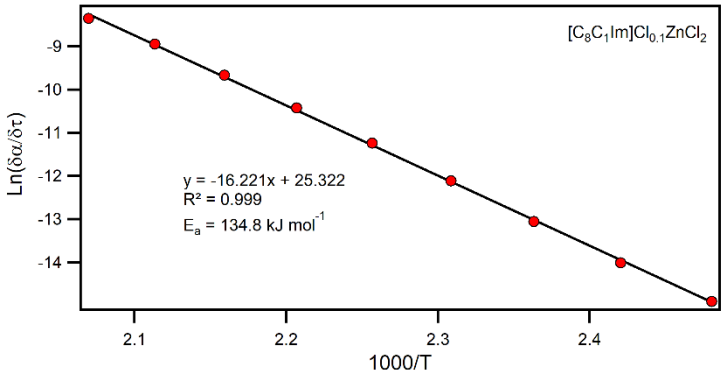

Figure S90 Stepwise isothermal kinetics for $[C_8C_1Im]Cl_{0.1}ZnCl_2$ under a nitrogen atmosphere using a heating rate of 10 °C min^{-1}

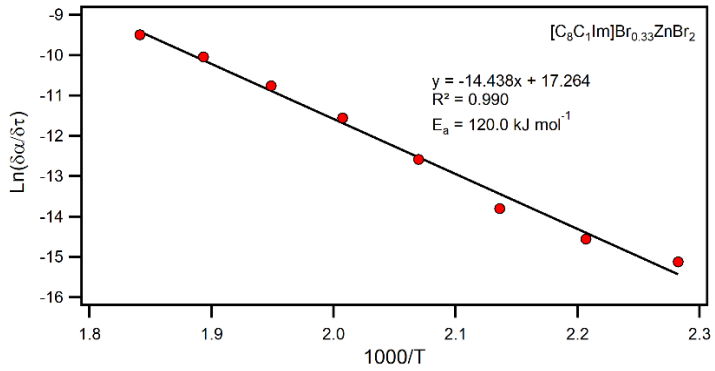

Figure S91 Stepwise isothermal kinetics for $[C_8C_1Im]Br_{0.33}ZnBr_2$ under a nitrogen atmosphere using a heating rate of 10 °C min^{-1}

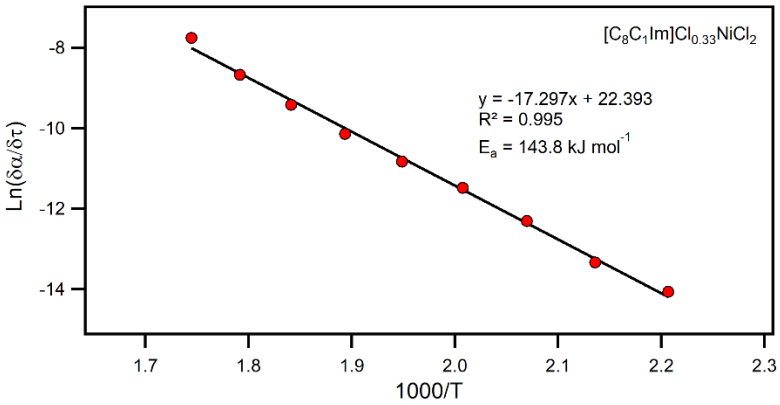

Figure S92 Stepwise isothermal kinetics for $[C_8C_1Im]Cl_{0.33}NiCl_2$ under a nitrogen atmosphere using a heating rate of 10 °C min^{-1}.

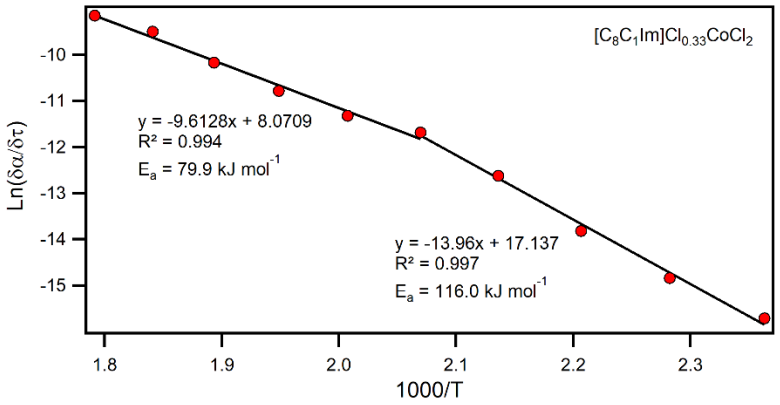

Figure S93 Stepwise isothermal kinetics for $[C_8C_1Im]Cl_{0.33}CoCl_2$ under a nitrogen atmosphere using a heating rate of 10 °C min^{-1}.

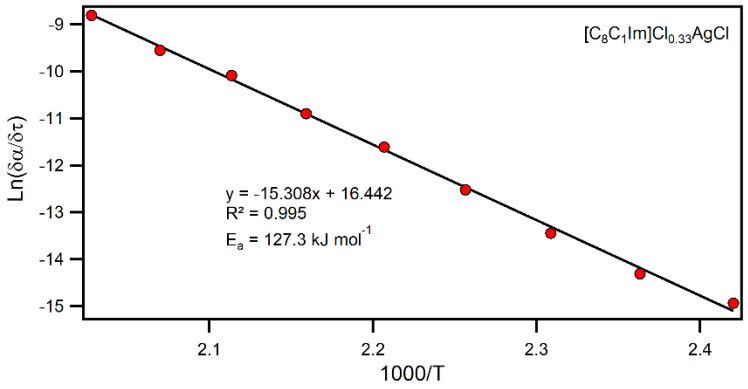

Figure S94 Stepwise isothermal kinetics for $[C_8C_1Im]Cl_{0.33}AgCl$ under a nitrogen atmosphere using a heating rate of 10 °C min^{-1}.

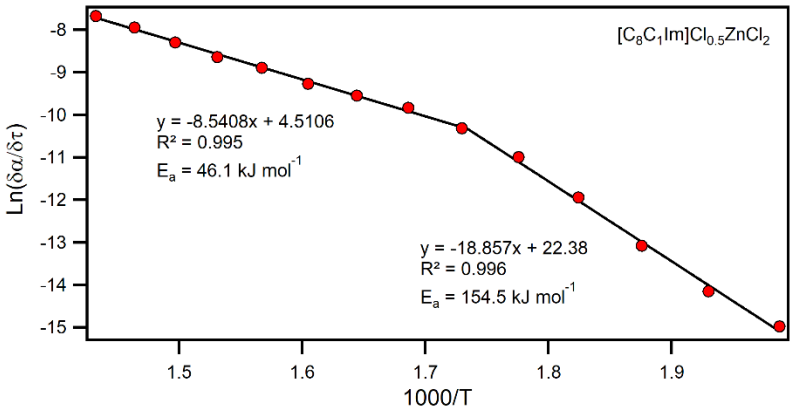

Figure S95 Stepwise isothermal kinetics for $[C_8C_1Im]Cl_{0.5}ZnCl_2$ under a nitrogen atmosphere using a heating rate of 10 °C min^{-1}.

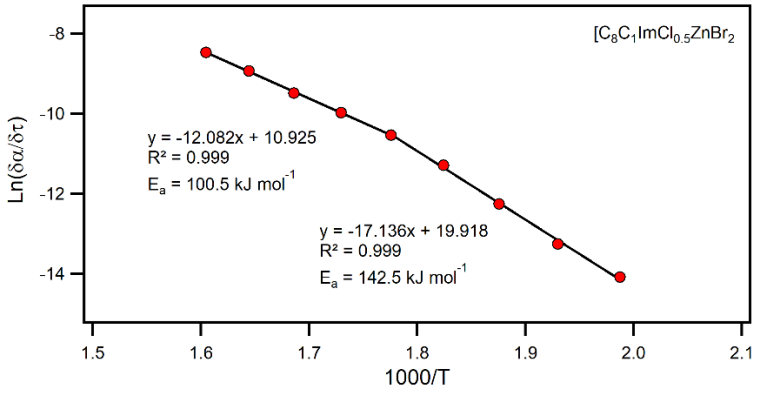

Figure S96 Stepwise isothermal kinetics for $[C_8C_1Im]Cl_{0.5}ZnBr_2$ under a nitrogen atmosphere using a heating rate of 10 °C min^{-1}.

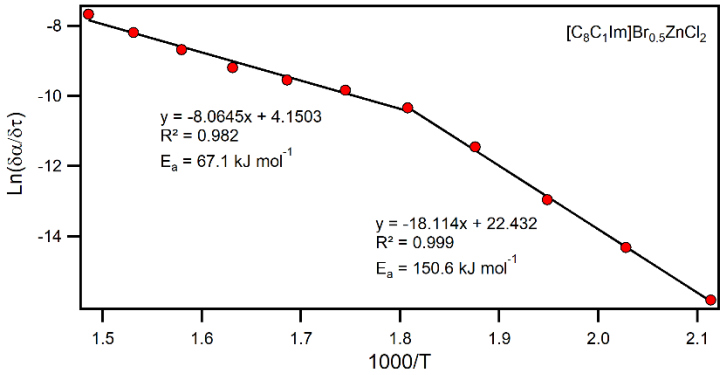

Figure S97 Stepwise isothermal kinetics for $[C_8C_1Im]Br_{0.5}ZnCl_2$ under a nitrogen atmosphere using a heating rate of 10 °C min^{-1}.

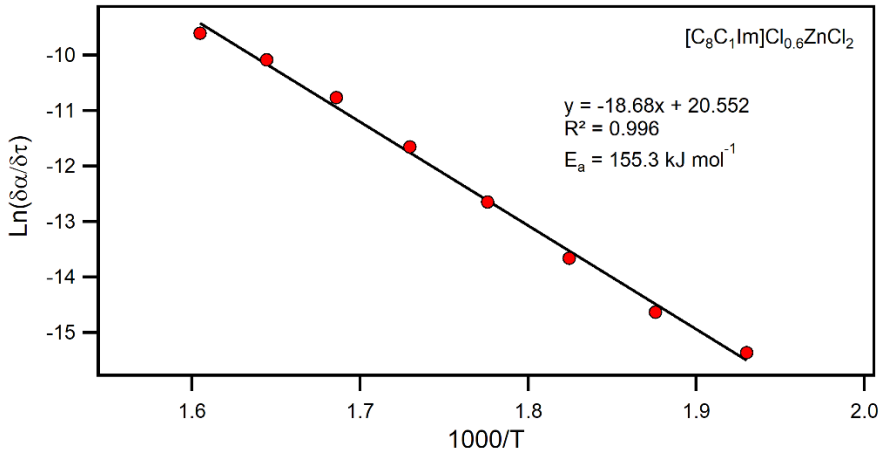

Figure S98 Stepwise isothermal kinetics for $[C_8C_1Im]Cl_{0.6}ZnCl_2$ under a nitrogen atmosphere using a heating rate of 10 °C min^{-1}.

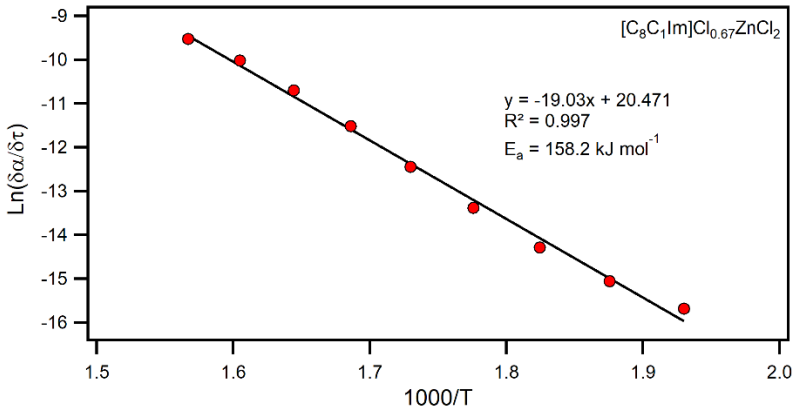

Figure S99 Stepwise isothermal kinetics for $[C_8C_1Im]Cl_{0.67}ZnCl_2$ under a nitrogen atmosphere using a heating rate of 10 °C min^{-1}.

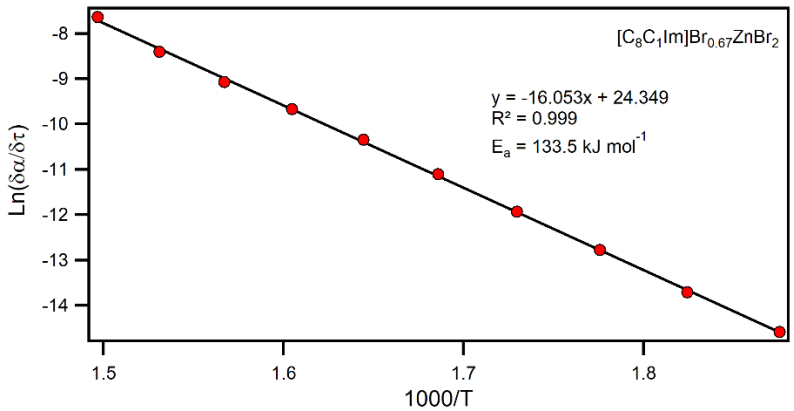

Figure S100 Stepwise isothermal kinetics for $[C_8C_1Im]Br_{0.67}ZnBr_2$ under a nitrogen atmosphere using a heating rate of 10 °C min^{-1}.

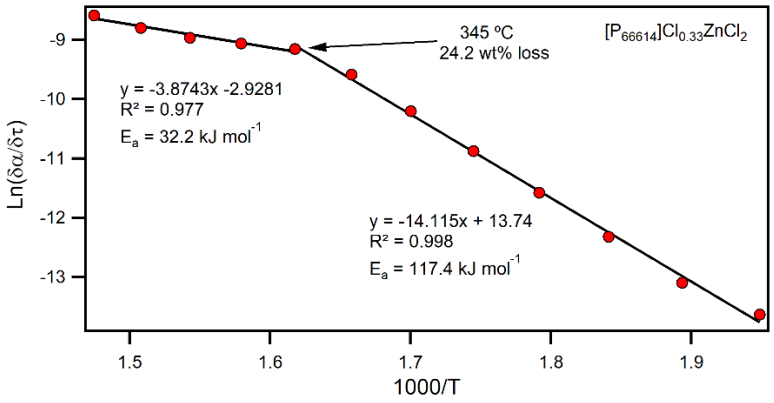

Figure S101 Stepwise isothermal kinetics for $[P_{66614}]Cl_{0.33}ZnCl_2$ under a nitrogen atmosphere using a heating rate of 10 °C min^{-1}.

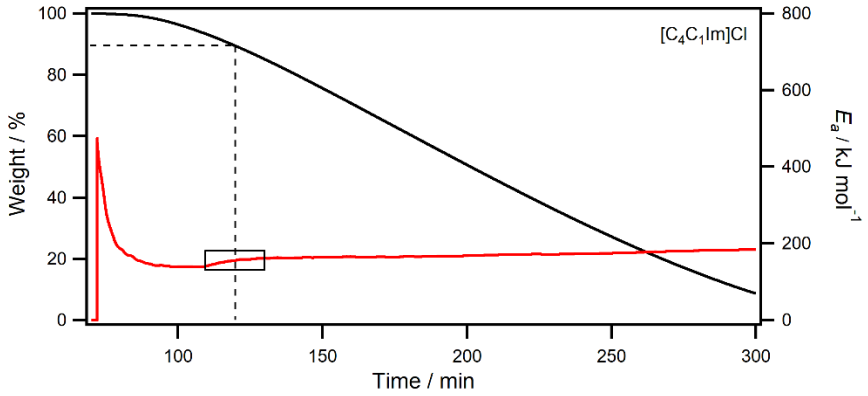

Figure S102 MTGA of $[C_4C_1Im]Cl$ under Hi-Res ramping (sensitivity = 1, resolution = 6) at 2 °C min^{-1} with a modulation temperature amplitude of 5 °C and a period of 200s.

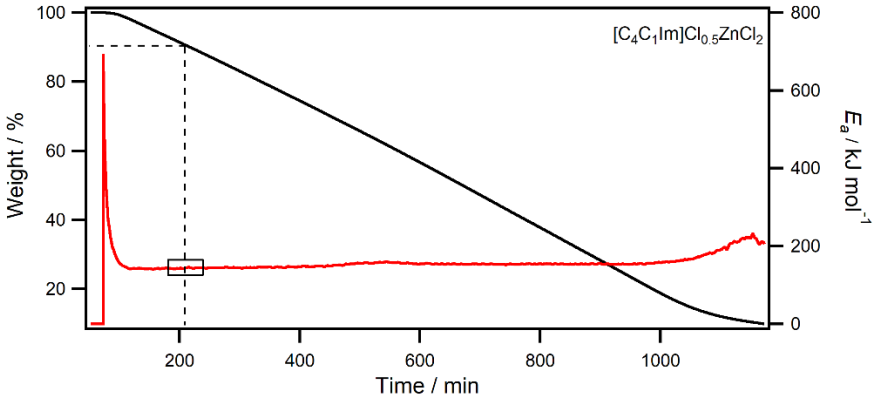

Figure S103 MTGA of $[C_4C_1Im]Cl_{0.5}ZnCl_2$ under Hi-Res ramping (sensitivity = 1, resolution = 6) at 2 °C min^{-1} with a modulation temperature amplitude of 5 °C and a period of 200s.

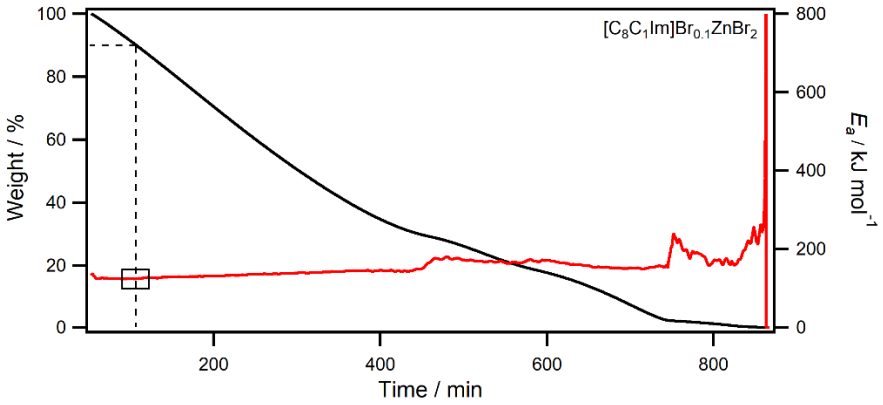

Figure S104 MTGA of $[C_8C_1Im]Br_{0.1}ZnBr_2$ under Hi-Res ramping (sensitivity = 1, resolution = 6) at 2 °C min^{-1} with a modulation temperature amplitude of 5 °C and a period of 200s.

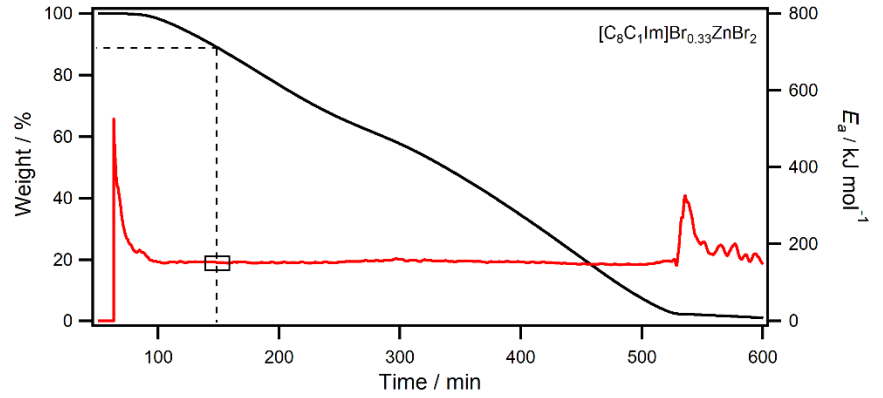

Figure S105 MTGA of $[C_8C_1Im]Br_{0.33}ZnBr_2$ under Hi-Res ramping (sensitivity = 1, resolution = 6) at 2 °C min^{-1} with a modulation temperature amplitude of 5 °C and a period of 200s.

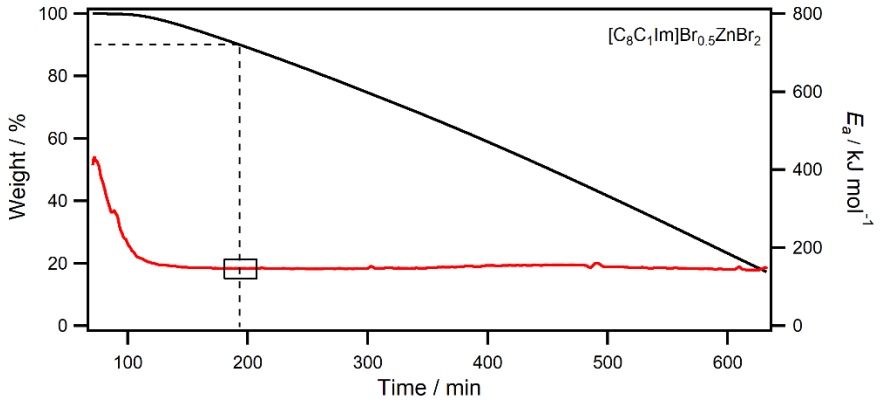

Figure S106 MTGA of $[C_8C_1Im]Br_{0.5}ZnBr_2$ under Hi-Res ramping (sensitivity = 1, resolution = 6) at 2 °C min^{-1} with a modulation temperature amplitude of 5 °C and a period of 200s.

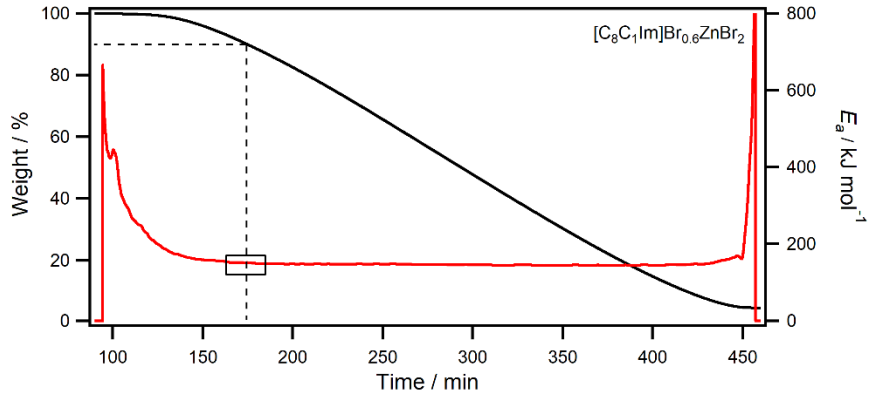

Figure S107 MTGA of $[C_8C_1Im]Br_{0.6}ZnBr_2$ under Hi-Res ramping (sensitivity = 1, resolution = 6) at 2 °C min^{-1} with a modulation temperature amplitude of 5 °C and a period of 200s.

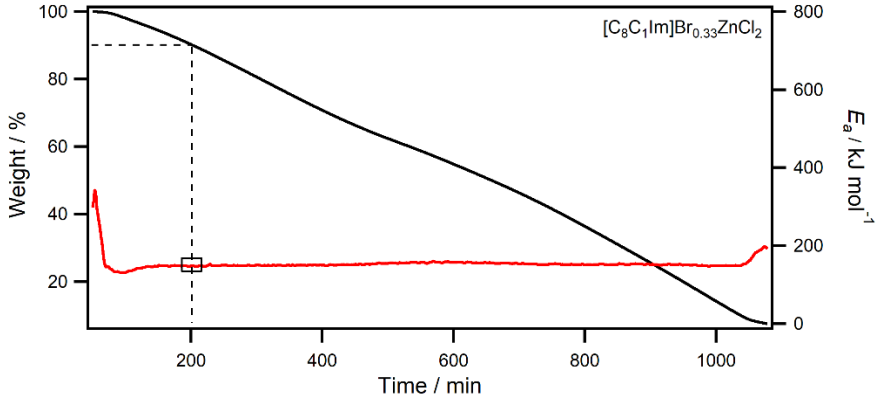

Figure S108 MTGA of $[C_8C_1Im]Br_{0.33}ZnCl_2$ under Hi-Res ramping (sensitivity = 1, resolution = 6) at 2 °C min^{-1} with a modulation temperature amplitude of 5 °C and a period of 200s.

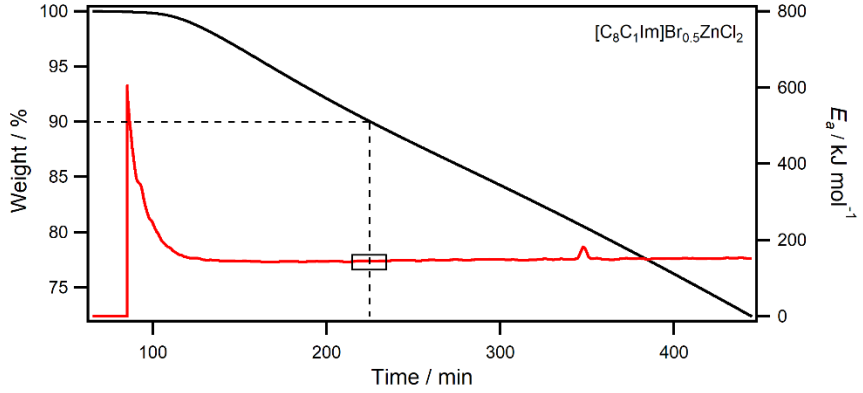

Figure S109 MTGA of $[C_8C_1Im]Br_{0.5}ZnCl_2$ under Hi-Res ramping (sensitivity = 1, resolution = 6) at 2 °C min^{-1} with a modulation temperature amplitude of 5 °C and a period of 200s.

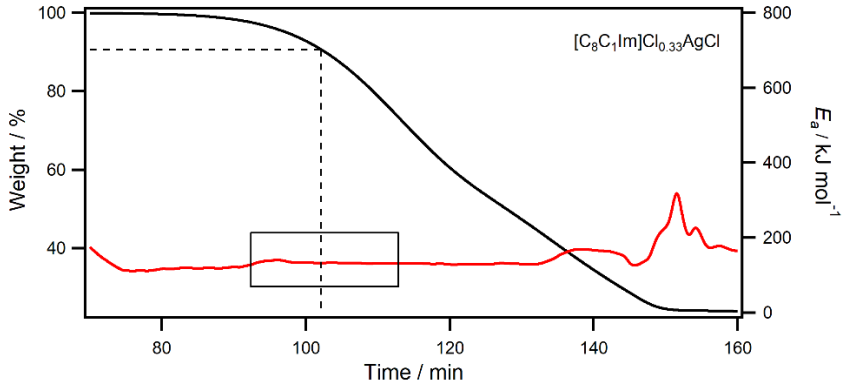

Figure S110 MTGA of $[C_4C_1Im]Cl_{0.33}AgCl$ under Hi-Res ramping (sensitivity = 1, resolution = 6) at 2 °C min^{-1} with a modulation temperature amplitude of 5 °C and a period of 200s.

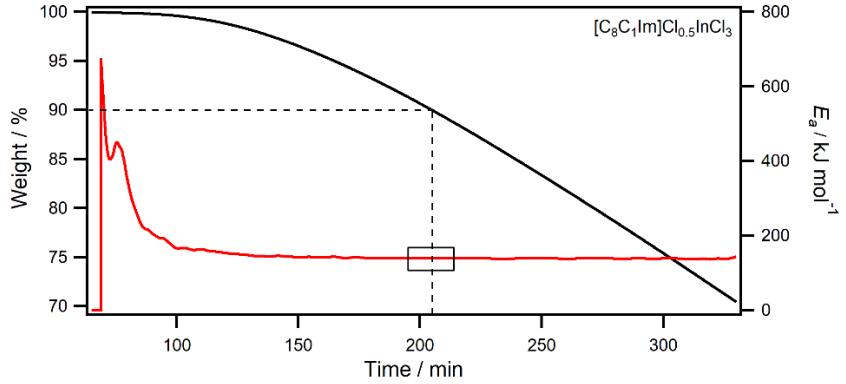

Figure S111 MTGA of $[C_8C_1Im]Cl_{0.5}InCl_3$ under Hi-Res ramping (sensitivity = 1, resolution = 6) at 2 °C min^{-1} with a modulation temperature amplitude of 5 °C and a period of 200s.

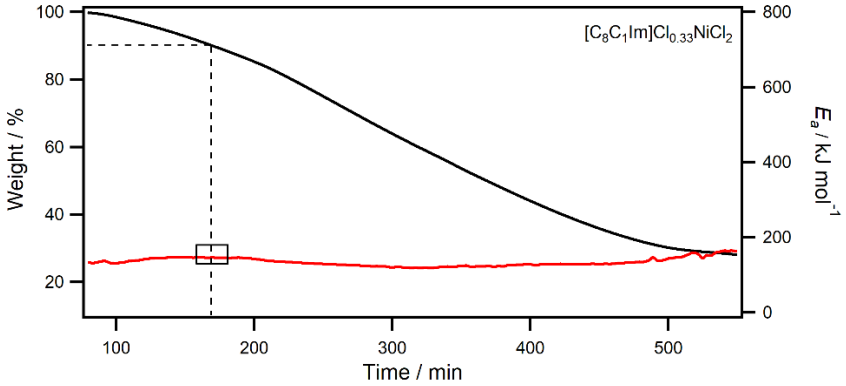

Figure S112 MTGA of $[C_8C_1Im]Cl_{0.33}NiCl_2$ under Hi-Res ramping (sensitivity = 1, resolution = 6) at 2 °C min^{-1} with a modulation temperature amplitude of 5 °C and a period of 200s.

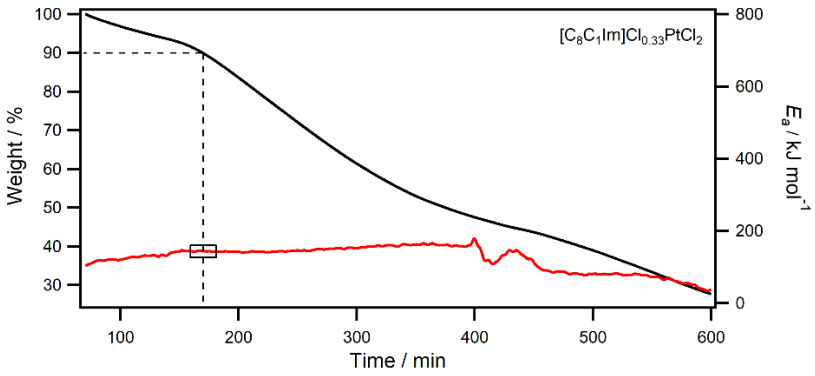

Figure S113 MTGA of $[C_8C_1Im]Cl_{0.33}PtCl_2$ under Hi-Res ramping (sensitivity = 1, resolution = 6) at 2 °C min^{-1} with a modulation temperature amplitude of 5 °C and a period of 200s.

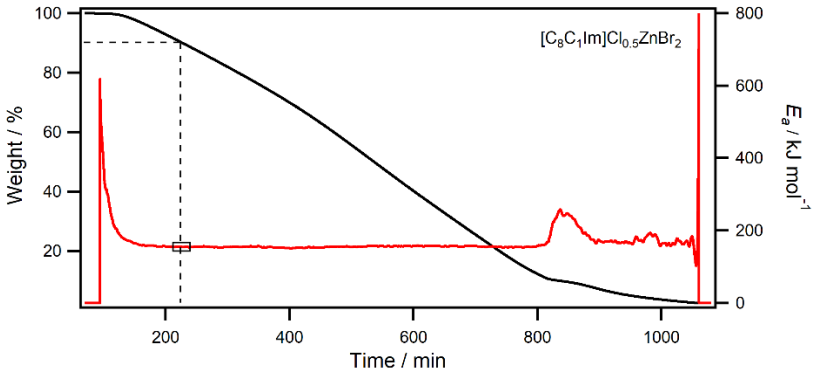

Figure S114 MTGA of $[C_8C_1Im]Cl_{0.5}ZnBr_2$ under Hi-Res ramping (sensitivity = 1, resolution = 6) at 2 °C min^{-1} with a modulation temperature amplitude of 5 °C and a period of 200s.

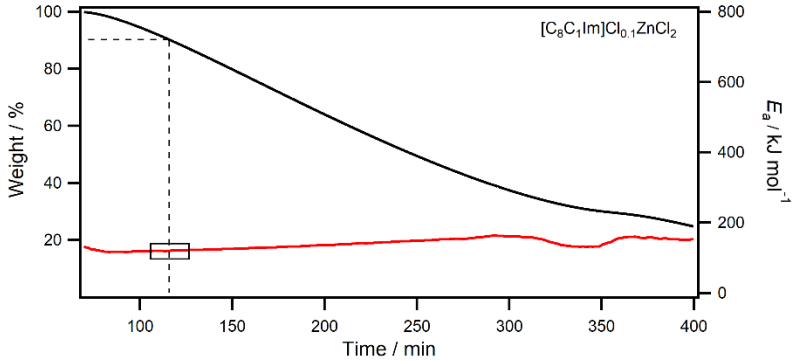

Figure S115 MTGA of $[C_8C_1Im]Cl_{0.1}ZnCl_2$ under Hi-Res ramping (sensitivity = 1, resolution = 6) at 2 °C min^{-1} with a modulation temperature amplitude of 5 °C and a period of 200s.

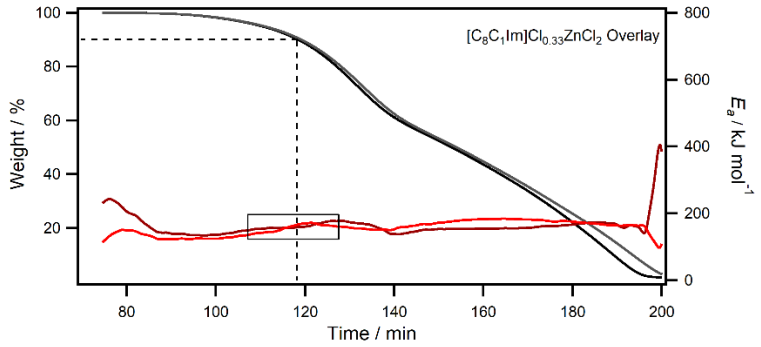

Figure S116 MTGA of $[C_8C_1Im]Cl_{0.33}ZnCl_2$ under Hi-Res ramping (sensitivity = 1, resolution = 6) at 2 °C min^{-1} with a modulation temperature amplitude of 5 °C and a period of 200s.

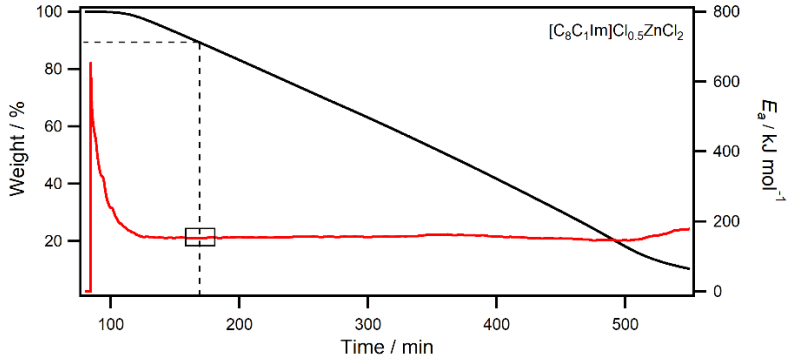

Figure S117 MTGA of $[C_8C_1Im]Cl_{0.5}ZnCl_2$ under Hi-Res ramping (sensitivity = 1, resolution = 6) at 2 °C min^{-1} with a modulation temperature amplitude of 5 °C and a period of 200s.

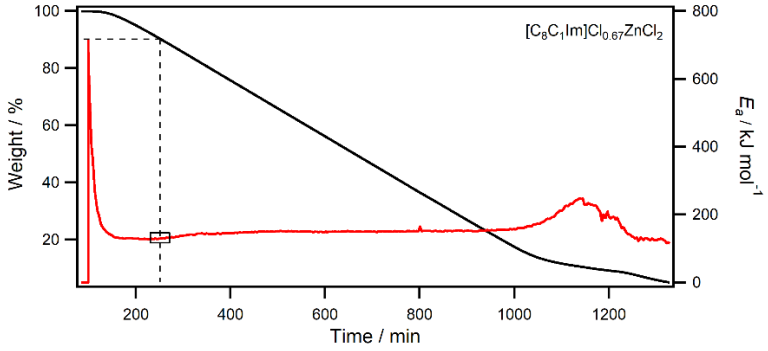

Figure S118 MTGA of $[C_8C_1Im]Cl_{0.67}ZnCl_2$ under Hi-Res ramping (sensitivity = 1, resolution = 6) at 2 °C min^{-1} with a modulation temperature amplitude of 5 °C and a period of 200s.

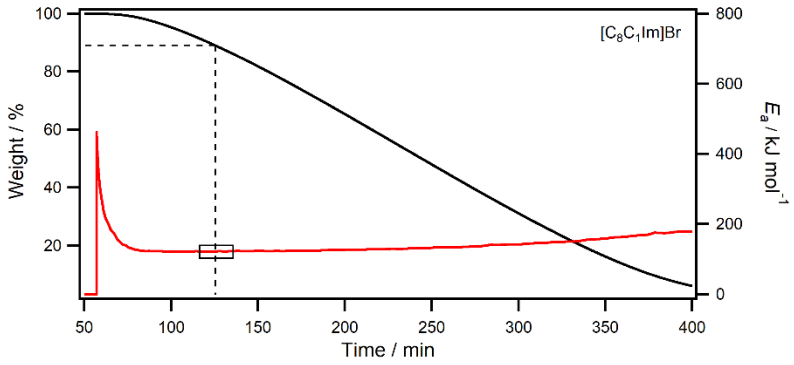

Figure S119 MTGA of $[C_8C_1Im]Br$ under Hi-Res ramping (sensitivity = 1, resolution = 6) at 2 °C min^{-1} with a modulation temperature amplitude of 5 °C and a period of 200s.

$T_{0.01/10}$ Long Term Thermal Stability

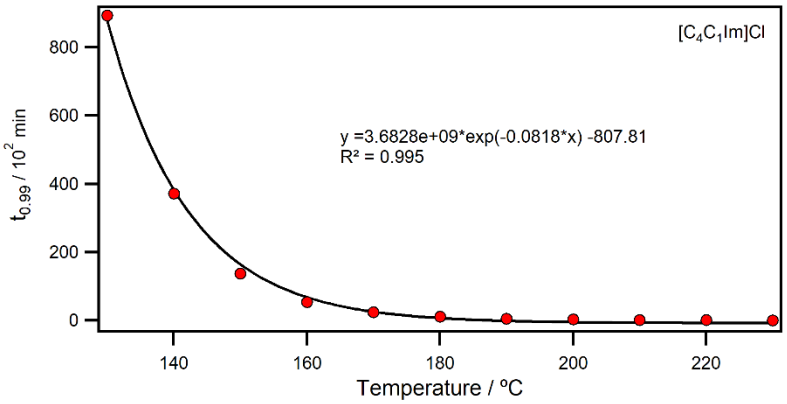

Figure S120 Fit used to calculate $T_{0.01/10}$ value for $[C_4C_1Im]Cl$.

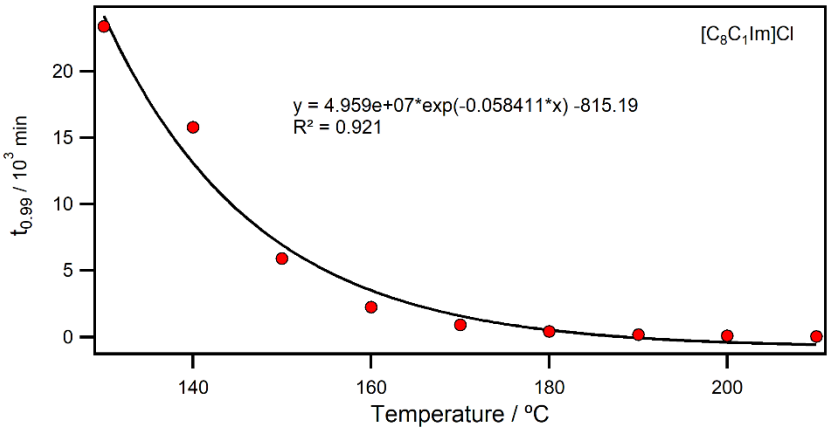

Figure S121 Fit used to calculate $T_{0.01/10}$ value for $[C_8C_1Im]Cl$.

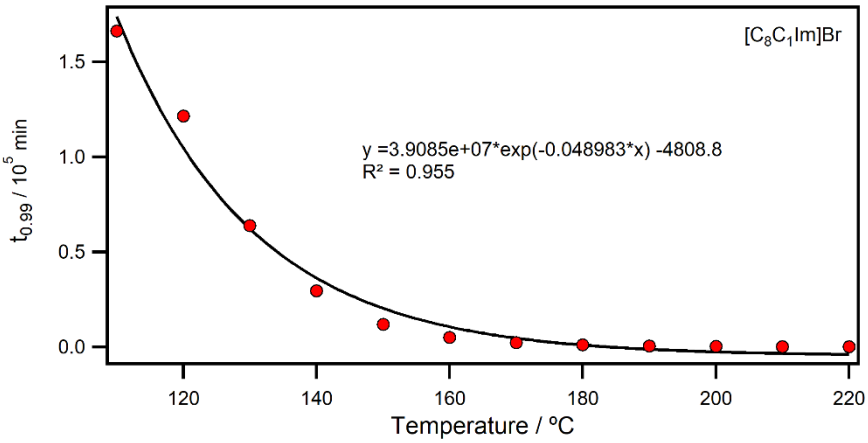

Figure S122 Fit used to calculate $T_{0.01/10}$ value for $[C_8C_1Im]Br$.

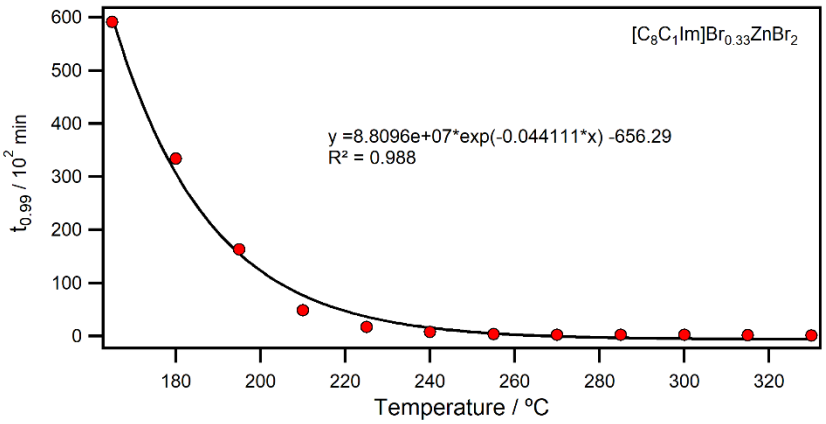

Figure S123 Fit used to calculate $T_{0.01/10}$ value for $[C_8C_1Im]Br_{0.33}ZnBr_2$.

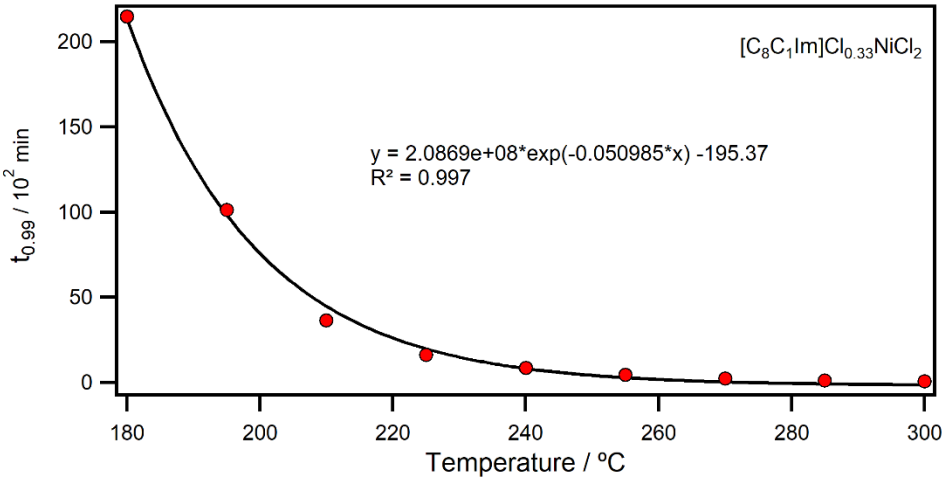

Figure S124 Fit used to calculate $T_{0.01/10}$ value for $[C_8C_1Im]Cl_{0.33}NiCl_2$.

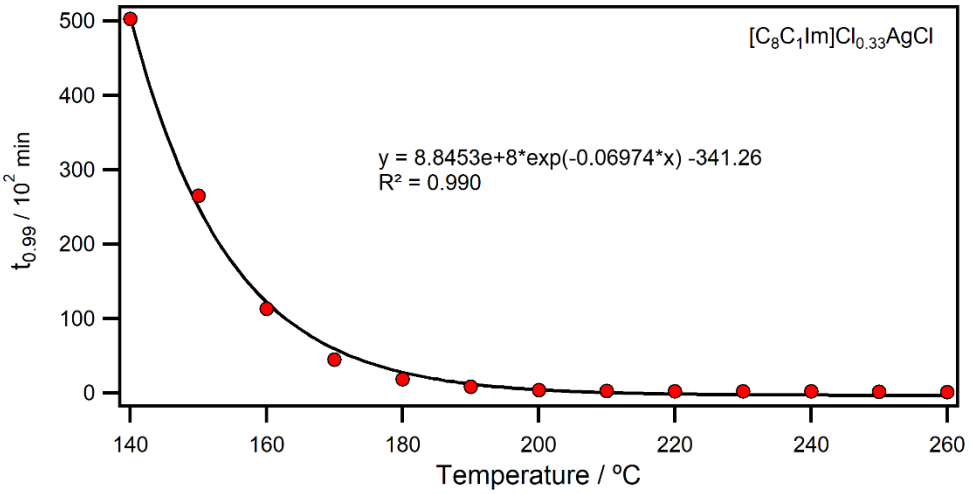

Figure S125 Fit used to calculate $T_{0.01/10}$ value for $[C_8C_1Im]Cl_{0.33}AgCl$.

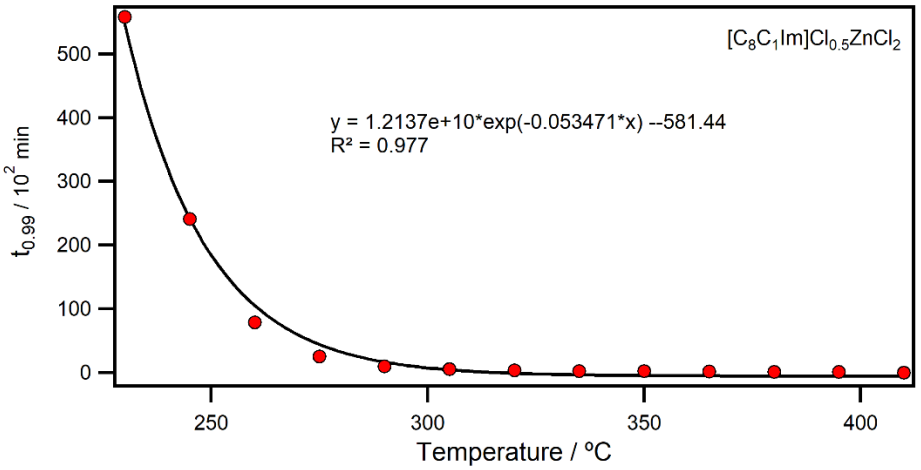

Figure S126 Fit used to calculate $T_{0.01/10}$ value for $[C_8C_1Im]Cl_{0.5}ZnCl_2$.

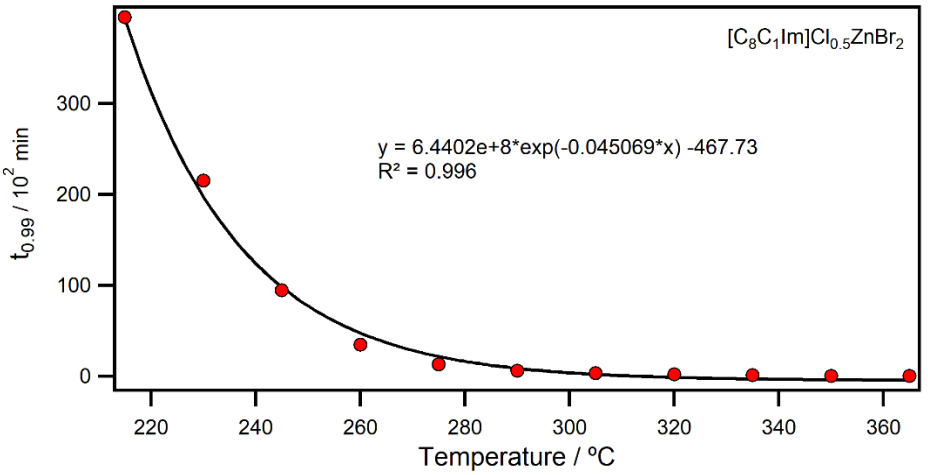

Figure S127 Fit used to calculate $T_{0.01/10}$ value for $[C_8C_1Im]Cl_{0.5}ZnBr_2$.

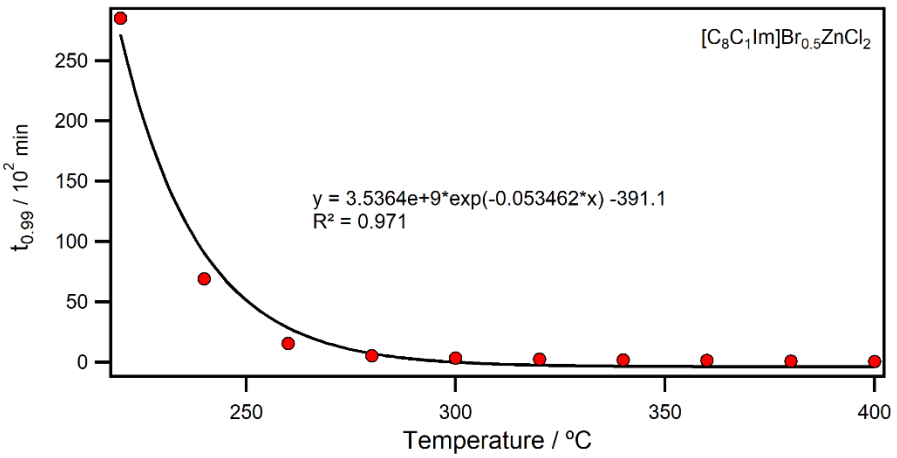

Figure S128 Fit used to calculate $T_{0.01/10}$ value for $[C_8C_1Im]Br_{0.5}ZnCl_2$.

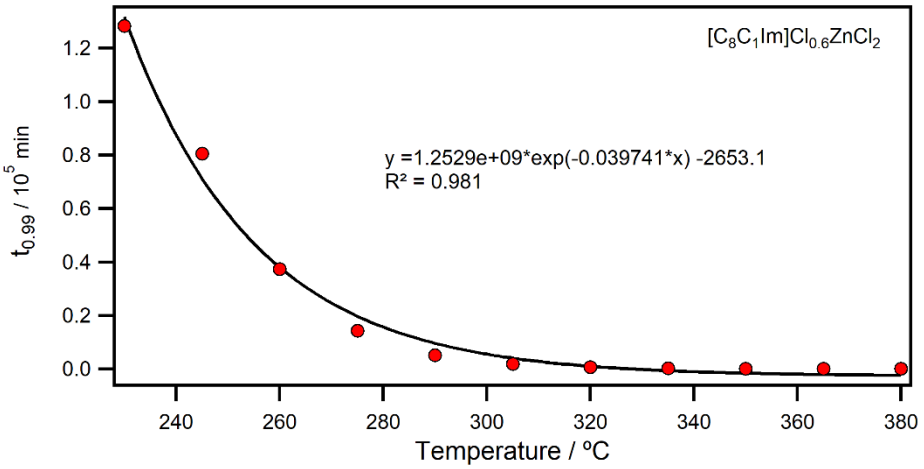

Figure S129 Fit used to calculate $T_{0.01/10}$ value for $[C_8C_1Im]Cl_{0.6}ZnCl_2$.

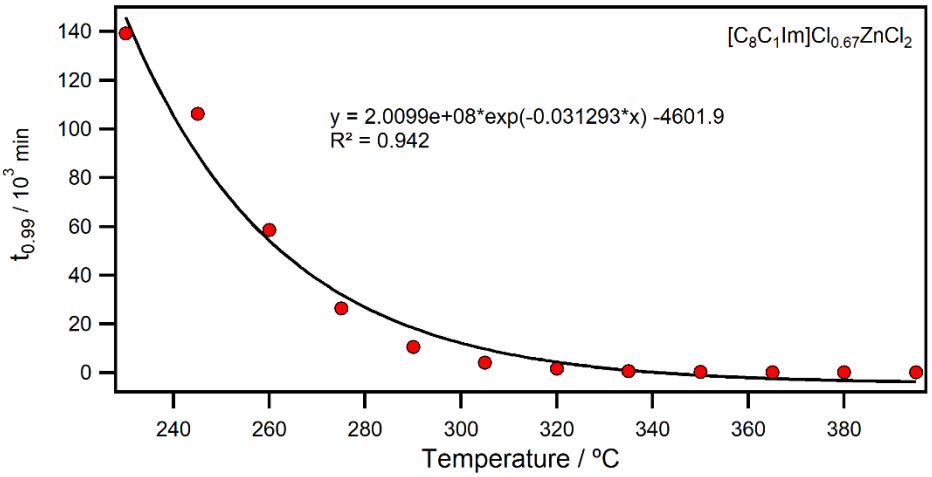

Figure S130 Fit used to calculate $T_{0.01/10}$ value for $[C_8C_1Im]Cl_{0.67}ZnCl_2$.

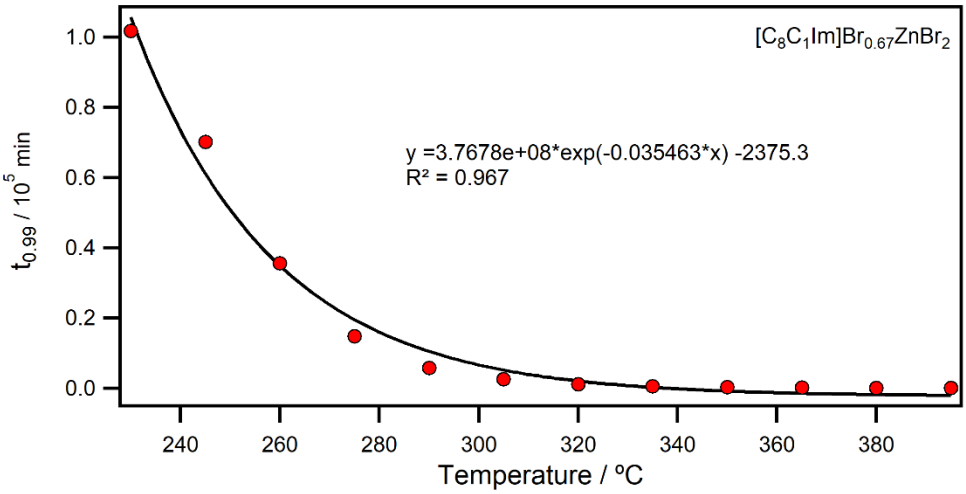

Figure S131 Fit used to calculate $T_{0.01/10}$ value for $[C_8C_1Im]Br_{0.67}ZnBr_2$.

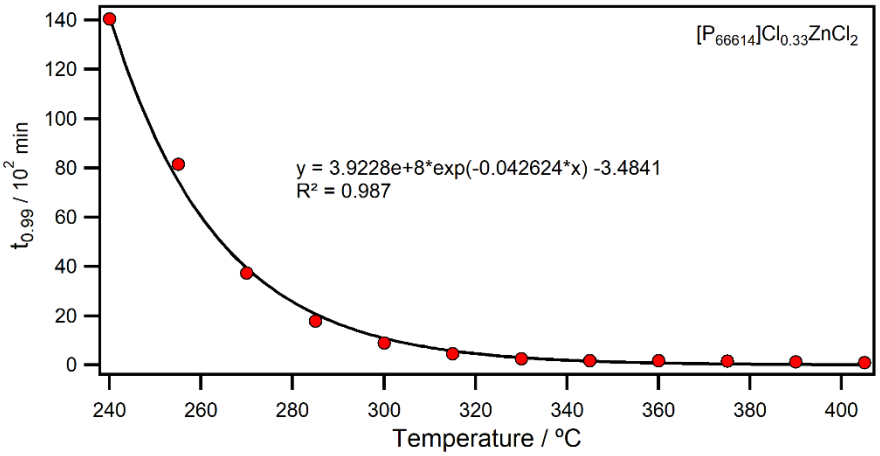

Figure S132 Fit used to calculate $T_{0.01/10}$ value for $[P_{66614}]Cl_{0.33}ZnCl_2$.

TGM-MS Data

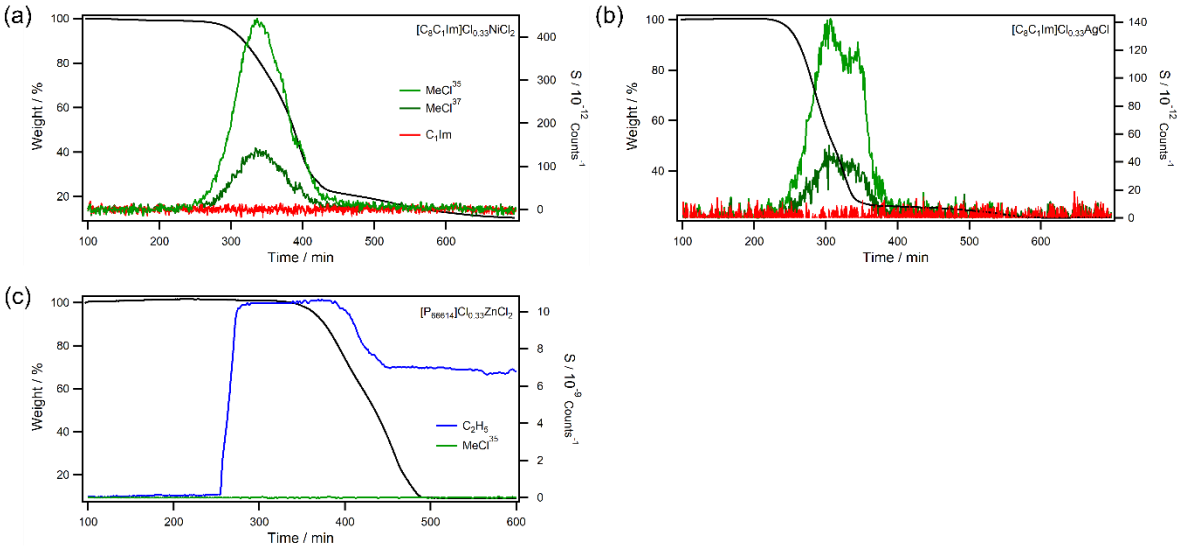

Figure S133 TGA-MS data for (a) $[C_8C_1Im]Cl_{0.33}NiCl_2$, (b) $[C_8C_1Im]Cl_{0.33}AgCl$, and (c) $[P_{66614}]Cl_{0.33}ZnCl_2$.

STA Data

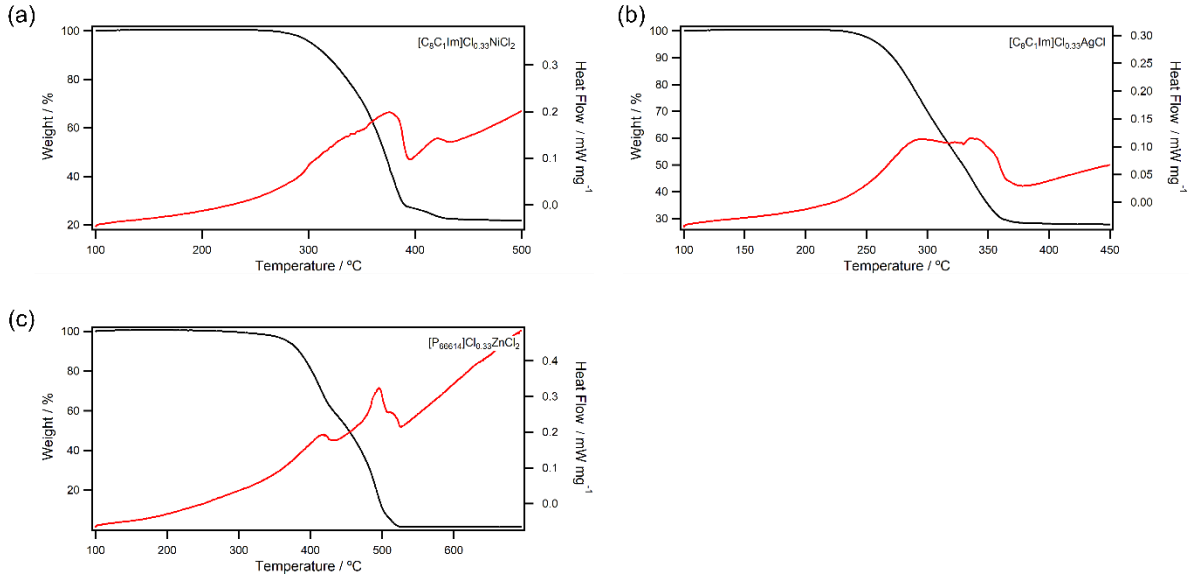

Figure S134 STA data for (a) $[C_8C_1Im]Cl_{0.33}NiCl_2$, (b) $[C_8C_1Im]Cl_{0.33}AgCl$, and (c) $[P_{66614}]Cl_{0.33}ZnCl_2$.

DSC Data

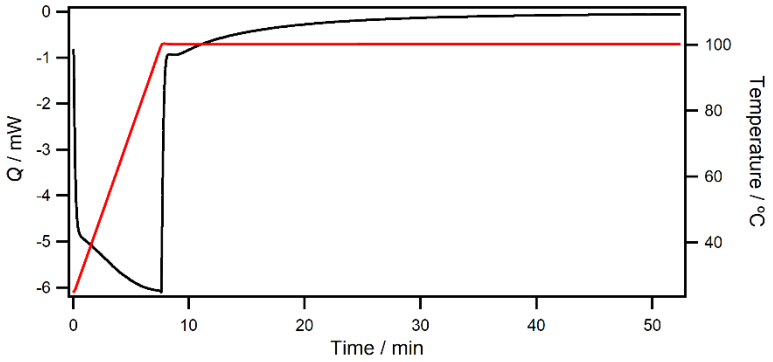

Figure S135 Heat Flow through $[C_8C_1Im]Cl_{0.33}ZnCl_2$ during drying isothermal step.

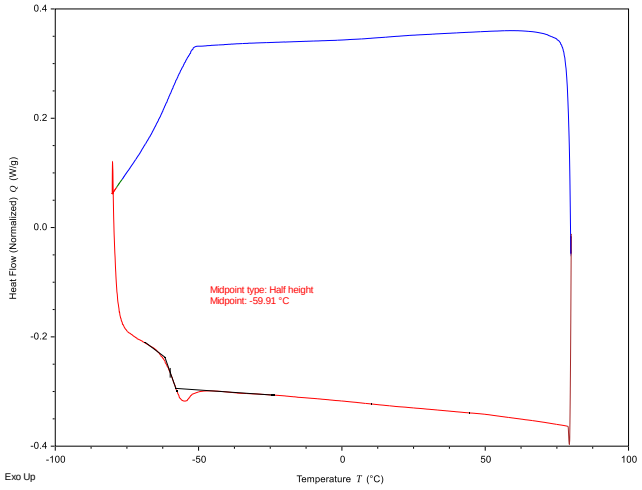

Figure S136 DSC data for $[C_8C_1Im]Cl$ at 10 °C min^{-1}.

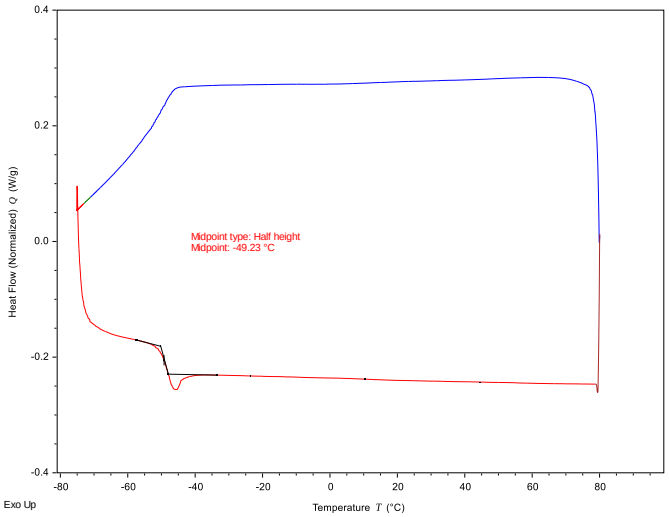

Figure S137 DSC data for $[C_4C_1Im]Cl_{0.5}ZnCl_2$ at 10 °C min^{-1}.

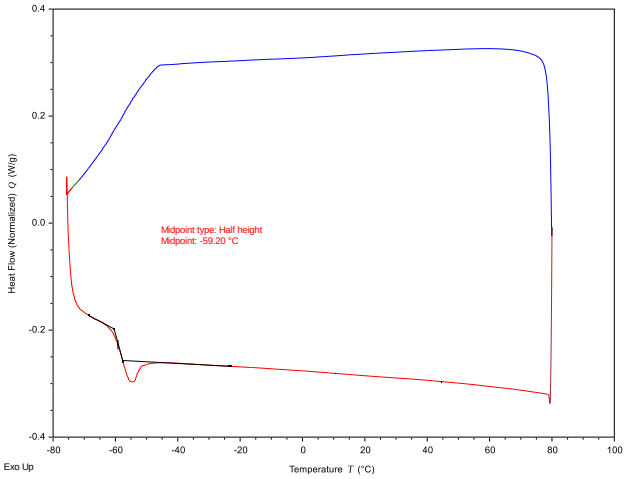

Figure S138 DSC data for $[C_4C_1Im]Cl_{0.33}ZnCl_2$ at 10 °C min^{-1}.

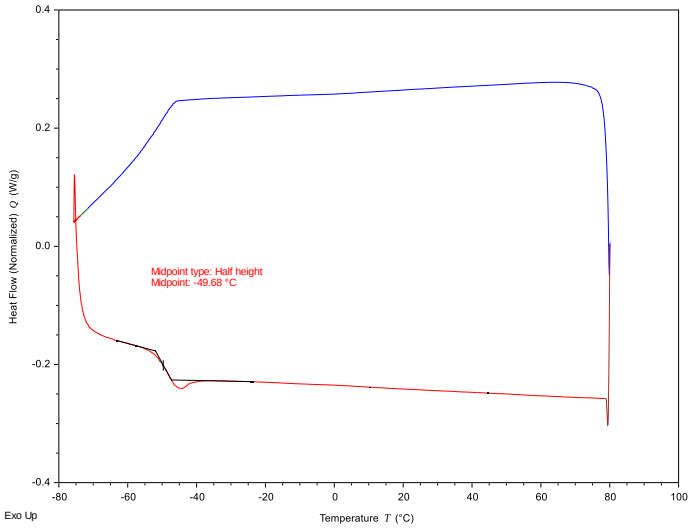

Figure S139 DSC data for $[C_8C_1Im]Br_{0.1}ZnBr_2$ at 10 °C min^{-1}.

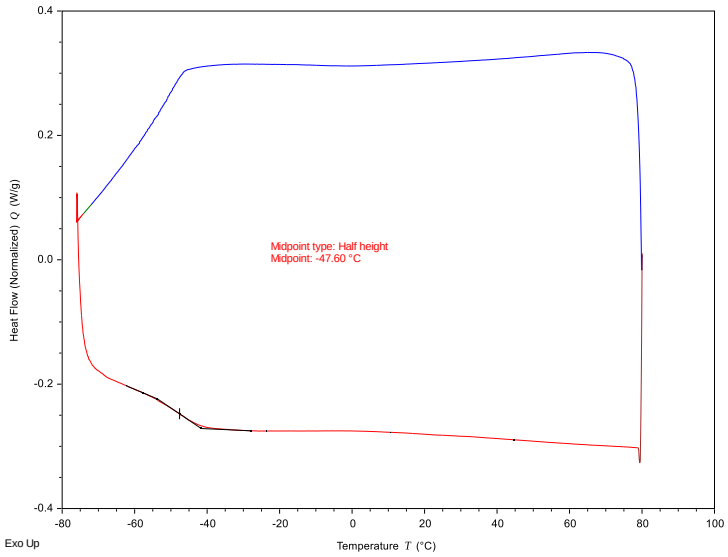

Figure S140 DSC data for $[C_8C_1Im]Cl_{0.5}InCl_3$ at 10 °C min^{-1}.

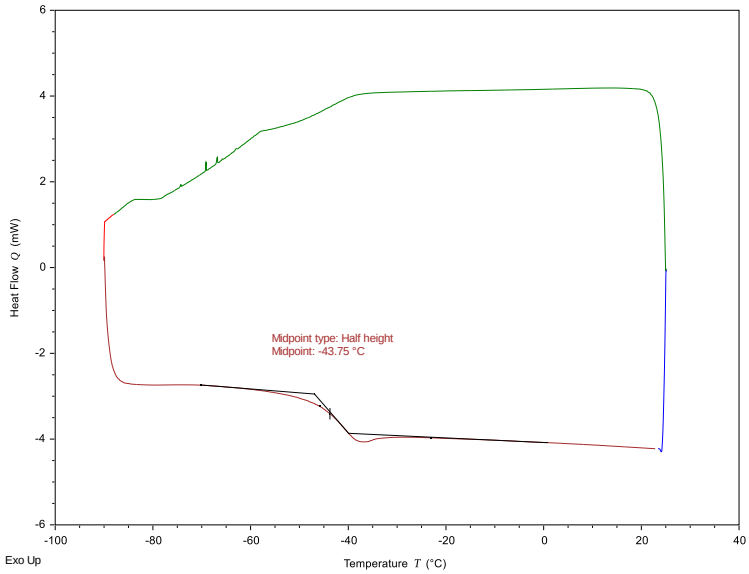

Figure S141 DSC data for $[C_8C_1Im]Cl_{0.33}NiCl_2$ at 10 °C min^{-1}.

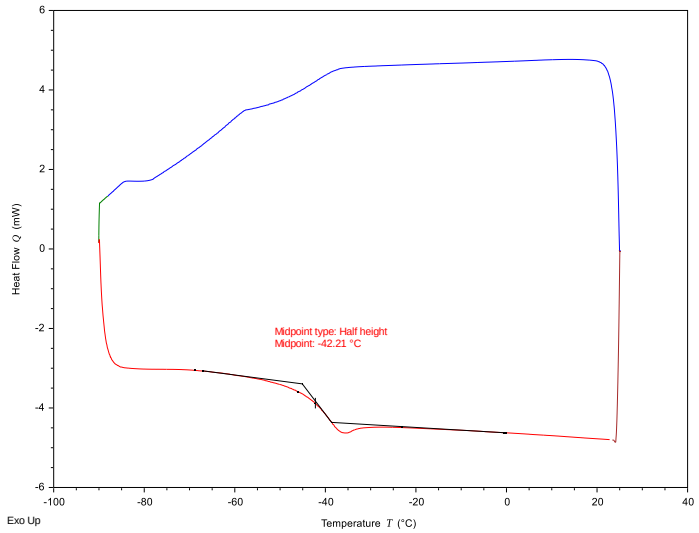

Figure S142 DSC data for $[C_8C_1Im]Cl_{0.33}CoCl_2$ at 10 °C min^{-1}.

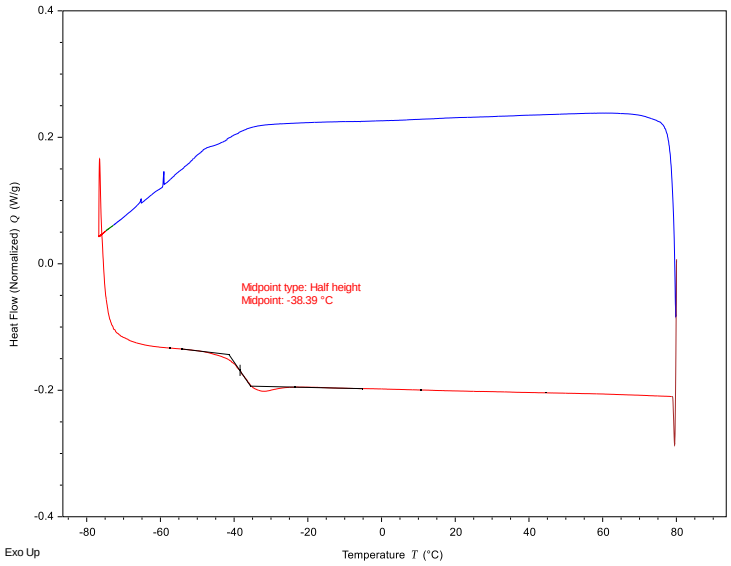

Figure S143 DSC data for $[C_8C_1Im]Cl_{0.67}ZnCl_2$ at 10 °C min^{-1}.

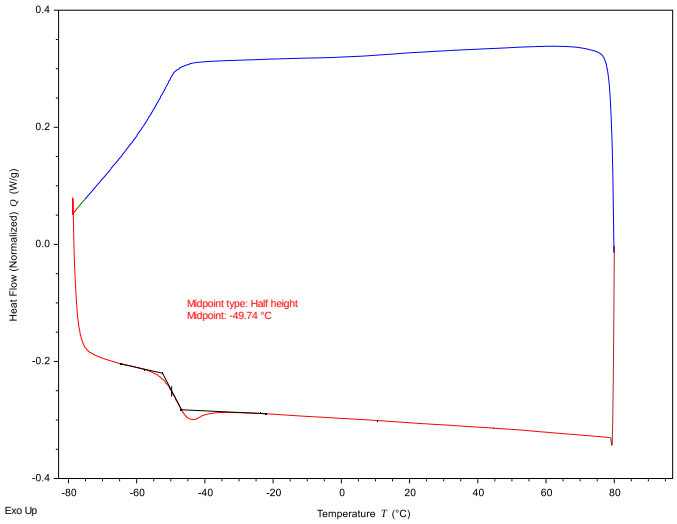

Figure S144 DSC data for $[C_8C_1Im]Cl_{0.1}ZnCl_2$ at 10 °C min^{-1}.

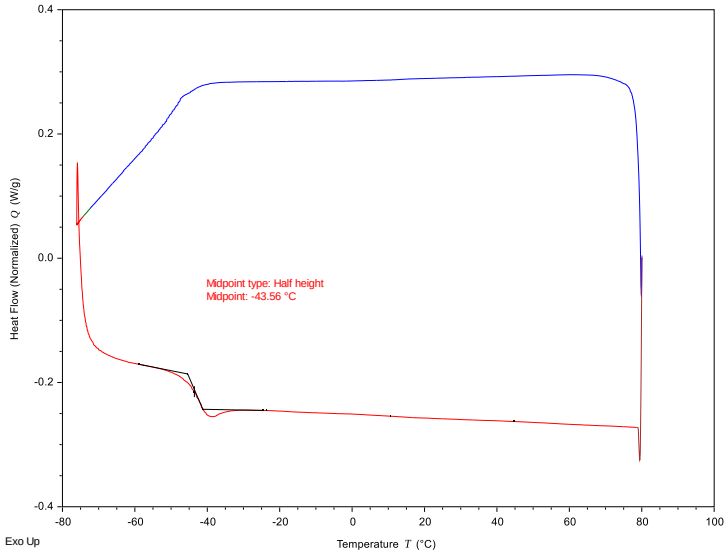

Figure S145 DSC data for $[C_8C_1Im]Cl_{0.4}ZnCl_2$ at 10 °C min^{-1}.

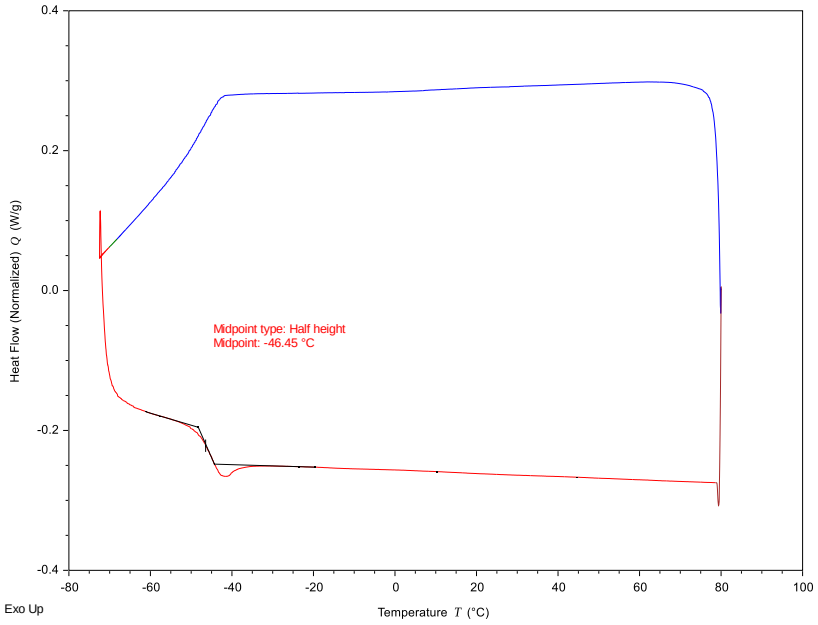

Figure S146 DSC data for $[C_8C_1Im]Cl_{0.43}ZnCl_2$ at 10 °C min^{-1}.

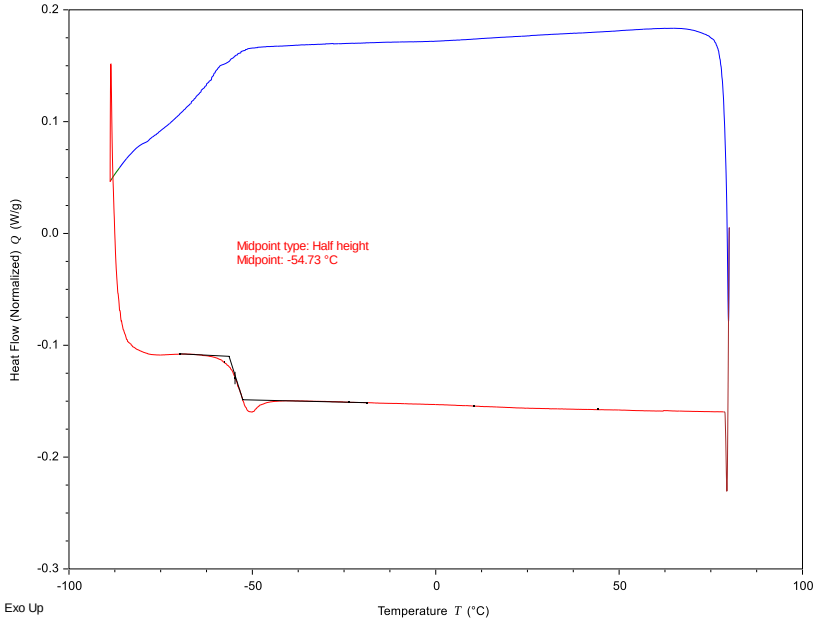

Figure S147 DSC data for $[C_8C_1Im]Br_{0.5}ZnBr_2$ at 10 °C min^{-1}.

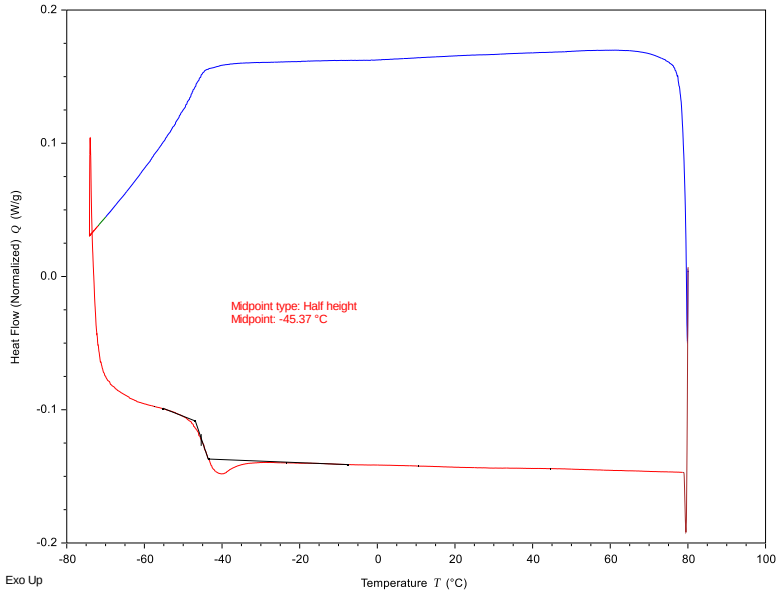

Figure S148 DSC data for $[C_8C_1Im]Br_{0.6}ZnBr_2$ at 10 °C min^{-1}.

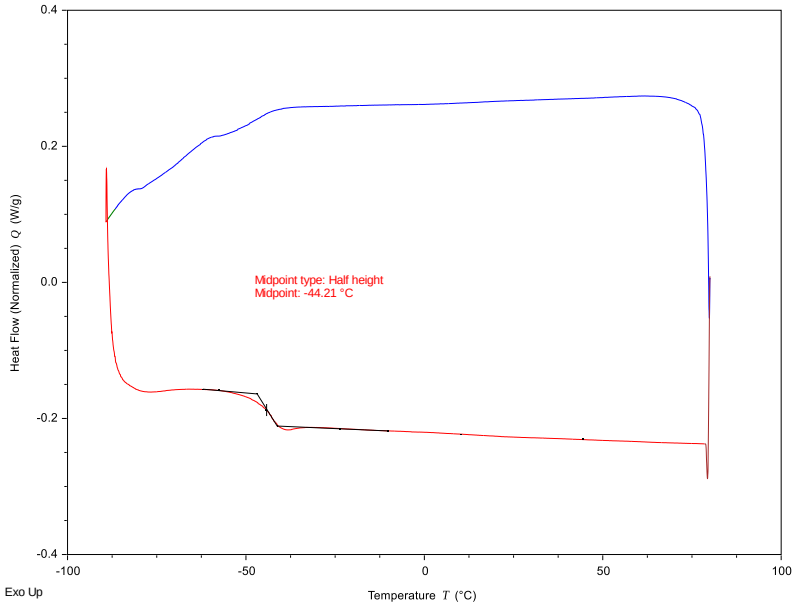

Figure S149 DSC data for $[C_8C_1Im]Br_{0.33}ZnBr_2$ at 10 °C min^{-1}.

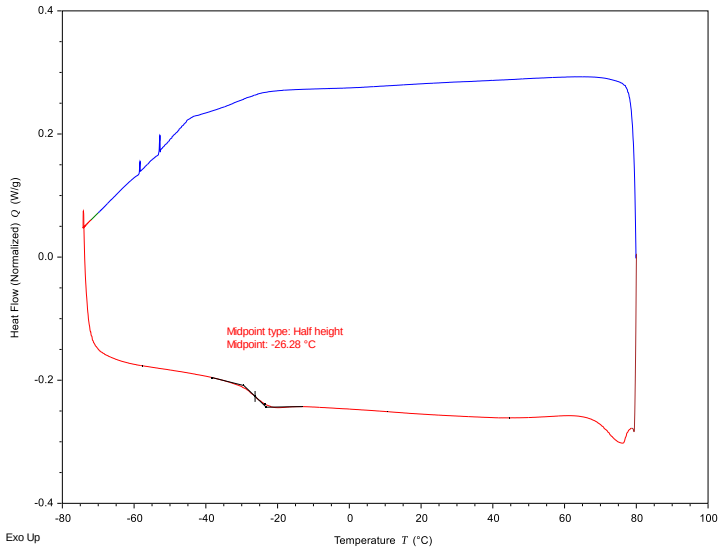

Figure S150 DSC data for $[C_8C_1Im]Cl_{0.33}PtCl_2$ at 10 °C min^{-1}.

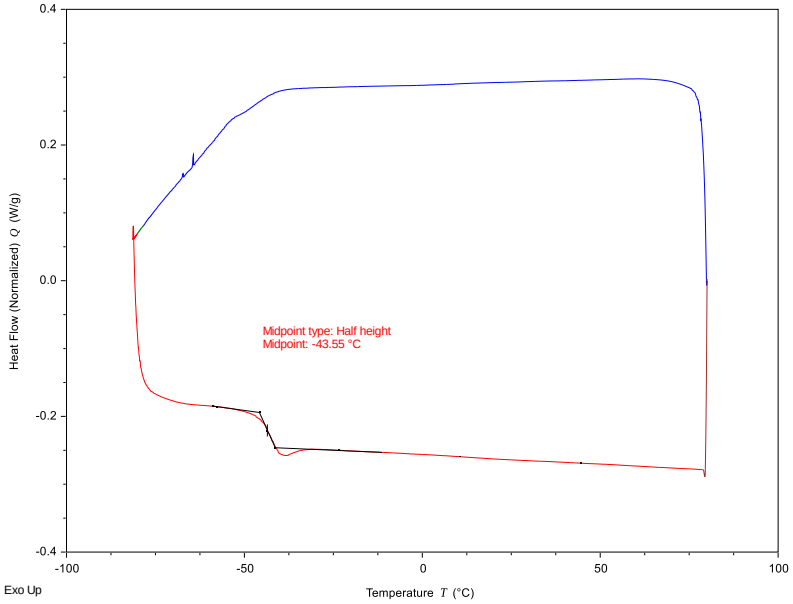

Figure S151 DSC data for $[C_8C_1Im]Cl_{0.33}ZnCl_2$ at 10 °C min^{-1}.

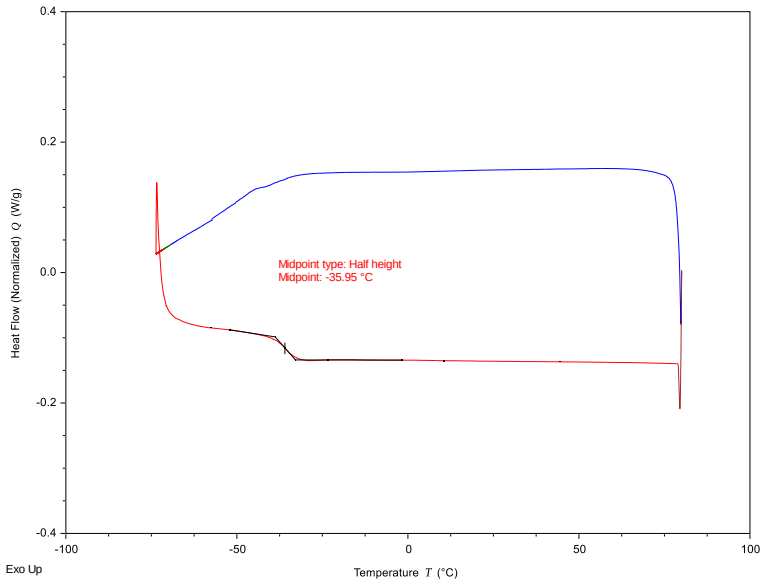

Figure S152 DSC data for $[C_8C_1Im]Br_{0.67}ZnBr_2$ at 10 °C min^{-1}.

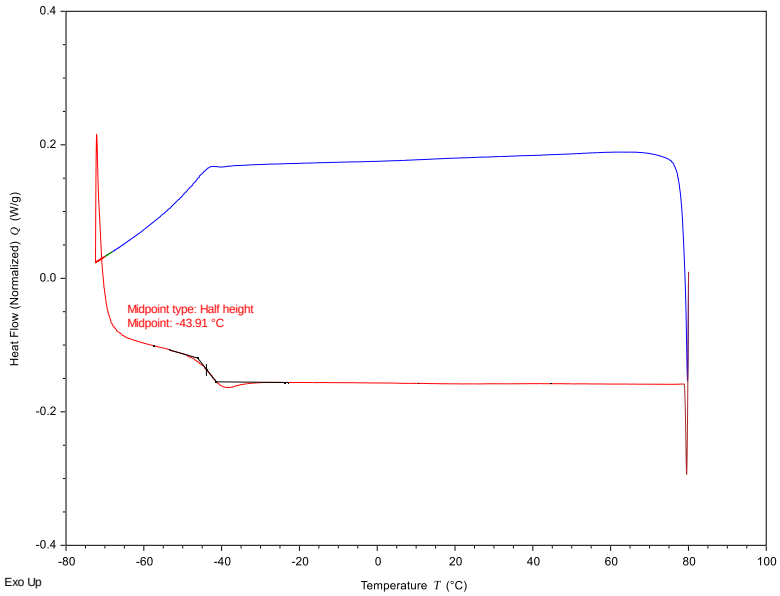

Figure S153 DSC data for $[C_8C_1Im]Br_{0.33}ZnCl_2$ at 10 °C min^{-1}.

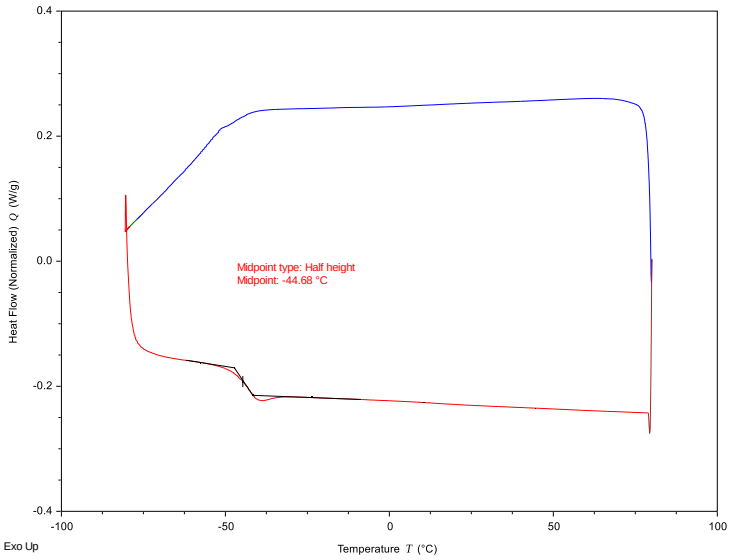

Figure S154 DSC data for $[C_8C_1Im]Br_{0.5}ZnCl_2$ at 10 °C min^{-1}.

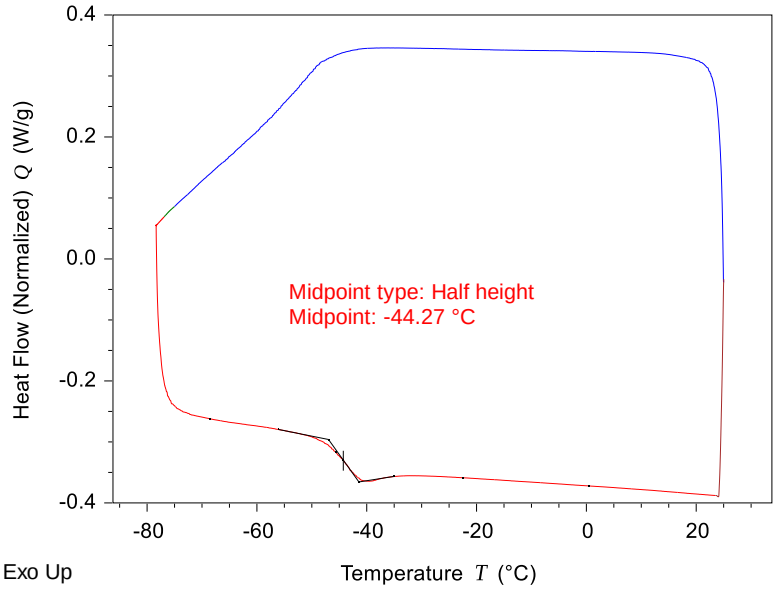

Figure S155 DSC data for $[C_8C_1Im]Cl_{0.33}ZnBr_2$ at 10 °C min^{-1}.

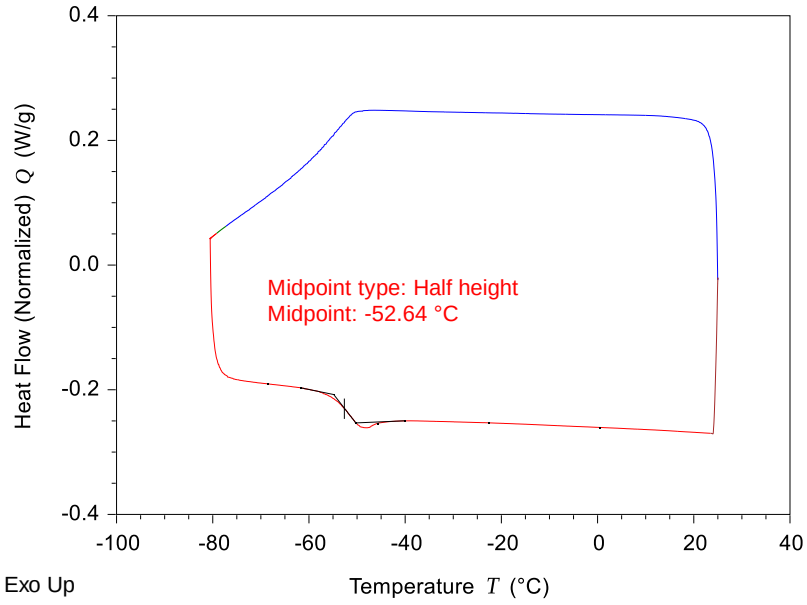

Figure S156 DSC data for $[C_8C_1Im]Cl_{0.5}ZnBr_2$ at 10 °C min^{-1}.

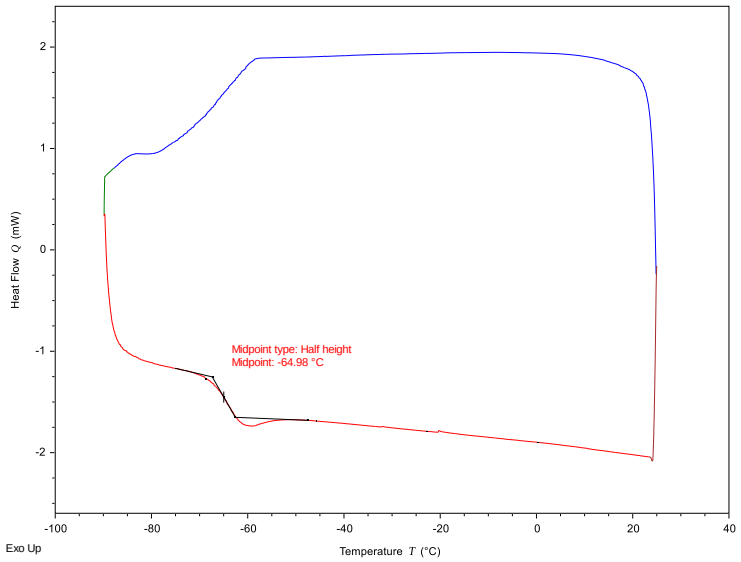

Figure S157 DSC data for $[C_8C_1Im]Br$ at 10 °C min^{-1}.

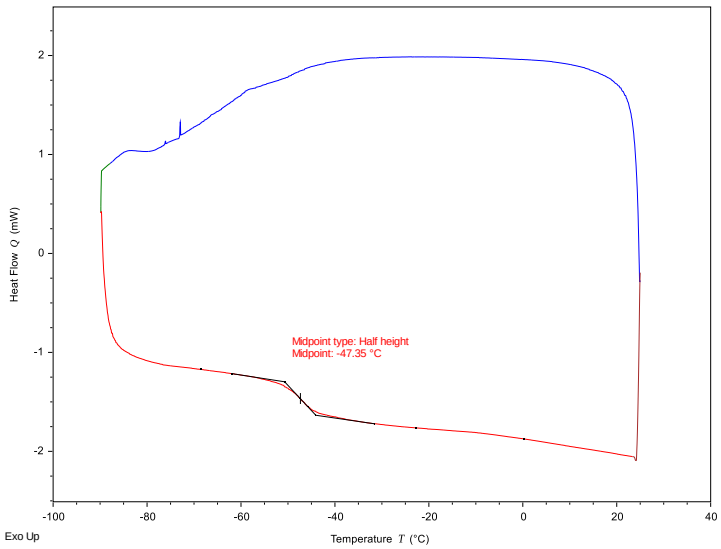

Figure S158 DSC data for $[C_8C_1Im]Cl_{0.5}ZnCl_2$ at 10 °C min^{-1}. Note the spikes on the cooling cycle (blue) are artefacts of cell.

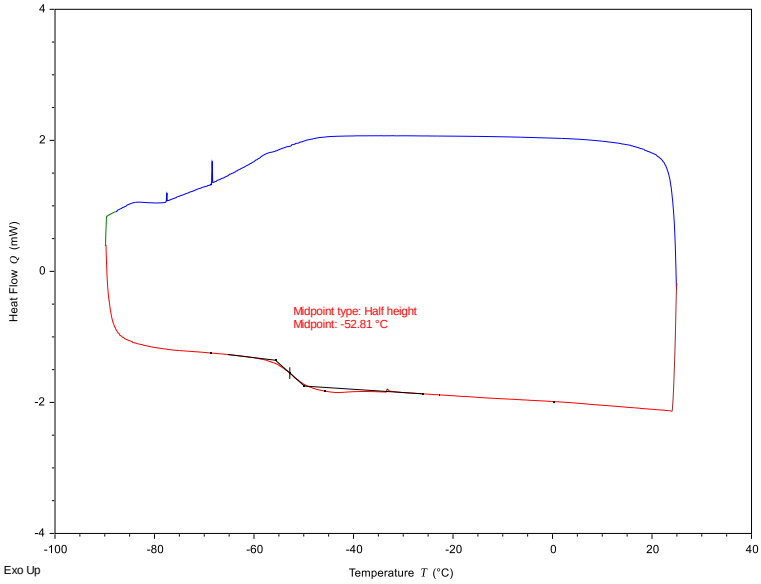

Figure S159 DSC data for $[C_8C_1Im]Cl_{0.6}ZnCl_2$ at 10 °C min^{-1}. Note the spikes on the cooling cycle (blue) are artefacts of cell.

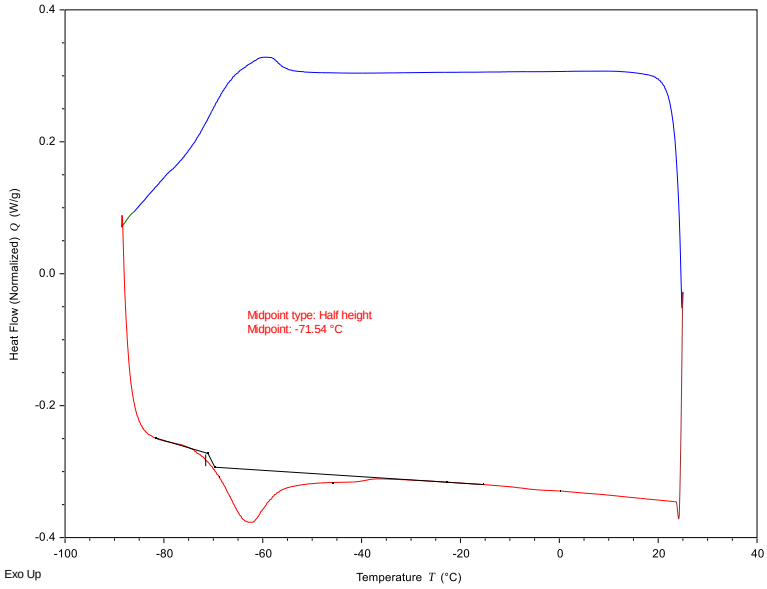

Figure S160 DSC data for $[P_{66614}]Cl_{0.33}AgCl$ at 10 °C min^{-1}.

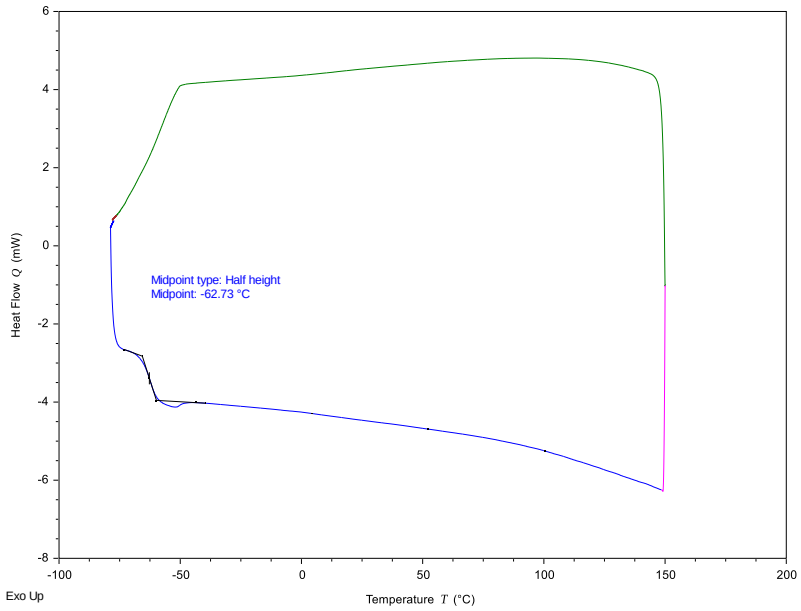

Figure S161 DSC data for $[C_4C_1Im]Cl$ at 10 °C min^{-1} (note: T_g of the supercooled liquid).

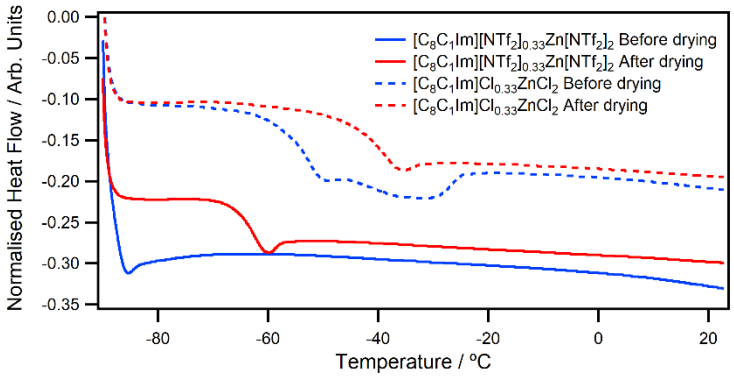

Figure S162 DSC data before and after *in situ* drying of $[C_8C_1Im]X_{0.33}ZnX_2$ samples with 10 wt% water for 45 minutes at 100 °C.

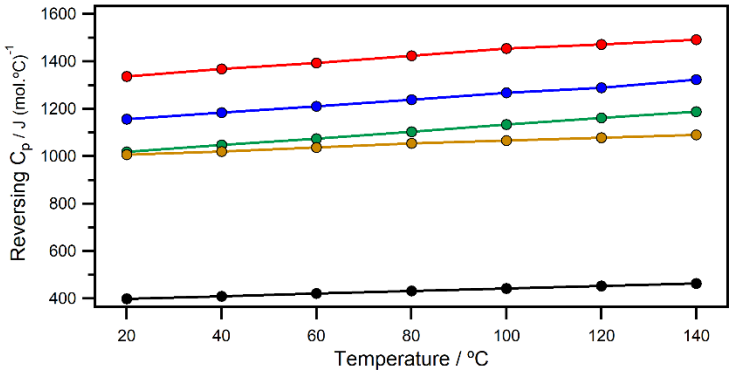

Figure S163 Reversing heat capacities of $[C_8C_1Im]Cl$ (black), $[C_8C_1Im]Cl_{0.33}ZnCl_2$ (green), $[C_8C_1Im]Cl_{0.5}ZnCl_2$ (blue), $[C_8C_1Im]Cl_{0.6}ZnCl_2$ (orange), $[C_8C_1Im]Cl_{0.67}ZnCl_2$ (red).

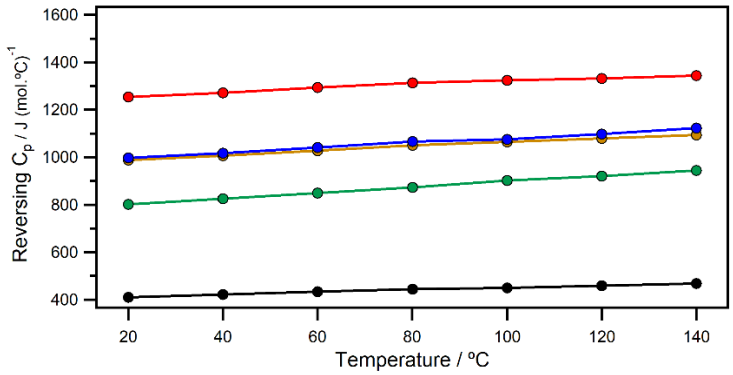

Figure S164 Reversing heat capacities of $[C_8C_1Im]Br$ (black), $[C_8C_1Im]Br_{0.33}ZnBr_2$ (green), $[C_8C_1Im]Br_{0.5}ZnBr_2$ (blue), $[C_8C_1Im]Br_{0.6}ZnBr_2$ (orange), $[C_8C_1Im]Br_{0.67}ZnBr_2$ (red).

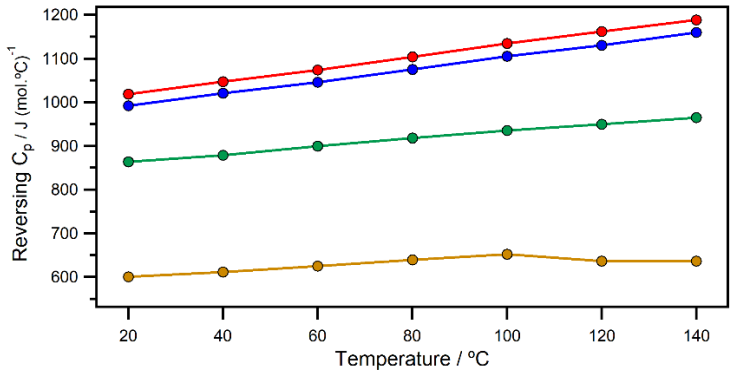

Figure S165 Reversing heat capacities of $[C_8C_1Im]Cl_{0.5}InCl_3$ (orange), $[C_8C_1Im]Cl_{0.33}NiCl_2$ (green), $[C_8C_1Im]Cl_{0.33}CoCl_2$ (blue), $[C_8C_1Im]Cl_{0.33}ZnCl_2$ (red).

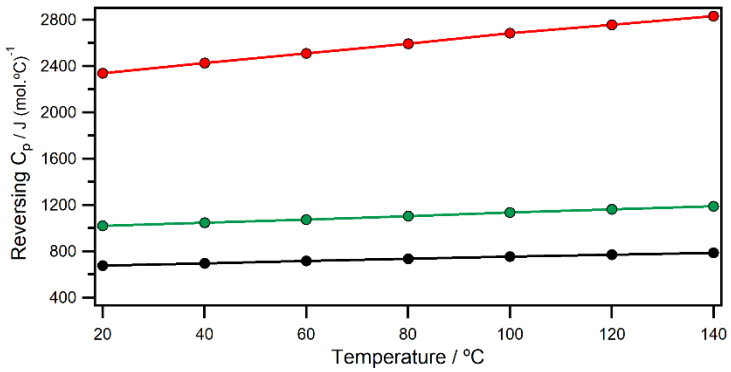

Figure S166 Reversing heat capacities of $[C_4C_1Im]Cl_{0.33}ZnCl_2$ (black), $[C_8C_1Im]Cl_{0.33}ZnCl_2$ (green), $[P_{66614}]Cl_{0.33}ZnCl_2$ (red).

DFT Data

Table S3 Dissociation energies (kJ mol^{-1}) for chlorozincate chloride dissociation.

	B3LYP-D3BJ	B3LYP-D3BJ (DCM)	B3LYP-D3BJ (HEX)
$[ZnCl_4]^{2-}$ —> $[ZnCl_3]^- + Cl^-$	-168	28.3	35.2
$[ZnCl_4]^{2-}$ —> $ZnCl_2 + 2Cl^-$	94.9	128.1	128.1
$[Zn_2Cl_6]^{2-}$ —> $[Zn_2Cl_5]^- + Cl^-$	-34.7	67.5	70.4
$[Zn_2Cl_6]^{2-}$ —> $[Zn_2Cl_5]^- + Cl^-$	-50.4	77.7	82.5
$[Zn_2Cl_6]^{2-}$ —> $[Zn_2Cl_4] + 2Cl^-$	274.8	181.5	176.3
$[Zn_3Cl_8]^{2-}$ —> $[Zn_3Cl_7]^- + Cl^-$	57.6	-34.7	-34
$[Zn_3Cl_8]^{2-}$ —> $[Zn_3Cl_6] + 2Cl^-$	370.3	76.7	69.3
$[Zn_4Cl_{10}]^{2-}$ —> $[Zn_4Cl_9]^- + Cl^-$	118	94.3	90.6
$[Zn_4Cl_{10}]^{2-}$ —> $[Zn_4Cl_8]^- + 2Cl^-$	430.2	204.8	194.4

Table S4 Dissociation energies (kJ mol^{-1}) for chlorozincate zinc chloride dissociation.

	B3LYP-D3BJ	B3LYP-D3BJ (DCM)	B3LYP-D3BJ (HEX)
$[Zn_4Cl_{10}]^{2-}$ —> $[Zn_3Cl_8]^{2-} + ZnCl_2$	176.8	172.5	166.0
$[Zn_3Cl_8]^{2-}$ —> $[Zn_2Cl_6]^{2-} + ZnCl_2$	212.1	-59.0	-64.9
$[Zn_2Cl_6]^{2-}$ —> $[ZnCl_4]^{2-} + ZnCl_2$	274.4	87.8	79.7

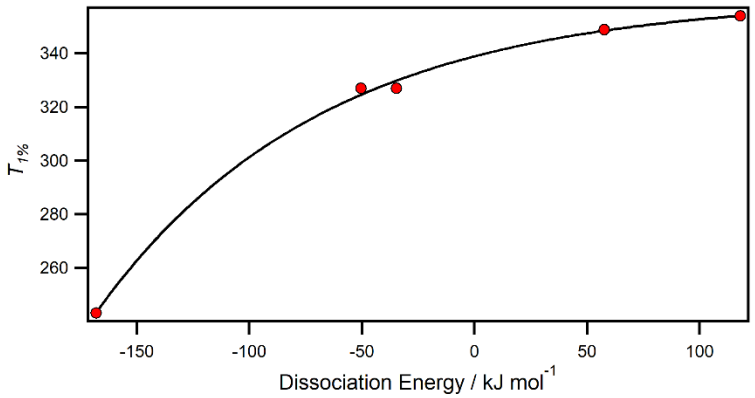

Figure S167 TGA derived $T_{1\%}$ values versus DFT calculated dissociation energies.

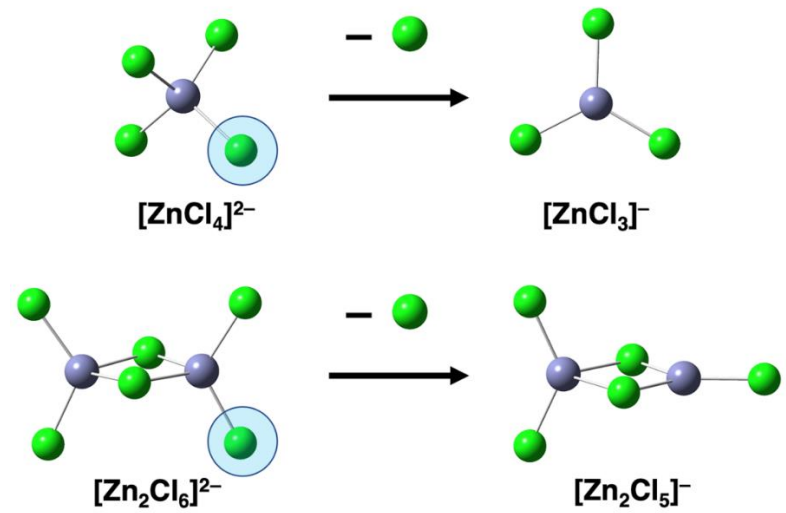

Figure S168 Example of chloride dissociation from chlorozincate complexes.

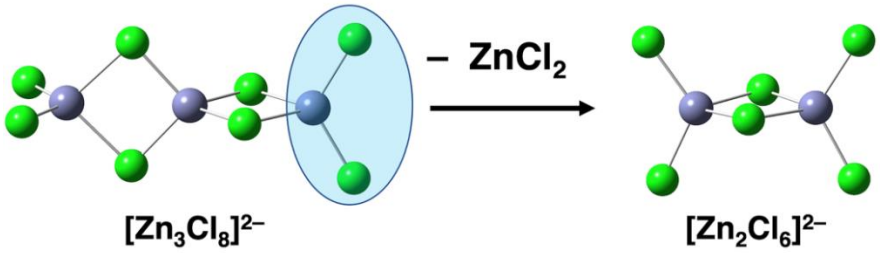

Figure S169 Example of zinc chloride dissociation from $[Zn_3Cl_8]^{2-}$.

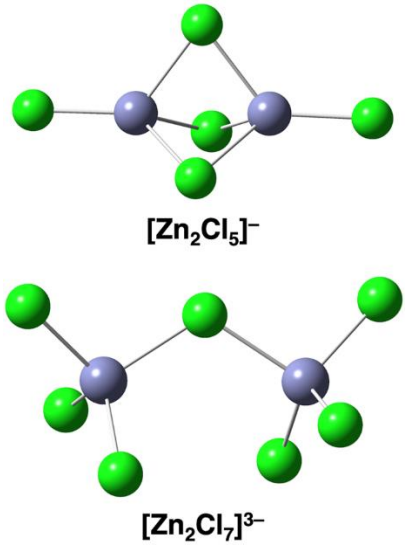

Figure S170 Unexpected $[Zn_2Cl_5]^-$ and $[Zn_2Cl_7]^{3-}$ anionic species.

Coordinates of optimised gas-phase Zinc Halide species using B3LYP-D3BJ/def2-TZVPP:

$[ZnCl_3]^-$

Zn	0.076300	1.180243	0.468461
Cl	2.006404	0.065527	0.468461
Cl	0.076300	3.409063	0.468461
Cl	-1.853803	0.065527	0.468461

$[ZnCl_4]^{2-}$

Zn	2.413878	0.233720	0.030488
Cl	1.054497	2.160611	-0.054078
Cl	1.051377	-1.692398	-0.004500
Cl	3.690382	0.258281	2.014898
Cl	3.859416	0.208563	-1.834380

$[Zn_2Cl_4]^0$

Zn	1.637852	-0.426219	0.777501
Zn	4.339027	0.563753	-0.532402
Cl	2.244221	0.090119	-1.396336
Cl	-0.175639	-1.091545	1.655901
Cl	6.152517	1.229076	-1.410804
Cl	3.732658	0.047412	1.641433

$[Zn_2Cl_5]^-$

Zn	2.181353	-0.138529	-0.072415
Zn	5.249786	0.669080	0.655413
Cl	1.166937	1.301707	-1.397634
Cl	1.496289	-2.021289	0.846862
Cl	7.296474	1.212553	1.138148
Cl	4.482165	-0.576091	-1.058790
Cl	3.349203	1.204841	1.741298

$[Zn_2Cl_6]^{2-}$

Zn	1.915227	0.233898	0.002759
Zn	5.295860	0.234166	0.035349
Cl	0.693896	2.151159	-0.024822
Cl	0.693872	-1.683543	0.006656
Cl	6.517215	2.151607	0.031451
Cl	6.517191	-1.683094	0.062929
Cl	3.588895	0.248153	1.744372
Cl	3.622191	0.219912	-1.706265

$[Zn_2Cl_7]^{3-}$

Zn	2.476764	-0.124136	0.087435
Zn	-2.474649	0.132633	-0.068199
Cl	0.001071	0.004244	0.009615
Cl	-3.366090	-1.734928	1.007561
Cl	-3.167339	2.079586	1.013043
Cl	-3.161842	0.170930	-2.296565
Cl	3.169477	-2.071091	-0.993791
Cl	3.368215	1.743429	-0.988338
Cl	3.163977	-0.162405	2.315798

$[Zn_3Cl_6]^0$

Zn	1.505241	0.311352	-1.296621
Zn	-1.144287	1.742666	-0.422940
Zn	-3.794609	3.175351	0.447025
Cl	3.300435	-0.657001	-1.888504
Cl	-2.926824	1.081800	0.912592
Cl	-2.024048	3.843365	-0.883527
Cl	-5.590334	4.144614	1.035785
Cl	0.980995	1.655651	0.511820
Cl	-0.607880	0.390618	-2.234795

$[Zn_3Cl_7]^-$

Zn	1.490779	0.877192	-1.550168
Zn	-1.283430	2.026905	-0.474508
Zn	-4.069838	3.176831	0.600244
Cl	3.362024	0.100561	-2.275806
Cl	-2.757563	0.985081	0.859337
Cl	-2.169096	4.046718	-0.891247
Cl	-5.758493	2.737740	-0.736951
Cl	-3.895134	4.238949	2.516918
Cl	0.995298	2.051162	0.331985
Cl	-0.603260	0.777082	-2.428262

$[Zn_3Cl_8]^{2-}$

Zn	1.646157	0.236884	-1.341316
Zn	-1.146145	1.741420	-0.426459
Zn	-3.936231	3.249042	0.490164
Cl	2.069961	-1.846253	-0.624128
Cl	3.098180	1.309427	-2.673422
Cl	-2.916148	1.053188	0.912185
Cl	-2.003542	3.847443	-0.904553
Cl	-5.781060	3.032874	-0.768165
Cl	-3.965165	4.478890	2.366491
Cl	0.968839	1.674652	0.533186
Cl	-0.633548	0.391713	-2.246908

$[Zn_4Cl_8]^0$

Zn	1.348026	0.224186	-1.454816
Zn	-1.027380	1.810908	-0.238043
Zn	-3.429798	3.410239	0.987867
Zn	3.750418	-1.375215	-2.680685
Cl	2.060774	-1.977103	-1.221634
Cl	3.051741	0.815275	-2.923347
Cl	-2.731075	1.219762	1.230493
Cl	-1.740173	4.012183	-0.471189
Cl	-5.058264	4.493563	1.817442
Cl	1.152499	1.479555	0.488743
Cl	-0.831847	0.555555	-2.181611
Cl	5.378873	-2.458569	-3.510244

$[Zn_4Cl_9]^-$

Zn	1.209852	0.268355	-1.448468
Zn	-1.346454	1.795283	-0.431730
Zn	-3.931624	3.362451	0.604828
Zn	3.789587	-1.254761	-2.473415
Cl	2.065015	-1.928578	-1.132975
Cl	3.044432	0.875131	-2.835799
Cl	-2.965468	0.997234	0.898367
Cl	-1.918068	3.913622	-0.895094
Cl	-5.664594	3.162400	-0.731207
Cl	-3.591273	4.409379	2.506590
Cl	0.904621	1.514581	0.424246
Cl	-0.856677	0.429099	-2.374428
Cl	5.535288	-2.285455	-3.165129

$[Zn_4Cl_{10}]^{2-}$

Zn	1.524886	0.270904	-1.285534
Zn	-1.204254	1.764156	-0.407302
Zn	-3.962409	3.270432	0.472333
Zn	4.283042	-1.235372	-2.165169
Cl	2.276829	-1.843115	-0.822072
Cl	3.282524	1.010777	-2.555487
Cl	-2.961891	1.024283	0.862652
Cl	-1.956197	3.878175	-0.870764
Cl	-5.723367	3.071134	-0.876892
Cl	-3.955210	4.425012	2.377162
Cl	0.934408	1.601189	0.566589
Cl	-0.613776	0.433871	-2.259424
Cl	4.275842	-2.389950	-4.069998
Cl	6.043999	-1.036074	-0.815944

Life Cycle Analysis

Modelling and simulation

This section details the properties used for the pseudo components in HYSYS V11 for process simulation. For estimating the enthalpy of formation, the molecular structures are first drawn and optimized in a molecular modelling and graphics software such as ArgusLab. The structure is then processed in a quantum chemistry tool MOPAC, an open source software used here for calculating the charge density profiles and enthalpies of formation. The enthalpy of formation of ionic liquids is obtained as shown in Equation 1 below from the Born-Haber cycle.[5]

$$\boldsymbol{\Delta H^{\circ}_{f_{IL}}} = \boldsymbol{\Delta H^{\circ}_{f_{Cation}}} + \boldsymbol{\Delta H^{\circ}_{f_{Anion}}} - \boldsymbol{\Delta H_L} \quad (1)$$

Where ΔH_L is the lattice energy calculated from Equation 2 below.[6]

$$\Delta H_L = U_{POT} + \left[p\left(\frac{n_m}{2} - 2\right) + q\left(\frac{n_x}{2} - 2\right)\right] RT \quad (2)$$

Where n_m and n_x are parameters that depend on the nature of the cation and anion, respectively. They are equal to 3 for monatomic ions, 5 for linear polyatomic ions, and 6 for non-linear polyatomic ions. p and q are the oxidation state of the cation and anion, respectively, and U_{POT} is the potential energy, which is calculated from Equation 3 as follows:

$$U_{POT} = \gamma\left(\frac{\rho_m}{M_m}\right)^{\frac{1}{3}} + \delta \quad (3)$$

Where ρ_m is the density and M_m is the molecular weight of the ionic liquid, while γ and δ are coefficients that depend on the stoichiometry of the ionic liquid.

Table S5 Aluminium hydroxide properties.

Property	Value	Units
MW	78.00	g mol^{-1}
Density	2420	Kg m^{-3}
ΔH_f	-1277000	kJ $kmol^{-1}$

Table S6 Aluminium properties.

Property	Value	Units
MW	26.98	g mol^{-1}
Density	2375	Kg m^{-3}
ΔH_f	-538300	kJ $kmol^{-1}$

Table S7 Triethylaluminium properties.

Property	Value	Units
MW	114.20	g mol^{-1}
BP	129.00	°C
Density	835	Kg m^{-3}
ΔH_f	-100000	kJ $kmol^{-1}$
T_c	335.10	°C
P_c	3503	kPa
V_c	0.38	m^3 $kmol^{-1}$
Acentricity	0.28	-

Table S8 Trioctylaluminium properties.

Property	Value	Units
MW	366.60	g mol^{-1}
BP	120.00	°C
Density	822.7	Kg m^{-3}
ΔH_f	-703200	kJ $kmol^{-1}$
T_c	323.40	°C
P_c	3532	kPa
V_c	0.38	m^3 $kmol^{-1}$
Acentricity	0.27	-

Table S9 1-chlorooctane properties.

Property	Value	Units
MW	148.70	g mol^{-1}
BP	183.00	°C
Density	875	Kg m^{-3}
ΔH_f	-218500	kJ $kmol^{-1}$
T_c	396.20	°C
P_c	3079	kPa
V_c	0.46	m^3 $kmol^{-1}$
Acentricity	0.36	-

Table S10 1-methylimidazole properties.

Property	Value	Units
MW	82.10	g mol^{-1}
BP	198.00[7]	°C
Density	1030[7]	Kg m^{-3}
ΔH_f	125700[8]	kJ $kmol^{-1}$
T_c	490.90	°C
P_c	6086	kPa
V_c	0.26	m^3 $kmol^{-1}$
Acentricity	0.35	-

Table S11 $[C_8C_1Im]Cl$ properties.

Property	Value	Units
MW	230.80	g mol^{-1}
BP	376.40[9]	°C
Density	1000[9]	Kg m^{-3}
ΔH_f	-64190	kJ $kmol^{-1}$
T_c	596.3[9]	°C
P_c	2032[9]	kPa
V_c	0.80[9]	m^3 $kmol^{-1}$
Acentricity	0.66[9]	-

Table S12 Zinc properties.

Property	Value	Units
MW	65.38	g/mol
BP	907	°C
Density	7140	Kg/m^3
ΔH_f	130400	kJ/kmol

Table S13 Zinc chloride properties.

Property	Value	Units
MW	136.30	g/mol
BP	732.00	°C
Density	2907	Kg/m^3
ΔH_f	-266000	kJ/kmol
T_c	982.30	°C
P_c	1845	kPa
V_c	1.41	$m^3/kmol$
Acentricity	1.25	-

Production Processes:

1-Octanol production:

The Ziegler process is used for producing 1-octanol. Herein, triethylaluminium is first produced from ethylene, aluminium, and hydrogen in a molar ratio of 3:1:1.5, respectively. The triethylaluminium further reacts with ethylene in 1:9 molar ratio under high temperature and pressure (120 °C and 120 bar) to form trioctylaluminium. Finally, it is oxidized before it reacts with water at 90 °C to produce 1-octanol and aluminium hydroxide.

1-Chlorooctane production:

The same process for producing 1-chlorobutane described in the work of Baaqel et al.[10] is used for modelling the production of 1-chlorooctane. Herein, 1-octanol reacts with excess hydrogen chloride at 120 °C. The mixture cools down to 25 °C before it is sent to flash tank to remove hydrogen chloride. The liquid mixture is then reheated to 69 °C before it is sent to another flash tank to remove the residuals containing 1-octanol and excess water.

$[C_8C_1Im]Cl$ production:

The modelling of the production process for $[C_8C_1Im]Cl$ is adapted from the modelled production of $[C_4C_1Im]Cl$ reported in the work of Baaqel et al.[10] In this process, 1-methylimidazole mixes with toluene in excess 1-chlorooctane at 112 °C. $[C_8C_1Im]Cl$ is then formed, and toluene and other unreacted materials are separated in a vacuum flash tank before they are recycled for reuse in the process.

Zinc chloride production:

Zinc chloride is prepared simply by reacting zinc and hydrogen chloride. The reaction forms zinc chloride and hydrogen as a by-product. Hydrogen is then removed in a flash tank to yield high purity zinc chloride. The hydrogen can be sold or used for other processes and hence a credit is applied in the form of reduced environmental impact and lower cost based on what would be incurred from its production.

$[C_8C_1Im]Cl_\chi ZnCl_2$ production:

The ionic liquids are prepared by mixing $[C_8C_1Im]Cl$ and $ZnCl_2$ using the desired ratio at 70 °C and using nitrogen as an inert gas to avoid unwanted oxidation or hydration.

Economic assessment

The tables below detail the breakdown of the costs accounted for in this work, prices of raw materials and costing results obtained from process simulation. CAPEX consists mainly of equipment costs and other costs such as engineering and offsite costs, while OPEX consists of costs of raw materials and utilities as well as fixed operation costs such as labour costs.

In this work, equipment costs were estimated using Equation (4):[11]

$$C_{ISBL} = \sum_{e \in Equipment} F_e C_e \quad (4)$$

Here, C_e is the cost of purchased equipment on a U.S. Gulf Coast basis as of January 2006 and F_e is the equipment installation factor. Due to unavailability of current equipment data, their costs are calculated from Equation (5).

$$C_e = a + bS^n \quad (5)$$

Here, a, b are cost constants, n is equipment type exponent and S is a size parameter. Finally, to account for inflation, capital cost need be escalated to reflect up to date cost. This is usually done using cost indices and calculated from Equation (6):

$$Cost_{new} = Cost_{old} \frac{Cost\ index_{new}}{Cost\ index_{old}} \quad (6)$$

In this work, the Chemical Engineering Plant Cost Index (CEPCI) for 2006 and 2019 are used. CEPCI is one of the most commonly-used published composite indices and was developed based on 4 main components: process equipment, construction labour, buildings and supervision and engineering.

Table S14 Breakdown of cost estimation.

CAPEX (C_{CAPEX})	OPEX (C_{OPEX})
Fixed Capital (C_{FC})	**Variable Cost of Production (C_{VCP})**
Onsite capital costs (ISBL)	Raw materials (CRM)
Equipment cost	Utilities (CU)
Offsite capital costs (OSBL) = 40% ISBL	
Engineering and construction costs (CEng) = 10% (CISBL + OSBL)	**Fixed Cost of Production (C_{FCP})**
Contingency charges (CCon) = 15% (ISBL + OSBL)	*Operation labour (COL)* = 720,000 USD*
	Supervision (CSup) = 25% COL = 180,000 USD
	Salaries (CSal) = 50% (COL + CSup) = 450,000 USD
	Maintenance (CMain) = 3% ISBL
	Land (CLand) = 1% (ISBL + OSBL)
	Taxes and Insurance (CTax) = 1.5% CFC
	General plant overhead (CGPO) = 65% (COL + CSup + CSal + CMain)
	*Based on 4.8 operator per shift with 3 shift positions and an average salary of $50k per operator.

Table S15 Commodity prices used in economic assessment.

Commodity	Price ($)
Hydrogen (kg)	4.29
Ethylene (kg)	1.21
Aluminium (kg)	2.66
Oxygen (kg)	0.25
Hydrogen chloride (kg)	0.20
1-methylimidazole (kg)	2.84
Deionized water (m^3)	0.13
Toluene (kg)	0.81
Zinc (kg)	1.66
Diethylether (kg)	1.79
Cooling water (kg)	0.50
Steam (1000 kg)	25
Electricity (kWh)	0.16

Table S16 Detailed CAPEX costs for 1-octanol.

Unit	Specifications		Eq. Cost ($/kg 1-octanol)
Flash Tank	Diameter (m) 1.26	Length (m) 4.42	3.60×10^{-5}
Reactor 1	Volume (m^3)	0.94	5.67×10^{-5}
Reactor 2	Volume (m^3)	3.05	9.41×10^{-5}
Reactor 3	Volume (m^3)	3.54	1.01×10^{-4}
Heater 1	Area (m^2)	15.48	
Heater 2	Area (m^2)	7.50	
Heater 3	Area (m^2)	114.79	
Heater 4	Area (m^2)	126.24	
Cooler 1	Area (m^2)	9.28	
Cooler 2	Area (m^2)	2.70	2.6×10^{-4}
Cooler 3	Area (m^2)	19.44	
Cooler 4	Area (m^2)	0.47	
Cooler 5	Area (m^2)	238.31	
Cooler 6	Area (m^2)	437.75	
Cooler 7	Area (m^2)	616.92	
Cooling Tower	Vol Flow (L/s)	3204.06	1.22×10^{-3}
Pump 1	Vol Flow (L/s)	3.11	6.89×10^{-6}
Pump 2	Vol Flow (L/s)	1.16	6.63×10^{-6}
Compressor 1	Power (kWh)	273.24	1.21×10^{-4}
Compressor 2	Power (kWh)	82.09	6.43×10^{-5}
Compressor 3	Power (kWh)	2468.04	4.26×10^{-4}
Compressor 4	Power (kWh)	168.62	9.34×10^{-5}
Compressor 5	Power (kWh)	10.36	2.59×10^{-5}

CAPEX Component	Total Cost ($/kg 1-octanol)
ISBL	2.5×10^{-3}
OSBL	1.0×10^{-4}
CEng	3.5×10^{-4}
CCon	5.3×10^{-4}

Table S17 Detailed OPEX costs for 1-octanol.

Feedstock/Utility	**Cost ($/kg 1-octanol)**
Hydrogen	0.03
Ethylene	1.04
Aluminium	0.20
Oxygen	0.03
Water	1.79×10^{-5}
Cooling Water	0.16
Electricity	5.44×10^{-3}
OPEX Component	**Total Cost ($/kg 1-octanol)**
C_{VCP}	1.47
C_{FCP}	0.01

Table S18 Detailed equipment costs for 1-chlorooctane.

Unit	**Specifications**		**Eq. Cost ($/kg 1-chlorooctane)**
Reactor	Volume (m^3)	4.99	1.21×10^{-4}
Heater 1	Area (m^2)	92.34	
Heater 2	Area (m^2)	122.74	6.08×10^{-5}
Cooler	Area (m^2)	70.82	
Cooling Tower	Vol Flow (L/s)	7.24	8.01×10^{-5}
Pump 1	Vol Flow (L/s)	11.74	8.35×10^{-6}
Pump 2	Vol Flow (L/s)	9.53	7.94×10^{-6}
Compressor	Power (kWh)	255.16	1.17×10^{-4}
CAPEX Component			**Total Cost ($/kg 1-chlorooctane)**
ISBL			3.96×10^{-4}
OSBL			1.58×10^{-4}
CEng			5.54×10^{-5}
CCon			8.31×10^{-5}

Table S19 Detailed OPEX costs for 1-chlorooctane.

Feedstock/Utility	**Cost ($/kg 1-chlorooctane)**
Hydrogen chloride	0.08
1-octanol	1.73
Steam	1.80×10^{-3}
Cooling Water	6.90×10^{-4}
Electricity	5.07×10^{-3}
OPEX Component	**Total Cost ($/kg 1-chlorooctane)**
C_{VCP}	1.83
C_{FCP}	9.64×10^{-3}

Table S20 Detailed CAPEX costs for $[C_8C_1Im]Cl$.

Unit	**Specifications**		**Eq. Cost ($/kg $[C_8C_1Im]Cl$)**
Flash Tank	Diameter (m) 2.85	Length (m) 9.98	4.77×10^{-5}
Reactor	Volume (m^3)	15.64	2.36×10^{-4}
Heater 1	Area (m^2)	196.83	2.33×10^{-4}
Heater 2	Area (m^2)	274.39	
Heater 3	Area (m^2)	131.18	
Cooler 1	Area (m^2)	701.27	
Cooler 2	Area (m^2)	90.20	
Cooler 3	Area (m^2)	21.92	
Cooling Tower	Vol Flow (L/s)	392.95	2.49×10^{-4}
Pump 1	Vol Flow (L/s)	10.09	8.04×10^{-6}
Pump 2	Vol Flow (L/s)	0.44	6.56×10^{-6}
Pump 3	Vol Flow (L/s)	47.82	1.64×10^{-5}
Pump 4	Vol Flow (L/s)	2.96	6.87×10^{-6}
Pump 5	Vol Flow (L/s)	38.91	1.42×10^{-5}
Pump 6	Vol Flow (L/s)	8.90	7.83×10^{-6}
CAPEX Component			**Total Cost ($/kg $[C_8C_1Im]Cl$)**
ISBL			8.25×10^{-4}
OSBL			3.30×10^{-4}
CEng			1.16×10^{-4}
CCon			1.73×10^{-4}

Table S21 Detailed OPEX costs for $[C_8C_1Im]Cl$.

Material	**Cost ($/kg $[C_8C_1Im]Cl$)**
1-methylimidazole	1.04
1-chlorooctane	1.95
Cooling Water	4.56×10^{-2}
Electricity	8.29×10^{-2}
OPEX Component	**Total Cost ($/kg $[C_8C_1Im]Cl$)**
C_{VCP}	3.03
C_{FCP}	0.01

Table S22 Detailed CAPEX costs for zinc chloride.

Unit	**Specifications**		**Eq. Cost ($/kg zinc chloride)**
Flash Tank	Diameter (m) 2.35	Length (m) 8.22	4.23×10^{-5}
Reactor	Volume (m^3)	1.81	7.38×10^{-5}
Heater	Area (m^2)	25.67	
Cooler 1	Area (m^2)	275.88	3.67×10^{-4}
Cooler 2	Area (m^2)	1993.49	
Cooling Tower	Vol Flow (L/s)	262.64	1.96×10^{-4}
Pump	Vol Flow (L/s)	1.71	6.70×10^{-6}
Compressor 1	Power (kWh)	309.31	1.30×10^{-4}
Compressor 2	Power (kWh)	1482.51	3.16×10^{-4}
CAPEX Component			**Total Cost ($/kg zinc chloride)**
ISBL			1.13×10^{-3}
OSBL			4.53×10^{-4}
CEng			1.58×10^{-4}
CCon			2.38×10^{-4}

Table S23 Detailed OPEX costs for zinc chloride.

Material	**Cost ($/kg zinc chloride)**
Zinc	0.80
Hydrogen chloride	0.11
Diethylether	0.26
Hydrogen	(0.24)
Cooling Water	0.03
Electricity	8.61×10^{-3}
OPEX Component	**Total Cost ($/kg zinc chloride)**
C_{VCP}	0.96
C_{FCP}	0.01

Table S24 Detailed CAPEX costs for $[C_8C_1Im]Cl_xZnCl_2$.

Unit	**Specifications**		**Eq. Cost ($/kg $[C_8C_1Im]Cl_xZnCl_2$)**
Flash Tank	Diameter (m) 0.58	Length (m) 2.03	1.79×10^{-5}
Heater	Area (m^2)	18.01	2.07×10^{-5}
Cooler	Area (m^2)	4.41	
Cooling Tower	Vol Flow (L/s)	10.00	8.17×10^{-5}
Pump 1	Vol Flow (L/s)	1.06	6.62×10^{-6}
Pump 2	Vol Flow (L/s)	5.24	7.21×10^{-6}
Compressor 1	Power (kWh)	19.69	3.33×10^{-5}
Compressor 2	Power (kWh)	117.94	7.74×10^{-5}
CAPEX Component			**Total Cost ($/kg $[C_8C_1Im]Cl_xZnCl_2$)**
ISBL			2.45×10^{-4}
OSBL			9.79×10^{-5}
CEng			3.43×10^{-5}
CCon			5.14×10^{-5}

Table S25 Detailed OPEX costs for $[C_8C_1Im]Cl_\chi ZnCl_2$.

Material	**Cost ($/kg $[C_8C_1Im]Cl_\chi ZnCl_2$)**			
	$[C_8C_1Im]Cl_{0.33}ZnCl_2$	**$[C_8C_1Im]Cl_{0.5}ZnCl_2$**	**$[C_8C_1Im]Cl_{0.6}ZnCl_2$**	**$[C_8C_1Im]Cl_{0.67}ZnCl_2$**
$[C_8C_1Im]Cl$	2.34	1.91	1.61	1.39
Zinc chloride	0.22	0.36	0.46	0.53
Hydrogen	4.40×10^{-3}	4.77×10^{-3}	5.03×10^{-3}	$5.22e \times 10^{-3}$
Steam	5.37×10^{-4}	6.21×10^{-4}	6.80×10^{-4}	7.23×10^{-4}
Electricity	1.42×10^{-4}	1.66×10^{-4}	1.80×10^{-4}	2.00×10^{-4}
OPEX Component	**Total Cost ($/kg $[C_8C_1Im]Cl_\chi ZnCl_2$)**			
C_{VCP}	2.57	2.28	2.08	1.93
C_{FCP}	9.50×10^{-3}	9.50×10^{-3}	9.50×10^{-3}	9.51×10^{-3}

Environmental assessment

This section elaborates on the proxy data, processes and flows used for the LCI phase in addition to the midpoint results from the characterization phase.

Table S26 Proxy data used in LCI.

Data Category	Proxy data	Proxy method
Air emissions	Raw materials	0.2% by mass of inflows are assumed to be vaporized or leaked
	Cooling water	4% by volume of total cooling water are assumed to be vaporized or leaked
	CO_2	90% by mass of carbon in waste stream is assumed to be completely burned in waste treatment to produce CO_2 as per the following complete combustion equation: $$C_X H_Y O_z + \left(X + \frac{Y}{4}\right) O_2 \rightarrow XCO_2 + \frac{Y}{2} H_2O$$
Water emissions	COD	The chemical oxygen demand (COD) or total oxygen consumed is assumed to be equivalent to the amount of oxygen needed to react with the amount of carbon remaining in the waste stream after treatment which is assumed to be 10% of total carbon.
	BOD	For worst case scenario, the biological oxygen demand (BOD) which is the oxygen consumed due to biological aerobic digestion by organisms is assumed to be equivalent to the amount of COD.
	TOC	The total organic carbon (TOC) which is the total amount of carbon is assumed to be equivalent to 10% of the total carbon in the waste stream which is the amount of carbon remaining after treatment.
	DOC	For waste case scenario, dissolved organic carbon (DOC) is assumed to be equivalent to TOC.

Table S27 1-octanol inventory.

Inventory Group	Inventory	Flow (amount/kg product)		Uncertainty Parameter (Lognormal)
		Amount	Unit	
Inputs from nature	Water, cooling, unspecified natural origin, RER	0.32	m3	1.0502
	Water, river, RER	0.16	m3	1.0502
	Water, well, in ground, RER	0.16	m3	1.0502
Inputs from technosphere (materials)	Hydrogen, liquid {RER}| market for | Cut-off	7.84×10^{-3}	kg	1.3269
	Chemical factory, organics {GLO}| market for | Cut-off	4.00×10^{-10}	p	2.9905
	Heat, district, or industrial, natural gas {RER}| market group for | Cut-off	1.20	MJ	1.0502
	Electricity, medium voltage {RER}| market group for | Cut-off	0.10	kWh	1.0502
	Heat, from steam, in chemical industry {RER}| market for heat, from steam, in chemical industry | Cut-off	0.13	MJ	1.0502
	Ethylene {RER}| ethylene production, average | Cut-off	0.86	kg	1.3269
	Water, deionised {Europe without Switzerland}| water production, deionised | Cut-off	0.14	kg	1.3269
	Aluminium, cast alloy {GLO}| market for | Cut-off	0.07	kg	1.3269
	Oxygen, liquid {RER}| market for | Cut-off	0.12	kg	1.3269
Emissions to air	Carbon dioxide	0.22	kg	1.0502
	Hydrogen	1.02×10^{-3}	kg	1.0502
	Water	0.01	kg	1.0502
	Ethene	1.72×10^{-3}	kg	1.0502
	Oxygen	2.46×10^{-4}	kg	1.0502
	Aluminium	1.49×10^{-4}	kg	1.0502
Emissions to water	Water, RER	0.32	m^3	1.0502
	Aluminium	5.19×10^{-3}	kg	1.0502
	Aluminium hydroxide	0.20	kg	1.0502
Outputs to technosphere	Wastewater, average {Europe without Switzerland}| market for wastewater, average | Cut-off	2.05×10^{-4}	m^3	1.0502

Table S28 1-chlorooctane inventory.

Inventory Group	Inventory	Flow (amount/kg product)		Uncertainty Parameter (Lognormal)
		Amount	Unit	
Inputs from nature	Water, cooling, unspecified natural origin, RER	1.38×10^{-3}	m^3	1.0502
	Water, river, RER	6.90×10^{-4}	m^3	1.0502
	Water, well, in ground, RER	6.90×10^{-4}	m^3	1.0502
Inputs from technosphere (materials)	1-octanol	1.17	kg	1.3269
	Chemical factory, organics {GLO}| market for | Cut-off	4.00×10^{-10}	p	2.9905
	Heat, district or industrial, natural gas {RER}| market group for | Cut-off	0.27	MJ	1.0502
	Electricity, medium voltage {RER}| market group for | Cut-off	8.61×10^{-3}	kWh	1.0502
	Heat, from steam, in chemical industry {RER}| market for heat, from steam, in chemical industry | Cut-off	0.03	MJ	1.0502
	Hydrochloric acid, without water, in 30% solution state {RER}| market for | Cut-off	0.41	kg	1.3269
Emissions to air	Hydrogen chloride	0.08	kg	1.0502
	1-Octanol	2.34×10^{-3}	kg	1.0502
	Butane, 1-chloro-	0.34	kg	1.0502
	Water	0.16	kg	1.0502
Emissions to water	Water, RER	1.38×10^{-3}	m^3	1.0502

Table S29 [C_8C_1Im]Cl inventory.

Inventory Group	Inventory	Flow (amount/kg product)		Uncertainty Parameter (Lognormal)
		Amount	Unit	
Inputs from nature	Water, cooling, unspecified natural origin, RER	0.08	m3	1.0502
	Water, river, RER	0.04	m^3	1.0502
	Water, well, in ground, RER	0.04	m3	1.0502
Inputs from technosphere (materials)	1-methylimidazole[12]	0.37	kg	1.3269
	Chemical factory, organics {GLO}| market for | Cut-off	4.00×10^{-10}	p	2.9905
	Heat, district, or industrial, natural gas {RER}| market group for | Cut-off	1.92	MJ	1.0502
	Electricity, medium voltage {RER}| market group for | Cut-off	4.73×10^{-4}	kWh	1.0502
	Heat, from steam, in chemical industry {RER}| market for heat, from steam, in chemical industry | Cut-off	0.21	MJ	1.0502
	1-chlorooctane	1.06	kg	1.3269
	Toluene, liquid {RER}| market for toluene, liquid | Cut-off	0.05	kg	1.3269
Emissions to air	Imidazole	7.32×10^{-4}	kg	1.0502
	Water	3.20×10^{-3}	kg	1.0502
	Butane, 1-chloro-	2.12×10^{-3}	kg	1.0502
	Carbon dioxide	0.92	kg	1.0502
	Toluene	9.10×10^{-5}	kg	1.0502
Emissions to water	Water, RER	0.08	m^3	1.0502
	COD, Chemical Oxygen Demand	0.07	kg	1.0502
	DOC, Dissolved Organic Carbon	0.03	kg	1.0502
	BOD5, Biological Oxygen Demand	0.07	kg	1.0502
	TOC, Total Organic Carbon	0.03	kg	1.0502
	Butane, 1-chloro-	0.03	kg	1.0502
	Chloride	4.36×10^{-4}	kg	1.0502
	Imidazole	2.40×10^{-3}	kg	1.0502
	Toluene	4.48×10^{-3}	kg	1.0502
Outputs to technosphere	Wastewater, average {Europe without Switzerland}| market for wastewater, average | Cut-off	4.12×10^{-4}	m^3	1.0502

Table S30 Zinc chloride inventory.

Inventory Group	Inventory	Flow (amount/kg product) Amount	Unit	Uncertainty Parameter (Lognormal)
Inputs from nature	Water, cooling, unspecified natural origin, RER	0.06	m3	1.0502
	Water, river, RER	0.03	m^3	1.0502
	Water, well, in ground, RER	0.03	m3	1.0502
Inputs from technosphere (materials)	Zinc concentrate {GLO}| market for | Cut-off	0.48	kg	1.3269
	Chemical factory, organics {GLO}| market for | Cut-off	4.00×10^{-10}	p	2.9905
	Electricity, medium voltage {RER}| market group for | Cut-off	4.73×10^{-4}	kWh	1.0502
	Hydrochloric acid, without water, in 30% solution state {RER}| market for | Cut-off	0.54	kg	1.3269
	Diethyl ether, without water, in 99.95% solution state {RER}| market for diethyl ether, without water, in 99.95% solution state | Cut-off	0.15	kg	1.3269
Emissions to air	Zinc	9.59×10^{-4}	kg	1.0502
	Water	2.43×10^{-3}	kg	1.0502
	Hydrogen chloride	1.07×10^{-3}	kg	1.0502
	Carbon dioxide	0.22	kg	1.0502
	Diethyl ether	2.92×10^{-4}	kg	1.0502
Emissions to water	Water, RER	0.06	m^3	1.0502
	COD, Chemical Oxygen Demand	0.02	kg	1.0502
	DOC, Dissolved Organic Carbon	6.77×10^{-3}	kg	1.0502
	BOD5, Biological Oxygen Demand	0.02	kg	1.0502
	TOC, Total Organic Carbon	6.77×10^{-3}	kg	1.0502
	Diethyl ether	0.01	kg	1.0502
Outputs to technosphere	Wastewater, average {Europe without Switzerland}| market for wastewater, average | Cut-off	1.05×10^{-4}	m^3	1.0502
Avoided products	Hydrogen, liquid {RER}| market for | Cut-off, U	0.01	kg	1.0502

Table S31 Inventory for different ratios of $[C_8C_1Im]Cl_\chi ZnCl_2$.

Inventory Group	Inventory	Flow (amount/kg product)				Unit
		Amount				
		$[C_8C_1Im]Cl_{0.33}ZnCl_2$	$[C_8C_1Im]Cl_{0.5}ZnCl_2$	$[C_8C_1Im]Cl_{0.6}ZnCl_2$	$[[C_8C_1Im]Cl_{0.67}ZnCl_2$	
Inputs from nature	Water, cooling, unspecified natural origin, RER	6.24×10^{-4}	6.34×10^{-4}	6.61×10^{-4}	7.56×10^{-4}	m3
	Water, river, RER	3.12×10^{-4}	3.17×10^{-4}	3.31×10^{-4}	3.78×10^{-4}	m^3
	Water, well, in ground, RER	3.12×10^{-4}	3.17×10^{-4}	3.31×10^{-4}	3.78×10^{-4}	m3
Inputs from technosphere (materials)	$[C_8C_1Im]Cl$	0.77	0.63	0.53	0.46	kg
	Zinc Chloride {RER}| production | Cut-off, U-Husain	0.23	0.37	0.47	0.54	kg
	Electricity, medium voltage {RER}| market group for | Cut-off	4.32×10^{-3}	4.64×10^{-3}	4.80×10^{-3}	5.11×10^{-3}	kWh
	Chemical factory, organics {GLO}| market for | Cut-off	4.0×10^{-10}	4.0×10^{-10}	4.0×10^{-10}	4.0×10^{-10}	p
	Heat, from steam, in chemical industry {RER}| market for heat, from steam, in chemical industry | Cut-off, U	9.12E-3	0.01	0.01	0.01	MJ
	Heat, district or industrial, natural gas {RER}| market group for | Cut-off, U	0.08	0.09	0.10	0.11	MJ
	Hydrogen, liquid {RER}| market for | Cut-off, U	1.03×10^{-3}	1.12×10^{-3}	1.18×10^{-3}	1.22×10^{-3}	kg
Emissions to air	Imidazole	1.31×10^{-3}	1.06×10^{-3}	8.98×10^{-4}	7.76×10^{-4}	kg
	Chloride	2.37×10^{-4}	1.93×10^{-4}	1.63×10^{-4}	1.41×10^{-4}	kg
	Water	2.50×10^{-5}	2.54×10^{-5}	2.65×10^{-5}	3.03×10^{-5}	kg
	Zinc chloride	4.56×10^{-4}	7.43×10^{-4}	9.40×10^{-4}	1.09×10^{-3}	kg
	Hydrogen	1.01×10^{-3}	1.10×10^{-3}	1.16×10^{-3}	1.20×10^{-3}	kg
Emissions to water	Water, RER	6.24×10^{-4}	6.34×10^{-4}	6.61×10^{-4}	7.56×10^{-4}	m^3

Table S32 LCA ReCiPe midpoint results for different ratios of $[C_8C_1Im]Cl_\chi ZnCl_2$.

Impact indicator	Unit	$[C_8C_1Im]Cl_{0.33}ZnCl_2$	$[C_8C_1Im]Cl_{0.5}ZnCl_2$	$[C_8C_1Im]Cl_{0.6}ZnCl_2$	$[C_8C_1Im]Cl_{0.67}ZnCl_2$
Global warming	kg CO_2 eq/kg	5.18	4.49	4.02	3.67
Stratospheric ozone depletion	kg CFC11 eq/kg	1.03×10^{-6}	9.59×10^{-7}	9.08×10^{-7}	8.71×10^{-7}
Ionizing radiation	kBq Co-60 eq/kg	0.31	0.28	0.26	0.25
Ozone formation, Human health	kg NOx eq/kg	8.18×10^{-3}	7.36×10^{-3}	6.79×10^{-3}	6.38×10^{-3}
Fine particulate matter formation	kg PM2.5 eq/kg	4.71×10^{-3}	4.27×10^{-3}	3.97×10^{-3}	3.75×10^{-3}
Ozone formation, Terrestrial ecosystems	kg NOx eq/kg	9.01×10^{-3}	8.08×10^{-3}	7.44×10^{-3}	6.97×10^{-3}
Terrestrial acidification	kg SO_2 eq/kg	1.27×10^{-2}	1.15×10^{-2}	1.07×10^{-2}	1.01×10^{-2}
Freshwater eutrophication	kg P eq/kg	1.54×10^{-3}	1.50×10^{-3}	1.48×10^{-3}	1.46×10^{-3}
Marine eutrophication	kg N eq/kg	5.74×10^{-3}	4.68×10^{-3}	3.96×10^{-3}	3.43×10^{-3}
Terrestrial ecotoxicity		56.29	78.51	93.79	104.87
Freshwater ecotoxicity		0.64	0.70	0.74	0.77
Marine ecotoxicity	kg 1,4-DCB/kg	0.85	0.95	1.03	1.08
Human carcinogenic toxicity		0.37	0.38	0.39	0.39
Human non-carcinogenic toxicity		13.28	18.46	22.03	24.62
Land use	m^2a crop eq/kg	7.24×10^{-2}	7.11×10^{-2}	7.02×10^{-2}	6.96×10^{-2}
Mineral resource scarcity	kg Cu eq/kg	0.04	0.05	0.06	0.07
Fossil resource scarcity	kg oil eq/kg	2.33	2.01	1.80	1.63
Water consumption	m^3/kg	0.32	0.27	0.24	0.21

Table S33 LCA ReCiPe endpoint results for different ratios of $[C_8C_1Im]Cl_\chi ZnCl_2$.

Impact indicator	Unit	$[C_8C_1Im]Cl_{0.33}ZnCl_2$	$[C_8C_1Im]Cl_{0.5}ZnCl_2$	$[C_8C_1Im]Cl_{0.6}ZnCl_2$	$[C_8C_1Im]Cl_{0.67}ZnCl_2$
Human health	DALY/kg	1.27×10^{-5}	1.29×10^{-5}	1.31×10^{-5}	1.32×10^{-5}
Ecosystem quality	Species.yr/kg	2.55×10^{-8}	2.28×10^{-8}	2.09×10^{-8}	1.96×10^{-8}
Resources	USD_{2013}/kg	0.89	0.77	0.69	0.63

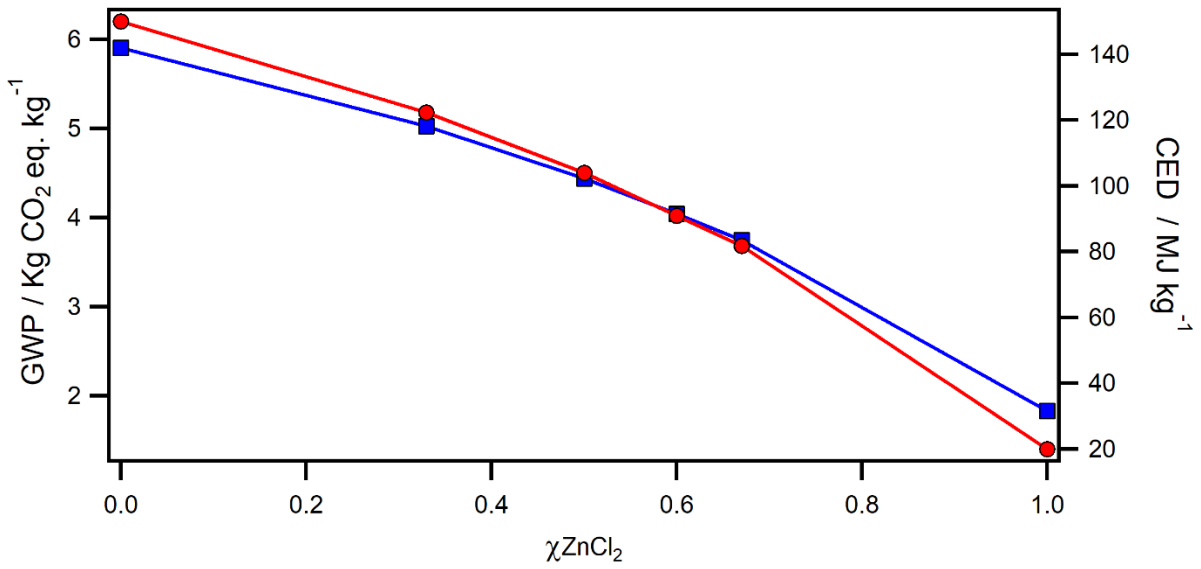

Figure S171 LCA derived global warming potential (red; left) and cumulative energy demand (blue; right) for the $[C_8C_1Im]Cl_\chi ZnCl_2$ series of ionic liquids.

References

(1) Bui-Le, L.; Clarke, C. J.; Bröhl, A.; Brogan, A. P. S.; Arpino, J. A. J.; Polizzi, K. M.; Hallett, J. P. Revealing the Complexity of Ionic Liquid–Protein Interactions through a Multi-Technique Investigation. *Commun. Chem.* **2020**, *3* (1), 1–9. https://doi.org/10.1038/s42004-020-0302-5.

(2) Clarke, C. J.; Hayama, S.; Hawes, A.; Hallett, J. P.; Chamberlain, T. W.; Lovelock, K. R. J.; Besley, N. A. Zinc 1s Valence-to-Core X-Ray Emission Spectroscopy of Halozincate Complexes. *J. Phys. Chem. A* **2019**, *123* (44), 9552–9559. https://doi.org/10.1021/acs.jpca.9b08037.

(3) Seymour, J.; Gousseva, E.; Large, A.; Held, G.; Hein, D.; Wartner, G.; Quevedo, W.; Seidel, R.; Kolbeck, C.; Clarke, C. J.; et al. Resonant Electron Spectroscopy: Identification of Atomic Contributions to Valence States. *Faraday Discuss.* **2022**. https://doi.org/10.1039/d1fd00117e.

(4) Seymour, J. M.; Gousseva, E.; Large, A. I.; Clarke, C. J.; Licence, P.; Fogarty, R. M.; Duncan, D. A.; Ferrer, P.; Venturini, F.; Bennett, R. A.; et al. Experimental Measurement and Prediction of Ionic Liquid Ionisation Energies. *Phys. Chem. Chem. Phys.* **2021**, *23* (37), 20957–20973. https://doi.org/10.1039/d1cp02441h.

(5) Gao, H.; Ye, C.; Piekarski, C. M.; Shreeve, J. M. Computational Characterization of Energetic Salts. *J. Phys. Chem. C* **2007**, *111* (28), 10718–10731. https://doi.org/10.1021/jp070702b.

(6) Jenkins, H. D. B.; Tudela, D.; Glasser, L. Lattice Potential Energy Estimation for Complex Ionic Salts from Density Measurements. *Inorg. Chem.* **2002**, *41* (9), 2364–2367. https://doi.org/10.1021/ic011216k.

(7) 1-Methylimidazole | Sigma-Aldrich https://www.sigmaaldrich.com/GB/en/product/sigma/m8878 (accessed May 6, 2022).

(8) Verevkin, S. P.; Zaitsau, D. H.; Emel'yanenko, V. N.; Paulechka, Y. U.; Blokhin, A. V.; Bazyleva, A. B.; Kabo, G. J. Thermodynamics of Ionic Liquids Precursors: 1-Methylimidazole. *J. Phys. Chem. B* **2011**, *115* (15), 4404–4411. https://doi.org/10.1021/jp201752j.

(9) Valderrama, J. O.; Rojas, R. E. Critical Properties of Ionic Liquids. Revisited. *Ind. Eng. Chem. Res.* **2009**, *48* (14), 6890–6900. https://doi.org/10.1021/ie900250g.

(10) Baaqel, H.; Hallett, J. P.; Guillén-Gosálbez, G.; Chachuat, B. Sustainability Assessment of Alternative Synthesis Routes to Aprotic Ionic Liquids: The Case of 1-Butyl-3-Methylimidazolium Tetrafluoroborate for Fuel Desulfurization. *ACS Sustain. Chem. Eng.* **2022**, *10* (1), 323–331. https://doi.org/10.1021/acssuschemeng.1c06188.

(11) Towler, G.; Sinnott, R. K. *Chemical Engineering Design - Principles, Practice and Economics of Plant and Process Design (2nd Edition)*; Butterworth-Heinemann, 2013.

(12) Baaqel, H.; Díaz, I.; Tulus, V.; Chachuat, B.; Guillén-Gosálbez, G.; Hallett, J. P. Role of Life-Cycle Externalities in the Valuation of Protic Ionic Liquids-a Case Study in Biomass Pretreatment Solvents. *Green Chem.* **2020**, *22* (10), 3132–3140. https://doi.org/10.1039/d0gc00058b.